Study of anticancer properties of PR-3 series compound(s) on Prostate cancer

THESIS SUBMITTED TO JAWAHARLAL NEHRU UNIVERSITY

FOR THE AWARD OF THE DEGREE OF

DOCTOR OF PHILOSOPHY

Guru Prasad Sharma

School of Life Sciences

Jawaharlal Nehru University

New Delhi-110067, India

January, 2017

SCHOOL OF LIFE SCIENCES
JAWAHARLAL NEHRU UNIVERSITY
NEW DELHI 110067
INDIA

CERTIFICATE

The research work embodied in the thesis entitled ***"Study of anticancer properties of PR-3 series compound(s) on Prostate cancer"*** has been carried out in School of Life Sciences, Jawaharlal Nehru University, New Delhi.

This work is original and has not been submitted so far, in part or in full, for award of any degree or diploma of any university.

Guru Prasad Sharma
(Candidate)

Dr. Neelima Mondal
(Supervisor)

Dean
School of Life Sciences

Dedicated

to my

Parents.....!

ACKNOWLEDGEMENTS

देहि सौभाग्यं आरोग्यं देहि में परमं सुखम् ।

रूपं देहि जयं देहि यशो देहि द्विषोजहि ।।

"Dear Goddess, bless me with good fortune, good health, good looks, success and fame. Dear vaishnavi you are the creator for the world. You have mesmerized the world. When you are pleased with someone you ensure his salvation from the cycle of life and death".

I am grateful to almighty for giving me opportunity and strength to accomplish my parent's dreams. This research work is the result of many years of hard work, during which I got the opportunity to work with many people who were more than supportive. It's a great pleasure to convey my sincere gratitude to them in my acknowledgement.

First and foremost, I would like to express my gratitude to my thesis supervisor, Dr. Neelima Mondal, for her mentorship, guidance and all kind of support over the course of my studies. Her enthusiasm and dedication has inspired me a lot and boosted my confidence to work independently. I sincerely thank her for showing confidence in me. I am also thankful to Professor Suman Dhar for his invaluable suggestions and support from time to time.

I would also like to acknowledge the sincere efforts of my advisory committee members especially Dr. Sher Ali, Dr. Abraham for critically evaluating my work presentations and providing inputs and comments.

My sincere regards to my work collaborator, Professor Amir Azam, for the synthesis of compounds and all kind of help in preparing the paper manuscript. I can't miss to express my gratitude to him for all the warm hospitality I received whenever I visited him.

I am thankful to the Dean, present and past, of our department under whom I carried out my work. I sincerely thank all the technical and clerical staff for their kind help in doing my experiments and paper works. I thank to the animal ethical committee, JNU, for providing me the space to do my animal experiments.

I express my sincere regards to the director ICGEB, New Delhi, for providing the experimental animals.

My special thanks to lokesh who helped me a lot in conducting animal and docking experiments.

My very special thanks go to all my lab mates for their encouragement, constructive suggestion, support and love. To Somesh, for introducing me the lab-work and techniques when I joined the lab. To Shazia, for all those conversations and light moments. I really cherished the morning and evening tea-time with Sumit, who lightened my hectic time. I have been really happy to have company of Sumiran, and Arti. Working with you all has been a wonderful experience. I also thank to my batchmates Apoorva and specially Isha for the kind support and help in our animal experiments.

My sincere thanks to Balwant ji for his light discussions and funny conversations in the lab, apart from assisting in the lab work.

I would like to acknowledge all the lab mates in previous lab at NII, New Delhi, when I was there on project. To Neha, Divya, Anwar, Aparna, Hari, Prakash, Kavita, Piyush, Sudheer, Praveen, Surabhi. I really had a great time with you all. I specially thank Prashant for providing critical suggestions and scientific inputs during my PhD and supporting me as younger brother.

To my dear friends, Dabbu, Himanshu Chaudhary, Md. Kalamuddin, Vikas, and Marry, the long time spent with you people was mesmerizing and the support you provided has been really great.

Funding for this project was provided in part by the UPE-II, DBT Builder, DST-PURSE II, DST-FIST and UGC-RNW. I was financially supported by the UGC-BSR fellowship.

My dear family members deserve super-special mention. I thank my parents, brothers, my sister, in-laws and all other members for their unconditional continuous encouragement, affection and support. All of you have been my pillars of strengths. My dear wife has always supported and cared me. My lovely daughter's smile, at the end of every day, made me get through times of frustration and rejuvenated me to work on next day.

Finally, I would like to thank each and everyone who have been the part of the success of this thesis and express my sincere apology for not mentioning them personally.

Guru Prasad Sharma

Abbreviations:

Ab	Antibody
ABL	Abelson murine leukemia viral oncogene homolog 1
APS	Ammonium persulphate
AR	Androgen receptor
ADME	Absorption, Distribution, Metabolism, and Excretion
ATP	Adenosine triphosphate
BSA	Bovine Serum Albumin
Bcl-2	B-cell lymphoma-2
cDNA	Complementary DNA
CA	Carbonic anhydrase
CDK	Cyclin Dependent Kinase
CAK	Cdk Activating Kinase
CKI	Cdk Kinase Inhibitor
CRPC	Castration-resistant Prostate Cancer
Caspase	Cysteine-aspartic proteases, cysteine aspartases
CAT	Catalase
DAPI	4', 6-Diamidino-2-phenylindone
DMEM	Dulbecco's Modified Eagle Medium
DMSO	Dimethyl sulphoxide
DNA	Deoxyribonucleic acid
DRE	Digital Rectal Exam
DCF-DA	Dichloro-dihydro-fluorescein diacetate
DTNB	5,5’-Dithiobis-(2-Nitrobenzoic acid)
DTT	Dithiothreitol
EDTA	Ethylene diamine tetraacetic acid
FBS	Fetal Bovine Serum
FIU	Fluorescence Intensity Unit
G	Gap, a phase in cell cycle
gm	Gram
GSH	Glutathione reductase
HPC1	Hereditary Prostate Cancer 1
IFA	Immunofluorescence Assay

`IP	Immunoprecipitation
kDa	Kilodalton
kb	Kilobase Pairs
M	Molar
min	Minutes
mg	Milligrams
ml	Millilitres
mM	Millimolar
mRNA	Messenger RNA
MMP	Mitochondrial membrane potential
MRC	Mitochondrial Respiratory Chain
MTT	(3-(4, 5-Dimethylthiazol-2-yl)-2, 5-Diphenyltetrazolium Bromide
MDA	Malondialdehyde
NBT	Nitro blue tetrazolium chloride
NEM	N–Ethylmaleimide
NADPH	Nicotinamide adenine dinucleotide phosphate
O.D.	Optical Density
OPT	1,10-Phenanthroline monohydrate
PCD	Programmed Cell Death
PBS	Phosphate buffer saline
PMS	Phenazine methosulphate
PCR	Polymerase chain reaction
PIN	Prostatic intraepithelial neoplasia
PKM2	Pyruvate kinase muscle isozyme M2
P/S	Penicillin Streptomycin
PARP	Poly (ADP-ribose) polymerase
PCV	Packed cell volume
RNA	Ribonucleic acid
rpm	Revolution per minute
RT-PCR	Reverse Transcription Polymerase Chain Reaction
ROS	Reactive Oxygen Species
SDS	Sodium dodecyl sulphate
SH	Sulfonyl Hydrazide
SOD	Superoxide dismutase

SDS-PAGE	Sodium dodecyl sulpahte polyacrylamide gel electrophoresis
TEMED	N,N,N’,N’-Tetramethylethylenediamine
TBE	Tris-Borate-EDTA
TRUS	Transrectal ultrasound
TBARS	Thiobarbituric acid reactive substance
TBA	Thiobarbituric acid
TCA	Trichloroacetic acid
WB	Western Blot
µg	Microgram
µl	Microlitre
µM	Micromolar
µg	Microgram

TABLE OF CONTENTS

CHAPTER-1

1.1. Review of literature

1.1.1. What is Prostate Cancer?

Prostate cancer results from the "unregulated functioning" of the prostate gland, "an exocrine gland of the male reproductive system" (Villers et al., 2008; Nelson et al., 2003). Androgen hormone, required for the growth of the prostate gland, binds to the "androgen receptor (AR)" and triggers the signaling cascade in the prostate gland (Tindall and Mohler, 2009; Heinlein and Chang, 2004). However, with the age over-activation of the AR leads to the activation of genes which promote the prostate cancer (Karayi and Markham, 2004; Shand and Gelmann, 2006). At the initial stage of this disease, though the signs are undetectable, the chronic symptoms include difficulty in urinating, pain in the pelvis and hematuria. In the early stage of the disease, prostate cancer cells rely on AR for their growth and in that case hormonal deprivation therapy is carried out (Widmark et al., 2009; Heinlein and Chang, 2004; Damber, 2005). The failure in early detection or even sometime prolong treatment of the disease results in an androgen-independent known as "advanced hormone refractory metastatic cancer" (Feldman and Feldman, 2001). The hormone refractory cancer cells do not respond to the androgen deprivation therapy. The metastatic-process involve the invasion of primary prostate cancer cells into the distant tissues. The major metastatic targets are usually bone marrow, and lymph nodes (Hejmadi, 2010). Early diagnosis includes the detection of PSA and followed with the treatments, however, the late diagnosis causes metastasis and usually results in mortality (Djulbegovic et al., 2010). Chemotherapy, radiation, and surgery are the major approaches which are maneuvered in the treatment of prostate cancer (Narayan et al., 2003). The mutations associated with tumor suppressor p53 (Downing et al., 2003), BRCA1 and BRCA2 (Cavanagh and Rogers, 2015), phosphatase and tensin homolog" (PTEN) (Phin et al., 2013) and "Kallmann syndrome 1" (KAI1) (Dong et al., 1995) have been reported in the manifestation of the disease.

1.1.2. Prostate cancer demography

"Prostate cancer is the sixth leading cause of cancer-born deaths globally and USA alone records around 32,000 lives every year" (Iarc., 2012). In developed countries like the USA, it is the second most diagnosed cancers (Ferlay et al., 2015). The developing countries have reported lesser number of cases, but incidence and mortality have been soaring recently (Boutayeb, 2006). Since most of the cases are detected at a very late stage, early detection is the need of the hour. Ethnicity is also one of the important factors. For instance, Asian men have the least incidence as compared to their African counterparts. The comparative depiction of "incidence and mortality rate" of prostate cancer is given below **(Table. 1.1)** (GLOBOCAN-2012).

Worldwide	**1095**	**307**	**3858**
More developed regions	742	142	2871
Less developed regions	353	165	987
India	**19**	**12**	**64**
WHO Americas region (PAHO)	413	85	1539
WHO East Mediterranean region (EMRO)	19	12	47
WHO Europe region (EURO)	420	101	1513
WHO South-East Asia region (SEARO)	39	25	123
WHO Western Pacific region (WPRO)	153	46	499
WHO Africa region (AFRO)	52	37	135
IARC membership (24 countries)	791	157	2998
United States of America	233	30	980
China	47	23	104
European Union (EU-28)	345	72	1277

Table. 1.1. Comparative cases of survival, mortality and prevalence rate of prostate cancer on global scale. The numbers are given in thousands. Indian data is highlighted (in red color). These figures have been taken from "GLOBOCAN -2102".

In India, several demographical studies have been conducted to evaluate the prostate cancer scenario, however these studies are limited. An exhaustive review has recently

reported that India may have low rate of incidences owing to the inadequate population based study and a proper prognosis program is required to assess the ground reality (Hariharan and Padmanabha, 2016).

1.1.3. Carcinogenesis and diagnosis of Prostate cancer

As stated above, "Prostate cancer is an uncontrolled growth of the prostate gland," and in they spread from the primary origin to the other tissues (Weinberg, 2013). The onset of prostate cancer has yet not been fully understood. However, some reports say that the beginning of prostate cancer is observed with the morphological changes in the prostate gland cells, called "Prostatic intraepithelial neoplasia" (PIN). Some reports have suggested that "PIN as a possible initiator of prostatic carcinogenesis, causing around 30 % cases in association with p53" (Brawer, 2005; Merrimen et al., 2009). In prostate cancer, the epithelial cells of PIN become irregular in shape and size resulting in a mass called "adenocarcinoma," and that provide the basis for the early diagnosis (Ayala and Ro, 2007). In some case, PIN development has been found without the occurrence of adenocarcinoma (Merrimen et al., 2009). The eukaryotic genome is always exposed to the constant genetic transformations. The genetic changes in non-coding regions are harmless, and most of the deleterious mutations are linked with the coding area of the genome (Weinberg, 2013). In the process of carcinogenesis, the above-stated transformations require six crucial factor, "Independent growth factors, enough availability of resources, evasion of apoptosis, continuous replication potential, expression of anti-apoptotic genes, and expression of factors promoting invasion and metastasis" (Hanahan and Weinberg, 2000; Chen et al., 2004). The prostate carcinogenesis and the genetics involved has yet not fully understood. However, the present reports have suggested that "the genes which are associated with the cellular growth, are the most susceptible to the mutations causing prostate cancer" (Abate-Shen, 2000; Ponder, 2001). These genes include "oncogenes, tumor suppressor genes, and DNA repair genes." These three groups of genes crosstalk with many axillary genes and trigger the onset of prostate cancer. Oncogenes originate from mutations in the proto-oncogenes such as "ras, myc and abl" (Pérez-Caro and Sánchez-García, 2007; Adrián et al., 2006). The proto-oncogenes are most susceptible to the genetic transformations and give rise to the abnormal proliferation (Chial et al., 2008). In majority of cancers, the tumor suppressor genes, p53 and retinoblastoma (Rb), are mutated and nonfunctional (Xu et al., 2014). The DNA repair genes are the molecular

engineers of the cells and maintain the intact genetic structure. The mutations in these genes often result in the catastrophic changes and lead to the abnormal genetic functions (Lahtz and Pfeifer, 2011). The prostate gland synthesizes PSA, "which help the spermatozoa pass through the female reproductive tract," is being used in the early detection of disease. The first use of PSA as a genetic marker and its first application in diagnosis were reported in 1982 and 1991 respectively (Koh and Atala, 2006). The standard level of PSA in seminal fluid varies from "0.45 to 2.10 mg/ml" while that in blood is very less (about 3-4 nanograms/ml) and sometimes undetectable. However, there have been various improvements in PSA testing to increase specificity and sensitivity (Goldfarb et al., 1986). The PSA levels diagnosed with the incidence of prostate cancer also vary and are affected by many environmental and genetic factors (Connolly et al., 2009; Lim et al., 2014). Other common diagnostic measures include "Digital Rectal Exam (DRE), Transrectal ultrasound (TRUS), biopsy, and Gleason scoring" (Skolarus et al., 2014). In spite of the development of advanced diagnostic measures the incidence of the disease are increasing.

1.1.4. Prostate Cancer risk factors

The well-known and established risk factors include "age, race, diet and the family history." There might be some other classified causative factors which lie in the cart of the research and discoveries. A number of factors are mulled in defining the nature of prostate cancer, the present studies are inclined majorly towards the genetic and environmental risks. Moreover, the prostate basal cells are the sites which are affected most by these risk factors (Goldstein et al., 2010). The two most responsible factors are given below.

1.1.4.1. Environmental risk factors

As the danger of incidence increases with old age, therefore, "approximately 90% of diagnosis are done beyond the age of 60-65" (Gann, 2002; Patel and Klein, 2009). In developed countries like the USA , the incidence rate is very high, and studies have shown that Asian men migrated to USA bear elavated risk of incidence than their native counterpart (Powell, 2011). These studies imply that some environmental factors might have been involved, though they are poorly understood. The higher rate of incidence in developed countries also imply that the better hygiene and better lifestyle have least counter effects on the prostate cancer cases. Some nutritional components have been

studied in context to the prostate incidence, and the reports have suggested the vitamin D, "a known inhibitor of the cell cycle and metastasis," exhibits protective role, though the exact mechanisms involved are still to be delineated (Garland et al., 2006). The lifestyle of different ethnic groups also makes them differentially sensitive to the disease (Optenberg et al., 2013). The population-based studied in various ethnic groups have suggested a better understanding that may improve the various diagnostic and screening techniques (Lilja et al., 2008). The physical activity though has not been well-stablished, in some cases it decreases the incidence rate and also results in the improvements in the men undergoing treatments (Parekh et al., 2012). Obesity, one of the major budding problems of the modern world, has been implicated in the incidence of prostate cancer by several studies (Calle et al., 2003). For example, "BMI," a scale of obesity index, has been reported to be linked with decreased level of PSA and often result in an adverse prognosis in the obese men (Barqawi et al., 2005). As per these data, it has been proposed that in the near future, western countries would observe an increase in prostate cancer (O'Malley and Taneja, 2006). The epidemic survey-based studies have implicated the diet containing high fat, as an inducer of the disease (Di Sebastiano and Mourtzakis, 2014). The use of vegetables and less use of red meat has been shown to reduce the incidence, though the molecular factors involved are not yet defined. In one report, the lycopene ,a constituent of tomato, has been shown to impinge on dihydrotestosterone hormone and activate apoptotic cascade in prostate cancer cells (Holzapfel et al., 2013). There are also the studies which have demonstrated the beneficial effects of red wine in reducing the risks (Watters et al., 2010). However, the overconsumption of alcoholic beverages also increases risk. The two important androgens, "Testosterone and dihydrotestosterone", are maintained in an optimal level normally in men. These increase in the level of these hormones confer potential risks to the development of prostate cancer disease (Kaplan et al., 2015). Basically, this is the hormonal misbalance which is acknowledged by several environmental factors.

1.1.4.2. Genetic risk factors

Since "the incidences of prostate cancer are also associated with the ethnicity," therefore the genetic history of men may underline the causes, linked to the incidence of prostate disease. The familial clustering of the disease suggests that the mode of inheritance may be either X-linked or recessive. The androgen receptor gene is frequently mutated and has

been shown to contribute to the incidence of prostate cancer (Smith et al., 1996). Recently, "the exhaustive genome-wide association studies" (GWAS) have disclosed some loci which may harbor prostate cancer genes (Gudmundsson et al., 2012; Amundadottir et al., 2006). In a GWAS survey on some family, the study has discovered two susceptible loci on the chromosomes. One locus was located on chromosome 1q24, "which is called HPC1 (Hereditary Prostate Cancer 1)" and another was located on chromosome X, "called Hereditary Prostate Cancer X (HPX)" (Smith et al., 1996; Xu et al., 1998). As per some studies, it has been reported that there is a higher risk of developing prostate cancer in men having affected father or brother than those having a family history without any such case (Steinberg et al., 1990; McDowell et al., 2013), "thereby suggesting a potential risk associated with HPC1 and HPX". "Polyamines" play a significant role in "cell growth, differentiation, and cell death" and abundantly found in prostate cells (Thomas and Thomas, 2001). The different forms of "polyamines, putrescine, spermidine and spermine," are controlled by androgens and decide the fate of prostate cellular discourse (Zeegers and Ostrer, 2005). In prostate cancer, higher levels of polyamines are found and implicated in further invasive infestations (Rhodes et al., 2002). The mutations associated with "BRCA1 and BRCA2" (Cavanagh and Rogers, 2015), tumor suppressor p53 (Downing et al., 2003) have been reported creating major risks . The anticancer protein, "phosphatase and tensin homolog" (PTEN) (Phin et al., 2013) and "Kallmann syndrome 1" (KAI1) (Dong et al., 1995). However, much is left to conclusively correlate the genetics with the onset of prostate cancer.

1.1.5. Cell cycle and its regulation in cancer

1.1.5.1. Cyclins

Cell cycle is driven by the mutual cooperation of cyclin/CDK complexes. Cyclins are the regulatory unit of these complexes and assist their respective kinases to advance the cell cycle. Their average molecular size ranges from 35 to 90 kDa (Morgan, 1997). The sequence homology based studies have revealed that cyclins have a "100-residue conserved section", called "cyclin box," and facilitates its interaction with CDK (Horton and Templeton, 1997). In mammals, cyclin family comprises around eight (from cyclin A to cyclin H), which are assigned the specific function in different tissue (Johnson and Walker, 1999). They bind and activate their associated kinases and march to the next cell cycle phase. After their successful functions, cyclins are degraded at various point of cell cycle.

The role of cyclin D1 has been reported as pro-oncogenic and contributes to the malignancy (Seiler et al., 2014; Umekita et al., 2002). Cyclin D1 is transcriptionally activated by oncogenes and its overexpression has been shown in the generation of CRPC condition in prostate cancer" (Drobnjak et al., 2000; He et al., 2007). The major cyclins and their kinase moiety have been depicted in figure 1.1.

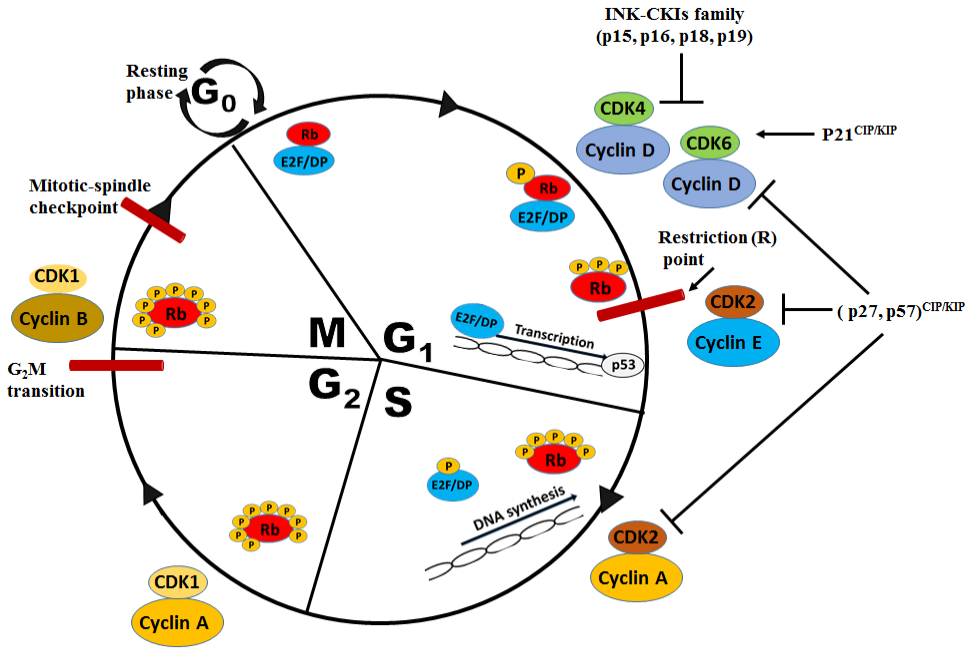

Fig. 1.1. Mammalian cell cycle and checkpoints.
Diagram shows various cell cycle phase and the cell cycle proteins involved in its progression. Red colour bar shows the checkpoints. Details are given in the text.

1.1.5.2. Cdks

"Cyclin-dependent protein kinases or CDKs" are the catalytic unit of cyclin/CDK complex. The active sites remain in dormant stage of an alone cdk and are activated by the association of its specific cyclin. The various phases of the cell cycle observe activation of phase-specific CDKs which are activated by their specific cyclins (Morgan, 1995). Apart from cyclins, most of the CDKs require additional activating factor to be fully functional. These additional activators include "CDK-Activating Kinase" or CAK" (Kaldis, 1999). The uninterrupted activation of CDKs may be deleterious for the cell, therefore, CDK-activities are governed by the "Cdk inhibitory subunits or CKIs". The CKIs have been discussed in

detail below. The kinase partners of different CDKs at various stages in the cell cycle are given in figure **(Fig. 1.1)**.

1.1.5.3. CKIs

In mammalian cell cycle, the progression through the G_1-phase and initiation of DNA synthesis are governed by various CDKs. As stated above, the continuous CDK activity is fatal for a healthy cell cycle, therefore CDKs are regulated by another class of inhibitors, called CDK inhibitors or CKIs (Lim and Kaldis, 2013). As the CDKs are diversified and express specifically to the stage of cell cycle, their regulation is also carried out by the different class of CKIs. Based on the specificity to respective CDK-targets, CKIs fall in two categories namely, "INK4 or inhibitors of CDK4", and "Cip/Kip family". The early G_1-CDKs, "CDK4 and CDK6" are inbited by INK4 inhibitors "($p16^{INK4a}$, $p15^{INK4b}$, $p18^{INK4c}$, and $p19^{INK4d}$)" (Schwaller et al., 1997). The INK4 are crucial in ensuring whether the cell is ready to cross the commitment point in G_1-phase. The Cip/Kip family, along with its specific members, "p21Waf1/CIP1, p27Kip1, p57Kip2", can inhibit CDK activity at any stage of the cell cycle (Nakayama and Nakayama, 1998). However, a recent report has shown that p21Waf1/CIP1 can activate cyclin D1-cdk4/6 complex (Abbas and Dutta, 2009). The members of p21 can interact and inhibit various cyclin/Cdk complexes but have also been reported to show preferential interaction with Cdk2 interacting cyclins (Cayrol et al., 1998). Also, p21 has is a c-terminus domain which interacts with "proliferating cell nuclear antigen or PCNA," an integral part of the "replication machinery." The p21-PCNA association can inhibit replication but not DNA repair property. A Recent report suggests that p21 biological functions depend on in context to the cellular localization and interactions (Pérez-tenorio et al., 2006; Schepers et al., 2003).

1.1.5.4. The p53 protein

"The tumor suppressor protein p53" is a well-studied transcription factor which transcribe crucial genes involved in the protection of cells from genetic damages (Green and Chipuk, 2006). P53 is highly sensitive to the processes like "DNA damage response, cell cycle arrest, apoptosis, autophagy, and metabolism", therefore the mutation in it causes the higher risk of about 50% of cancer development (Olivier et al., 2010). Mdm2, which is transcribed by p53, regulates p53 by activating the ubiquitin-proteasome system (Kubbutat et al., 1997). On receiving DNA-damage signals, the resultant responsive kinases such as

"ATM, Chk1, and Chk2", phosphorylate p53 and enhance its transcriptional potential (Smith et al., 2010). The transcriptional property of p53 is to facilitate the expression of pro-apoptotic proteins like "Bax, puma and noxa in the nucleus" (Amaral et al., 2010). The cytosolic p53 can induce apoptosis by binding to pro-apoptotic proteins, "Bcl-2, Bcl-XL, Bax, and Bak", which further can induce "mitochondrial outer membrane potential or MOMP" (Moll, 2005; Mihara et al., 2003). Cancer cells have modified glucose metabolism, wherein a large chunk of ATP are produced by aerobic glycolysis of pyruvate. The p53 transcribes the gene, "TP53-induced glycolysis and apoptosis regulator or TIGAR", which lowers fructose-2,6-bisphosphate levels in cells and frther redirect glucose to the pentose phosphate pathway to generate sufficient reducing power (Bensaad et al., 2006; Green and Chipuk, 2006).

1.1.5.5. Caspases

"Caspases or **c**ysteine-**asp**artic prote**ases**, **c**ysteine **asp**art**ase,"** are the family of protease enzymes and play a major role in "programmed cell death or PCD" (McIlwain et al., 2013). Caspases cleave polypeptide chains with the help of sulfur atom in cysteine. Almost all living cells have the caspases, and their number and cellular functions differ in different species. The recent developments in sequence analysis have reported that "Drosophila has probably seven caspases" (Cashio et al., 2005) and "mammalian cell lines are found with 14 caspases" (Elmore, 2007). Caspases are typically localized to the cytoplasm. Based on their sequence alignment, they are classified into two groups, "the Ced-3 and ICE" (Thornberry and Lazebnik, 1998; Shi, 2002). The Ced-3 caspases namely "caspases 2, 3, 6, 7, 8, 9 and 10" perform activation and progression of apoptotic cascade, while "Interleukin-1 converting enzyme or ICE" caspases namely "caspases 1, 4, 5, 11 and 13" exert pro-inflammatory events such as cytokine mobilization (Nicholson and Thornberry, 1997; Nuñez et al., 1998). The apoptotic pathway implicates the Ced-3 caspases which are subdivided in two categories namely "initiator caspases" and "executor caspases". Initiator caspases include caspase 2, 8, 9, 10 and are activated by the protein other than caspases. The executor caspases include caspase 3, 6 , 7 and are activated by the initiator caspases and that further leads to the modulation of the proteins implicated in apoptotic pathway (Shi, 2004a). Under apoptotic conditions, the activation of an initiator caspase and the downstream caspases is well-regulated and is often assisted by the multi-component complex (Vaux et al., 1988). When an apoptotic signal is received, the

procaspases get activated and are cleaved into 20 and 11 kDa subunits. The 20 kDa subunit is further auto-processed into an active subunit of 17 kDa, producing a dimer of these two subunits (Salvesen and Dixit, 1999; Shi, 2004b). The assembly of multi-complex is added by different protein recruitment domains found on these caspases (Hu et al., 2014). The initiator caspases are activated via two pathways, "extrinsic pathway or intrinsic pathway".

The extrinsic pathway comprises at least five different cell death receptors from "transmembrane tumor necrosis factor or TNF" receptor superfamily. The two receptors, "Fas and the type I TNF receptor," have been extensively studied (Griffith et al., 1995). All death receptors have a death domain directed to the cytoplasm and a death effector domains (DED). These death receptors, on binding to TNF, further recruits additional adaptor proteins like "Fas-associated death domain or FADD" (Siegmund et al., 2001). As shown in the diagram **(Fig. 1.2)**, FADD activates caspase 8 and 10 and gives rise to the formation a complex known as the "death-inducing signaling complex or DISC" (Peter and Krammer, 2003). The intrinsic pathway or mitochondrial pathway, requires a set of different complex circuits comprising "cytochrome c, procaspases 2, 3 and 9 and various apoptosis inducing agents". These pro-apoptotic agents reside in the "mitochondrial intermembrane space" and are ejected in cytoplasm upon receiving apoptotic signals (Susin et al., 1999; Misevičien et al., 2011). From the present available reports, it is understood that "caspase-9 is activated by the formation of a complex of Apaf-1, cytochrome c, and procaspase-9", and that assembly somehow also provides the launching station for the activation of effector caspases and further apoptosis (caspase 3, 7).

1.1.5.6. Cell cycle regulation by cyclin-CDK complexes

A large no of cells in human body, at the same time, do not engage in active cell cycle and remain in an inactive state called quiescent state. A small fraction of cells is actively proliferating and primarily reside in the milieu of self-renewal tissue known as epithelial and bone marrow (Wilson and Trumpp, 2006). A normal cell cycle is composed of four sequential phases, "G_1, S, G_2, and M". The resting phase or G_0 represents a state when cells are out of cell cycle division because of unavailability of mitotic cues (Humphrey and Pearce, 2010). M phase is followed by G_1 phase, which marks the time when the cell is most sensitive to the various cues from signaling networks. In both yeast and mammalian cells, G_1 phase is also unique for having a critical checkpoint (Foster et al., 2010). Once the

cell passes through this checkpoint, it becomes bound to enter S-phase where DNA synthesis takes place. Next to G_1 comes S phase, wherein DNA replicates itself. Next, comes G_2 or Gap-phase which separates S phase to M phase and this phase makes cells ready to enter mitosis (Teer and Dutta, 2006). The M phase follows the G_2 phase; "wherein a cell gives rise to the formation of two daughter cells." The journey of the standard cell cycle in eukaryotes is inspected and directed by complexes containing "cyclins, the regulatory moiety," and, "cyclin-dependent kinase (CDK) family of serine/threonine kinases," the catalytic moiety (Morgan, 1995). As shown in the diagram **(Fig. 1.1)**, the progression through G_1-phase is driven by the activity of Cyclin D-CDK4/6 and cyclin E-CDK2. These G_1 cyclin-CDKs prepare the cells to cross the restriction point (R) and enter the S-phase (Blagosklonny and Pardee, 2002; Teer and Dutta, 2006)**.** Cyclin A is involved in the DNA synthesis, and cyclinA-CDK2 activity maintains the proper progression of S-phase. Further, cyclin A-CDK1 complex readies cells to enter G_2M-phase, and the progression through G_2M and entry into mitotic phase is facilitated by cyclin B-CDK1 activities (Humphrey and Pearce, 2010). The multilevel regulation of the cell cycle is implicated in the design of inhibitors for cancer treatments.

1.1.5.7. Cell cycle regulation by transcription factors

Apart from cell cycle regulation by Cyclin-CDK complexes, these complexes themselves are regulated by transcriptional regulations. The induction of different isoforms of cyclin D starts in the G_0 phase, a cell cycle preparatory phase. Except for D-cyclins, the levels of various cyclins vary through the course of the cell cycle (Sherr, 1995). Early phase of the cell cycle is marked by the phosphorylation of tumor suppressor protein "retinoblastoma or Rb" by cyclin D-CDK4/6 complex which is required for the further cell cycle progression (Parry et al., 1995). The transcription factor E2F transcribes the genes required for the cell growth and proliferation (Khleif et al., 1996). The unphosphorylated form of Rb protein keeps the transcription factor E2F in inactive state. The cyclin D-CDK4/6-induced phosphorylation of Rb results in the release of E2F. The E2F family regulates the expression of multiple cell cycle proteins", such as "cyclins E and cyclin A, cdc2, CDK1, thymidine kinase, and DNA polymerase α" (van den Heuvel and Dyson, 2008). In late G_1-phase, cyclin E-CDK2 complex further phosphorylates Rb into a hyperphosphorylated state, thereby ruling out the reunion of Rb and E2F (Cayrol et al., 1998). Some reports have indicated that even in Rb null cells, the cyclin E-CDK2 activity cannot be compromised,

that can be explained by the existence of other substrates for cyclin E-CDK2 (Hwang and Clurman, 2005; Yu and Sicinski, 2004). Cyclin A is also partially regulated by E_2F. The expression of cyclin A starts piling from late G1-pase and persist until the end of S-phase. Cyclin A-CDK2 activity keeps Rb in hyperphosphorylated form, which is indispensable for the completion of S phase. Cyclin A also interacts and facilitates the synthesis of DNA in S-phase as shown by some reports (Bashir et al., 2000). Before entering the mitotic-phase, there is a small halt in the cell cycle which is meant for DNA repair process. This small repairing phase is called G2 checkpoint and is crucial in getting rid of the unwanted mutations in mitotic phase. The mitotic-phase is observed by the expression of cyclins A, and different forms of cyclin B. These M-phase cyclins in association with CDK1 phosphorylate many proteins which are implicated in the DNA unwinding and facilitates the formation of the mitotic spindle (Gavet and Pines, 2010; Ubersax et al., 2003). The transcriptional regulation ensures the time-specific expression of cell cycle proteins and their mutation may result in uncontrolled cell cycle progression and cancer development.

1.1.5.8. Cell cycle regulation by ubiquitination

In addition to factors mentioned above, "the ubiquitin- mediated proteolysis of cyclin and CDK" plays a crucial part in the cell- cycle regulation (Nakayama and Nakayama, 2006). The various cyclins have different life spawn and are degraded accordingly via ubiquitination, where a degrading cyclin covalently binds to ubiquitin complexes. The degradation of G1-phase cyclins is promoted by the "ubiquitin-conjugating enzyme" (Mitchison and Salmon, 2001). The Ubiquitination of Cyclin E is preceded by the autophosphorylation via its association with cdk2 on Thr380 residue, which is an example of an autoregulatory function (Won and Reed, 1996). Unlike cyclin E, the degradation of cyclin B involves the assembly of proteins, known as the "anaphase-promoting complex or APC." The APC is negatively regulated by the mitotic checkpoint protein MAD2 (Li et al., 1998). A protein, undergoing degradation, possess a nine amino acid long signature pattern, known as "destruction box", is recognized by the APC. Another ubiquitin ligase involved in cell cycle regulation is a multi-protein E3 ligase called "SCF complex or Skp, Cullin, F-box containing complex" (Wei et al., 2004). This class indirectly regulates the proteins by degrading the protein involved in the proteolysis of cyclins. For example, the ubiquitination of "cyclin-dependent kinase inhibitors, p21, and p27" regulates G1/S cyclins in cell cycle.

1.1.6. Apoptotic pathways in cancer

"Apoptosis is a tightly-regulated and well-executed physiological process of programmed cell death" in which the initial trigger is signaled by various of genetic insults (Fulda, 2009). The process of apoptosis is marked by cellular changes that include, "membrane-blebbing, nuclear fragmentation, and chromatin condensation" and that lead to the generation of apoptotic bodies and eventually cell death (Lowe and Lin, 2000). These apoptotic bodies are scavenged by phagocytic cells, thereby ruling out the chance of immunogenic responses. Cancer development is associated with evasion of apoptosis (Lowe and Lin, 2000). Depending upon the executing molecular players, the process of apoptosis can be the extrinsic or intrinsic. Individually, both apoptotic pathways can activate the caspases-dependent apoptosis as given in the diagram **(Fig. 1.2)**.

1.1.6.1. Extrinsic pathway of apoptosis

As discussed previously in this chapter, the extrinsic pathway starts by stimulation of death receptors belonging to TNF superfamily. Two receptors of this family, "Fas and TRAIL" initially get oligomerized upon binding with their respective ligands. These death receptors, on binding to TNF, further recruits other additional proteins like "Fas-associated death domain or FADD". (Siegmund et al., 2001; Houston and O'Connell, 2004). As discussed above, FAAD associates with the adapter caspases and form DISC. The activation of Bid, a member of pro-apoptotic Bcl-2 family, by caspase 8 locates itself on the outer membrane of mitochondria and facilitates its association with Bax/Bak proteins **(Fig. 1.2)**. The activation of Bax/Bak induces the apoptotic signaling cascade of the intrinsic pathway (Dlugosz et al., 2006; Edlich et al., 2011).

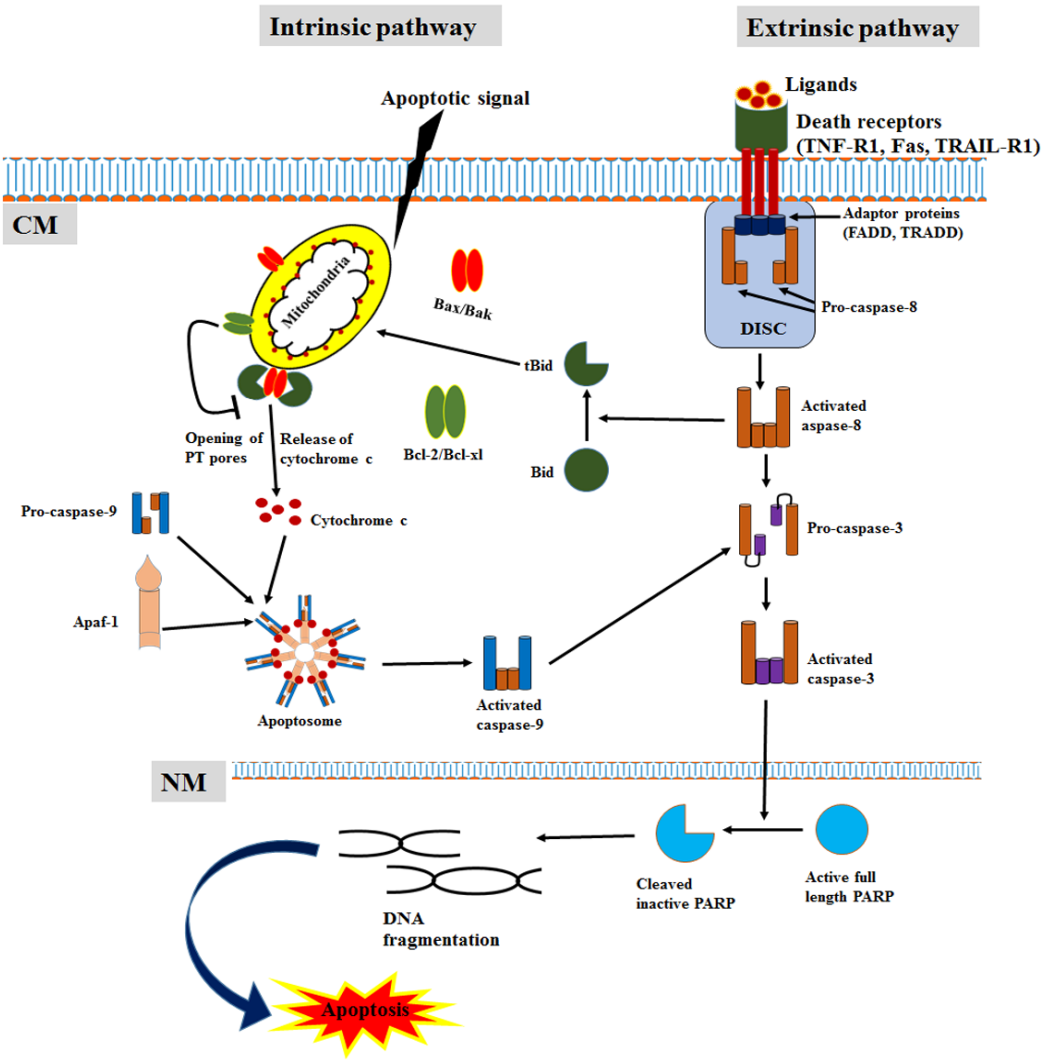

Fig. 1.2. Apoptotic pathways in mammalian cells.

Diagram shows the signalling course of extrinsic and intrinsic apoptotic pathways.

1.1.6.2. Intrinsic pathway of apoptosis

The intrinsic pathway of apoptosis, which involves the mitochondria-associated proteins, is is triggered by several factors like, "DNA damage, hypoxia and growth factor deprivation,". Upon receiving apoptotic signals, mitochondria induces the expression of pro and ant-apoptotic proteins which are characterized by the presence of "Bcl-2 homology domains or BH" (Indran et al., 2011). The anti-apoptotic members, "Bcl-2, Bcl-XL, Bcl-w, and Mcl-1" which lie in outer membrane, have four BH-domains (Kutuk and Letai, 2008). While, the pro-apoptotic family proteins, "Bax and Bak" are characterized by the presence of three BH domains and are linked in modulating the MOMP (Brenner and

Mak, 2009; Kutuk and Letai, 2008). Upon receiving apoptotic signals, the cytosolic Bax gets recruited along with Bak, on outer mitochondrial membrane and forms "hetero- and homo-oligomers" (Dewson and Kluck, 2009). These oligomers facilitate the channel opening and the release of cytochrome c and "AIF or apoptosis inducing factor" (Candé et al., 2004). The released cytochrome c merge with factors like "Apaf-1, ATP and pro-caspase 9" and further lead to the formation of wheel-like structure, "apoptosome" (Pop et al., 2006). In addition to that, the release of cytochrome c disrupts the mitochondrial membranes and results in the subsequent loss of "mitochondrial membrane potential or MMP" (Ly et al., 2003). MMP loss is also brought about by the opening of voltage-gated " mitochondrial permeability transition pore or MPTP" (Gogvadze et al., 2006). There have been reports where ROS is claimed as "one of the stimulants of MPTP opening" (Morin et al., 2009). All these events eventually lead to the sudden flow of solutes via MPTP and cause rupturing of OM and cell death (Elmore, 2007; Kroemer and Martin, 2005).

1.1.6.3. Mitochondrial cell death effectors

The activators of effector caspases can be grouped into two broad categories; caspase-dependent activators and caspase-independent activators. The previous one is further sub-divided as direct caspase activators and indirect caspase activators. The release of cytochrome c and the subsequent formation of apoptosome are implicated in the direct caspase activation (Pradelli et al., 2010). Apoptosis is negatively regulated by some proteins, called "inhibitor of apoptosis proteins or IAPs,". IAPs are also known as indirect caspase activators and the example of such inhibitory proteins are "Smac/DIABLO and Omi/HtrA2" (Indran et al., 2011; Brenner and Mak, 2009). The concluding step of caspase-dependent apoptosis is commonly regarded as the activation of effector caspases, but many reports are there showing that these effector caspases can act on other downstream substrates which include "poly (ADP-ribose) polymerase or PARP **(Fig. 1.2)** and some cytoskeletal proteins" (Reed, 2000).

Following the drop in MOMP, along with cytochrome c, the caspase-independent proteins are also released in the cytoplasm (Pradelli et al., 2010). These proteins induce cell death via another mechanism, called "caspase-independent programmed cell death or CICD" (Constantinou et al., 2009). One such protein and the valuable player of CICD is the mitochondrial endonuclease, "EndoG" (David et al., 2006; Pradelli et al., 2010). Another protein, "AIF," is cleaved and activated by the "calpain or cathepsin" proteases upon

MOMP (Boya and Kroemer, 2008; Boya et al., 2003). In metastatic cancers, AIF is reported to be down-regulated, which may contribute to chemotherapy resistance (Pommier et al., 2004). The PARP, "well-known DNA repair protein," can also induce programmed cell death, through the production of "poly-ADP-ribose or PAR," which further stimulates mitochondria to release AIF (Wang et al., 2011; Yu et al., 2006). In cancer cells, the active PARP is involved in repairing the single strand break and allows cancer cells to proliferate without any hindrance. This makes PARP a legitimate target for cancer therapy. Some PARP inhibitors (PARPi) have been synthesized and are running in clinical trials.

1.1.7. Cancer metabolism

In cancer cells, the metabolic phenotypes are different and complex from normal dividing cells (Cairns et al., 2011). The power source, mitochondria appears to be structurally and functionally different and is under high metabolic pressure (Fulda et al., 2010). Cancer cells, despite high availability of oxygen, rely heavily on the glycolysis to form ATP (DeBerardinis et al., 2008). This phenomenon is termed as "aerobic glycolysis" or the "Warburg effect" (Warburg, 1956). Also, cancer cells differ from their normal counterparts by having "increased gluconeogenesis, reduced pyruvate oxidation and increased lactic acid production" (Modica-Napolitano and Singh, 2002; Modica-Napolitano et al., 2007). These metabolic differences add to a cancer cell in malignancy (Modica-Napolitano and Singh, 2002; Fulda, 2009). These metabolic changes modulate the mitochondrial physiology in three ways. Firstly, "the hexokinase or HK" binds to the "voltage-dependent anionic channel or VDAC," a component of MPTP on the outer mitochondrial membrane in cancer cells (Mathupala et al., 2009). The conversion of glucose to glucose-6-phosphate is mediated by VDAC-bound HK, which can export residual ATP from mitochondria, and thereby supplying abundant energy for the glycolysis (Da-Silva et al., 2004; Mathupala et al., 2009).

A second key change in cancer cells is the preferential conversion of pyruvate to lactic acid by lactate dehydrogenase, "a rate limiting step in the glycolysis" and that leads to the acidification of the tumor microenvironment (Feron, 2009; Koukourakis et al., 2005). An acidic microenvironment promotes the invasive and metastatic potential of cancer cells (Estrella et al., 2013; Gatenby and Gawlinski, 2003). The third key change is the hyperpolarization of cancer cell mitochondria as a result of "high glycolytic ATP

production" (Hockenbery, 2010; Vyas et al., 2016). These conserved features of cancer cell mitochondria provide the opportunity to be targeted in cancer therapy.

1.1.8. Reactive Oxygen Species (ROS) in cancer

ROS are generated as "natural metabolic by-products of oxygen" and include "peroxides, superoxide, hydroxyl radical, and singlet oxygen" (Lobo et al., 2010; Pham-Huy et al., 2008). ROS is a combined term for "highly reactive species" such as "superoxide anion (O2•−), hydrogen peroxide (H2O2) and hydroxyl radical (OH•)" (Liou and Storz, 2010). To maintain the homeostasis, deleterious effects of these species are taken care by antioxidant defense machinery comprising "catalase or CAT," "superoxide dismutase or SOD," and "glutathione or GSH" (Fulda et al., 2010). Mitochondria are the primary source of ROS species which can induce mitochondrial permeabilization and subsequent activation of the intrinsic pathway of apoptosis (Webster, 2012). The "mitochondrial DNA or mtDNA," encodes 13 essential subunits of "mitochondrial respiratory chain or MRC" which have been reported to be damaged by the high level of ROS (Paradies et al., 2002). Cancer cells are always under high level of oxidative stress and have devised the mechanism to cope up with the elevated ROS level. The high level of ROS in cancer cells are regulated to an extent, and a further increase in their levels can render the cells to apoptosis and cell death (Khan et al., 2012; Wang and Yi, 2008). On its apoptosis-inducing capacity, molecules that promote ROS production may be exploited as novel therapeutics agent by elevating ROS levels beyond a tolerable threshold to induce PCD (Chen et al., 2008; Pelicano et al., 2004).

1.1.9. MAPK pathways in cancer

"The extracellular signals" transport information from outside to the inside of a cell. To the inside of the cell, these information are delivered to a complex machinery which transform them into various physiological functions viz. "growth, proliferation, migration, PCD, chromatin modulation etc."(Zhang et al., 2002). MAPKs or "Mitogen-Activated Protein Kinase" are the family of three different and sequential kinases namely "MAPKKK, MAPKK, and MAPK" that carry out the transfer of extracellular signals to the intracellular processing unit. In a mammalian cell, six types of MAPKs have been reported which are "ERK1/2, ERK/34, ERK5, ERK7/8, JNK1/2/3 and p38 α/β/γ/□ "(Krens et al., 2006; Roux and Blenis, 2004). The JNK and p38 family are also called "stress-activated MAPKs."

Some reports have shown that a single mutation at any level of the pathway can lead to the cell cycle deregulation and development of cancer. Followings are the brief description about the functional implication of MAPKs at their various level in carcinogenesis.

1.1.9.1. ERK pathway

This pathway is triggered by binding of the growth-promoting molecules to the Trk receptors. The activated Trks further phosphorylate downstream kinases, "Ras, Raf, MEKs and ERKs" in a sequential manner. Cancer-associated mutations can occur at any level of this kinase cascade, however, "Ras and Raf" have been found the most sensitive one (Roberts and Der, 2007). Ras is a GTP-activated kinase which can not only activate its downstream kinase Raf but also recruit some scaffolding proteins like "SUR-8/SHOC-2 and KSR" (Dhawan et al., 2016; Galperin et al., 2012). The knock study of "KSR" has revealed its potential role in the carcinogenesis. Raf occurs in three forms, "B-Raf, Raf-1 and A-Raf", of which "B-Raf" has the highest kinase potential and mutation probability (Galabova-Kovacs et al., 2006). The various forms of Raf can also modulate each other and thereby enhance the phosphorylation of MKs, and that is more than their individual phosphorylating capacity. The Raf-activated MKs are positively phosphorylated at, "S218, S222, and S298" (Coles and Shaw, 2002), while phosphorylation at "S212" (Gopalbhai et al., 2003) inhibits MKs. The activated ERKs many cellular targets that include "Kinases, Phosphatases, Transcription factors and cytoskeletal proteins," which regulate "cell growth and proliferation" (Chambard et al., 2007). These complex cascades in ERK pathway are monitored by the protein which is expressed in the early event of signaling and includes "Fas, Jun, Myc." In addition to these proteins, ERK signaling can express the "CDK-inhibitors," which create a "negative feedback-loop mechanism" (Murphy et al., 2004).

1.1.9.2. SAPK pathway

These class of kinases is activated upon receiving the "stress signals." As, the cancer cells are always under constant stresses like "hypoxia, substrate detachment, inflammation, and metabolic deregulation", therefore these kinases respond to them as "antiproliferative" or "anti-apoptotic." The "JNK pathway" is majorly triggered by "cytokines, UV-damage, deprivation of growth factors" (Weston and Davis, 2007). The members of this family are encoded by three genes, "Jnk1, Jnk2, and Jnk3", and form 10 different isoforms by the "alternative splicing." JNKs, at upstream, are activated by "MEK4 & MEK7", which

themselves are activated by "different MAPKKKs." JNKs, at downstream, can bind and activate various factors, "AP1, ATF-2, NF-ATc1, STAT3, and p53" and modulate the "cell cycle machinery" (Ip and Davis, 1998).

Another class of SAPKs, p38MAPK, is said to be induced majorly by environment stimuli which are generated by some stress. Many studies on p38MAPK's potential role in promoting apoptosis have implicated several cell cycle factors such as "cyclins, cell-cycle checkpoints, p53" (Recchia et al., 2009; Reinhardt et al., 2007). Apart from that, p38 can even phosphorylate pro-apoptotic proteins and trigger apoptosis. The recent years have observed some unconventional functions of p38MAPK and that have put it on the hot table of prospective inventions (Thornton and Rincon, 2009). Some interesting studies have advocated p38 in the cell survival of many cancers. For example, it has been shown that p38 activation is indispensable for strengthening the apoptosis-inducing capability of well-known drugs, such as "etoposide, doxorubicin, cisplatin, Taxol, Vincristine" (Reinhardt et al., 2007). The "survival role of p38" has been attributed to its immediate substrate MK2, which gets phosphorylated in response to "DNA damages." The "small heat shock protein" Hsp27, has been reported in many cell survival promoting processes, such as "actin organization, chaperoning, ROS-inhibition, inhibition of apoptosis" (Arrigo et al., 2005). MK2 has been shown to phosphorylate Hsp27, and that may explain the p38 and Hsp27 nexus in the survival of cancer cells (Guay et al., 1997). The survival potential of p38, shown by many recent findings, has set the platform, where it can be targeted in cancer therapy.

1.1.10. Prostate Cancer therapeutics

The type of cancer therapy is dependent on the kind of cancer and the extent of advancement of cancer. The standard chemotherapy is adopted for treating the advanced stage cancer and sometimes used along with surgery. Chemotherapy has ended up with adverse effects and toxicity in patients (Extermann et al., 2012). For instance, the 5-fluorouracil (5-FU), "a pyrimidine analog and inhibitor of DNA synthesis," has been used in cancer therapeutics for many decades (Gamelin et al., 1996). Other drugs include "antimetabolites such as methotrexate, DNA alkylating agents such as cyclophosphamide (Emadi et al., 2009) or cisplatin, the antimitotics (Lobert and Correia, 1992; Huszar et al., 2009) such as paclitaxel and docetaxel, and topoisomerase inhibitors (Lock and Ross, 1987; Pommier, 2012) such as

etoposide and camptothecins". The above-stated targeting agents cause severe side effects. Hence they are now combined with other agents that reduce the systemic toxicity.

With the advancement of innovative approaches, dissecting the signaling cascades associated with cancer, "target-based therapy" is now being adopted in many cancer treatment. The first instance of targeted approach was witnessed as the use of imatinib for the treatment of chronic myeloid leukemia in the last decade (Deininger et al., 2005). Later on, some monoclonal antibodies were developed and approved clinically (Weiner et al., 2010). One of the widely used anticancer drug, tamoxifen, can induce apoptosis by inhibiting the mitochondrial respiratory chain (MRC) (Pandey et al., 2011). In recent scenario, the combinatorial approach is preferred in which two are more anticancer drugs are used to enhance the cancer cell-killing effect (Al-Lazikani et al., 2012). Despite much advancements, the major drawback using these drugs has been the development of resistance to the drugs and systemic toxicity (Ramos and Bentires-Alj, 2014; Holohan et al., 2013). To overcome the problem of toxicity and resistance to some extent, plants and microorganisms are thought to be the incredible sources. The various phytochemicals such as "alkaloids, flavonoids, and isothiocyanates," have been studied with potential medicinal properties (Nobili et al., 2009; Amin et al., 2009).

Some of the above mentioned cancer therapies have been the major breakthrough of the 20th century. In the early non-metastatic condition, the prostate cancer can be treated by the hormonal therapy or in combination with other therapy like surgery or radiation (Damber, 2005)**.** However, the early detection of prostate cancer is not possible and many cases, and there are the potential side effects conferred by the hormonal therapy i.e. "mode change, muscle shrinkage, and pain, osteoporosis, increased risk of diabetes, weight loss or gain, impotence and heart attack." In metastatic cells the localized prostate cancer cells are spread to other parts of the body and can no longer be cured by hormonal therapy, the pathological condition is called hormonal refractory prostate cancer. Many FDA-approved drugs are being used for the treatment of advanced forms of cancer either alone or in combination with one or more drugs (Fowler et al., 2010; Blagosklonny, 2004; Wu et al., 2015). Still, more drugs are running on clinical trial with an aim to impart better treatment and with minimized side effects.

1.1.11. Challenges and questions

Above mentioned therapies have many side-effects. Other therapeutic complications include intake, stability and maintenance of drugs and their defined use in targeting the tumor vasculature (Silberstein et al., 2013), hence we need to develop such anticancer agent which should bear the attributes of "the desired and tissue selective effects with novel structures or new mechanism(s) of action".

These factors will have to be kept in mind while designing the novel anticancer compounds. In the recent scenario, a multi-faceted approach is being embraced in which all interdisciplinary fields like chemistry, met-lab and wet-lab altogether characterize the pharmaceutical compounds. According to Dr.James Fuchs, ***"minuscule changes that may seem insignificant can have dramatic effects on these toxicity properties,"***

1.2. Research objectives

One of the main reasons for the systemic toxicity of the available drugs is the use of very high dose. Thus, there is a need for the development of potent anticancer agents having the desired tissue selective effects at minimal doses. "The introduction of sulphonamide group is a provocative tactic in drug designing for enhancing pharmacological potency and the ADME attributes of the chemical matter" (Dai et al., 2011). Sulphonamides have retained the interest of the researchers due to their significant and versatile biological activities (Supuran et al., 2003; Abbate et al., 2004; Drews, 2000). Sulfonamide and their derivatives are known for their anti-cancer properties; they act as "inhibitors of carbonic anhydrase or CA" (Guler et al., 2010; Supuran et al., 2001). "Benzenesulfonamide derivatives" have been reported as a well-known CA inhibitors, and may such compounds have been used in designing the inhibitors with different medicinal chemistry applications (Garg H.G., 1972; CALVERT W. WHITEHEAD, 1960). "Sulfonylhydrazide and their analogs" constitute a class of cancer chemotherapeutic agents (Brynes et al., 1978). Arylsulfonylhydrazones of 2- formylpyridine 1-oxide have been found as promising antineoplastic agents in some experimental murine tumor system (May and Sartorelli, 1978). Taking account of these facts, a series of compounds, known as PR-3 series, were screened for their anticancer properties on metastatic prostate cancer cell lines. These compounds were provided by Professor Amir Azam, Jamia Milia University, New Delhi. The biological characterization of these compounds were done under the following objectives:

1. To evaluate the effect of PR-3 series compounds in prostate cell lines by checking the viability of the cells and analysis of cell cycle.
2. To study expression level of different proteins and their cellular localization in prostate cancer cell lines after treating with PR-3 series compounds.
3. To elucidate the pathway(s) affected by the PR-3 series compounds.

1.3. References

Abate-Shen, C. (2000). 'Molecular genetics of prostate cancer'. *Genes & development*, 14(19): 2410–2434.

Abbas, T. and Dutta, A. (2009). 'P21 in Cancer: Intricate Networks and Multiple Activities'. *Nature Reviews Cancer*, 9(6): 400–414.

Abbate, F., Casini, A., Owa, T., Scozzafava, A. and Supuran, C.T. (2004). 'Carbonic anhydrase inhibitors: E7070, a sulfonamide anticancer agent, potently inhibits cytosolic isozymes I and II, and transmembrane, tumor-associated isozyme IX'. *Bioorganic and Medicinal Chemistry Letters*, 14(1): 217–223.

Adrián, F.J., Ding, Q., Sim, T., Velentza, A., Sloan, C., Liu, Y., Zhang, G., et al. (2006). 'Allosteric inhibitors of Bcr-abl–dependent cell proliferation'. *Nature Chemical Biology*, 2(2): 95–102.

Al-Lazikani, B., Banerji, U. and Workman, P. (2012). 'Combinatorial drug therapy for cancer in the post-genomic era'. *Nature Biotechnology*, 30(7): 679–692.

Amaral, J.D., Xavier, J.M., Steer, C.J. and Rodrigues, C.M. (2010). 'The role of p53 in apoptosis.' *Discovery medicine*, 9(45): 145–152.

Amin, A.R.M.R., Kucuk, O., Khuri, F.R. and Shin, D.M. (2009). 'Perspectives for cancer prevention with natural compounds'. *Journal of Clinical Oncology*, 27(16): 2712–2725.

Amundadottir, L.T., Sulem, P., Gudmundsson, J., Helgason, A., Baker, A., Agnarsson, B. a, Sigurdsson, A., et al. (2006). 'A common variant associated with prostate cancer in European and African populations.' *Nat Genet*, 38(6): 652–8.

Arrigo, A., Virot, S., Chaufour, S., Firdaus, W., Kretz-Remy, C. and Diaz-Latoud, C. (2005). 'Hsp27 consolidates intracellular redox homeostasis by upholding glutathione in its reduced form and by decreasing iron intracellular levels.' *Antioxidants & redox signaling*, 7(3–4): 414–22.

Ayala, A.G. and Ro, J.Y. (2007). 'Prostatic intraepithelial neoplasia: recent advances.' *Archives of pathology & laboratory medicine*, 131(8): 1257–1266.

Barqawi, A.B., Golden, B.K., O'Donnell, C., Brawer, M.K. and Crawford, E.D. (2005). 'Observed effect of age and body mass index on total and complexed PSA: Analysis from a national screening program'. *Urology*, 65(4): 708–712.

Bashir, T., Horlein, R., Rommelaere, J. and Willwand, K. (2000). 'Cyclin A activates the DNA polymerase delta -dependent elongation machinery in vitro: A parvovirus DNA replication model.' *Proceedings of the National Academy of Sciences of the United States of America*, 97: 5522–5527.

Bensaad, K., Tsuruta, A., Selak, M.A., Vidal, M.N.C., Nakano, K., Bartrons, R., Gottlieb, E., et al. (2006). 'TIGAR, a p53-Inducible Regulator of Glycolysis and Apoptosis'. *Cell*, 126(1): 107–120.

Blagosklonny, M. V. (2004). 'Analysis of FDA approved anticancer drugs reveals the future of cancer therapy'. *Cell Cycle*, 3(8): 1035–1042.

Blagosklonny, M. V. and Pardee, A.B. (2002). 'The restriction point of the cell cycle.' *Cell cycle (Georgetown, Tex.)*, 1(2): 103–110.

Boutayeb, A. (2006). 'The double burden of communicable and non-communicable diseases in developing countries'. *Transactions of the Royal Society of Tropical Medicine and Hygiene*, 100(3): 191–199.

Boya, P., Andreau, K., Poncet, D., Zamzami, N., Perfettini, J.-L., Metivier, D., Ojcius, D.M., et al. (2003). 'Lysosomal membrane permeabilization induces cell death in a mitochondrion-dependent fashion.' *The Journal of experimental medicine*, 197(10): 1323–34.

Boya, P. and Kroemer, G. (2008). 'Lysosomal membrane permeabilization in cell death.' *Oncogene*, 27(50): 6434–6451.

Brawer, M.K. (2005). 'Prostatic intraepithelial neoplasia: an overview.' *Reviews in urology*, 7: 11–18.

Brenner, D. and Mak, T.W. (2009). 'Mitochondrial cell death effectors'. *Current Opinion in Cell Biology*, 21(6): 871–877.

Brynes, S., Burckart, G.J. and Mokotoff, M. (1978). 'Potential inhibitors of L-asparagine biosynthesis. 4. Substituted sulfonamide and sulfonylhydrazide

analogues of L-asparagine.' *Journal of medicinal chemistry*, 21(1): 45–49.

Cairns, R., Harris, I. and Mak, T. (2011). 'Regulation of cancer cell metabolism'. *Nature Reviews Cancer*, 11(2): 85–95.

Calle, E.E., Rodriguez, C., Walker-Thurmond, K. and Thun, M.J. (2003). 'Overweight, obesity, and mortality from cancer in a prospectively studied cohort of U.S. adults'. *N Engl J Med*, 348(17): 1625–1638.

CALVERT W. WHITEHEAD, J.J.T. (1960). 'The Reaction of Saccharin with Amines. N-Substituted-3-Amino-1,2-benzisothiazole-1,1-dioxides'. *J. Org. Chem*, 25(3): 413–416.

Candé, C., Vahsen, N., Garrido, C. and Kroemer, G. (2004). 'Apoptosis-inducing factor (AIF): caspase-independent after all.' *Cell death and differentiation*, 11: 591–595.

Cashio, P., Lee, T. V and Bergmann, A. (2005). 'Genetic control of programmed cell death in Drosophila melanogaster.' *Seminars in cell & developmental biology*, 16(2): 225–35.

Cavanagh, H. and Rogers, K.M.A. (2015). 'The role of BRCA1 and BRCA2 mutations in prostate, pancreatic and stomach cancers'. *Hereditary Cancer in Clinical Practice*, 13(1): 16.

Cayrol, C., Knibiehler, M. and Ducommun, B. (1998). 'p21 binding to PCNA causes G1 and G2 cell cycle arrest in p53-deficient cells'. *Oncogene*, 16(3): 311–320.

Chambard, J.C., Lefloch, R., Pouysségur, J. and Lenormand, P. (2007). 'ERK implication in cell cycle regulation'. *Biochimica et Biophysica Acta - Molecular Cell Research*, 1773(8): 1299–1310.

Chen, J., De, S., Brainard, J. and Byzova, T. V. (2004). 'Metastatic properties of prostate cancer cells are controlled by VEGF'. *Cell Commun Adhes*, 11(1): 1–11.

Chen, Y., McMillan-Ward, E., Kong, J., Israels, S.J. and Gibson, S.B. (2008). 'Oxidative stress induces autophagic cell death independent of apoptosis in transformed and cancer cells.' *Cell death and differentiation*, 15(1): 171–182.

Chial, B.H., Write, P.D., Right, S. and Education, N. (2008). 'Proto-oncogenes to Oncogenes to Cancer'. *Nature Education*, 1: 1–5.

Coles, L.C. and Shaw, P.E. (2002). 'PAK1 primes MEK1 for phosphorylation by Raf-1 kinase during cross-cascade activation of the ERK pathway.' *Oncogene*, 21(14): 2236–44.

Connolly, D., Black, a, Murray, L.J., Nambirajan, T., Keane, P.F. and Gavin, a. (2009). 'Repeating an abnormal prostate-specific antigen (PSA) level: how relevant is a decrease in PSA?' *Prostate cancer and prostatic diseases*, 12(1): 47–51.

Constantinou, C., Papas, K. and Constantinou, A. (2009). 'Caspase-Independent Pathways of Programmed Cell Death: The Unraveling of New Targets of Cancer Therapy?' *Current Cancer Drug Targets*, 9(6): 717–728.

Da-Silva, W.S., Gómez-Puyou, A., De Gómez-Puyou, M.T., Moreno-Sanchez, R., De Felice, F.G., De Meis, L., Oliveira, M.F., et al. (2004). 'Mitochondrial bound hexokinase activity as a preventive antioxidant defense. Steady-state ADP formation as a regulatory mechanism of membrane potential and reactive oxygen species generation in mitochondria'. *Journal of Biological Chemistry*, 279(38): 39846–39855.

Dai, H.X., Stepan, A.F., Plummer, M.S., Zhang, Y.H. and Yu, J.Q. (2011). 'Divergent C-H functionalizations directed by sulfonamide pharmacophores: Late-stage diversification as a tool for drug discovery'. *Journal of the American Chemical Society*, 133(18): 7222–7228.

Damber, J.-E. (2005). 'Endocrine therapy for prostate cancer.' *Acta oncologica (Stockholm, Sweden)*, 44(6): 605–609.

David, K.K., Sasaki, M., Yu, S.-W., Dawson, T.M. and Dawson, V.L. (2006). 'EndoG is dispensable in embryogenesis and apoptosis.' *Cell death and differentiation*, 13(7): 1147–1155.

DeBerardinis, R.J., Lum, J.J., Hatzivassiliou, G. and Thompson, C.B. (2008). 'The Biology of Cancer: Metabolic Reprogramming Fuels Cell Growth and Proliferation'. *Cell Metabolism*, 7(1): 11–20.

Deininger, M., Buchdunger, E. and Druker, B.J. (2005). 'The development of imatinib as a therapeutic agent for chronic myeloid leukemia'. *Blood*, 105(7): 2640–2653.

Dewson, G. and Kluck, R.M. (2009). 'Mechanisms by which Bak and Bax permeabilise mitochondria during apoptosis.' *Journal of cell science*, 122(Pt 16): 2801–2808.

Dhawan, N.S., Scopton, A.P. and Dar, A.C. (2016). 'Small molecule stabilization of the KSR inactive state antagonizes oncogenic Ras signalling'. *Nature*, 537(7618): 112–116.

Djulbegovic, M., Beyth, R.J., Neuberger, M.M., Stoffs, T.L., Vieweg, J., Djulbegovic, B. and Dahm, P. (2010). 'Screening for prostate cancer: systematic review and meta-analysis of randomised controlled trials.' *BMJ (Clinical research ed.)*, 341(3): c4543.

Dlugosz, P.J., Billen, L.P., Annis, M.G., Zhu, W., Zhang, Z., Lin, J., Leber, B., et al. (2006). 'Bcl-2 changes conformation to inhibit Bax oligomerization.' *The EMBO journal*, 25(11): 2287–2296.

Dong, J.T., Lamb, P.W., Rinker-Schaeffer, C.W., Vukanovic, J., Ichikawa, T., Isaacs, J.T. and Barrett, J.C. (1995). 'KAI1, a metastasis suppressor gene for prostate cancer on human chromosome 11p11.2.' *Science (New York, N.Y.)*, 268(5212): 884–886.

Downing, S.R., Russell, P.J. and Jackson, P. (2003). 'Alterations of p53 are common in early stage prostate cancer.' *The Canadian journal of urology*, 10(4): 1924–1933.

Drews, J. (2000). 'Drug Discovery: A Historical Perspective'. *Science*, 287(5460): 1960–1964.

Drobnjak, M., Osman, I., Scher, H.I., Fazzari, M. and Cordon-Cardo, C. (2000). 'Overexpression of cyclin D1 is associated with metastatic prostate cancer to bone'. *Clin Cancer Res*, 6(5): 1891–1895.

Edlich, F., Banerjee, S., Suzuki, M., Cleland, M.M., Arnoult, D., Wang, C.,

Neutzner, A., et al. (2011). 'Bcl-xL retrotranslocates Bax from the mitochondria into the cytosol'. *Cell*, 145(1): 104–116.

Elmore, S. (2007). 'Apoptosis: a review of programmed cell death.' *Toxicologic pathology*, 35(4): 495–516.

Emadi, A., Jones, R.J. and Brodsky, R. a. (2009). 'Cyclophosphamide and cancer: golden anniversary.' *Nature reviews. Clinical oncology*, 6(11): 638–647.

Estrella, V., Chen, T., Lloyd, M., Wojtkowiak, J., Cornnell, H.H., Ibrahim-Hashim, A., Bailey, K., et al. (2013). 'Acidity generated by the tumor microenvironment drives local invasion'. *Cancer Research*, 73(5): 1524–1535.

Extermann, M., Boler, I., Reich, R.R., Lyman, G.H., Brown, R.H., Defelice, J., Levine, R.M., et al. (2012). 'Predicting the risk of chemotherapy toxicity in older patients: The chemotherapy risk assessment scale for high-age patients (CRASH) score'. *Cancer*, 118(13): 3377–3386.

Feldman, B.J. and Feldman, D. (2001). 'The development of androgen-independent prostate cancer.' *Nature reviews. Cancer*, 1(1): 34–45.

Ferlay, J., Soerjomataram, I., Dikshit, R., Eser, S., Mathers, C., Rebelo, M., Parkin, D.M., et al. (2015). 'Cancer incidence and mortality worldwide: Sources, methods and major patterns in GLOBOCAN 2012'. *International Journal of Cancer*, 136(5): E359–E386.

Feron, O. (2009). 'Pyruvate into lactate and back: From the Warburg effect to symbiotic energy fuel exchange in cancer cells'. *Radiotherapy and Oncology*, 92(3): 329–333.

Foster, D.A., Yellen, P., Xu, L. and Saqcena, M. (2010). 'Regulation of G1 Cell Cycle Progression: Distinguishing the Restriction Point from a Nutrient-Sensing Cell Growth Checkpoint(s).' *Genes & cancer*, 1(11): 1124–31.

Fowler, J.F., Chappell, R.J. and Ritter, M.A. (2010). 'New treatments for metastic prostate cancer.' *The Medical letter on drugs and therapeutics*, 52(1346): 69–70.

Fulda, S. (2009). 'Tumor resistance to apoptosis'. *International Journal of Cancer*,

124(3): 511–515.

Fulda, S., Galluzzi, L. and Kroemer, G. (2010). 'Targeting mitochondria for'. *Nature Publishing Group*, 9(6): 447–464.

Galabova-Kovacs, G., Kolbus, A., Matzen, D., Meissl, K., Piazzolla, D., Rubiolo, C., Steinitz, K., et al. (2006). 'ERK and beyond: Insights from B-Raf and Raf-1 conditional knockouts'. *Cell Cycle*, 5(14): 1514–1518.

Galperin, E., Abdelmoti, L. and Sorkin, A. (2012). 'Shoc2 is targeted to late endosomes and required for Erk1/2 activation in EGF-stimulated cells'. *PLoS ONE*, 7(5).

Gamelin, E.C., Danquechin-Dorval, E.M., Dumesnil, Y.F., Maillart, P.J., Goudier, M.J., Burtin, P.C., Delva, R.G., et al. (1996). 'Relationship between 5-fluorouracil (5-FU) dose intensity and therapeutic response in patients with advanced colorectal cancer receiving infusional therapy containing 5-FU'. *Cancer*, 77(3): 441–451.

Gann, P.H. (2002). 'Risk factors for prostate cancer.' *Reviews in urology*, 4 Suppl 5(Suppl 5): S3–S10.

Garg H.G., A. V. (1972). 'Chemistry and biological activity of N-acyl-4-arylazopyrazoles'. *J. Pharm. Sci.*, 61: 130–132.

Garland, C.F., Garland, F.C., Gorham, E.D., Lipkin, M., Newmark, H., Mohr, S.B. and Holick, M.F. (2006). 'The role of vitamin D in cancer prevention'. *American Journal of Public Health*, 96(2): 252–261.

Gatenby, R.A. and Gawlinski, E.T. (2003). 'The glycolytic phenotype in carcinogenesis and tumor invasion: Insights through mathematical models'. *Cancer Research*, 63(14): 3847–3854.

Gavet, O. and Pines, J. (2010). 'Progressive Activation of CyclinB1-Cdk1 Coordinates Entry to Mitosis'. *Developmental Cell*, 18(4): 533–543.

Gogvadze, V., Orrenius, S. and Zhivotovsky, B. (2006). 'Multiple pathways of cytochrome c release from mitochondria in apoptosis'. *Biochimica et Biophysica Acta - Bioenergetics*, 1757(5–6): 639–647.

Goldfarb, D.A., Stein, B.S., Shamszadeh, M. and Petersen, R.O. (1986). 'Age-related changes in tissue levels of prostatic acid phosphatase and prostate specific antigen.' *The Journal of urology*, 136(6): 1266–9.

Goldstein, A.S., Huang, J., Guo, C., Garraway, I.P. and Witte, O.N. (2010). 'Identification of a cell of origin for human prostate cancer.' *Science (New York, N.Y.)*, 329(5991): 568–71.

Gopalbhai, K., Jansen, G., Beauregard, G., Whiteway, M., Dumas, F., Wu, C. and Meloche, S. (2003). 'Negative regulation of MAPKK by phosphorylation of a conserved serine residue equivalent to Ser212 of MEK1'. *Journal of Biological Chemistry*, 278(10): 8118–8125.

Green, D.R. and Chipuk, J.E. (2006). 'p53 and Metabolism: Inside the TIGAR'. *Cell*, 126(1): 30–32.

Griffith, T.S., Brunner, T., Fletcher, S.M., Green, D.R. and Ferguson, T.A. (1995). 'Fas ligand-induced apoptosis as a mechanism of immune privilege.' *Science (New York, N.Y.)*, 270(5239): 1189–1192.

Guay, J., Lambert, H., Gingras-Breton, G., Lavoie, J.N., Huot, J. and Landry, J. (1997). 'Regulation of actin filament dynamics by p38 map kinase-mediated phosphorylation of heat shock protein 27.' *Journal of cell science*, 110 (Pt 3: 357–68.

Gudmundsson, J., Sulem, P., Gudbjartsson, D.F., Masson, G., Agnarsson, B.A., Benediktsdottir, K.R., Sigurdsson, A., et al. (2012). 'A study based on whole-genome sequencing yields a rare variant at 8q24 associated with prostate cancer'. *Nature Genetics*, 44(12): 1326–1329.

Guler, O.O., De Simone, G. and Supuran, C.T. (2010). 'Drug design studies of the novel antitumor targets carbonic anhydrase IX and XII.' *Current medicinal chemistry*, 17: 1516–1526.

Hanahan, D. and Weinberg, R.A. (2000). 'The hallmarks of cancer'. *Cell*, 100: 57–70.

Hariharan, K. and Padmanabha, V. (2016). 'Demography and disease characteristics

of prostate cancer in India'. *Indian Journal of Urology*, 32(2): 103.

He, Y., Franco, O.E., Jiang, M., Williams, K., Love, H.D., Coleman, I.M., Nelson, P.S., et al. (2007). 'Tissue-specific consequences of cyclin D1 overexpression in prostate cancer progression'. *Cancer Research*, 67(17): 8188–8197.

Heinlein, C.A. and Chang, C. (2004). 'Androgen receptor in prostate cancer'. *Endocrine Reviews*, 25(2): 276–308.

Hejmadi, M. (2010). *Introduction to Cancer Biology*

van den Heuvel, S. and Dyson, N.J. (2008). 'Conserved functions of the pRB and E2F families.' *Nature reviews. Molecular cell biology*, 9(9): 713–24.

Hockenbery, D.M. (2010). 'Targeting mitochondria for cancer therapy'. *Environmental and Molecular Mutagenesis*, 51(5): 476–489.

Holohan, C., Van Schaeybroeck, S., Longley, D.B. and Johnston, P.G. (2013). 'Cancer drug resistance: an evolving paradigm'. *Nature Reviews Cancer*, 13(10): 714–726.

Holzapfel, N.P., Holzapfel, B.M., Champ, S., Feldthusen, J., Clements, J. and Hutmacher, D.W. (2013). 'The potential role of lycopene for the prevention and therapy of prostate cancer: From molecular mechanisms to clinical evidence'. *International Journal of Molecular Sciences*, 14(7): 14620–14646.

Horton, L.E. and Templeton, D.J. (1997). 'The cyclin box and C-terminus of cyclins A and E specify CDK activation and substrate specificity.' *Oncogene*, 14(4): 491–498.

Houston, A. and O'Connell, J. (2004). 'The Fas signalling pathway and its role in the pathogenesis of cancer'. *Current Opinion in Pharmacology*, 4(4): 321–326.

Hu, Q., Wu, D., Chen, W., Yan, Z., Yan, C., He, T., Liang, Q., et al. (2014). 'Molecular determinants of caspase-9 activation by the Apaf-1 apoptosome.' *Proceedings of the National Academy of Sciences of the United States of America*, 111(46): 16254–61.

Humphrey, T. and Pearce, A. (2010). 'Cell Cycle'. *Cell Cycle*, 9(11): 2063–2064.

Huszar, D., Theoclitou, M.-E., Skolnik, J. and Herbst, R. (2009). 'Kinesin motor proteins as targets for cancer therapy.' *Cancer metastasis reviews*, 28: 197–208.

Hwang, H.C. and Clurman, B.E. (2005). 'Cyclin E in normal and neoplastic cell cycles.' *Oncogene*, 24(17): 2776–2786.

Iarc., I.A. for R. on C.W.H.O. (2012). 'GLOBOCAN 2012: Estimated Cancer Incidence, Mortality and Prevalence Worldwide in 2012.' *Globocan*: 1–6.

Indran, I.R., Tufo, G., Pervaiz, S. and Brenner, C. (2011). 'Recent advances in apoptosis, mitochondria and drug resistance in cancer cells'. *Biochimica et Biophysica Acta (BBA) - Bioenergetics*, 1807(6): 735–745.

Ip, Y.T. and Davis, R.J. (1998). 'Signal transduction by the c-Jun N-terminal kinase (JNK)--from inflammation to development.' *Current opinion in cell biology*, 10(2): 205–219.

Johnson, D.G. and Walker, C.L. (1999). 'Cyclins and cell cycle checkpoints.' *Annual review of pharmacology and toxicology*, 39: 295–312.

Kaldis, P. (1999). 'The cdk-activating kinase (CAK): From yeast to mammals'. *Cellular and Molecular Life Sciences*, 55(2): 284–296.

Kaplan, A.L., Hu, J.C., Morgentaler, A., Mulhall, J.P., Schulman, C.C. and Montorsi, F. (2015). 'Testosterone Therapy in Men With Prostate Cancer'. *European Urology*, 69(5): 894–903.

Karayi, M.K. and Markham, a F. (2004). 'Molecular biology of prostate cancer.' *Prostate Cancer and Prostatic Diseases*, 7(1): 6–20.

Khan, M.I., Mohammad, A., Patil, G., Naqvi, S.A.H., Chauhan, L.K.S. and Ahmad, I. (2012). 'Induction of ROS, mitochondrial damage and autophagy in lung epithelial cancer cells by iron oxide nanoparticles'. *Biomaterials*, 33(5): 1477–1488.

Khleif, S.N., DeGregori, J., Yee, C.L., Otterson, G.A., Kaye, F.J., Nevins, J.R. and Howley, P.M. (1996). 'Inhibition of cyclin D-CDK4/CDK6 activity is associated with an E2F-mediated induction of cyclin kinase inhibitor activity.' *Proceedings of the National Academy of Sciences of the United States of*

America, 93(9): 4350–4.

Koh, C.J. and Atala, A. (2006). 'Recent advances in the field of urology'. *Current Urology Reports*, 7(1): 43–49.

Koukourakis, M.I., Giatromanolaki, A., Sivridis, E., Gatter, K.C. and Harris, A.L. (2005). 'Pyruvate dehydrogenase and pyruvate dehydrogenase kinase expression in non small cell lung cancer and tumor-associated stroma.' *Neoplasia (New York, N.Y.)*, 7(1): 1–6.

Krens, S.F.G., Spaink, H.P. and Snaar-Jagalska, B.E. (2006). 'Functions of the MAPK family in vertebrate-development'. *FEBS Letters*, 580(21): 4984–4990.

Kroemer, G. and Martin, S.J. (2005). 'Caspase-independent cell death.' *Nature medicine*, 11(7): 725–730.

Kubbutat, M.H., Jones, S.N. and Vousden, K.H. (1997). 'Regulation of p53 stability by Mdm2.' *Nature*, 387(June 1997): 299–303.

Kutuk, O. and Letai, A. (2008). 'Regulation of Bcl-2 family proteins by posttranslational modifications.' *Current molecular medicine*, 8(2): 102–118.

Lahtz, C. and Pfeifer, G.P. (2011). 'Epigenetic changes of DNA repair genes in cancer'. *Journal of Molecular Cell Biology*, 3(1): 51–58.

Li, F., Ambrosini, G., Chu, E.Y., Plescia, J., Tognin, S., Marchisio, P.C. and Altieri, D.C. (1998). 'Control of apoptosis and mitotic spindle checkpoint by survivin.' *Nature*, 396(6711): 580–584.

Lilja, H., Ulmert, D. and Vickers, A.J. (2008). 'Prostate-specific antigen and prostate cancer: prediction, detection and monitoring.' *Nature reviews. Cancer*, 8(4): 268–78.

Lim, J., Bhoo-Pathy, N., Sothilingam, S., Malek, R., Sundram, M., Bahadzor, B.H., Ong, T.A., et al. (2014). 'Ethnicity is an independent determinant of age-specific PSA level: Findings from a multiethnic Asian setting'. *PLoS ONE*, 9(8).

Lim, S. and Kaldis, P. (2013). 'Cdks, cyclins and CKIs: roles beyond cell cycle

regulation.' *Development*, 140(15): 3079–93.

Liou, G.-Y. and Storz, P. (2010). 'Reactive oxygen species in cancer.' *Free radical research*, 44(5): 479–96.

Lobert, S. and Correia, J.J. (1992). 'Antimitotics in cancer chemotherapy'. *Cancer Nurs*, 15(1): 22–33.

Lobo, V., Patil, A., Phatak, A. and Chandra, N. (2010). 'Free radicals, antioxidants and functional foods: Impact on human health.' *Pharmacognosy reviews*, 4(8): 118–26.

Lock, R.B. and Ross, W.E. (1987). 'DNA topoisomerases in cancer therapy.' *Anti-cancer drug design*, 2(2): 151–64.

Lowe, S.W. and Lin, a W. (2000). 'Apoptosis in cancer.' *Carcinogenesis*, 21(3): 485–495.

Ly, J.D., Grubb, D.R. and Lawen, A. (2003). 'The mitochondrial membrane potential (δψm) in apoptosis; an update'. *Apoptosis*, 8(2): 115–128.

Mathupala, S.P., Ko, Y.H. and Pedersen, P.L. (2009). 'Hexokinase-2 bound to mitochondria'. *Seminars in Cancer Biology*, 19(1): 17–24.

May, J.A. and Sartorelli, A.C. (1978). 'Antineoplastic properties of arylsulfonylhdrazones of 3-formylpyridazine 2-oxide and 4-formylpyrimidine 3-oxide'. *Journal of medicinal chemistry*, 21(12): 1333—1335.

McDowell, M., Occhipinti, S. and Chambers, S. (2013). 'The Influence of Family History on Cognitive Heuristics, Risk Perceptions, and Prostate Cancer Screening Behavior.' *Health Psychol*, 32(11): 1158–1169.

McIlwain, D.R., Berger, T. and Mak, T.W. (2013). 'Caspase functions in cell death and disease.' *Cold Spring Harbor perspectives in biology*, 5(4).

Merrimen, J.L., Jones, G., Walker, D., Leung, C.S., Kapusta, L.R. and Srigley, J.R. (2009). 'Multifocal high grade prostatic intraepithelial neoplasia is a significant risk factor for prostatic adenocarcinoma.' *The Journal of urology*, 182(2): 485–90; discussion 490.

Mihara, M., Erster, S., Zaika, A., Petrenko, O., Chittenden, T., Pancoska, P. and Moll, U.M. (2003). 'p53 has a direct apoptogenic role at the mitochondria'. *Molecular Cell*, 11(3): 577–590.

Misevičien, L., Anusevičius, Ž., Šarlauskas, J., Sevrioukova, I.F. and Čnas, N. (2011). 'Redox reactions of the FAD-containing apoptosis-inducing factor (AIF) with quinoidal xenobiotics: A mechanistic study'. *Archives of Biochemistry and Biophysics*, 512(2): 183–189.

Mitchison, T.J. and Salmon, E.D. (2001). 'Mitosis: a history of division.' *Nature cell biology*, 3(1): E17-21.

Modica-Napolitano, J.S., Kulawiec, M. and Singh, K.K. (2007). 'Mitochondria and human cancer.' *Current molecular medicine*, 7: 121–131.

Modica-Napolitano, J.S. and Singh, K.K. (2002). 'Mitochondria as targets for detection and treatment of cancer.' *Expert reviews in molecular medicine*, 4(9): 1–19.

Moll, U.M. (2005). 'P53 has a direct pro-apoptotic action at the mitochondria'. In *25 Years of p53 Research*. pp. 165–181.

Morgan, D.O. (1997). 'CYCLIN-DEPENDENT KINASES: Engines, Clocks, and Microprocessors'. *Annual Review of Cell and Developmental Biology*, 13(1): 261–291.

Morgan, D.O. (1995). 'Principles of CDK regulation.' *Nature*, 374(6518): 131–134.

Morin, D., Assaly, R., Paradis, S. and Berdeaux, A. (2009). 'Inhibition of mitochondrial membrane permeability as a putative pharmacological target for cardioprotection.' *Current medicinal chemistry*, 16(33): 4382–4398.

Murphy, L.O., MacKeigan, J.P. and Blenis, J. (2004). 'A network of immediate early gene products propagates subtle differences in mitogen-activated protein kinase signal amplitude and duration.' *Molecular and cellular biology*, 24(1): 144–53.

Nakayama, K.I. and Nakayama, K. (1998). 'Cip/Kip cyclin-dependent kinase inhibitors: Brakes of the cell cycle engine during development'. *BioEssays*, 20(12): 1020–1029.

Nakayama, K.I. and Nakayama, K. (2006). 'Ubiquitin ligases: cell-cycle control and cancer.' *Nature reviews. Cancer*, 6(5): 369–81.

Narayan, S., Smith, D.C. and Sandler, H.M. (2003). 'Chemotherapy for localized, high-risk prostate cancer'. *Seminars in Radiation Oncology*, 13(2): 152–157.

Nelson, W.G., De Marzo, A.M. and Isaacs, W.B. (2003). 'Prostate cancer.' *The New England journal of medicine*, 349(4): 366–81.

Nicholson, D.W. and Thornberry, N.A. (1997). 'Caspases: Killer proteases'. *Trends in Biochemical Sciences*, 22(8): 299–306.

Nobili, S., Lippi, D., Witort, E., Donnini, M., Bausi, L., Mini, E. and Capaccioli, S. (2009). 'Natural compounds for cancer treatment and prevention'. *Pharmacological Research*, 59(6): 365–378.

Nuñez, G., Benedict, M. a, Hu, Y. and Inohara, N. (1998). 'Caspases: the proteases of the apoptotic pathway.' *Oncogene*, 17(25): 3237–3245.

O'Malley, R.L. and Taneja, S.S. (2006). 'Obesity and prostate cancer.' *The Canadian journal of urology.*, 13 Suppl 2: 11–17.

Olivier, M., Hollstein, M. and Hainaut, P. (2010). 'TP53 mutations in human cancers: origins, consequences, and clinical use.' *Cold Spring Harbor perspectives in biology*, 2(1).

Optenberg, S.A., Thompson, I.M., Friedrichs, P., Wojcik, B., Stein, C.R. and Kramer, B. (2013). 'Race, treatment, and long-term survival from prostate cancer in an equal-access medical care delivery system.' *JAMA : the journal of the American Medical Association*, 274(20): 1599–605.

Pandey, S., Chatterjee, S.J., Ovadje, P., Mousa, M. and Hamm, C. (2011). 'The efficacy of dandelion root extract in inducing apoptosis in drug-resistant human melanoma cells'. *Evidence-based Complementary and Alternative Medicine*, 2011.

Paradies, G., Petrosillo, G., Pistolese, M. and Ruggiero, F.M. (2002). 'Reactive oxygen species affect mitochondrial electron transport complex I activity through oxidative cardiolipin damage'. In *Gene*. pp. 135–141.

Parekh, N., Lin, Y., Craft, L.L., Vadiveloo, M. and Lu-Yao, G.L. (2012). 'Longitudinal associations of leisure-time physical activity and cancer mortality in the Third National Health and Nutrition Examination Survey (1986-2006)'. *Journal of Obesity*, 2012.

Parry, D., Bates, S., Mann, D.J. and Peters, G. (1995). 'Lack of cyclin D-Cdk complexes in Rb-negative cells correlates with high levels of p16INK4/MTS1 tumour suppressor gene product.' *The EMBO journal*, 14(3): 503–11.

Patel, A.R. and Klein, E.A. (2009). 'Risk factors for prostate cancer'. *Nat Clin Pract Urol*, 6(2): 87–95.

Pelicano, H., Carney, D. and Huang, P. (2004). 'ROS stress in cancer cells and therapeutic implications'. *Drug Resistance Updates*, 7(2): 97–110.

Pérez-Caro, M. and Sánchez-García, I. (2007). 'BCR-ABL and Human Cancer'. In *Apoptosis, Cell Signaling, and Human Diseases*. pp. 3–33.

Pérez-tenorio, G., Berglund, F., Merca, A.E., Nordenskjöld, B.O., Rutqvist, L.E., Skoog, L. and Stål, O. (2006). 'Cytoplasmic p21 WAF1 / CIP1 correlates with Akt activation and poor response to tamoxifen in breast cancer'. *International Journal of Oncology*: 1031–1042.

Peter, M.E. and Krammer, P.H. (2003). 'The CD95(APO-1/Fas) DISC and beyond'. *Cell Death & Differentiation*, 10(1): 26–35.

Pham-Huy, L.A.., He, H.. and Pham-Huy, C.. (2008). 'Free radicals, antioxidants in disease and health'. *International Journal of Biomedical Science*, 4(2): 89–96.

Phin, S., Moore, M.W. and Cotter, P.D. (2013). 'Genomic Rearrangements of PTEN in Prostate Cancer.' *Frontiers in oncology*, 3(September): 240.

Pommier, Y. (2012). *DNA Topoisomerases and Cancer*

Pommier, Y., Sordet, O., Antony, S., Hayward, R.L. and Kohn, K.W. (2004). 'Apoptosis defects and chemotherapy resistance: molecular interaction maps and networks.' *Oncogene*, 23(16): 2934–49.

Ponder, B.A. (2001). 'Cancer genetics.' *Nature*, 411(6835): 336–41.

Pop, C., Timmer, J., Sperandio, S. and Salvesen, G.S. (2006). 'The Apoptosome Activates Caspase-9 by Dimerization'. *Molecular Cell*, 22(2): 269–275.

Powell, I.J. (2011). 'The precise role of ethnicity and family history on aggressive prostate cancer: A review analysis'. *Archivos Espanoles de Urologia*, 64(8): 711–719.

Pradelli, L. a., Bénéteau, M. and Ricci, J.-E. (2010). 'Mitochondrial control of caspase-dependent and -independent cell death'. *Cellular and Molecular Life Sciences*, 67(10): 1589–1597.

Ramos, P. and Bentires-Alj, M. (2014). 'Mechanism-based cancer therapy: resistance to therapy, therapy for resistance'. *Oncogene*, 34(August): 3617–3626.

Recchia, A.G., Musti, A.M., Lanzino, M., Panno, M.L., Turano, E., Zumpano, R., Belfiore, A., et al. (2009). 'A cross-talk between the androgen receptor and the epidermal growth factor receptor leads to p38MAPK-dependent activation of mTOR and cyclinD1 expression in prostate and lung cancer cells'. *International Journal of Biochemistry and Cell Biology*, 41(3): 603–614.

Reed, J.C. (2000). 'Warner-Lambert/Parke Davis award lecture: Mechanisms of apoptosis'. *American Journal of Pathology*, 157(5): 1415–1430.

Reinhardt, H.C., Aslanian, A.S., Lees, J.A. and Yaffe, M.B. (2007). 'p53-Deficient Cells Rely on ATM- and ATR-Mediated Checkpoint Signaling through the p38MAPK/MK2 Pathway for Survival after DNA Damage'. *Cancer Cell*, 11(2): 175–189.

Rhodes, D.R., Barrette, T.R., Rubin, M.A., Ghosh, D. and Chinnaiyan, A.M. (2002). 'Meta-analysis of microarrays: Interstudy validation of gene expression profiles reveals pathway dysregulation in prostate cancer'. *Cancer Research*, 62(15): 4427–4433.

Roberts, P.J. and Der, C.J. (2007). 'Targeting the Raf-MEK-ERK mitogen-activated protein kinase cascade for the treatment of cancer.' *Oncogene*, 26(22): 3291–310.

Roux, P.P. and Blenis, J. (2004). 'ERK and p38 MAPK-activated protein kinases: a family of protein kinases with diverse biological functions.' *Microbiology and molecular biology reviews : MMBR*, 68(2): 320–44.

Salvesen, G.S. and Dixit, V.M. (1999). 'Caspase activation: the induced-proximity model.' *Proceedings of the National Academy of Sciences of the United States of America*, 96(20): 10964–7.

Schepers, H., Geugien, M., Eggen, B.J.L. and Vellenga, E. (2003). 'Constitutive cytoplasmic localization of p21(Waf1/Cip1) affects the apoptotic process in monocytic leukaemia.' *Leukemia : official journal of the Leukemia Society of America, Leukemia Research Fund, U.K*, 17(11): 2113–21.

Schwaller, J., Pabst, T., Koeffler, H.P., Niklaus, G., Loetscher, P., Fey, M.F. and Tobler, A. (1997). 'Expression and regulation of G1 cell-cycle inhibitors (p16INK4A, p15INK4B, p18INK4C, p19INK4D) in human acute myeloid leukemia and normal myeloid cells.' *Leukemia*, 11(1): 54–63.

Di Sebastiano, K. and Mourtzakis, M. (2014). 'The Role of Dietary Fat throughout the Prostate Cancer Trajectory'. *Nutrients*, 6(12): 6095–6109.

Seiler, R., Thalmann, G.N., Rotzer, D., Perren, A. and Fleischmann, A. (2014). 'CCND1/CyclinD1 status in metastasizing bladder cancer: a prognosticator and predictor of chemotherapeutic response.' *Modern pathology : an official journal of the United States and Canadian Academy of Pathology, Inc*, 27(1): 87–95.

Shand, R.L. and Gelmann, E.P. (2006). 'Molecular biology of prostate-cancer pathogenesis.' *Current opinion in urology*, 16(3): 123–131.

Sherr, C.J. (1995). 'D-type cyclins'. *Trends in Biochemical Sciences*, 20(5): 187–190.

Shi, Y. (2004a). 'Caspase activation, inhibition, and reactivation: a mechanistic view.' *Protein science : a publication of the Protein Society*, 13(8): 1979–87.

Shi, Y. (2004b). 'Caspase activation: Revisiting the induced proximity model'. *Cell*, 117(7): 855–858.

Shi, Y. (2002). 'Mechanisms of caspase activation and inhibition during apoptosis'.

Molecular Cell, 9(3): 459–470.

Siegmund, D., Mauri, D., Peters, N., Juo, P., Thome, M., Reichwein, M., Blenis, J., et al. (2001). 'Fas-associated Death Domain Protein (FADD) and Caspase-8 Mediate Up-regulation of c-Fos by Fas Ligand and Tumor Necrosis Factor-related Apoptosis-inducing Ligand (TRAIL) via a FLICE Inhibitory Protein (FLIP)-regulated Pathway'. *Journal of Biological Chemistry*, 276(35): 32585–32590.

Silberstein, J.L., Pal, S.K., Lewis, B. and Sartor, O. (2013). 'Current clinical challenges in prostate cancer.' *Translational andrology and urology*, 2(3): 122–36.

Skolarus, T.A., Wolf, A.M.D., Erb, N.L., Brooks, D.D., Rivers, B.M., Underwood III, W., Salner, A.L., et al. (2014). 'American Cancer Society prostate cancer survivorship care guidelines'. *CA Cancer Journal for Clinicians*, 64(4): 225–249.

Smith, J., Mun Tho, L., Xu, N. and A. Gillespie, D. (2010). 'The ATM-Chk2 and ATR-Chk1 pathways in DNA damage signaling and cancer'. *Advances in Cancer Research*, 108(C): 73–112.

Smith, J.R., Freije, D., Carpten, J.D., Grönberg, H., Xu, J., Isaacs, S.D., Brownstein, M.J., et al. (1996). 'Major susceptibility locus for prostate cancer on chromosome 1 suggested by a genome-wide search.' *Science (New York, N.Y.)*, 274(5291): 1371–1374.

Steinberg, G.D., Carter, B.S., Beaty, T.H., Childs, B. and Walsh, P.C. (1990). 'Family history and the risk of prostate cancer.' *The Prostate*, 17: 337–347.

Supuran, C., Briganti, F., Tilli, S., Chegwidden, W. and Scozzafava, a. (2001). 'Carbonic anhydrase inhibitors: sulfonamides as antitumor agents?' *Bioorg Med Chem*, 9(3): 703–714.

Supuran, C.T., Scozzafava, A. and Casini, A. (2003). 'Carbonic anhydrase inhibitors'. *MEDICINAL RESEARCH REVIEWS*, 23(2): 146–189.

Susin, S. a, Lorenzo, H.K., Zamzami, N., Marzo, I., Snow, B.E., Brothers, G.M.,

Mangion, J., et al. (1999). 'Molecular characterization of mitochondrial apoptosis-inducing factor.' *Nature*, 397(6718): 441–446.

Teer, J.K. and Dutta, A. (2006). 'Regulation of S phase'. *Results and Problems in Cell Differentiation*, 42: 31–63.

Thomas, T. and Thomas, T.J. (2001). 'Polyamines in cell growth and cell death: molecular mechanisms and therapeutic applications.' *Cellular and molecular life sciences : CMLS*, 58: 244–258.

Thornberry, N. and Lazebnik, Y. (1998). 'Caspases: enemies within.' *Science*, 281: 1312–1316.

Thornton, T.M. and Rincon, M. (2009). 'Non-classical p38 map kinase functions: Cell cycle checkpoints and survival'. *International Journal of Biological Sciences*, 5(1): 44–52.

Tindall, D. and Mohler, J. (2009). *Androgen action in prostate cancer*

Ubersax, J. a, Woodbury, E.L., Quang, P.N., Paraz, M., Blethrow, J.D., Shah, K., Shokat, K.M., et al. (2003). 'Targets of the cyclin-dependent kinase Cdk1.' *Nature*, 425(6960): 859–864.

Umekita, Y., Ohi, Y., Sagara, Y. and Yoshida, H. (2002). 'Overexpression of cyclinD1 predicts for poor prognosis in estrogen receptor-negative breast cancer patients'. *International Journal of Cancer*, 98(3): 415–418.

Vaux, D.L., Cory, S. and Adams, J.M. (1988). 'Bcl-2 gene promotes haemopoietic cell survival and cooperates with c-myc to immortalize pre-B cells.' *Nature*, 335: 440–442.

Villers, A., Haffner, J. and Bouye, S. (2008). 'What is prostate cancer ?' *Bulletin de l'Academie Nationale de Medecine*, 192(5): 1003–1012.

Vyas, S., Zaganjor, E. and Haigis, M.C. (2016). 'Mitochondria and Cancer'. *Cell*, 166(3): 555–566.

Wang, J. and Yi, J. (2008). 'Cancer cell killing via ROS: To increase or decrease, that is a question'. *Cancer Biology and Therapy*, 7(12): 1875–1884.

Wang, Y., Kim, N.S., Haince, J.-F., Kang, H.C., David, K.K., Andrabi, S.A., Poirier, G.G., et al. (2011). 'Poly(ADP-ribose) (PAR) binding to apoptosis-inducing factor is critical for PAR polymerase-1-dependent cell death (parthanatos).' *Science signaling*, 4(167): ra20.

Warburg, O. (1956). 'Injuring of Respiration the Origin of Cancer Cells'. *Science*, 123(3191): 309–14.

Watters, J.L., Park, Y., Hollenbeck, A., Schatzkin, A. and Albanes, D. (2010). 'Alcoholic beverages and prostate cancer in a prospective US cohort Study'. *American Journal of Epidemiology*, 172(7): 773–780.

Webster, K.A. (2012). 'Mitochondrial membrane permeabilization and cell death during myocardial infarction: roles of calcium and reactive oxygen species'. *Future Cardiol*, 8(6): 863–884.

Wei, W., Ayad, N.G., Wan, Y., Zhang, G.-J., Kirschner, M.W. and Kaelin, W.G. (2004). 'Degradation of the SCF component Skp2 in cell-cycle phase G1 by the anaphase-promoting complex.' *Nature*, 428(6979): 194–198.

Weinberg, R.A. (2013). *The Biology of Cancer, 2nd ed.*

Weiner, L.M., Surana, R. and Wang, S. (2010). 'Monoclonal antibodies: versatile platforms for cancer immunotherapy.' *Nature reviews. Immunology*, 10(5): 317–27.

Weston, C.R. and Davis, R.J. (2007). 'The JNK signal transduction pathway'. *Current Opinion in Cell Biology*, 19(2): 142–149.

Widmark, A., Klepp, O., Solberg, A., Damber, J.-E., Angelsen, A., Fransson, P., Lund, J.-A., et al. (2009). 'Endocrine treatment, with or without radiotherapy, in locally advanced prostate cancer (SPCG-7/SFUO-3): an open randomised phase III trial.' *Lancet*, 373(9660): 301–308.

Wilson, A. and Trumpp, A. (2006). 'Bone-marrow haematopoietic-stem-cell niches.' *Nature reviews. Immunology*, 6(2): 93–106.

Won, K.A. and Reed, S.I. (1996). 'Activation of cyclin E/CDK2 is coupled to site-specific autophosphorylation and ubiquitin-dependent degradation of cyclin E.'

The EMBO journal, 15(16): 4182–4193.

Wu, P., Nielsen, T.E. and Clausen, M.H. (2015). 'FDA-approved small-molecule kinase inhibitors'. *Trends in Pharmacological Sciences*, 36(7): 422–439.

Xu, J., Meyers, D., Freije, D., Isaacs, S., Wiley, K., Nusskern, D., Ewing, C., et al. (1998). 'Evidence for a prostate cancer susceptibility locus on the X chromosome'. *Nat Genet*, 20(2): 175–179.

Xu, X.L., Singh, H.P., Wang, L., Qi, D.-L., Poulos, B.K., Abramson, D.H., Jhanwar, S.C., et al. (2014). 'Rb suppresses human cone-precursor-derived retinoblastoma tumours.' *Nature*, 514(7522): 385–8.

Yu, Q. and Sicinski, P. (2004). 'Mammalian cell cycles without cyclin E-CDK2'. *Cell Cycle*, 3(3): 292–295.

Yu, S.-W., Andrabi, S.A., Wang, H., Kim, N.S., Poirier, G.G., Dawson, T.M. and Dawson, V.L. (2006). 'Apoptosis-inducing factor mediates poly(ADP-ribose) (PAR) polymer-induced cell death.' *Proceedings of the National Academy of Sciences of the United States of America*, 103(48): 18314–9.

Zeegers, M.P. and Ostrer, H. (2005). 'Genes in the polyamine biosynthesis pathway may be involved in prostate cancer susceptibility'. *Future Oncol*, 1(5): 683–688.

Zhang, W., Liu, H.T. and Tu LIU, H. (2002). 'MAPK signal pathways in the regulation of cell proliferation in mammalian cells'. *Cell Research*, 12(1): 9–18.

CHAPTER-2

SCREENING AND PRELIMINARY EVALUATION OF THE COMPOUNDS

2.1 Introduction

Worldwide, the incidences of prostate cancer are increasing. The androgen secretory glands are usually hyperactivated in prostate cancer and the androgen hormone androgen receptor in the prostate gland. Initially, prostate tumors respond well to hormonal therapy. However, due to either prolonged hormonal therapy or late diagnosis, the disease becomes insensitive to the initial treatments, and the condition is known as "Castration-Resistant Prostate Cancer or CRPC." The various methods for the treatment of cancer comprise "surgery, radiation, chemotherapy, hormone therapy, biological therapy, and targeted therapy" (Pongrakhananon, 2013). For better effect, the chemotherapeutic methods are exploited, either alone or in combination with other drugs, for the cancer treatments (Schumann et al., 2015; Al-Lazikani et al., 2012; Mishra et al., 2013). Although advances have been made in early detection, prevention, and treatment, still effective therapies against late-stage metastatic prostate cancer are awaited. The presently available drugs, despite promising results, bear severe side effects and systemic toxicity (Grossmann and Zajac, 2011; Taylor et al., 2009; Sharifi et al., 2005; Ziolkowska et al., 2012).

The sulphonamides have retained the interest of the researchers due to their significant and versatile biological activities and the ability to enhance "pharmacological potency of the lead chemical matter" (Dai et al., 2011; Supuran et al., 2003). Sulfonamide and their derivatives are known for their anti-cancer properties; wherein they act as inhibitors of "carbonic anhydrase or CA (Guler et al., 2010; Supuran et al., 2001). Benzenesulfonamide derivatives showed well-known CA inhibitory properties, and a broad range of such compounds have been used in the design of inhibitors with various medicinal chemistry applications(Garg H.G., 1972; CALVERT W. WHITEHEAD, 1960). Sulfonylhydrazide and their analogs constitute a class of cancer chemotherapeutic agents(Brynes et al., 1978).

Arylsulfonylhydrazones of 2-formylpyridine N-oxide **(Figure. 2a)** and 2-formylpyridine 1-oxide have been shown to possess potent activity against several transplanted murine tumor (May and Sartorelli, 1978; Loh et al., 1980). Sulphonylhydrazones are known as a class of compounds with potent antineoplastic properties. A series of sulphonylhydrazone derivatives were prepared by substituting at various positions of the phenyl rings of toluene sulphonylhydrazones and named as "PR-3 series". The parameter necessary for anticancer activity were evaluated with a purpose to develop compounds with more favorable therapeutic indices.

In this chapter, the preliminary screening data showed that four of these compounds (**SH-1, SH-2, SH-3,** and **SH-4**) affected androgen-independent metastatic prostate cancer cell lines, DU145 and PC-3 and conferred the least toxicity to noncancerous-fibroblast cell line, NIH-3T3. Two of these compounds viz. SH-1 or *N*'-[(1*E*)-(2,5-dimethoxyphenyl)methylene]-4-methylbenzenesulfonohydrazide and SH-2 or (E)-*N-(*1-(3-chlorophenyl)propylidene)-4-methylbenzene sulfonohydrazide (**Fig. 2b),** were taken for the further detailed study**.** The IC_{50} of the two compounds were found to be 60µM and 70 µM for DU145 and PC-3 cell lines respectively. SH-1 arrested cells in S-phase and SH-2 detained in the G_1 phase of the cell cycle in both the prostate cancer cell lines and both induced a strong polyploidy and cell death. Corresponding to the effect on the cell cycle, SH-1 inhibited Cyclin A while SH-2 inhibited cyclin D1 and cyclin E. Both compounds cleaved the PARP and inhibited survivin and Bcl-2.

2.2 Methodology

2.2.1 Cell lines and reagents

The human prostate carcinoma cell lines, "DU145 and PC-3", and human fibroblast cell line, NIH-3T3 were obtained from "American Type Culture Collection (Manassas, VA)" and grown in DMEM media supplemented with 10% heat-inactivated fetal bovine serum. Fetal bovine serum and penicillin-streptomycin were obtained from Invitrogen. MTT or "[3-(4,5-Dimethylthiazol-2-Yl)-2,5-Diphenyltetrazolium Bromide]" dye (M2128) was obtained from Sigma-Aldrich. Antibodies were PARP1 (sc-7150), cyclin A (sc-751), cyclin D1 (sc-450), cyclin E

(sc-25303), survivin (sc-17779), bcl-2 (7382) and actin (sc-1615). Other routine chemicals were obtained in their commercially available highest purity grade.

2.2.2 MTT assay

Effect of the compounds on cell proliferation was measured using MTT assay as described by Narayanaswamy, N. *et al.* (Narayanaswamy et al., 2015). Briefly, prostate cancer cell line, PC-3, and DU145, and noncancerous-fibroblast cell line, NIH-3T3, were plated (6000-8000/well) in triplicate in 96 well plates. The cells were incubated in the presence of various concentrations of the compound in a final volume of 200 µl for different time lengths (24, 48 and 72h) at 37°C in a 5% CO_2 humidified chamber. Cells treated with the vehicle alone (DMSO) served as a control. At the end of each time point, 20 µl of MTT solution (5 mg/ml in 1X PBS) added to each well and incubated for another 5 hours. After discarding the supernatant at the end of 5 hours, the resultant formazan crystals produced were dissolved in 200µM of DMSO. The absorbance value (A) measured at 570 nm by a microplate ELISA reader.

2.2.3 Cell cycle assay

FACS-fluorescence activated cell sorting methodology was used to determine the effect on cell cycle progression either in the presence of selected concentration of synthetic compounds. The cells (120000/well) were plated in 6-well plates. The concentration of compound corresponding to IC_{50} was added to the cells for different time periods (24, 48 and 72 hours). Cells were harvested at the stipulated time point and washed twice with 1x cold PBS. Cells were then fixed in 70% ethanol and incubated overnight at 4°C. Cells were stained with propidium iodide, and data was acquired of 10,000 cells. The acquired data was further analyzed by flow cytometry using "ModFit LT (Verity Software House) software".

2.2.4 Western blot

Western blot technique was used to check and analyze the expression level of the various cell cycle proteins in response to the screened synthetic compounds. The cells (7x 10^4/ml) were plated in 100mm^2 dishes. Cells treated with corresponding

IC_{50} concentrations of screened compounds were harvested at different time points. Proteins were extracted in lysis buffer and lysed on end to end rotator for 3 hours at 4ºC. After lysis, samples were centrifuged at 13,000 rpm and 4ºC for 30 minutes. Protein was quantified by "Bradford assay" and analyzed on SDS-PAGE. The proteins were transferred to "PVDF membrane" and incubated with specific antibodies to detect the protein of interest by "ECL method".

2.2.5 Statistical analysis

Each experiment was repeated more than three times and significance was measured by one way or two way ANNOVA. The data shown are the mean value from three independent experiments. $\alpha = p<0.05$, $\beta = p<0.01$, $\gamma = p<0.001$ compared to control.

2.3 Results

2.3.1 Screening of compounds by cell cytotoxicity assay on DU145 and PC-3 cell lines.

The cytotoxicity of PR-3 series compounds was evaluated on two androgen-independent metastatic prostate cancer cell lines, "DU145 and PC-3", by MTT assay. Three different concentrations 50, 100 and 150 µM were used, and treatments were given for 72 hours. The preliminary screening indicated that four compounds namely SH-1, SH-2, SH-3, and SH-4 elicited toxicity in both cell lines **(Figure. 2.1a and b)**. Both SH-1 and SH-2 elicited the cell death by 52% and 38% in DU145, and 31% and 25% in PC-3 cells respectively. MTT data also indicated that SH-4 was the least toxic among the four compounds **(Figure. 2.1)**. Rest other compounds did not confer toxicity even at higher concentrations. SH-1 and SH-2 were taken for the detailed study. The IUPAC name of SH-1 and SH-2 are *N*'-[(1*E*)-(2,5-dimethoxyphenyl)methylene]-4-methylbenzenesulfonohydrazide and (E)-*N*-*(*1-(3-chlorophenyl)propylidene)-4-methylbenzene sulfonohydrazide respectively **(Fig. 2.2b)**.

For the determination of IC_{50} values, both SH-1 and SH-2 concentrations were further titrated in both DU145 and PC-3 cell lines. For SH-1, 5, 10, 40, 60, 65, 70, 75 and 80µM concentrations, and for SH-2, 10, 20, 40, 50, 60, 80 and 90 µM concentrations values were taken. The treatments were given for 24, 48, and 72 hours. The results showed that the minimum concentration of the compounds which induced toxicity significantly was 10µM for SH-1 and 40µM for SH-2 in both cancer cells. SH-1 **(Figure. 2.3a)** at 10µM induced 20% and 28% and SH-2 **(Figure. 2.3b)** at 40µM induced 28% and 36% cell death in DU145 and PC-3 respectively. It was interesting to observe that, at lower concentration ranges, both SH-1 and SH-2 exerted more toxicity in the PC-3 cell line. That might be due to differential sensitivity of cancer cells towards different concentrations. IC_{50} values for compound SH-1 and SH-2 were calculated graphically after 72 hours treatments and found to be 60µM in DU145 cell line and 70µM in PC-3 cell line respectively for both compounds **(Figure. 2.4a)**.

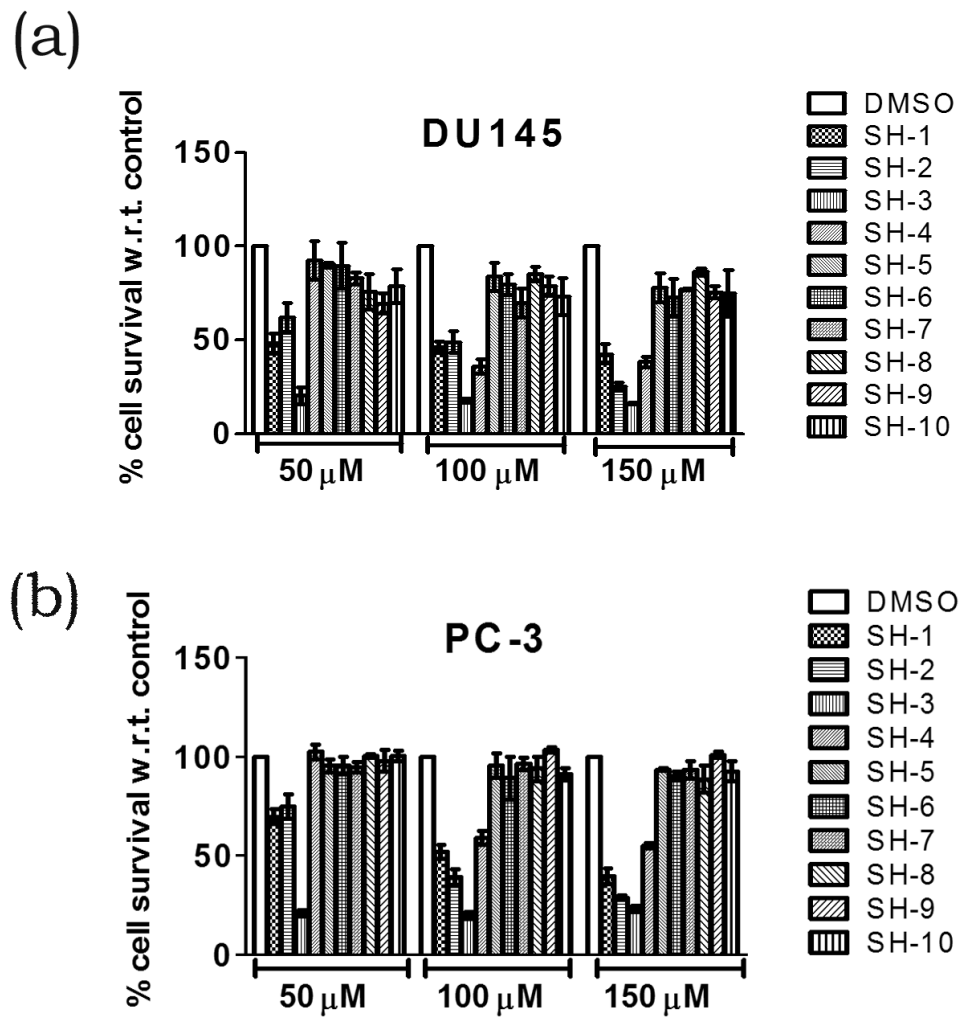

Figure. 2.1- Screening of PR-3 series synthetic compounds on prostate cancer cell lines DU145 and PC-3.

Cell cytotoxicity assay was done by MTT on prostate cancer cell lines (a) DU145 and (b) PC-3. Briefly, cells were plated in 96 well plates and treated with 50 µM, 100 µM and 150 µM of synthetic compounds for 72 hours' period. After 72 hours MTT dye was added and incubated for 4 hours in a CO_2 incubator. The formed crystals were dissolved in DMSO and OD was taken at 570nM. The results shown here indicated that of all synthetic compounds, four compounds namely SH-1, SH-2, SH-3, and SH-4 elicited cytotoxic effects on both cell lines. The data shown are the mean from three parallel experiments, and each experiment was done in triplicate.

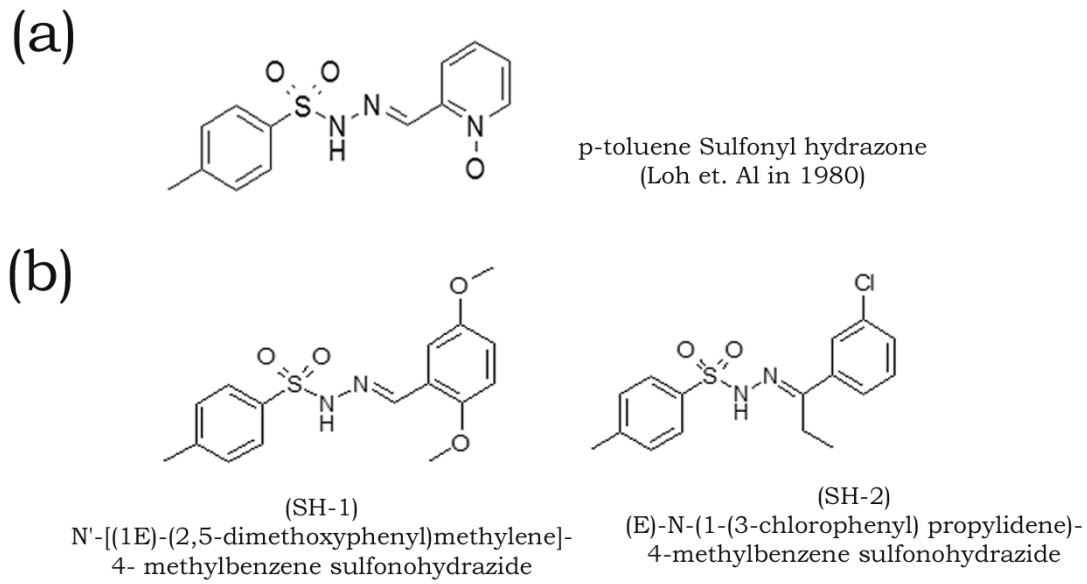

Figure. 2.2- The structure of screened hydrazone compounds.

The structure of Arylsulfonylhydrazones by William Loh et. Al in 1980 (a). Structure and chemical name of screened synthetic compounds SH-1 and SH-2 (b). Both these compounds were purified to their significant biological level.

Next, the toxicities of these compounds were accessed in the fibroblast cell line, "NIH 3T3". The data indicated that more than 80% cells were viable at 72 hours even at the IC_{50} concentration **(Figure. 2.4b)**. The results inferred that both compounds induced cytotoxicity in cancer cells more than in noncancerous fibroblast cells.

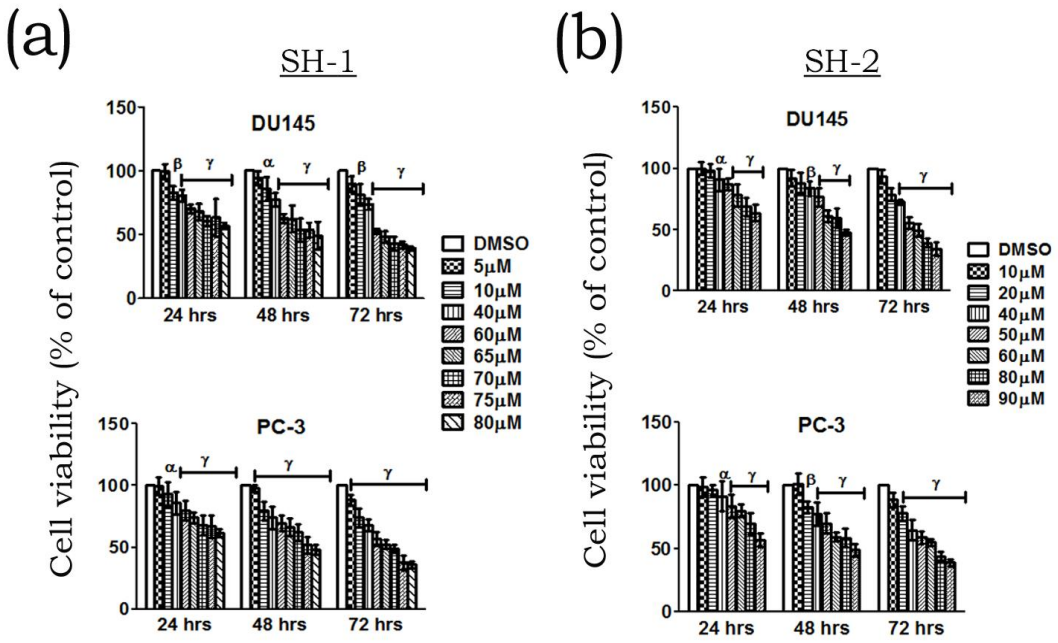

Figure. 2.3- Cytotoxicity assay of SH-1 and SH-2 on prostate cancer cell lines, DU145 and PC-3.

Cell cytotoxicity assay of SH-1(a) and SH-2 (b) on prostate cancer cell lines, DU145 and PC-3. Briefly, cells were plated in 96 well plates and treated with different concentrations of SH-1 and SH-2 for 24hours, 48hours and 72 hours' period. After incubation for the respective time point, MTT dye was added and incubated for 4 hours in a CO_2 incubator. The formed crystals were dissolved in DMSO and OD was taken at 570nM. The figure indicates that minimum significant inhibitory concentration of compound SH-1 was 10µM and that of SH-2 was 40µM. The graphical analysis of the inhibitory values indicated that IC_{50} values of SH-1 and SH-2 were 60 µM and 70 µM in DU145 and PC-3 cell lines respectively. The data shown are the mean from three parallel experiments. $\alpha = p<0.05$, $\beta = p<0.01$, $\gamma = p<0.001$ compared to control and each experiment was done in triplicate.

(a)

Compounds	IC_{50} (μM)	
	DU145	PC-3
SH-1	60.0±2.16	70.0±3.15
SH-2	60.0±5.19	70.0±2.63

(b)

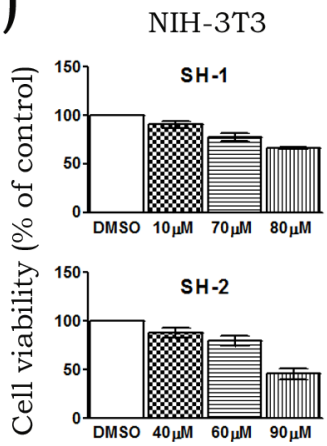

Figure.2.4- Effect of the toxicity of SH-1 and SH-2 on fibroblast cell lines, NIH 3T3.

From figure 2.2, graphically calculated IC_{50} values are given for SH-1 and SH-2. (b) For cytotoxicity assay in normal fibroblast cell, cells were plated in 96 well plates and treated with various indicated concentrations of SH-1 and SH-2 for 72 hours' time period. After 72 hours MTT dye was added and incubated for 4 hours in CO_2 incubator. The formed crystals were dissolved in DMSO and OD was taken at 570nM. MTT data indicated that at IC_{50} concentration, more that 80% cells were available in fibroblast. The data shown are the mean from three parallel experiments.

2.3.2 Evaluation of screened compounds SH-1 and SH-2 on cell cycle

Based on the preliminary assays where growth and proliferation inhibitory effects of SH-1 and SH-2 on human prostate cancer cells were evaluated, the effect of these compounds on cell cycle was checked by flow cytometric analysis as described in methods. Cells were exposed to either SH-1 or SH-2 for 24, 48 and 72 hours. Histograms of flow cytometric data indicated that both SH-1 and SH-2 conferred considerable amount of cell death in both cell lines in a time-dependent manner. Administration of the IC_{50} concentrations of compounds resulted in an aberrant cell cycle profile, which might be the result of their strong toxic effects as evident from the increased cell death. IC_{50} of SH-1 led to a drastic increase in the polyploidy, though there was the indication of S-phase arrest at 24 hours point. SH-1-induced cell death was 63% in DU145 and 58% in PC-3 against 3.38% and 5.8% in the corresponding control after 72 hours treatment **(Figure. 2.5 and table. 2.1)**. IC_{50} of

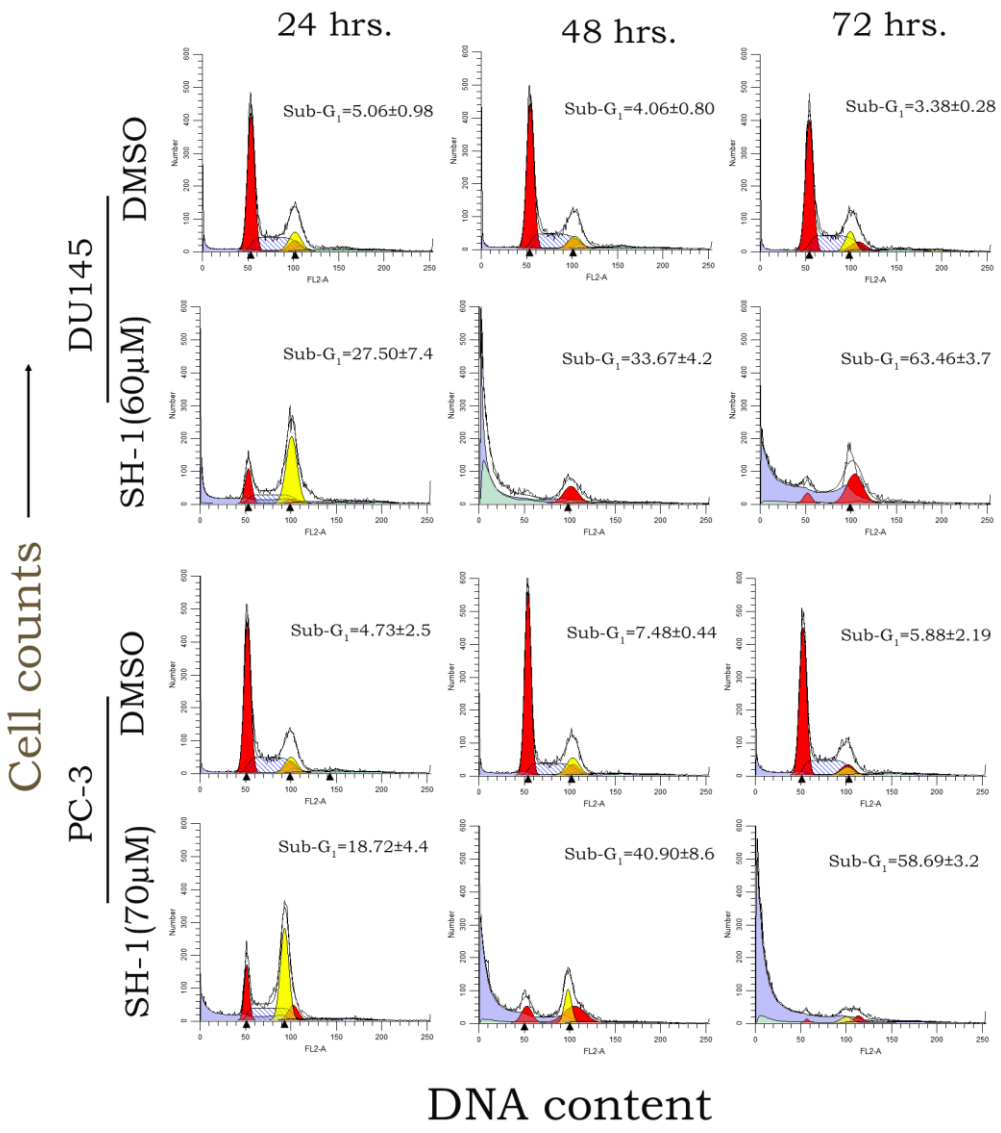

Figure.2.5- Evaluation of SH-1 on cell cycle profile.

Cell cycle analysis was done by FACS. Briefly, DU145 and PC-3 **c**ells were plated (60,000 cells/ml) in 6-well plates and treated with 60µM and 70µM of respectively with compound SH-1 for indicated time points. The DNA content of 10,000 events was analyzed by flow cytometry using modFit LT (verity software house) software. SH-1 treated cells showed high toxic effects and increased total tetraploidy. The percentage of all cellular populations is given in the table (Table-2.1). The experiment was done two or three times and yielded similar results.

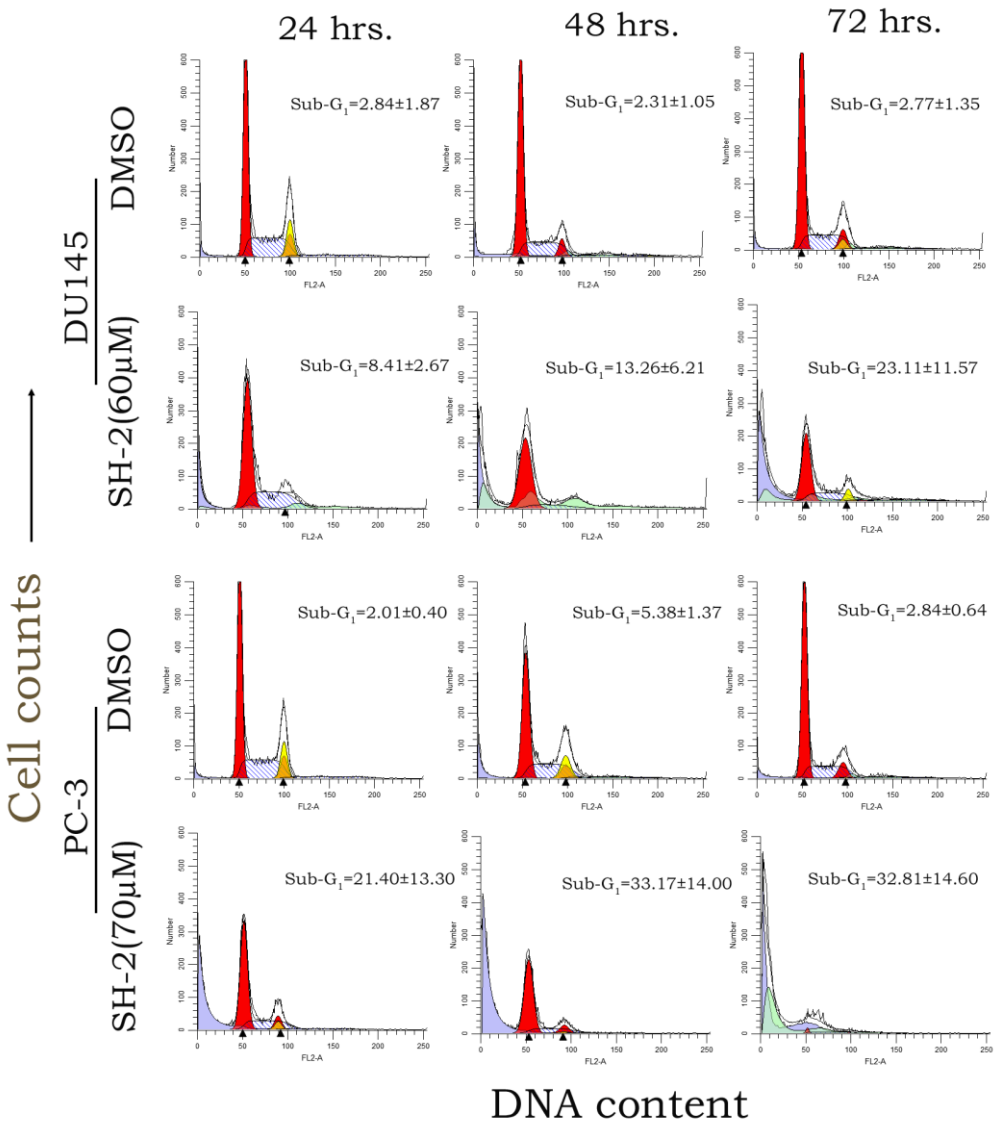

Figure.2.6- Evaluation SH-2 on cell cycle profile.

Cell cycle analysis was done by FACS. Briefly, DU145 and PC-3 **c**ells were plated (60,000 cells/ml) in 6-well plates and treated with 60µM and 70µM respectively with SH-2 for indicated time points. The DNA content of 10,000 events was analyzed by flow cytometry using modFit LT (verity software house) software. SH-2 treated cells also showed toxic effects along with G_1-arrest of the cell cycle. The percentage of all cellular populations is given in the table (Table-2.2). The experiment was done two or three times and yielded similar results.

SH-2 resulted in persistence of cells in G_1-phase in both cancer cell lines **(Figure. 2.6 and table. 2.2)**. SH-2-induced cell death was 23.11% in DU145 and 32.81% in PC-3 against 2.77% and 2.84% in respective control after 72 hours treatment

(Figure. 2.6 and table. 2.2). Due to a higher amount of cell death, cell cycle showed less number of cell cycle events, which were around less than half of the total modeled events **(Table. 2.1 and 2.2)**. Cell cycle data suggested that both cancer cells were more sensitive to SH-1 than SH-2 at their respective inhibitory concentrations.

Table-2.1

	Time Point		Diploid	Tetraploid (T)	Cellular distribution of total cells			Sub-G_1 cells	Modelled events	Cell cycle events
					G1	S	G_2M+T			
DU145	24 hours	Control	81.51±3.17	18.48±3.17	52.57±4.23	28.16±2.39	**19.24±6.60**	***5.06±0.98***	9691.0±95.3	7654.6±462.0
		SH-1(60μM)	78.84±12.31	21.15±12.31	12.24±2.04	17.91±9.53	**69.24±11.39**	***27.50±7.4***	9311.6±167.3	6117.3±670.5
	48 hours	Control	85.81±1.98	14.18±1.98	54.95±3.51	28.89±1.96	**16.14±5.33**	***4.06±0.80***	9396.0±28.9	8551.3±193.4
		SH-1(60μM)	43.26±5.92	56.63±5.92	9.97±1.33	2.97±4.60	**86.94±4.98**	***33.67±4.2***	9221.0±58.2	4892.0±841.3
	72 hours	Control	85.76±5.68	14.23±5.68	54.13±7.97	28.47±1.86	**18.0±5.13**	***3.38±0.28***	9598.3±143.8	8215.0±69.9
		SH-1(60μM)	73.78±6.52	26.21±6.52	17.58±1.75	0.00±0.00	**82.41±1.74**	***63.46±3.7***	8966.3±58.79	1349.0±123.8
PC-3	24 hours	Control	85.20±5.87	14.80±5.87	48.47±6.56	29.89±1.99	**21.60±4.57**	***4.73±2.5***	9301.3±278.6	8164.0±165.7
		SH-1(70μM)	44.71±10.20	55.29±10.20	18.59±3.20	22.52±4.49	**58.86±1.40**	***18.72±4.4***	9538.3±231.1	7187.0±297.5
	48 hours	Control	82.90±3.70	17.10±3.70	51.64±6.66	24.61±2.55	**23.7±4.51**	***7.48±0.44***	9651.0±141.7	8126.6±304.8
		SH-1(70μM)	25.01±9.15	74.09±9.15	19.18±3.17	3.88±2.54	**76.90±0.68**	***40.90±8.6***	9377.6±209.9	3112.6±409.3
	72 hours	Control	86.76±2.18	13.24±2.18	50.70±6.72	30.81±3.32	**18.33±3.58**	***5.88±2.19***	9472.3±42.18	8460.3±89.2
		SH-1(70μM)	70.23±5.87	29.77±5.87	16.50±6.32	2.30±3.56	**80.32±9.36**	***58.69±3.2***	9358.0±276.7	558.3±90.36

Table-2.1- Cell cycle distribution of various cellular populations after exposed to IC_{50} concentration of compound SH-1.

DNA content of 10,000 events was used for analysis. Populations in bold and underlined represent effective G_2M cells. Populations in bold and italics show the dead cells. Values represent means ± standard deviations for at least two separate experiments performed in triplicate.

Table-2.2

	Time Point		Diploid	Tetraploid (T)	Cellular distribution of total cells			Sub-G_1 cells	Modelled events	Cell cycle events
					G1	S	G_2M+T			
DU145	24 hours	Control	72.66±17.00	26.30±17.00	**37.51±7.53**	28.40±8.31	32.63±15.03	***2.84±1.87***	9021.0±117.0	8425.0±280.8
		SH-2(60μM)	94.40±8.66	5.59±8.66	**60.09±2.60**	32.0±7.45	7.89±10.0	***8.41±2.67***	9010.3±264.8	7006.0±317.9
	48 hours	Control	86.0±8.12	14.0±8.12	**50.32±5.33**	28.79±2.39	20.86±7.47	***2.31±1.05***	9338.3±186.6	8661.3±507.3
		SH-2(60μM)	100±0.0	0.0±0.0	**78.51±7.77**	20.35±8.49	15.32±21.4	***13.26±6.21***	8686.3±504.8	4493.3±186.5
	72 hours	Control	88.6±4.5	11.4±4.5	**55.37±0.6**	29.26±2.81	16.27±0.98	***2.77±1.35***	9576.6±272.0	8785.6±139.4
		SH-2(60μM)	92.60±6.5	7.30±6.5	**61.94±0.50**	27.56±8.99	10.58±8.32	***23.11±11.57***	8749.3±24.1	4402.6±106.4
PC-3	24 hours	Control	85.86±2.00	14.14±2.00	**47.24±1.13**	31.74±2.92	20.90±1.99	***2.01±0.40***	9572.3±57.5	9133.3±360.3
		SH-2(70μM)	79.83±5.38	20.16±5.38	**54.38±3.0**	22.98±4.24	22.61±7.15	***21.40±13.30***	8996.6±311.8	5695.3±412.9
	48 hours	Control	84.87±6.74	15.12±6.74	**49.55±5.27**	30.02±3.22	20.4±8.48	***5.38±1.37***	9184.3±99.92	8653.6±203.8
		SH-2(70μM)	82.05±6.46	17.95±6.46	**64.79±1.69**	15.62±4.24	19.56±5.29	***33.17±14.00***	9063.6±162.0	4775.0±576.0
	72 hours	Control	91.80±1.14	8.20±1.14	**57.93±2.65**	27.96±3.86	14.07±1.22	***2.84±0.64***	9639.3±232.1	8880.0±155.0
		SH-2(70μM)	95.09±6.00	4.90±6.00	**70.23±3.58**	13.03±1.89	16.73±4.29	***32.81±14.60***	8538.3±723.4	3771.0±90.7

Table-2.2- Cell cycle distribution of various cellular populations after exposed to IC_{50} concentration of compound SH-2.

DNA content of 10,000 events was used for analysis. Populations in bold and underlined represent effective G_{1}- phase cells. Populations in bold and italics show the dead cells. Values represent means ± standard deviations for at least two separate experiments performed in triplicate.

2.3.3 Evaluation of SH-1 and SH-2 on expression of the cyclins

A typical cell cycle is regulated and progressed by the cyclins. The level of each cyclin varies in different cell cycle phase, and any aberration in their phase-specific expression level may lead to the cell cycle deregulation. In corroboration with the cell cycle data, the effect of SH-1 and SH-2 was checked on the expression of the cyclins in both prostate cancer cell lines by western blots. Western blot data indicated that cyclin A expression level was downregulated by 90-100% in SH-1-treated cancer cells. **(Figure. 2.7a).** Whereas, approximately 50-70% of the cyclin E and cyclin D1 expression was blocked by 24 hours and the inhibition further increased with time in SH-2-treated samples. Inhibition of cyclin E and D1 suggested G_1-phase cell cycle arrest **(Figure. 2.7b)**.

These data suggested that the inhibition in respective cyclins might have halted the cell cycle at the respective stage and prolonged exposure resulted in the polyploidy and cell death as evident by the cell cycle data.

2.3.4 Evaluation of SH-1 and SH-2 on apoptosis

The cell cycle data indicated that both compounds induced the sub-G_1 cell populations, which represent dead cells. The cleavage of "poly-[ADP-ribose] polymerase or PARP", a DNA repair enzyme, indicates apoptosis. To check whether the cell death caused by either compound was due to apoptosis, western blot with PARP-antibody was done, and that indicated significant cleavage of full-length PARP **(Figure. 2.7a and b)**. The densitometry calculation of band intensities of the cleaved PARP by 24 hours of exposure to SH-1 and SH-2 showed about 2 to 3-fold increase. Cleaved product increased with increase in time along with a decrease in the full-length protein, indicating the apoptotic effect of SH-1 and SH-2 on the both cancerous cells.

Cancer cells show deregulated apoptotic machinery. The intrinsic pathway of apoptosis involves the disciplined activation of the effector caspases by pro-apoptotic and anti-apoptotic factors. Bcl-2 is a member of the bcl-2 family is an anti-apoptotic factor, which suppresses apoptosis and is associated with the mitochondrial membrane. The Bcl-2 expression was examined in these cancer cells at different time points. Data indicated the time-dependent inhibition of Bcl-2 in both cells. Post 24 hours exposure, SH-1 inhibited Bcl-2 expression by approximately 90-100% **(Figure. 2.7a)**, and SH-2 inhibited by 80-90% **(Figure. 2.7b)** in DU145 and PC-3. The inhibition of Bcl-2 further increased with time in both DU145 and PC-3.

Survivin is overexpressed in many cancers, including prostate cancer which positively promotes the conditions for metastasis and tumorigenesis(Zhu et al., 2005; Jha et al., 2012). Survivin is a member of "IAP or Inhibitor of Apoptosis" family which has been reported to

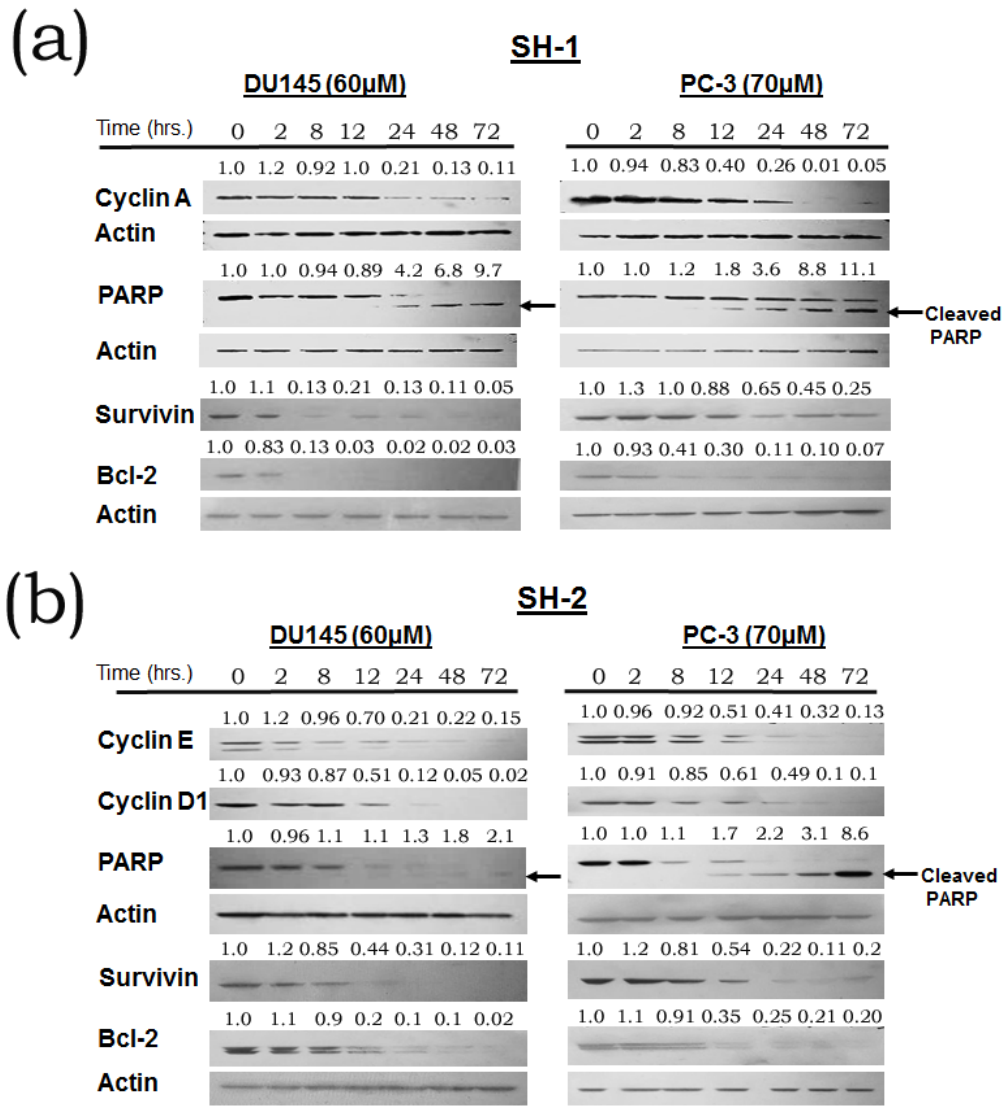

Figure.2.7- Evaluation of SH-1 and SH-2 on the expression of cell cycle proteins.

Cell cycle protein expression was checked by western blotting. Briefly, DU145 and PC-3 **c**ells were plated at 70,000cells/ml in 100mm^2 dishes with 10 ml media/dish and treated with 60µM and 70µM respectively with either compound SH-1 or SH-2 for indicated time points. Whole-cell lysates were prepared, and an equal amount of protein were loaded to run SDS-PAGE and analyzed by Western blot. SH-1 treated cells indicated the downregulation of cyclin A, S-phase cyclin (a) while SH-2 exposed cells showed downregulation of cyclin E and cyclin D1, both G1-phase cyclins (b). Both compounds cleaved the PARP and inhibited Bcl-2 and survivin proteins in both cancer cells. Each blot was quantitated and normalized with actin and the values were represented as relative to the control. Actin served as a loading control. Each blot was repeated and yielded similar results.

interact and activate the cell survival pathways and to directly inhibit caspases and other apoptotic proteins (Chen et al., 2016) Inhibition of survivin expression is prominent in DU145 compared to PC-3 cell line. In the presence of SH-1, by 12 hours, approximately 80% survivin expression was inhibited in DU145 as compared to 12% in the PC-3 cell line. By 72 hours, the inhibition in PC-3 cell line increased to 60% whereas in the case of DU145, the expression of survivin was almost entirely blocked **(Figure. 2.7a)**. 45-55% of inhibition in survivin expression was observed by 12 hours of SH-2 exposure in both cancer cells, which increased with increase in treatment time **(Figure. 2.7b)**. The inhibition of pro-oncogenic protein Bcl-2 and survivin further indicated the implication of intrinsic apoptosis by these compounds.

2.4 Discussion

Many studies have been published exploring the chemotherapeutic potential of many anticancer compounds; however, during the course of treatment, a higher dosage of drugs are administered which often result in toxicity in the distant tissues, known as systemic toxicity. These undesired complications impart a big question mark on the potency of these anticancer compounds. This chapter mainly focused on the preliminary screening of the PR-3 series synthetic compounds, provided by Professor Amir Azam, Jamia Milia University, New Delhi. Total 10 compounds were taken from the PR-3 series and preliminary screening for anti-proliferating activity was checked by MTT assay. Metastatic prostate cancer cell lines, DU145 and PC-3, were used for the assay. Out of these 10 compounds, 4 of them, namely, SH1, SH-2, SH-3, and SH-4, showed the anti-proliferative effect on the two cancer cell lines. Among these 4 compounds, SH-1 and SH-2 were taken for the further detailed study. Cytotoxic effect of these two compounds was also checked on the noncancerous-fibroblast cell line, NIH 3T3. It was shown that both the synthetic compounds, SH-1 and SH-2, strongly induced cytotoxicity in the prostate cancer cells as compared to the non-cancerous cells, as demonstrated by MTT assay. Toxicity data also indicated that SH-1 was more toxic than SH-2 at lower concentrations. The IC_{50} for both compounds were found to be 60μM and 70μM in DU145 and PC-3 respectively. In contrast, at these concentrations, 80-90% non-

cancerous cells were viable showing least toxicity to these compounds. Uncontrolled cell proliferation is one of the signatures of the cancer cells. Thus, one way of treatment is to target the cell cycle. The *in vitro* cell cycle data demonstrated that treatment of prostate cancer cells with these compounds at their respective IC_{50} concentrations resulted in the arrest of cell cycle in early time point but conferred significant cell death in later time points. At 24 hours post-treatment, SH-1 induced an increase in S-phase cells, while SH-2 did that in G_1-phase of the cell cycle. Longer treatments with either compound caused a considerable amount of polyploidy at cell death.

A typical cell cycle is controlled by many complex factors at several points in the cyclic progression. Major controlling complexes are the heterodimer of cyclins and CDKs which are the regulatory and the catalytic units respectively (Bybee and Thomas, 1991). Cyclins D, cyclin E, cyclin A, and cyclin B along with CDK2, CDK4/6, and CDK1 play a major role in the typical progression of cells through different phases of the cell cycle (Sherr and Roberts, 2004). The aberrations in these cell cycle regulators may trigger the uncontrolled proliferation and malignancy (Williams and Stoeber, 2012; Foster, 2008). Therefore, targeting Cyclin/CDKs complexes is advocated to be a promising and efficient strategy for the treatments of cancer in many anticancer treatments approaches. Flow cytometric data showed S-phase cell cycle arrest at an early time point in the presence of SH-1 and G1-phase arrest in the presence of SH-2. Inhibition of cyclin A in the presence of SH-1 and cyclin D and cyclin E in the presence of SH-2 were observed in both cancer cells. From these data we concluded that the SH-1-induced S-phase arrest was brought about by the inhibition of S-phase-specific Cyclin A and SH-2-induced G_1-phase arrest was by the inhibition of G_1 specific Cyclin D and cyclin E in both cancer cells. Prolonged treatment with either of the compounds resulted in induction of high amount of polyploidy and cell death. Our cell cycle data indicated that treatment of both cancer cell lines with either compound resulted in an increase in a sub-G_1 apoptotic cell population in a time-dependent manner. To investigate whether the cell death was due to cellular apoptosis, we performed the western blot of PARP, a well-characterized DNA repair protein and an indicator of apoptosis. The cleaved product of PARP increased with increase in the treatment time, indicating that arrested cells were apoptosized with an increase in time**.** Survivin is

overexpressed in many cancers, including prostate cancer which might promote the conditions for metastasis and tumorigenesis (Zhu et al., 2005)'(Jha et al., 2012) and its high expression in the primary tumor are frequently associated with a poor prognosis for patients (Jha et al., 2012). The downregulation of survivin and Bcl-2 indicated that the either compound induced apoptosis might be following the intrinsic course of action in both cancer cells.

From these preliminary studies, it may be concluded that these compounds may prove to be promising antiproliferative agents in metastatic prostate cancer cell lines DU145 and PC-3. More importantly, both compounds were more cytotoxic to the cancer cell lines examined than to the non-cancerous fibroblasts cells. Further work was carried out with these two screened compounds to unearth the molecular targets and mechanism involved in the induction of apoptosis in the cancer cells.

2.5 References

Al-Lazikani, B., Banerji, U. and Workman, P. (2012). 'Combinatorial drug therapy for cancer in the post-genomic era'. *Nature Biotechnology*, 30(7): 679–692.

Brynes, S., Burckart, G.J. and Mokotoff, M. (1978). 'Potential inhibitors of L-asparagine biosynthesis. 4. Substituted sulfonamide and sulfonylhydrazide analogues of L-asparagine.' *Journal of medicinal chemistry*, 21(1): 45–49.

Bybee, A. and Thomas, N.S. (1991). 'Cell cycle regulation.' *Blood Rev.*, 5: 177–192.

CALVERT W. WHITEHEAD, J.J.T. (1960). 'The Reaction of Saccharin with Amines. N-Substituted-3-Amino-1,2-benzisothiazole-1,1-dioxides'. *J. Org. Chem*, 25(3): 413–416.

Chen, X., Duan, N., Zhang, C. and Zhang, W. (2016). 'Survivin and tumorigenesis: Molecular mechanisms and therapeutic strategies'. *Journal of Cancer*, 7(3): 314–323.

Dai, H.X., Stepan, A.F., Plummer, M.S., Zhang, Y.H. and Yu, J.Q. (2011). 'Divergent C-H functionalizations directed by sulfonamide pharmacophores: Late-stage diversification as a tool for drug discovery'. *Journal of the American Chemical Society*, 133(18): 7222–7228.

Foster, I. (2008). 'Cancer: A cell cycle defect'. *Radiography*, 14(2): 144–149.

Garg H.G., A. V. (1972). 'Chemistry and biological activity of N-acyl-4-arylazopyrazoles'. *J. Pharm. Sci.*, 61: 130–132.

Grossmann, M. and Zajac, J.D. (2011). 'Androgen deprivation therapy in men with prostate cancer: How should the side effects be monitored and treated?' *Clinical Endocrinology*, 74(3): 289–293.

Guler, O.O., De Simone, G. and Supuran, C.T. (2010). 'Drug design studies of the novel antitumor targets carbonic anhydrase IX and XII.' *Current medicinal chemistry*, 17: 1516–1526.

Jha, K., Shukla, M. and Pandey, M. (2012). 'Survivin expression and targeting in

breast cancer.' *Surgical oncology*, 21(2): 125–131.

Loh, W., Cosby, L.A. and Sartorelli, A.C. (1980). 'Synthesis and antineoplastic activity of phenyl-substituted phenylsulfonylhydrazones of 1-pyridinecarboxaldehyde 1-oxide'. *Journal of Medicinal Chemistry*, 23(6): 631–634.

May, J.A. and Sartorelli, A.C. (1978). 'Antineoplastic properties of arylsulfonylhdrazones of 3-formylpyridazine 2-oxide and 4-formylpyrimidine 3-oxide'. *Journal of medicinal chemistry*, 21(12): 1333—1335.

Mishra, J., Drummond, J., Quazi, S.H., Karanki, S.S., Shaw, J.J., Chen, B. and Kumar, N. (2013). 'Prospective of colon cancer treatments and scope for combinatorial approach to enhanced cancer cell apoptosis'. *Critical Reviews in Oncology/Hematology*, 86(3): 232–250.

Narayanaswamy, N., Das, S., Samanta, P.K., Banu, K., Sharma, G.P., Mondal, N., Dhar, S.K., et al. (2015). 'Sequence-specific recognition of DNA minor groove by an NIR-fluorescence switch-on probe and its potential applications'. *Nucleic Acids Research*, 43(18): 8651–8663.

Pongrakhananon, V. (2013). 'Cancer Treatment - Conventional and Innovative Approaches'. *Cancer Treatment - Conventional and Innovative Approaches*: 618.

Schumann, C., Taratula, O., Khalimonchuk, O., Palmer, A.L., Cronk, L.M., Jones, C. V., Escalante, C.A., et al. (2015). 'ROS-induced nanotherapeutic approach for ovarian cancer treatment based on the combinatorial effect of photodynamic therapy and DJ-1 gene suppression'. *Nanomedicine: Nanotechnology, Biology, and Medicine*, 11(8): 1961–1970.

Sharifi, N., Gulley, J.L. and Dahut, W.L. (2005). 'Androgen deprivation therapy for prostate cancer.' *JAMA : the journal of the American Medical Association*, 294(2): 238–244.

Sherr, C.J. and Roberts, J.M. (2004). 'Living with or without cyclins and cyclin-dependent kinases.' *Genes & development*, 18(22): 2699–2711.

Supuran, C., Briganti, F., Tilli, S., Chegwidden, W. and Scozzafava, a. (2001). 'Carbonic anhydrase inhibitors: sulfonamides as antitumor agents?' *Bioorg Med Chem*, 9(3): 703–714.

Supuran, C.T., Scozzafava, A. and Casini, A. (2003). 'Carbonic anhydrase inhibitors'. *Medicinal Research Reviews*, 23(2): 146–189.

Taylor, L.G., Canfield, S.E. and Du, X.L. (2009). 'Review of major adverse effects of androgen-deprivation therapy in men with prostate cancer'. *Cancer*, 115(11): 2388–2399.

Williams, G.H. and Stoeber, K. (2012). 'The cell cycle and cancer'. *Journal of Pathology*, 226(2): 352–364.

Zhu, H., Chen, X.-P., Zhang, W.-G., Luo, S.-F. and Zhang, B.-X. (2005). 'Expression and significance of new inhibitor of apoptosis protein survivin in hepatocellular carcinoma.' *World Journal of Gastroenterology*, 11(25): 3855–3859.

Ziolkowska, E., Zarzycka, M., Wisniewski, T. and Zyromska, A. (2012). 'The side effects of hormonal therapy at the patients with prostate cancer'. *Wspolczesna Onkologia*, 16(6): 491–497.

CHAPTER-3

CELL CYCLE ARREST AND REPLICATION BLOCK

3.1 Introduction

The journey of a cell in a cell cycle passes through a well-regulated and timely-executed signalling events that ensure the normal progression and further cell division. The mammalian cyclins the regulatory proteins bind to and activate specific "Cyclin Dependent Kinases or CDKs" (Johnson and Walker, 1999). A normal cell cycle has four phases, namely G_1, S, G_2 and M. The G1 and G2 are the preparatory phases which groom the cells to enter in "DNA-synthetic or S-phase" and "Mitotic-phase or M-phase" respectively. These different phases are housed with various cell cycle checkpoints which prepare the cells ready to enter next phase. These checkpoints are further governed by non-cyclin proteins which are triggered by the environmental cues. CDKs are the driving-units of cell cycle and have their own regulation machinery such as CKIs. The inhibition of cyclin-CDK complex or deregulation of CKIs contribute to that abnormal cell cycle and generation of cancer (Malumbres and Barbacid, 2001). The multifaceted levels of regulation has reinforced the cell cycle in developing many anticancer agents like "alkaloids, taxanes". For instance, It has been shown that targeting G_1-CDKs may block the expression of some proto-oncogenes such as "c-myc and cyclin D1" (Puyol et al., 2010). The ectopic expression of cyclin D1, which is the maiden cyclin to be expressed in a cell cycle, has been shown to induce prostate carcinoma (Drobnjak et al., 2000). A number of cyclin-CDK synthetic inhibitors are running under various phases of clinical trials, for example "Flavopiridol (Phelps et al., 2009), Indisulam (Rowinsky et al., 2003), AZD5438 (Boss et al., 2009), SNS-032 (Chen et al., 2009), Bryostatin-1 (Marshall et al., 2002), Seliciclib (McClue et al., 2002), PD-0332991 (Toogood et al., 2005), and SCH-727965 (Parry et al., 2010)".

The p21, a CDK inhibitor of "Cip/Kip" family, can interact and inhibit various cyclin/CDK complexes but has also been reported to show preferential interaction with Cdk2 interacting cyclins (Cayrol et al., 1998). A study by Abbas et al. has shown that p21 can activate cyclin D1/CDK4-CDK6 complex (Abbas and Dutta,

2009). Apart from p53, BRCA1 also induces the expression of p21 (Warfel and El-Deiry, 2013). The c-terminus domain of p21 interacts with "proliferating cell nuclear antigen or PCNA", an integral part of the "replication machinery" (Funk et al., 1997; Cazzalini et al., 2008). Another report by Perez-tenorio et al. has indicated that the biological functions p21 depend on the cellular localization and thus interactions with different sets of proteins (Pérez-tenorio et al., 2006).

The draw back with most of the anticancer synthetic compounds is the nonspecific tissue-toxicity which is incurred due to the usage of higher. In this chapter, fibroblast cell line, NIH-3T3, was used as a mock to noncancer cells and the toxicity of the compounds were evaluated. The morphological examination and cell-migration assay were conducted. The compounds were assessed for the expression of different cell cycle proteins in cancer cells.

3.2. Methodology

3.2.1 Cell lines and reagents

Human prostate carcinoma cell lines DU145, PC-3 and human fibroblast cell line NIH-3T3 and maintained **(The detail is provided in chapter-1)** described in chapter 2. Antibodies used were PARP1 (sc-7150), cyclin A (sc-751), cyclin D1 (sc-450), cyclin E (sc-25303), cyclin B1 (sc-7393), cdk2 (sc-6248), cdk4 (sc-260), BRCA1 (sc-642), p21 (sc-6246), PCNA (sc-56) and actin (sc-1615) and other chemicals were A/G PLUS-Agarose beads (sc-2003) from santacruz. Other chemicals used were Histone H1 type3 (H5505), propidium iodide (P4170), and obtained from sigma Aldrich. Other commonly used chemicals were obtained in their commercially available highest purity grade.

3.2.2 Cell morphology analysis

Briefly, Cells were plated in 30mm^2 culture-dishes at 60% confluency and exposed to individual compound for 72 hours. Images were captured pre and post 72 hours drug treatments under bright field microscope (NIKON ECLIPSE Tis) at 20X (scale bar: 100µm) and analysed (NIS Elements D). Cell shapes and membrane integrity were observed and analysed. Experiment was repeated and similar results were observed

3.2.3 Wound-healing assay

For wound-healing assays, cells were plated in a 6-well plate and the wound was introduced by scratching the monolayer with a 1-ml sterile tip. Cells were than exposed to compounds in culture media for 72 hours. Wound widths at 0 and 72 hours was measured using bright field microscope at 5X (NIKON ECLIPSE Tis) and analysed (NIS Elements D) with three independent experiments (scale bar: 200µm).

3.2.4 Cell cycle analysis

FACS or "fluorescence activated cell sorting" methodology was used to determine the effect on cell cycle progression in presence of selected concentration of either synthetic compound. The cells (6x 10^4/ml) were plated in 6-well plates. The compounds were added to the cells for different time periods (24, 48 and 72 hours). For the withdrawal experiments, 3 days post treatment, the media was replaced with the fresh one and further incubated for 3 days. In another set, cells were treated with compounds for 6 days. All cells were harvested at their stipulated time intervals, washed with 1Xcold PBS, fixed in 70% ethanol and incubated overnight at 4°C. Propidium iodide was used to stain the DNA and data was acquired of 10,000 cells. The acquired data was further analysed by flow cytometry (BD Biosciences) using "ModFit LT (Verity Software House) software".

3.2.5 Western blot

Western blotting was used to check and analyse the expression level of various cell cycle proteins in response to the synthetic compounds. The cells (7x 10^4/ml) were plated in 100mm^2 dishes. **(The detail is provided in chapter-1).**

3.2.6 Quantitative Real Time-PCR (qRT-PCR)

Real-time PCR of p21 was performed using the Power SYBR-Green master mix (Applied Biosystems). Briefly, Total RNA was isolated using QIAzol lysis reagent (QIAGEN). cDNA was generated from 1.0 µg of total RNA by reverse transcription system (Verso cDNA Synthesis Kit, Thermo Scientific) with oligo(dT) as per manufacturer's instruction. For qRT-PCR, the "SYBR-Green master mix" was used,

and the reaction was set up according to the manufacturer's instructions. Triplicate samples were subjected to qPCR using a 7500 Real-Time PCR System (Applied Biosystems) with the maximum cycle number of 40. The relative abundance of genes of interest was calculated by expression based on "cycle threshold or Ct" values normalized to GAPDH. The qRT-PCR products were also verified by electrophoresis on 1.5% agarose gel and visualized using ethidium bromide staining. Three independent batches of RNA samples were used for qRT-PCR analysis, and data were presented as mean ± SD and analyzed by one-way ANOVA ($p < 0.05$ was considered statistically significant). Primer pairs and run method, used in the experiments, have been listed in the appendix section.

3.2.7 *In-vitro* CDK2 kinase assay

About 150-200µg of whole cell lysate was incubated with ~1µg of the cyclin A or cyclin E, primary antibody for 6 hour at 4°C on end-to-end rotor in a 500-µl reaction volume. Subsequently, 40µl of equilibrated Protein A/G PLUS-Agarose beads (santacruz) were incubated with the antibody–protein complex for 14–16 hour at 4°C. The beads were washed with ice-cold 1XPBS twice and suspended in 1X kinase assay buffer. The catalytic activity of respective cyclin-associated CDK2 activity was assayed in the reaction buffer containing kinase assay buffer, "100 µM [γ-^{32}P] ATP (6000 Ci/mmol) and 2.5µg of histone H1". Reaction was typically carried out for 40 min at 30°C and was terminated by boiling the assay mix in Laemmli's buffer for 5 min at 100°C, followed by SDS–PAGE. Radioactive phosphate incorporation in histone H1 was analyzed by autoradiography of SDS–PAGE gels.

3.2.8 Coimmunoprecipitation

About 300µg of whole cell lysate was incubated with ~1µg of the desired primary antibody for 6 hour at 4°C on end-to-end rotor in a 500-µl reaction volume. Subsequently, 40µl of equilibrated Protein A/G PLUS-Agarose beads (santacruz) were incubated with the antibody–protein complex for 14–16 hour at 4°C. The complex bound to beads were washed twice with ice-cold 1XPBS and once with complete lysis buffer. Beads were suspended in 30µl lysis buffer and boiled in

Laemmli buffer for 5 min at 100°C. The supernatant was run on "SDS-PAGE" followed by immunoblotting with desired antibody.

3.2.9 Immunofluorescence assay

Cancer cells ($7x10^3$ cells/ml) were seeded in 6-well plates over the cover slip and exposed to desired concentration of DMSO or compounds for the 48 hours. Post 48 hours incubation, cells were processed and subjected to specific primary antibody (1:50, overnight, 4°C) and FITC labelled secondary antibody (1:10,000, room temperature, 1 hour). DAPI (1:1000) was used to counterstain nucleus. Coverslips were mounted in antifade (sigma) on the slides. Slides were observed at 60X (scale bar: 20µm) under "ANDOR SPINNING DISK confocal microscope" using "ANDOR iQ 2.7 software". Fluorescence intensities from images of randomly selected microscopic fields of cells were semi-quantitatively analyzed by "NIS Elements AR version-3.000 software". For each set of data more than 50 cells were quantified.

3.2.10 Statistical analysis

All experiments were minimally carried out for three times. Statistical analyses were carried out using "Graph Pad Prism software". Experimental data are expressed as means ±S.D. and the significance of differences was analyzed by "ANOVA" test. Values of $P < 0.05$ were assumed statistically significant. Blots were densitometrically quantitated and represented as relative.

3.3 Results

3.3.1 SH-1 induced S-phase arrest and SH-2 induced G_1-phase arrest in DU145 and PC-3 cell lines

The major drawback with present anticancer compounds is the induction of systemic toxicity, resistance caused due to the usage of very high dosage and prolonged treatment. Taking the clue from MTT data, two different concentrations were selected for each compound. First one was the minimum concentration that inhibited cancer cells significantly i.e. 10µM for SH-1 and 40µM for SH-2, which were called the subcytotoxic concentration. The second values were the IC_{50} values, 60µM for SH-1 and 70 µM for SH-2. In chapter-1, we demonstrated that IC_{50} concentrations of SH-1 and SH-2 exerted extensive toxicity in both cancer cells. Here, the subcytotoxic concentrations of the compounds were assessed on the cell cycle profile by flow cytometric analysis. After exposed to either SH-1 or SH-2 for stipulated time intervals, cells were processed for flow cytometry as per the method described previously. The results indicated that 10µM of SH-1 and 40µM of SH-2 resulted in cell cycle arrest in S-phase **(Fig. 3.1)** and G_1-phase respectively of the cell cycle **(Fig. 3.2)**. Compared to the untreated cells, SH-1 treatment increased S-phase population from 28% to 40.09%, 41.0%, and 44.77% by 24, 48, and 72 hours respectively in DU145 cells **(Table. 3.1)**. Similarly, an increase of about 10% was observed by 48 hours in the S-phase of PC-3 cells **(Table. 3.1)**. SH-1-induced S-phase arrest was more prominent in DU145 as compared to PC-3 cells throughout the incubation times. The other cell cycle phases observed a concomitant reduction with increase in S-phase cells. SH-2-arrested G_1-phase cells increased by approximately 5% in DU145 and by 13% in PC-3 cells after 72 hours of treatments **(Table. 3.2)**. The increase in G_1-phase was accompanied by a corresponding reduction in the other phases of cell cycle population. SH-1-arrested S-phase cells and SH-2-arrested G_1-phase cells were plotted graphically, which showed a prominent increase in the cell cycle arrest with increase in the exposure time **(Fig. 3.3)**. The different cell cycle populations obtained after treatment with either SH-1 **(Table. 3.1)** or SH-2 **(Table. 3.2)** were given in details. Both compounds resulted in cell death, as indicated by sub-G_1 cell population, which increased with time in both DU145 and PC-3 cell.

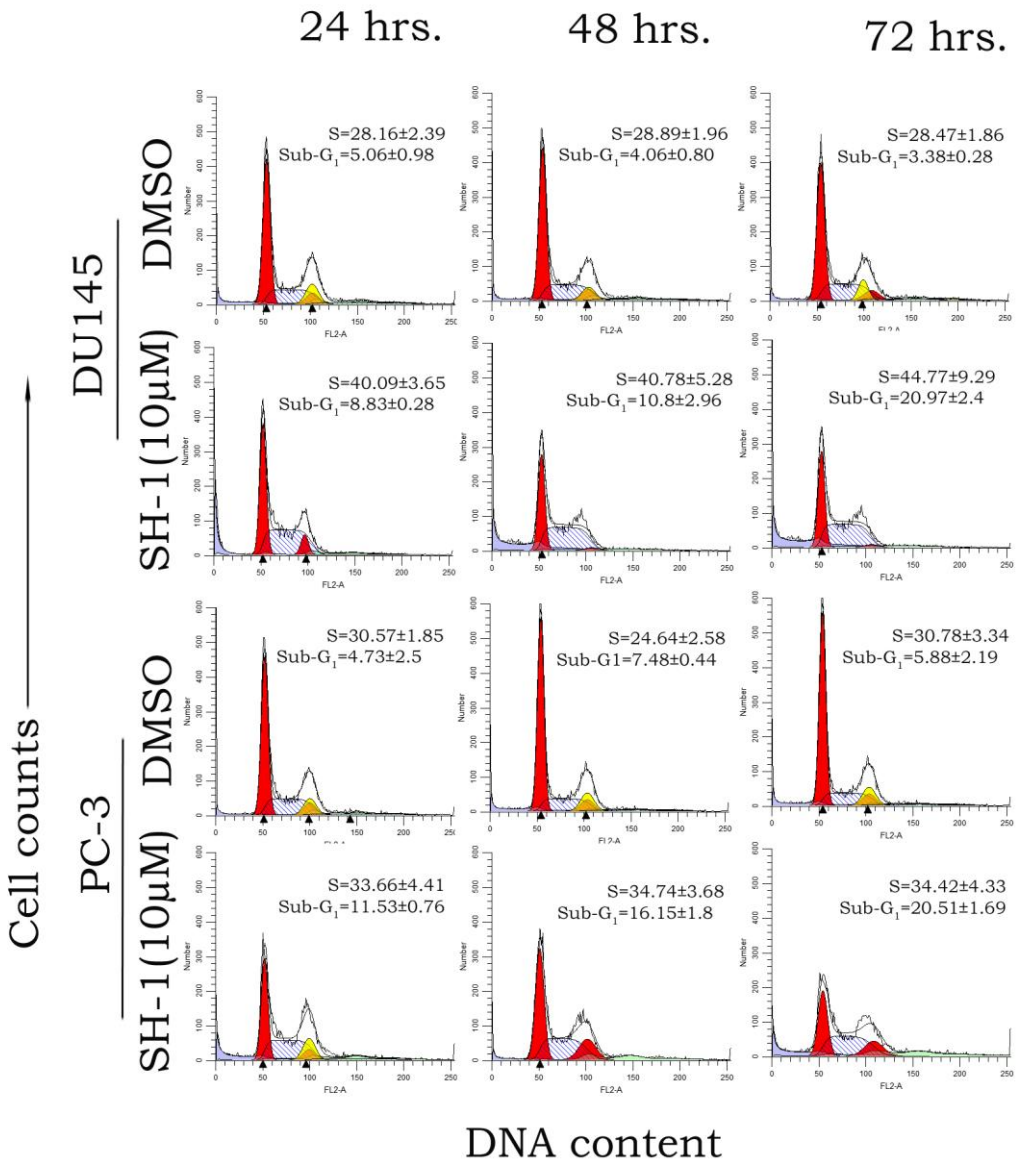

Figure. 3.1. Effect of subcytotoxic concentrations of SH-1 on cell cycle profile.

Cells were plated in 6-well plates and treated with 10µM of compound SH-1 for 24, 48 and 72 hours. The DNA content was analyzed by flow cytometry using Modfit LT (Verity Software House) software. SH-1 arrested cells in S-phase. The number of arrested cells and dead cells increased with time. The detailed cellular population distribution is given in the table. 1.

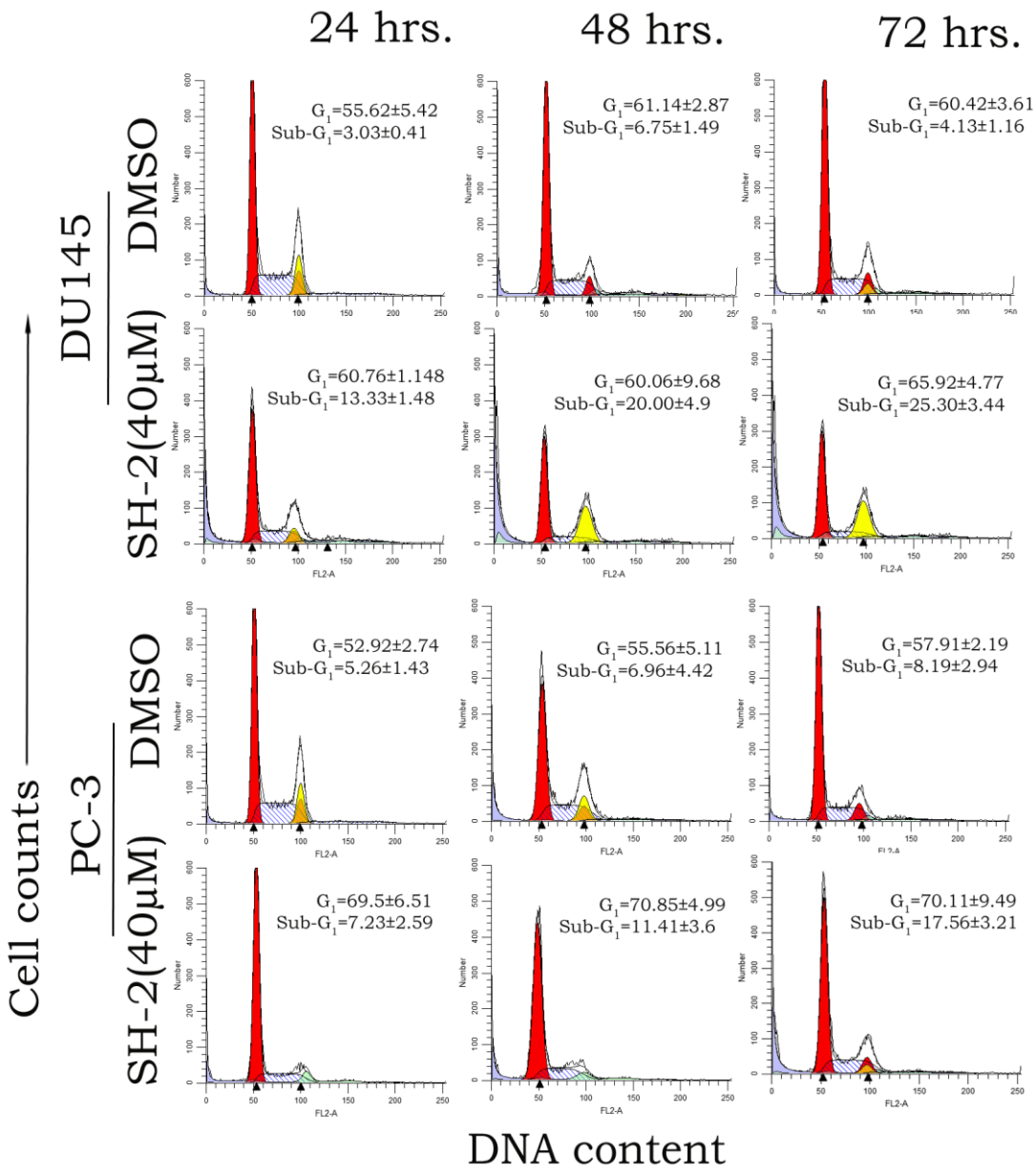

Figure. 3.2. Effect of subcytotoxic concentrations of SH-2 on cell cycle profile.

Cells were plated in 6-well plates and treated with 40μM of compound SH-2 for 24, 48 and 72 hours. The DNA content was analyzed by flow cytometry using Modfit LT (Verity Software House) software. SH-2 arrested cells in G_1-phase. The number of arrested cells and dead cells increased with time. The detailed cellular population distribution is given in the table. 2.

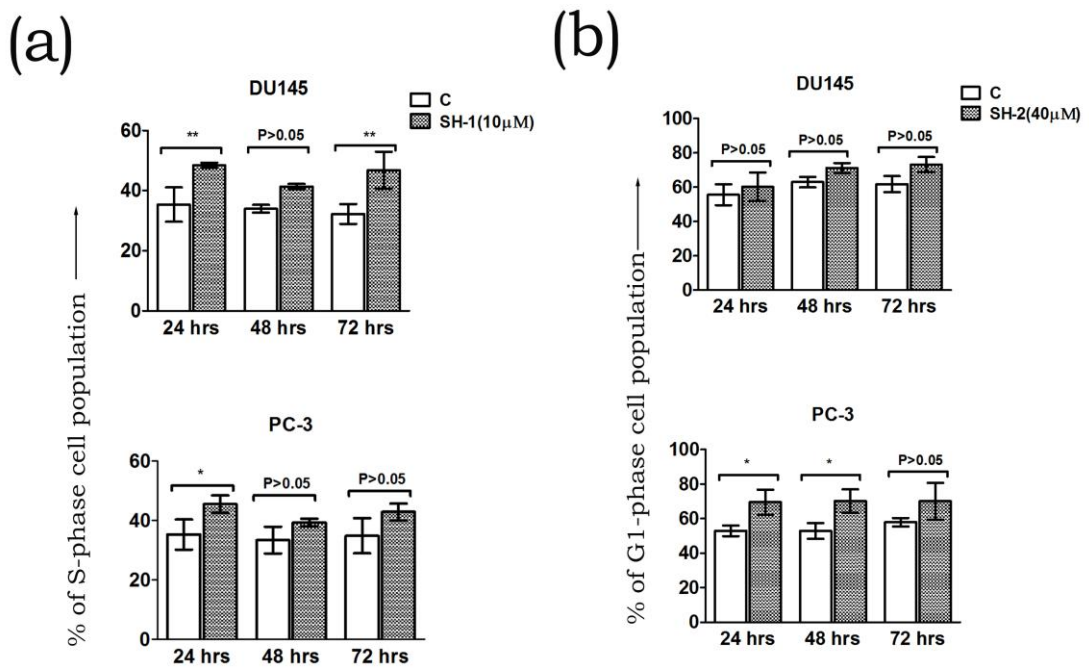

Figure. 3.3. The bar diagram representation of respectively arrested cells.

The arrested cells were plotted against their respective control in both cell lines. (a) Representation of SH-1 arrested S-phase for 24, 48 and 72 hours. (b) Representation of SH-2 arrested G_1-phase for 24, 48 and 72 hours. The data shown are the mean ±S.D. from three independent experiments. *$p<0.05$, **$p<0.01$, represented as compared to control.

Table. 3.1

	Time Point		Diploid	Tetraploid (T)	Cell cycle distribution of total cells			Sub-G_1 cells	Modelled events	Cell cycle Events
					G1	S	G_2M+T			
DU145	24 hours	Control	85.18±3.17	14.81±3.17	52.57±4.23	**28.16±2.39**	19.24±6.60	***5.06±0.98***	9691.0±95.3	7654.6±462.0
		SH-1(10μM)	90.88±12.31	9.11±12.31	38.79±7.71	**40.09±3.65**	21.10±9.36	***8.83±0.28***	9382.0±56.9	7648.3±42.18
	48 hours	Control	88.52±1.98	11.48±1.98	54.95±3.51	**28.89±1.96**	16.14±5.33	***4.06±0.80***	9396.0±28.9	8551.3±193.4
		SH-1(10μM)	92.84±5.92	7.16±5.92	45.59±4.64	**40.78±5.28**	13.44±2.00	***10.8±2.96***	9791.6±48.4	8102.0±155.2
	72 hours	Control	89.28±5.68	10.71±5.68	54.13±7.97	**28.47±1.86**	18.0±5.13	***3.38±0.28***	9598.3±143.8	8215.0±69.9
		SH-1(10μM)	89.79±6.52	10.20±6.52	39.44±1.07	**44.77±9.29**	15.76±8.50	***20.97±2.4***	9663.3±53.9	8302.3±195.2
PC-3	24 hours	Control	84.03±5.87	15.96±5.87	49.01±7.76	**30.57±1.85**	20.39±7.10	***4.73±2.5***	9301.3±278.6	8164.0±165.7
		SH-1(10μM)	78.88±10.20	21.11±10.20	41.26±9.57	**33.66±4.41**	25.07±12.3	***11.53±0.76***	9649.6±138.6	7923.3±75.6
	48 hours	Control	88.31±3.70	11.66±3.70	56.6±1.09	**24.64±2.58**	18.72±3.38	***7.48±0.44***	9651.0±141.7	8126.6±304.8
		SH-1(10μM)	89.03±9.15	10.96±9.15	46.6±4.05	**34.74±3.68**	18.65±6.45	***16.15±1.8***	9599.3±89.46	8337.6±480.7
	72 hours	Control	86.76±2.18	13.23±2.18	51.20±7.23	**30.78±3.34**	17.86±4.13	***5.88±2.19***	9472.3±42.18	8460.3±89.2
		SH-1(10μM)	80.21±5.87	19.01±5.87	41.27±1.89	**34.42±4.33**	23.49±1.20	***20.51±1.69***	9617.3±30.65	7527.0±292.5

Table-3.1- Cell cycle distribution of various cellular populations after exposure to subcytotoxic concentration of compound SH-1.

DNA content of 10,000 events was used for analysis. Populations in bold and underlined represent effective S-phase cells. Populations in bold and italics show the dead cells. Modelled cells are the total cells being counted in FACS, and cell cycle events represent the actual number of cells in the cell cycle. Values represent means ± standard deviations for at least two separate experiments performed in triplicate.

Table. 3.2

	Time Point		Diploid	Tetraploid (T)	Cell cycle distribution of total cells			Sub-G1 cells	Modelled events	Cell cycle Events
					G1	S	G_2M+T			
DU145	24 hours	Control	88.46±2.36	11.53±2.36	**55.62±5.42**	30.61±0.50	13.74±5.74	***3.03±0.41***	9681.0±106.9	8325.0±280.8
		SH-2(40μM)	88.93±3.16	11.07±3.16	**60.76±1.148**	26.2±7.44	13.34±0.66	***13.33±1.48***	9067.6±706.9	7238.0±317.9
	48 hours	Control	93.60±2.37	6.396±2.37	**61.14±2.87**	27.91±2.92	10.93±1.56	***6.75±1.49***	9500.6±253.9	8019.3±323.3
		SH-2(40μM)	84.59±16.11	15.40±16.11	**60.06±9.68**	22.68±5.31	17.25±14.11	***20.00±4.9***	9023.3±767.8	7236.0±186.5
	72 hours	Control	95.15±1.24	4.85±1.24	**60.42±3.61**	28.12±3.20	11.47±1.89	***4.13±1.16***	9328.6±249.2	8191.6±494.1
		SH-2(40μM)	88.02±8.69	11.97±8.69	**65.92±4.77**	22.29±3.67	14.02±11.86	***25.30±3.44***	9247.6±840.7	7629.0±106.4
PC-3	24 hours	Control	87.47±1.94	12.77±1.94	**52.92±2.74**	34.54±4.56	12.53±1.94	***5.26±1.43***	9540.3±134.2	8139.3±191.3
		SH-2(40μM)	98.44±1.21	1.47±1.21	**69.5±6.51**	25.19±5.51	5.21±4.05	***7.23±2.59***	9394.6±171.7	8168.0±392.5
	48 hours	Control	93.91±1.15	6.08±1.15	**55.56±5.11**	33.19±9.76	11.23±4.70	***6.96±4.42***	9191.6±150.1	7402.3±498.2
		SH-2(40μM)	99.21±0.63	0.78±0.63	**70.85±4.99**	26.47±7.03	2.67±3.40	***11.41±3.6***	9455.0±69.3	7957.6±649.1
	72 hours	Control	90.09±5.60	9.91±5.60	**57.91±2.19**	31.56±6.81	10.51±4.67	***8.19±2.94***	9355.6±227.1	7621.3±421.6
		SH-2(40μM)	93.52±1.76	6.46±1.76	**70.11±9.49**	24.68±9.94	6.46±1.77	***17.56±3.21***	9436.6±228.5	7802.3±451.0

Table-3.2- Cell cycle distribution of various cellular populations after exposure to subcytotoxic concentration of compound SH-2.

DNA content of 10,000 events was used for analysis. Populations in bold and underlined represent effective G_1-phase cells. Populations in bold and italics show the dead cells. Modelled cells are the total cells being counted in FACS, and cell cycle events represent the actual number of cells in the cell cycle. Values represent means ± standard deviations for at least two separate experiments performed in triplicate

3.3.2 Evaluation of cell cycle after the withdrawal of SH-1 or SH-2 in DU145 and PC-3 cells.

Next, the question was asked whether the cells recovered after the removal of the compounds from the medium. For the withdrawal experiment two sets of treatments were used. In one set, cells were exposed to the either of the compound for six days continuously. In second set, cells were first incubated with either compound for three days and then media was replaced without adding the compound. Cells exposed to either of the compound for three days, served as the reference. Cell cycle data

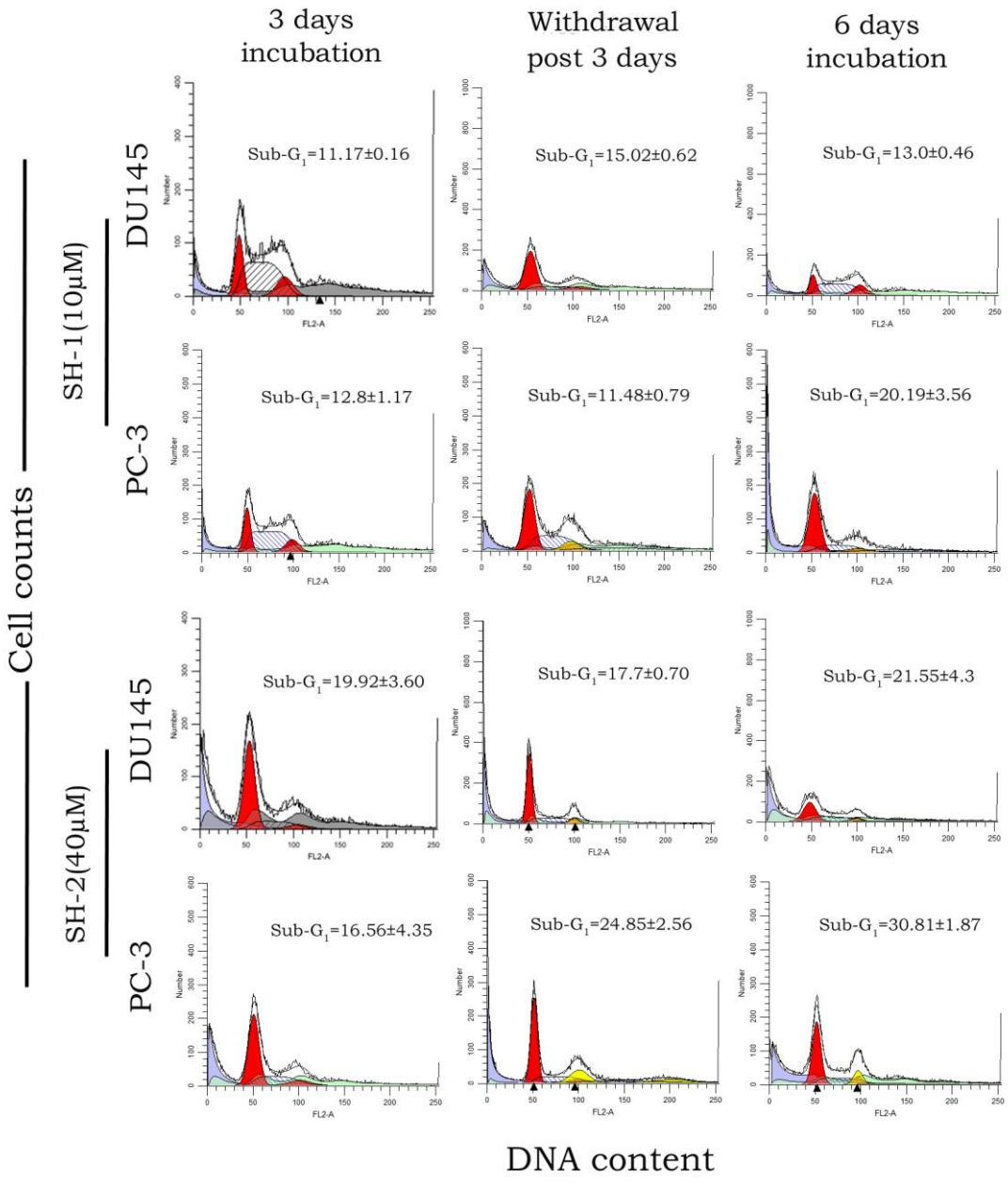

Figure. 3.4 - Effect of withdrawal of SH-1 and SH-2 on cell cycle profile.

Cells were plated in 6-well plates and treated with 10µM and 40µM of SH-1 and SH-2 respectively for 3days. The DNA content was analyzed by flow cytometry using Modfit LT (Verity Software House) software. The number of dead cells increased with time. The detailed cellular population distribution is given in the table. 3.

showed increase in cell death even after withdrawal of either SH-1 or SH-2. The percentage of cell death induced in both sets remained almost similar in both cancer cells exposed to either compound (**Fig. 3.4 and table. 3.3)**.

Table. 3.3

	Time Point	Diploid	Tetraploid (T)	Cell cycle distribution of total cells			Sub-G1 cells	Modelled events	Cell cycle Events
				G1	S	G_2M+T			
DU145	SH-1 (10μM) 3days	100.0±0.0	0.0±0.0	23.01±1.26	59.24±1.74	17.74±2.05	***11.17±0.16***	9126.0±193.7	4624.3±240.8
	SH-1 (10μM) 3days*	100.0±0.0	0.0±0.0	63.17±2.95	25.69±3.51	11.13±1.01	***15.02±0.62***	9501.6±26.98	4594.0±169.9
	SH-1 (10μM) 6days	100.0±0.0	0.0±0.0	22.89±2.42	59.22±1.44	17.89±1.77	***13.0±0.46***	9358.6±89.91	4923.3±329.3
	SH-2 (40μM) 3days	100.0±0.0	0.0±0.0	67.43±1.99	25.35±2.00	7.21±1.05	***19.92±3.60***	9569±25.71	4021±120.8
	SH-2 (40μM) 3days*	95.82±3.23	4.17±3.23	61.34±1.83	26.62±1.04	11.97±2.7	***17.7±0.70***	8961.6±189.5	4488.0±406.5
	SH-2 (40μM) 6days	100.0±0.0	0.0±0.0	59.99±2.31	18.38±3.64	21.5±2.99	***21.55±4.3***	9218.4±136.2	2658.6±129.1
PC-3	SH-1 (10μM) 3days	100.0±0.0	0.0±0.0	19.77±4.67	60.12±0.97	20.11±5.66	***12.8±1.17***	9013.0±305.9	4358.0±360.8
	SH-1 (10μM) 3days*	82.91±1.70	17.09±1.70	40.26±2.39	38.97±1.79	23.71±1.57	***11.48±0.79***	9537.6±18.9	6515.0±160.9
	SH-1 (10μM) 6days	93.78±9.62	6.21±9.62	60.59±5.77	24.85±2.53	14.49±8.24	***20.19±3.56***	9542.6±131.9	5527.3±303.3
	SH-2 (40μM) 3days	100.0±0.0	0.0±0.0	65.97±3.15	24.84±4.72	9.18±1.73	***16.56±4.35***	9589.0±52.5	4925.0±586.5
	SH-2 (40μM) 3days*	66.1±1.96	33.88±1.96	42.95±1.08	17.85±0.86	39.16±1.82	***24.85±2.56***	8154.3±160.8	4985.0±586.5
	SH-2 (40μM) 6days	83.19±0.88	16.80±0.88	52.67±1.43	23.85±0.61	23.85±	***30.81±1.87***	9523.6±74.2	4014.6±36.1

* Replaced media with fresh one without compound and incubated for 6 days

Table-3.3- Cell cycle distribution of various cellular populations after compound withdrawal

DNA content of 10,000 events was used for analysis. Populations in bold and italics show the sub-G_1 cells. Modelled cells are the total cells being counted in FACS, and cell cycle events represent the actual number of cells in the cell cycle. Values represent means ± standard deviations for at least two separate experiments performed in triplicate.

Although, after six days of compound exposure, the pattern of arrested cells was unclear, there was an extensive amount of death which caused lesser number of cell cycle events **(table. 3.3)**.

Overall, the cell cycle study suggested that the inhibitory effect of compounds might be responsible rendering of arrested cells to cell death. Even on withdrawal of the compounds, cells exhibited a considerable amount of death.

3.3.3 Evaluation of SH-1 and SH-2 on cell cycle profile in fibroblast cell line NIH-3T3

Very high dosages of anticancer drugs are used which, apart from killing cancer cells, also affect the non-cancerous healthy cells.

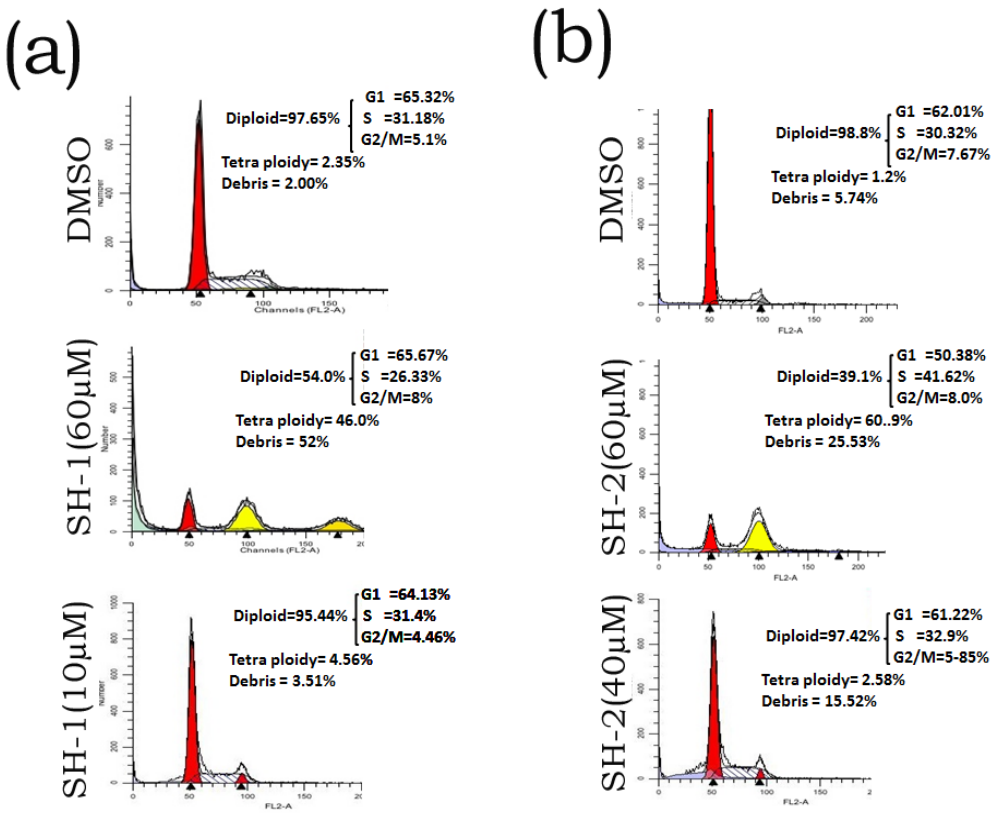

Figure. 3.5. Evaluation of SH-1 and SH-2 on cell cycle in fibroblast cell line NIH-3T3.

The assessment of both SH-1 and SH-2 was done on normal fibroblast cell line NIH-3T3 by FACS. Briefly, cells were plated in 6-well plates and treated with 10µM and 60µM of SH-1 and 40µM and 60µM of SH-2 for 72 hours. Cell cycle was done as per the methods described earlier. The data indicated the induction of a strong polyploidy and cell death by both compounds at 60µM (a) & (b). Fibroblast cells were not affected by either 10µM of SH-1 (a) or 40µM of SH-2 (b). The experiment was repeated and yielded similar results.

To check how the tested compounds affect the non-cancerous cells, we studied the cell cycle profile of fibroblast cells, NIH-3T3, in presence IC_{50} and the subcytotoxic concentrations of either SH-1 or SH-2. First we checked the cell cycle profile in presence of IC_{50} concentration of both SH-1 and SH-2. Cell cycle data indicated that the IC_{50} concentration of SH-1 resulted in 46% tetraploidy and 52% cell death **(Figure. 3.5a)** while that of SH-2 induced 60% tetraploidy and 25.5% cell death **(Figure. 3.5b)** post 72 hour treatment. These results show that the non-cancerous cells were adversely affected by both the compounds at their IC_{50} concentrations. Next we took the subcytotoxic concentrations, the minimum concentration that inhibited cancer cells significantly i.e. 10µM for SH-1 and 40µM for SH-2. The cell

cycle profile indicated that these subcytotoxic concentrations of either compounds were not harmful to the fibroblast cells **(Figure. 3.5a and b)**. Since, the aim of the study was to kill cancer cells without compromising the effect on normal cells and to minimize the systemic toxicity, further experiments were conducted with the subcytotoxic concentrations of SH-1 (10µM) and SH-2 (40µM).

3.3.4 The subcytotoxic concentration of SH-1 and SH-2 caused morphological changes and inhibition of cell migration in DU145 and PC-3 but not in fibroblast NIH-3T3

Using the subcytotoxic concentrations, both compounds were examined for their effect on cell morphology and cell migration in DU145, PC-3, and NIH-3T3. Cells were seeded in "6-well plates" and at 60-70% confluency of cells, cells were exposed to 10µM of SH-1 and 40µM of SH-2 and incubated for 72 hours. DMSO was used as a control. Images were captured at 20X pre and post incubation. As shown in the results **(Fig. 3.6)**, treatment with either SH-1 or SH-2 led to the shrinkage of the cancerous cells and the cells looked roundish with dense cytoplasm and irregular cell membrane with the small protrusion. Cell numbers were also decreased due to death. Fibroblast cells were unaffected, and cell confluency of treated cells was at par with that of the control cells **(Fig. 3.6)**.

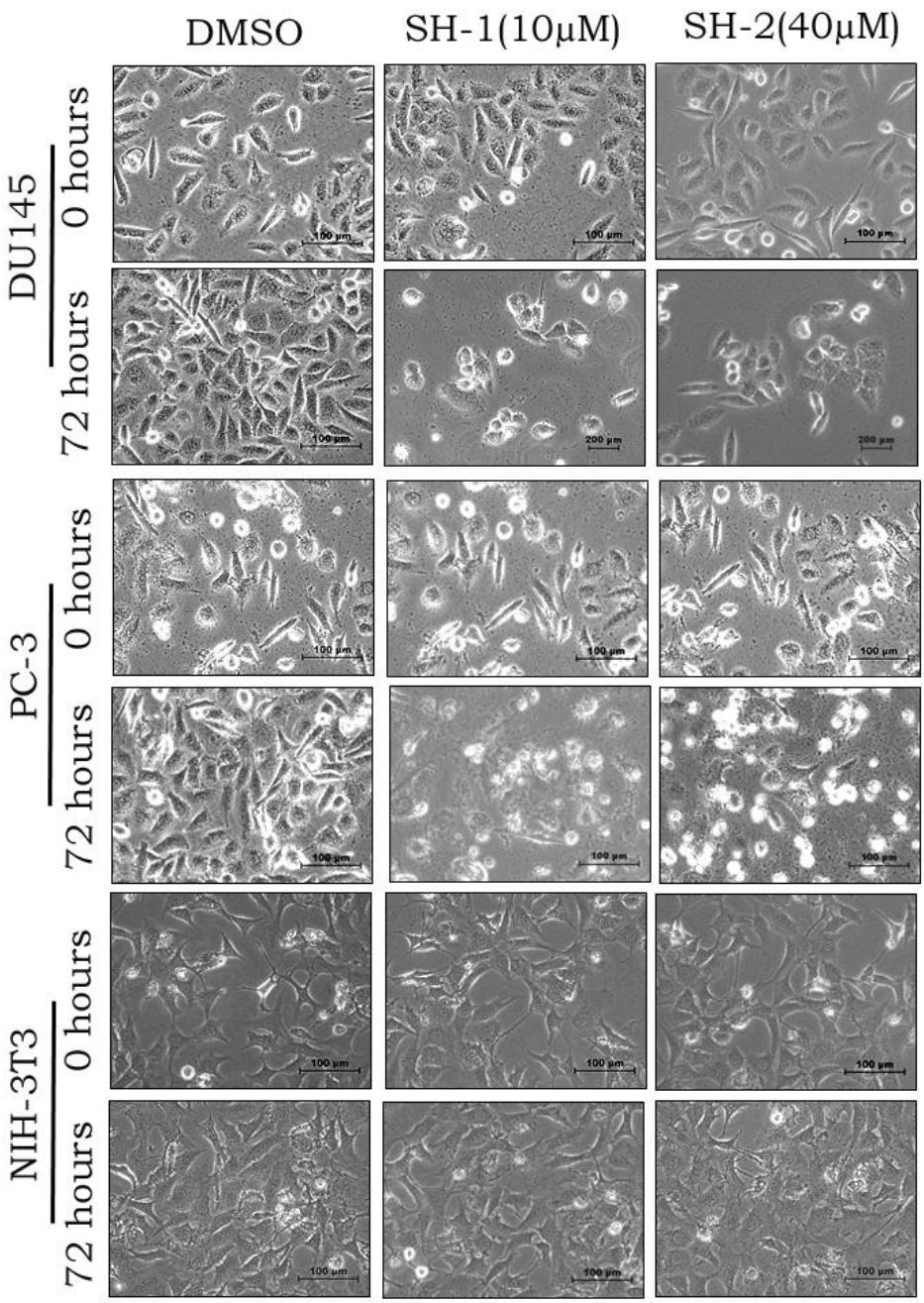

Figure. 3.6. Evaluation of SH-1 and SH-2 on cell morphology.

Cells were plated in 60 mm^2 dishes, and at 60% confluence, cells were treated with 10µM of SH-1 and 40µM of SH-2 for 72 hours. Cell morphology was examined of pre and post compound treated cells under bright field microscope at 20X. DMSO was used as a control. Fibroblast data indicated that SH-1 and SH-2 have least effect. The data shown are the mean from three parallel experiments.

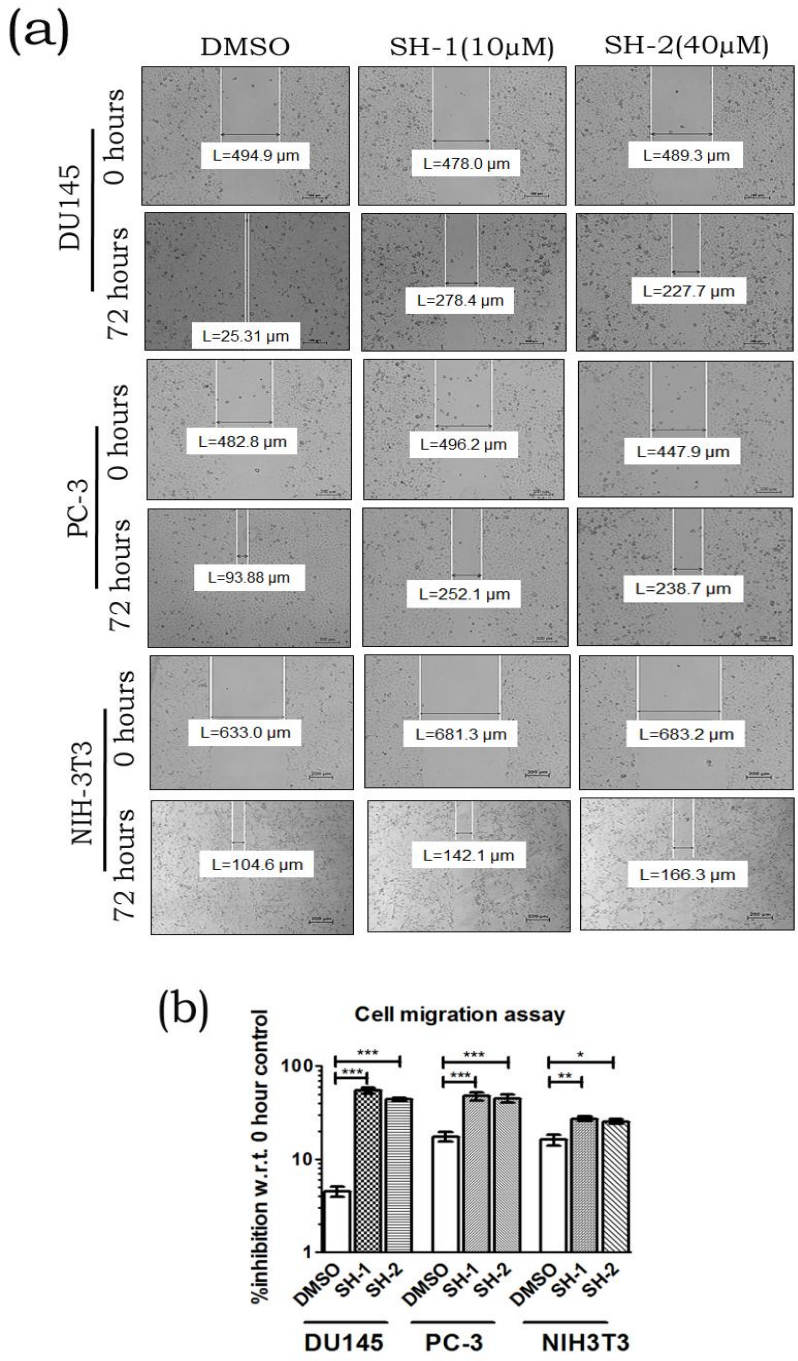

Figure. 3.7. Evaluation of SH-1 and SH-2 on cell migration.

Cells were plated in 60 mm^2 dishes, and at 90% confluence, a scratch was introduced in all samples before treatment. Media was changed, and cells were treated with 10µM of SH-1 and 40µM SH-2 for 72 hours. DMSO was used as vehicle control. (a) Widths were measured pre and post compound treatments at 5X on a brightfield microscope. Data indicated that both SH-1 and SH-2 affect cell morphology and cell migration in cancer cell lines. Fibroblast data stated that SH-1 and SH-2 are less efficient on them. (b) Bar diagram representation of cell migration data of DU145, PC-3 and NIH-3T3. The mean ±S.D. from three independent experiments. *$p<0.05$, **$p<0.01$ and ***$p<0.001$ represented as compared to control.

For the wound-healing assay, the cells were grown to confluence and scratch was introduced. Media was replaced, and pretreatment wound-widths were measured. Cells were exposed to either of the compound for 72 hours, and again wound-widths were measured. The results showed that the untreated cancer cells migrated to fill up space more rapidly as compared to the treated cells **(Fig. 3.7a)**. The noncancer cells, treated with SH-1 or SH-2, indicated that cells proliferated and migrated to fill the space in both treated and untreated samples and the wound-widths measured were almost the same **(Fig. 3.7a)**. The widths of scratch were measured, and values were plotted as percentage inhibition with respect to control. The relative comparison of bar diagrams indicated that the cell migration slowed down in presence of either of the compounds in both cancer cells. The histogram showed that cell migration of DU145 was inhibited by 50% and 40%, while that of PC-3 was inhibited by 30% and 28% by SH-1 and SH-2 treatments respectively **(Fig. 3.7b).** These data suggested that both compounds affected cell morphology and migration significantly in cancer cells.

3.3.5 SH-1 inhibited the expression of cyclin A, CDK2 activity and their nuclear localization in DU145 and PC-3

Cyclins and CDKs play a constructive role in cell cycle regulation. Compounds were evaluated on the expression level of respective cyclins and CDKs in both cancer cells for the stipulated times. Western blotting data indicated that the subcytotoxic concentration, 10µM of SH-1 inhibited cyclin A to a significant extent **(Fig. 3.8a)**. The densitometry of respective bands indicated that SH-1 inhibited cyclin A by 70% in DU145 and by almost 100% in PC-3 cells after 48 hours treatments **(Fig. 3.8a)**. At 72 hours post-treatment, SH-1 upregulated cyclin B1 by more than 1.5-fold, but the expression of "cyclin D1 and cyclin E" remained more or less unaffected in DU145 **(Fig. 3.8a)**. In PC-3 cells, cyclin B1, cyclin D1 and cyclin E were inhibited by 30%, 49% and 9% respectively at 72 hours post-treatment **(Fig. 3.8a)**.

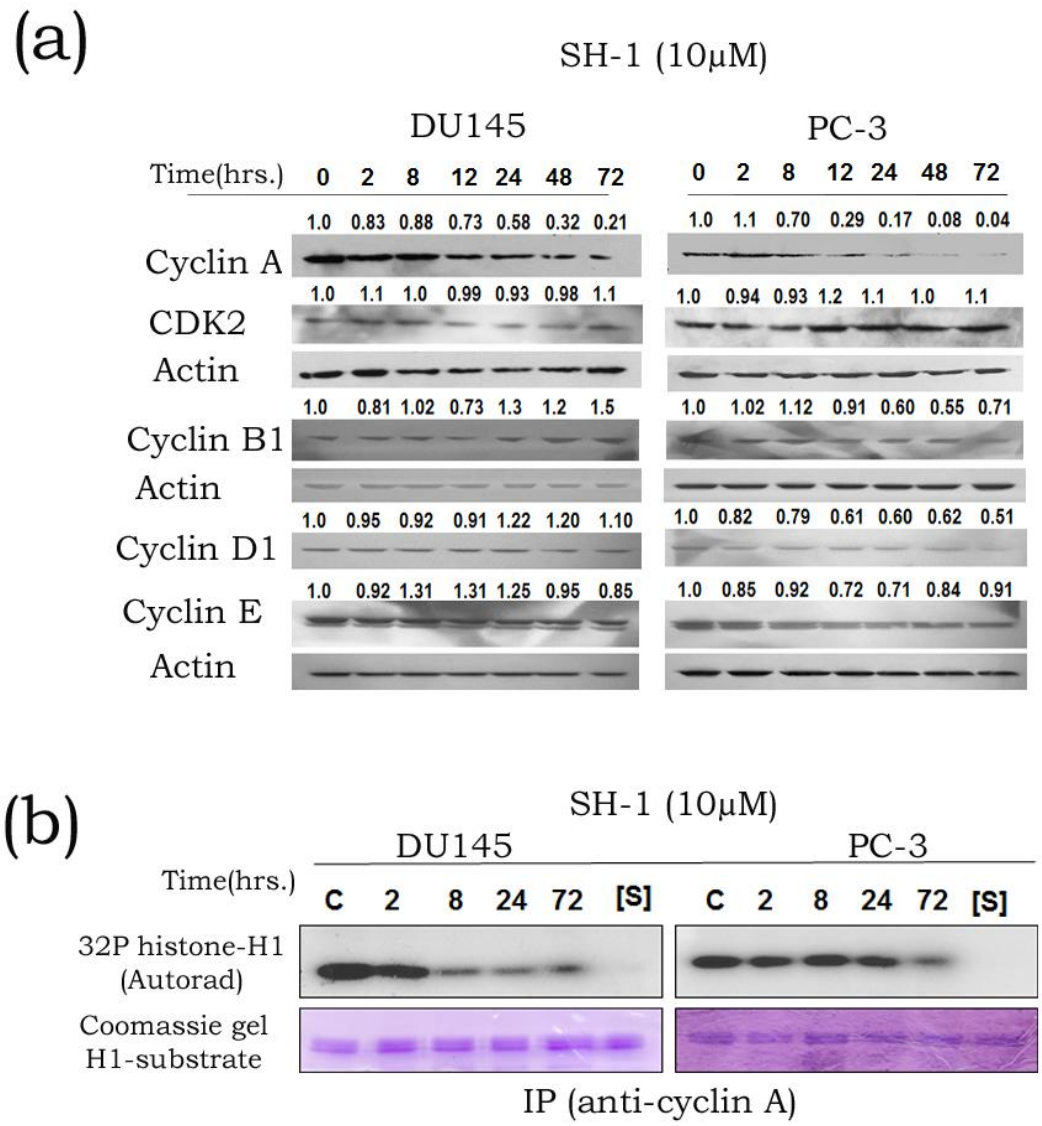

Figure. 3.8. Compound SH-1 inhibits cyclin A and CDK2 kinase activity.

Cells were plated and after overnight incubation, treated with 10μM of SH-1 for the indicated times. (a) Western blot showing the protein expression of cyclin A, cyclin B, cyclin D1 and cyclin E in cancer cells. Actin served as a loading control. Each blot was quantitated and normalized with actin, and the values were represented as relative to the control. (b) Kinase assay was done to access the CDK2 activity; 200μg protein was used for immunoprecipitation either with anti-cyclin A. IP beads were processed and used for *in-vitro* radio-isotope based kinase assay. Histone-H1 was used as the substrate. Coomassie stained Histone-H1 served as loading control. All experiments were repeated and yielded similar results.

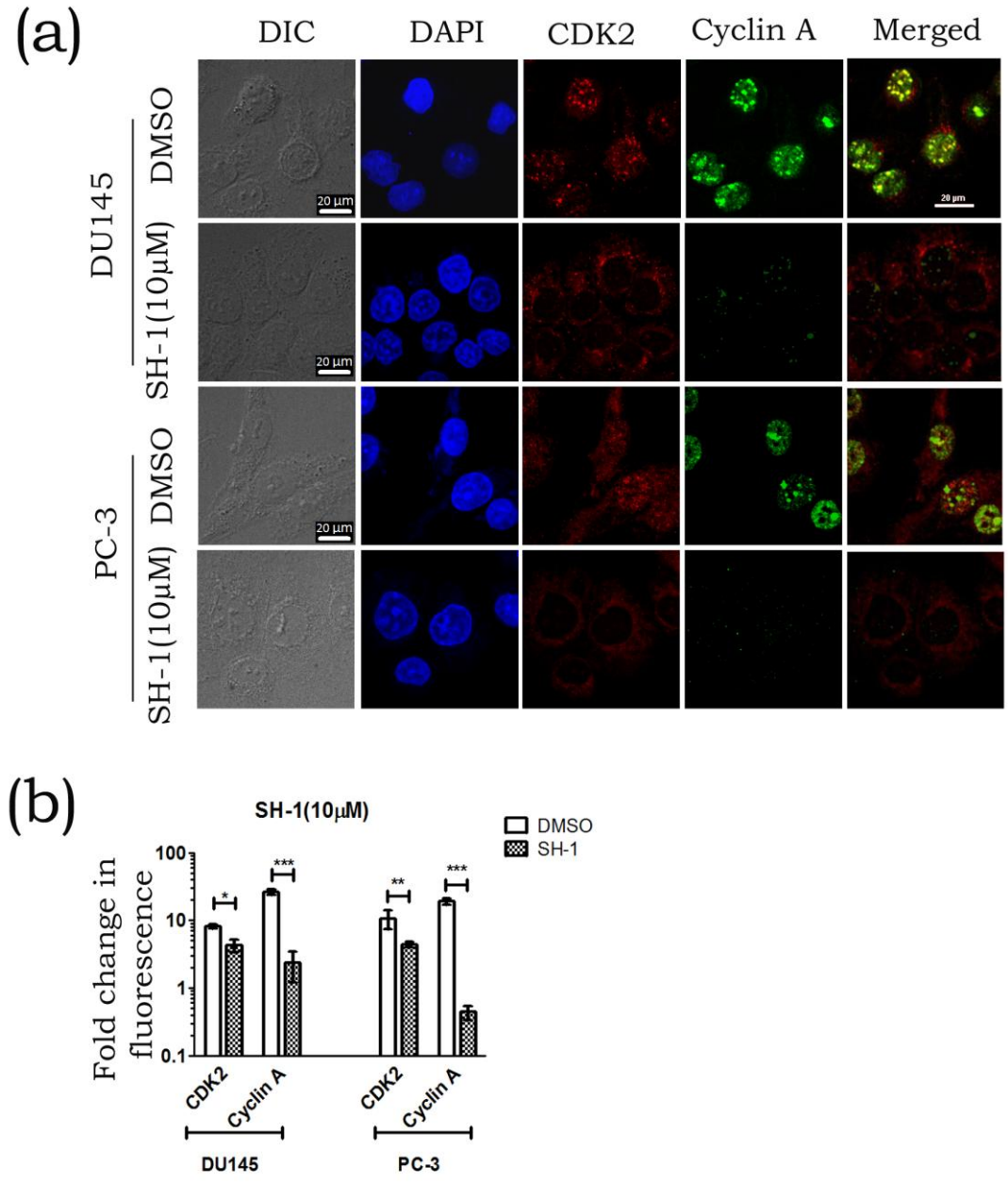

Figure. 3.9. Compound SH-1 inhibits nuclear localization of cyclin A and CDK2.

DU145 and PC-3 cells were plated on coverslips in 6-well plates and treated with 10μM of SH-1 for 48 hours. Cells were fixed in 4% PFA followed by permeabilization with 0.01% Triton-x-100. After incubating with respective primary (1:50 dilution) and secondary (1:10,000) FITC labeled antibody, cells were mounted on slides in antifade mounting media. DAPI was used to counterstain nucleus. Slides were observed at 60X under ANDOR SPINNING DISK confocal microscope using ANDOR iQ 2.7 software (scale bar: 20μm). (a) The merged image is showing co-localization of cyclin A and CDK2. (b) Quantitation from microscopic images was done using n number (n>50) of cells for each set. All experiments were repeated and yielded similar results. *p<0.05, **p<0.01 and ***p<0.001 represented as compared to control.

The cyclins control the progression of the cell cycle through the specific protein kinases known as "cyclin-dependent protein kinases or CDKs". The protein expression of CDK2 remained unchanged in both cancerous cells treated with either compound **(Fig. 3.8a).** Next we checked cyclins associated CDK activity. Immunoprecipitation was carried out using whole cell lysate with anti-cyclin A antibody. Kinase assay was set up using histone H1 as substrate as per the method described. The data indicated an increase in the inhibition of "cyclin A-associated CDK2 activity" with increase in time and that was in tune with the inhibition of cyclin A **(Fig. 3.8b)**. Nuclear localization of the cyclin-CDK complex is necessary for its active participation in cell cycle regulation. The localization of the cyclin A and CDK2 was examined after treating the cells with SH-1. Immunofluorescence data indicated that in control cells, both cyclin A and CDK2 co-localized in the nucleus, as shown in the merged panel, in both cancer cell lines **(Fig. 3.9a).** SH-1 treatment resulted in the cytoplasmic localization of CDK2 and inhibition of cyclin A in both cell lines **(Fig. 3.9a).** The quantification of cyclin and CDK2 was done which indicated about 48% and 78% inhibition of nuclear-cyclin A in DU145 and PC-3 cells respectively **(Fig. 3.9b).**

Taken together, western blot, kinase activity, and localization data indicated that SH-1 inhibited cell cycle by inhibiting the cyclin A and associated CDK2 activity.

3.3.6 SH-2 inhibited the expression of cyclin E, CDK2 activity and their nuclear localization in DU145 and PC-3

The expression of cyclins and CDKs were examined in SH-2 treated cancer cells at various time points. Western blot data indicated that 40µM of SH-2 inhibited G_1 cyclins, "Cyclin E and cyclin D1", entirely in both DU145 and PC-3 cells at 72 hours post-treatment **(Fig. 3.10a)**. The inhibition of these early G_1 cyclins might have resulted in G_1-phase arrest. Cyclin B1 was downregulated by approximately 20% in both cancer cells, while cyclin A showed inhibition of 30% in PC-3 and remained constant in DU145 cells **(Fig. 3.10a)**. We also checked the expression level of kinase partners, CDKs, and found that SH-2 inhibited both CDK2 and CDK4 expression significantly in both cancer cells **(Fig. 3.10a)**.

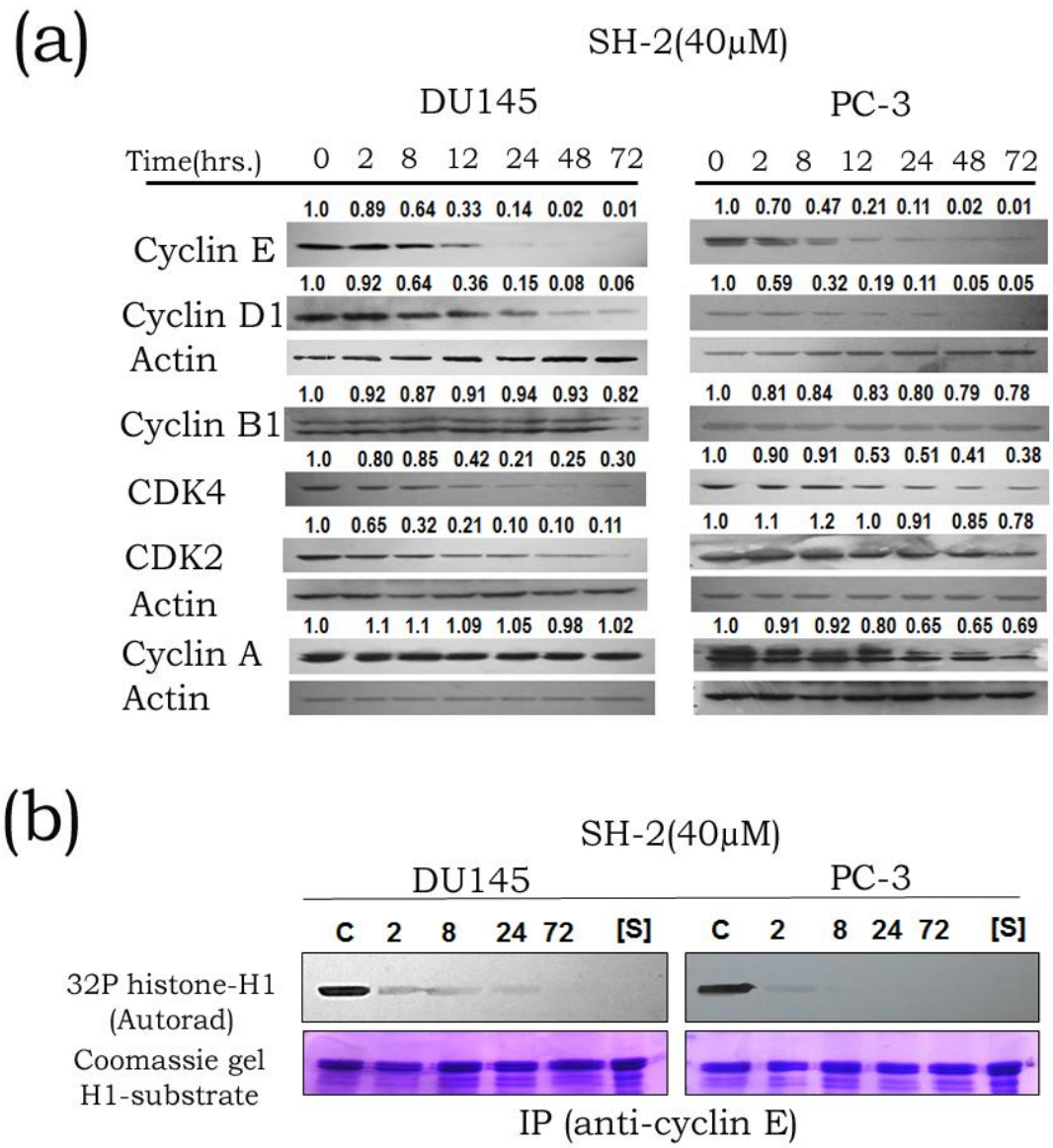

Figure. 3.10. Compound SH-2 inhibits cyclin E, cyclin D1, and CDK2 kinase activity.

Cells were plated and after overnight incubation, treated with 40μM of SH-2 for the indicated times. (a) Western blot showing the protein expression of cyclin A, cyclin B, cyclin D1 and cyclin E in cancer cells. Actin served as a loading control. Each blot was quantitated and normalized with actin, and the values were represented as relative to the control. (b) Kinase assay was done to access the CDK2 activity; 200μg protein was used for immunoprecipitation with anti-cyclin E. IP beads were processed and used for *in-vitro* radio-isotope based kinase assay. Histone-H1 was used as the substrate. Coomassie stained Histone-H1 served as loading control. All experiments were repeated and yielded similar results.

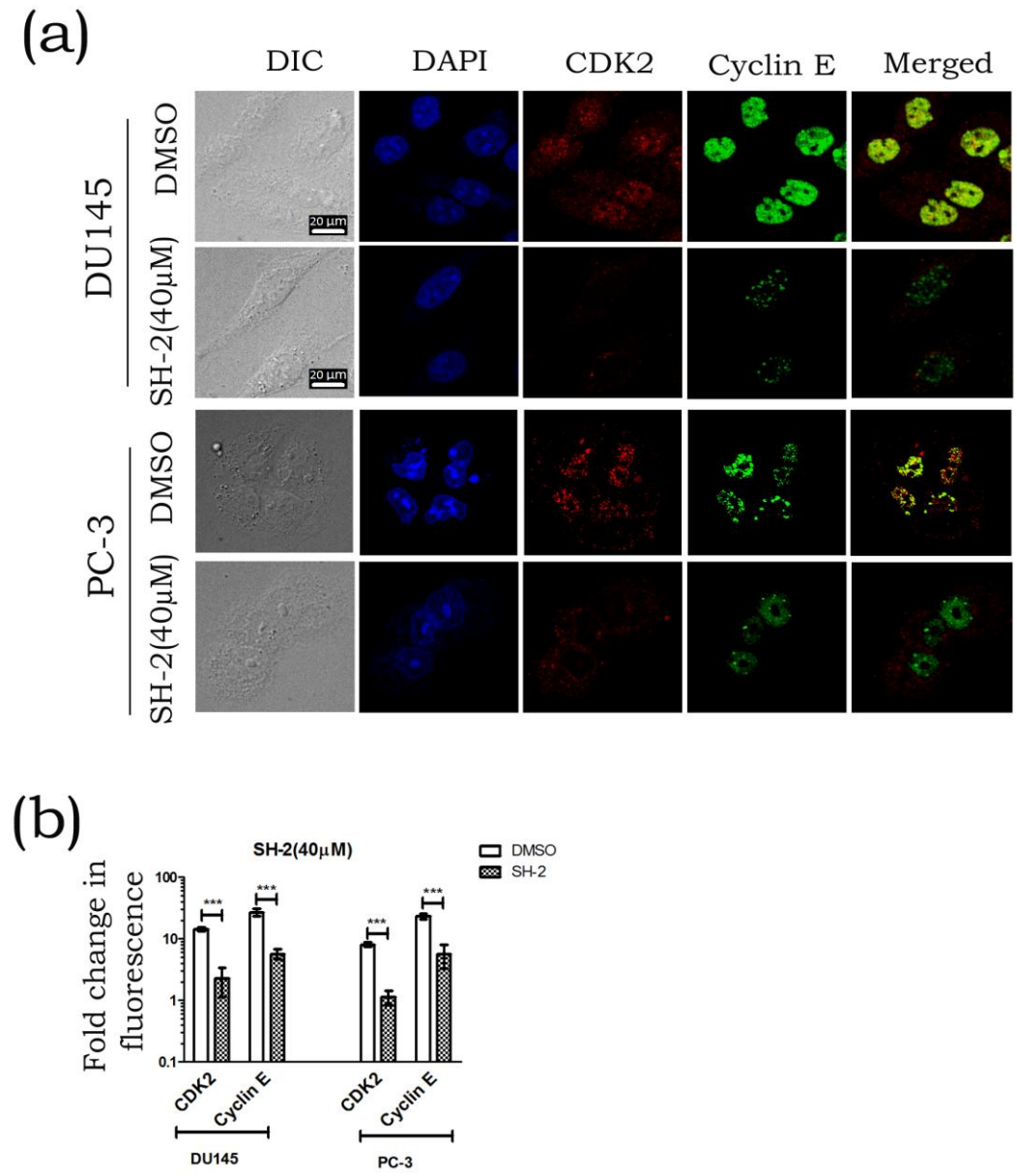

Figure. 3.11. Compound SH-1 inhibits nuclear localization of cyclin E and CDK2.

DU145 and PC-3 cells were plated on coverslips in 6-well plates and treated with 40µM of SH-2 for 48 hours. Cells were fixed in 4% PFA followed by permeabilization with 0.01% Triton-x-100. After incubating with respective primary (1:50 dilution) and secondary (1:10,000) FITC labeled antibody, cells were mounted on slides in antifade mounting media. DAPI was used to counterstain nucleus. Slides were observed at 60X under ANDOR SPINNING DISK confocal microscope using ANDOR iQ 2.7 software (scale bar: 20µm). (a) The merged image is showing co-localization of cyclin E and CDK2. (b) Quantitation from microscopic images was done using n number (n>50) of cells for each set. All experiments were repeated and yielded similar results. *p<0.05, **p<0.01 and ***p<0.001 represented as compared to control.

Further, we studied the cyclin E-associated CDK2 activity. Immunoprecipitation was carried out using whole cell lysate with anti-cyclin E antibody. The data indicated a clear inhibition of cyclin E-associated CDK2 activity by more than 90% in both cells post-24 hours treatment **(Fig. 3.10b)**. Immunofluorescence data indicated that in control cells, there was abundant expression of both cyclin E and CDK2 and that co-localized in the nucleus, as shown in the merged panel and in both cancer cell lines **(Fig. 3.11a).** SH-2 induced inhibition and cytoplasmic localization of CDK2 and inhibition of cyclin E in both cell lines **(Fig. 3.11a).** The quantification of cyclin E and CDK2 indicated about 32% and 41% inhibition in DU145, and about 30% and 48% inhibition in PC-3 cells **(Fig. 3.11b).**

Taken together, western blot, kinase activity, and localization data indicated that SH-2 inhibited cell cycle by inhibiting the cyclin E, cyclin D1 and associated "CDK2 activity".

3.3.7 SH-1 and SH-2 upregulated the nuclear expression of p21 and BRCA1 in DU145 and PC-3

The CDK inhibitor p2 blocks the interaction of "cyclinA-CDK2" as well as "cyclin E-CDK2" and prevents cell cycle progression and proliferation. The expression of p21 was accessed in both cancer cells treated with either of the compound. Western blotting data showed significant upregulation of p21 24 hours-treatment onwards and that increased with the incubation time. By 72 hours of treatment with either compound, p21 expression was upregulated by 3-4 fold in DU145 and 6-7 fold in PC-3 cells **(Fig. 3.12b).** Tumor suppressor protein p53 regulates the expression of p21. But PC-3 is $p53^{-/-}$ cell line. Therefore we looked for another upstream transcriptional regulator of p21. Many studies have shown that tumor suppressor protein BRCA1 transcriptionally activates p21 (**Fig. 3.12a)**. BRCA1 expresses in both DU145 and PC-3 and its expression was checked in compound treated cancer cells. Western blotting data showed a prominent increase in BRCA1 expression post 72 hours treatments with SH-1, 8-11 fold increase, and SH-2, 4 fold increase, in both cancer cells **(Fig. 3.12b**). BRCA1 upregulation by either compound in both cell lines was in corroboration with the upregulation of p21 **(Fig. 3.12b**). With increase in the treatment time, both p21 and BRCA1 were further upregulated.

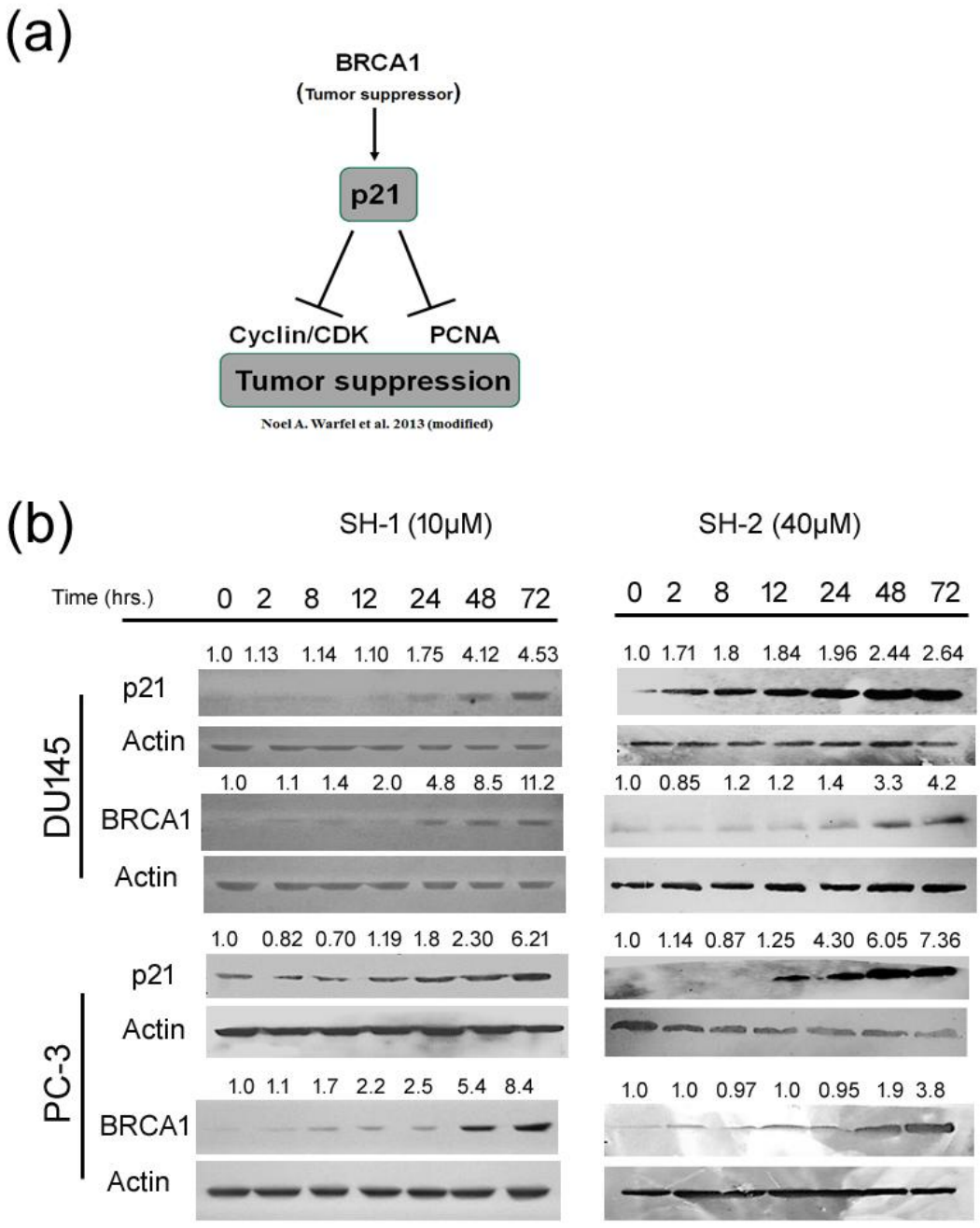

Figure. 3.12. Compound SH-1 and SH-2 induce expression of BRCA1 and p21.

(a) Flow diagram of p21 showing regulation and its downstream signaling. Cells were plated and after overnight incubation treated with10μM and 40μM of compounds SH-1 and SH-2 respectively for the indicated time. (b) Western blot showing the protein expression of p21 and BRCA1 in both cancer cells. Actin served as a loading control. Each blot was quantitated and normalized with actin, and the values were represented as relative to the control. All experiments were repeated and yielded similar results.

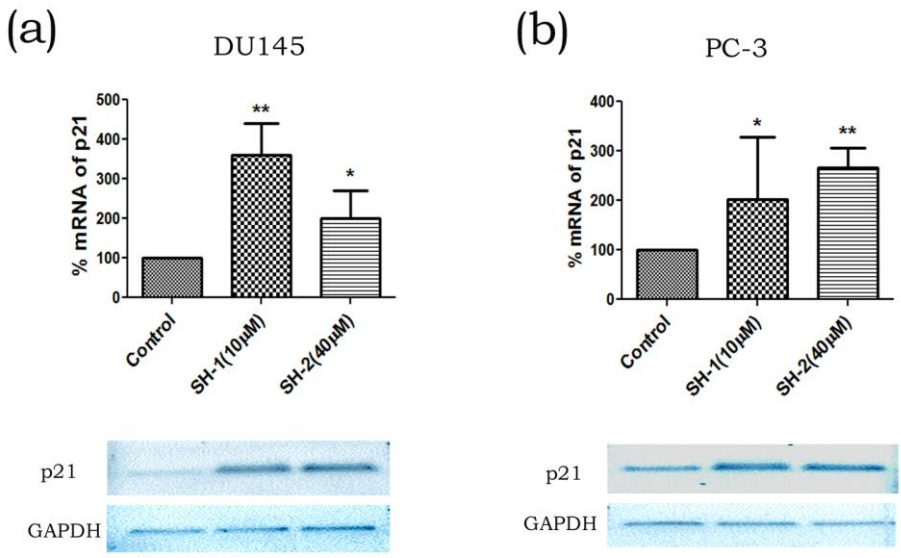

Figure. 3.13. Compound SH-1 and SH-2 induce expression p21-mRNA.

Cells were plated and after overnight incubation treated with10μM and 40μM of compounds SH-1 and SH-2 respectively for 72 hours. Total RNA was isolated using QIAzol method, and cDNA was prepared. Quantitative PCR was done using a SYBR-green master mix. Corresponding CT values were normalized to control and plotted values in (a) DU145 and (b) PC-3. All experiments were repeated and yielded similar results. *p<0.05, **p<0.01 represented as compared to control.

In addition to the protein level, the p21 mRNA level were also examined. Real-time data showed that p21 mRNA was upregulated by 2-3 fold in DU145 **(Fig. 3.13a)** and by 2-2.5 fold in PC-3 **(Fig. 3.13b)** cells by the either compound. The cellular localization of BRCA1 and p21 are known to play an important role in apoptosis, therefore, we next checked the cellular localization of BRCA1 and p21 upon treatment with either compound. Immunofluorescence data showed a very low expression of BRCA1 and p21 in the untreated cells. In compound treated cells, both BRCA1, and p21 localized majorly to the nucleus. The merged panel indicated that BRCA1 interacts with p21 in nucleus upon compound treatments in both DU145 **(Fig. 3.14a)** and PC-3 **(Fig. 3.15a)**. The quantification of BRCA1 and p21 indicated about 40-50% increase in the expression of both p21 and BRCA1 in DU145 **(Fig. 3.14b)**. In SH-2-treated PC-3 cells, BRCA1 was upregulated by about 60% and p21 was induced by about 35% **(Fig. 3.15b)**.

These data suggested that both compounds induced BRCA1 that might have increased the expression of p21 in both cancer cell lines.

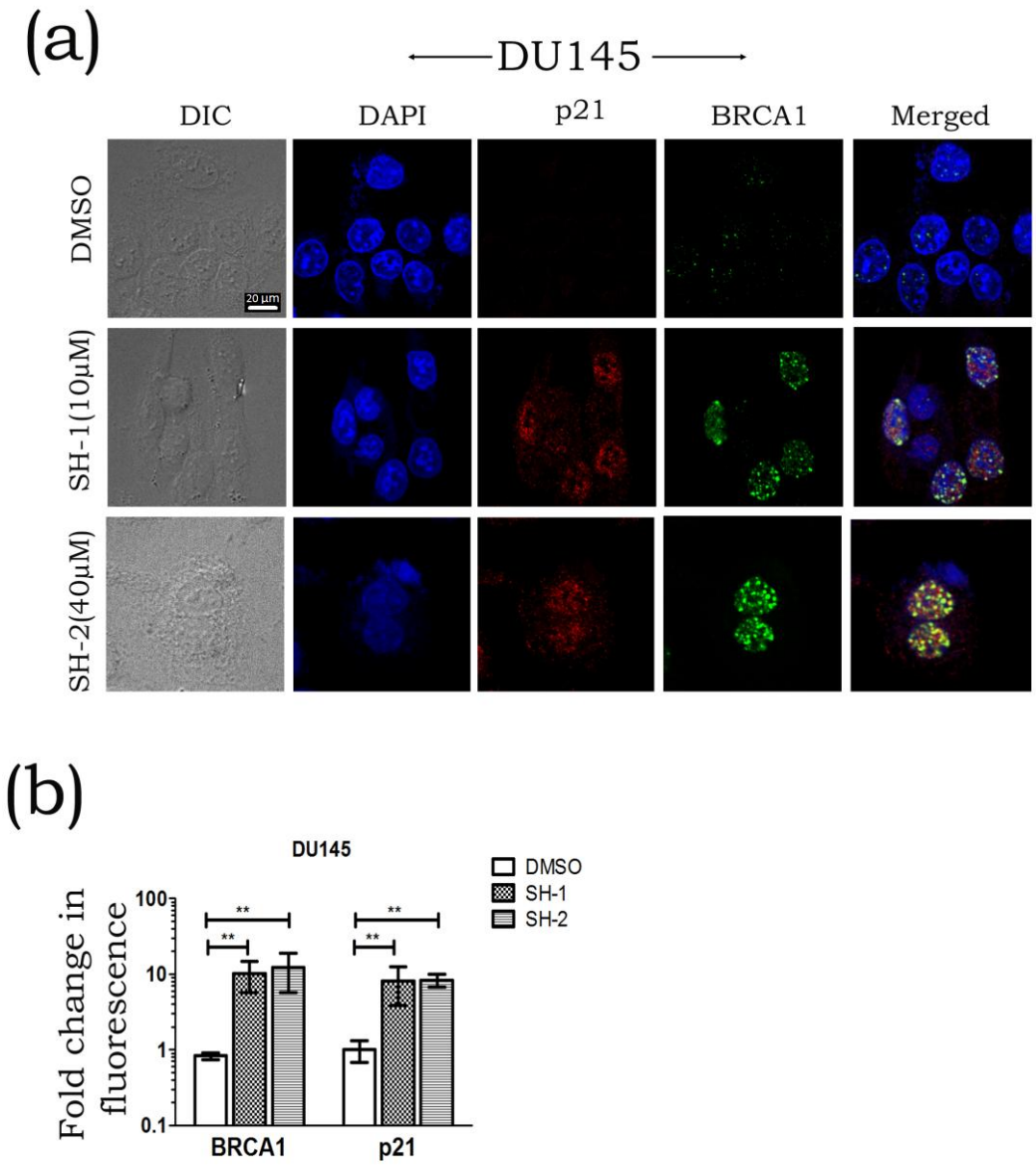

Figure. 3.14. Compound SH-1 and SH-2 induce nuclear localization of BRCA1 and p21 in the DU145 cell.

DU145 cells were plated on coverslips in 6-well plates and treated with10µM and 40µM of compounds SH-1 and SH-2 respectively for 48 hours. Cells were fixed in 4% PFA followed by permeabilization with 0.01% Triton-x-100. After incubating with BRCA1 and p21 primary (1:50 dilution) and secondary (1:10,000) FITC labeled antibody, cells were mounted on slides in antifade mounting media. DAPI was used to counterstain nucleus. Slides were observed at 60X under ANDOR SPINNING DISK confocal microscope using ANDOR iQ 2.7 software (scale bar: 20µm). (a) The merged image is showing co-localization of BRCA1 and p21. (b) Quantitation from microscopic images was done using n number (n>50) of cells for each set. All experiments were repeated and yielded similar results. *p<0.05, **p<0.01 and ***p<0.001 represented as compared to control.

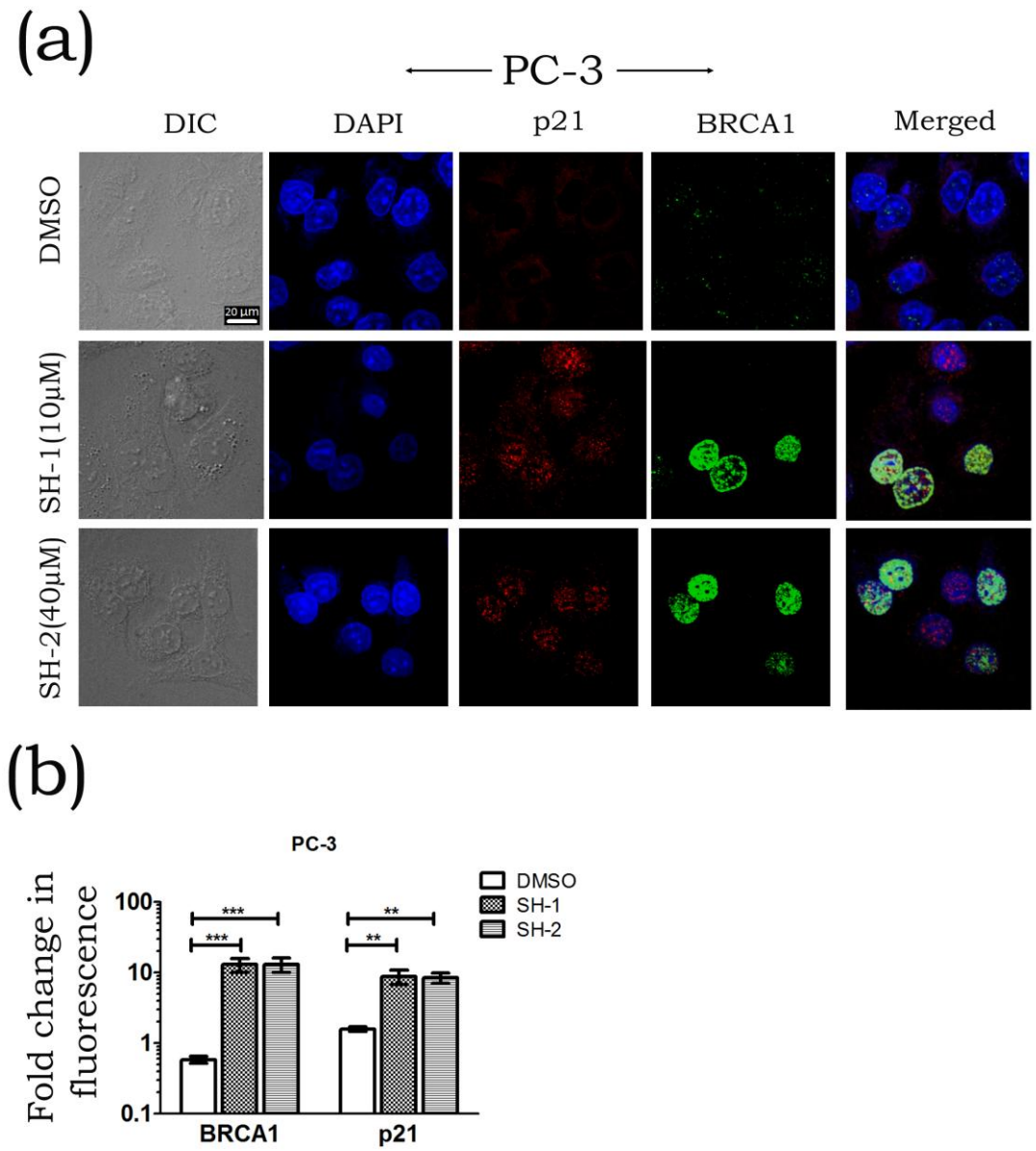

Figure. 3.15. Compound SH-1 and SH-2 induce nuclear localization of BRCA1 and p21 in the PC-3 cell.

PC-3 cells were plated on coverslips in 6-well plates and treated with10μM and 40μM of compounds SH-1 and SH-2 respectively for 48 hours. Cells were fixed in 4% PFA followed by permeabilization with 0.01% Triton-x-100. After incubating with BRCA1 and p21 primary (1:50 dilution) and secondary (1:10,000) FITC labeled antibody, cells were mounted on slides in antifade mounting media. DAPI was used to counterstain nucleus. Slides were observed at 60X under ANDOR SPINNING DISK confocal microscope using ANDOR iQ 2.7 software (scale bar: 20μm). (a) The merged image is showing co-localization of BRCA1 and p21. (b) Quantitation from microscopic images was done using n number (n>50) of cells for each set. All experiments were repeated and yielded similar results. *p<0.05, **p<0.01 and ***p<0.001 represented as compared to control.

3.3.8 SH-1 and SH-2 inhibited PCNA, associated with p21 in DU145 and PC-3

The p21 binds and inhibits PCNA, a key agent in DNA replication. Next, the question was asked whether PCNA was getting affected or not by either compound. Western blotting data indicated that both SH-1 and SH-2 inhibited PCNA in both cell lines **(Fig. 3.16)**.

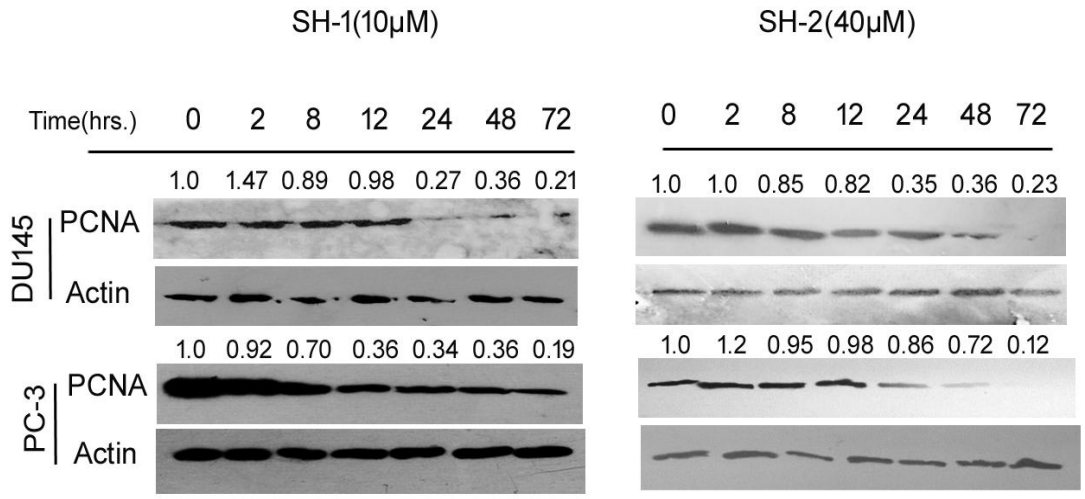

Figure. 3.16. Effect of subcytotoxic concentrations of SH-1 and SH-2 on PCNA expression.

Cells were plated and after overnight incubation treated with10μM and 40μM of compounds SH-1 and SH-2 respectively for the indicated time. Western blot showing the protein expression of PCNA in both cancer cells. Actin served as a loading control. Each blot was quantitated and normalized with actin, and the values were represented as relative to the control. All experiments were repeated and yielded similar results.

The densitometry values of respective blots showed about 80-90% PCNA inhibition by 72 hours in presence of either of the compound in both cancer cells (**Fig. 3.16)**. Studies have reported that p21 has a binding site for PCNA at its c-terminus **(Fig. 3.17a)**. p21 interacts with PCNA and inhibits its DNA synthesis capability (Cayrol et al., 1998).

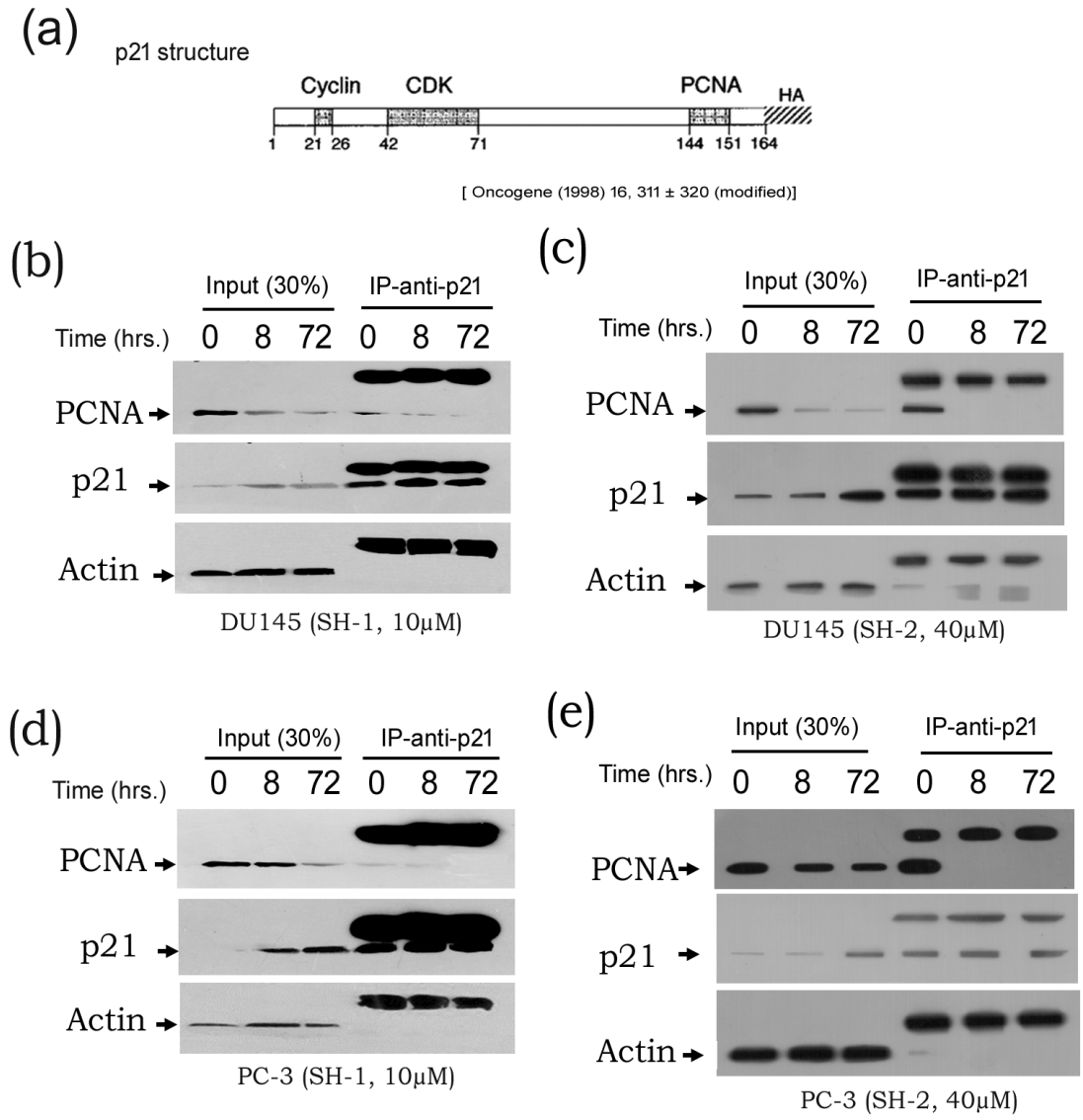

Figure. 3.17. SH-1 SH-2 induce the p21 associated inhibition of PCNA in DU145 and PC-3.

(a) p21 structure, showing PCNA binding domain. Briefly, cells were plated and after overnight incubation, treated with 10μM of SH-1 and 40μM of SH-2 for the indicated time. 400μg protein was used for immunoprecipitation with anti-p21. IP beads were used to run the SDS-PAGE. Western blot showing the protein expression of PCNA and p21 in DU145 (b) & (c) and PC-3 (d) & (e). All experiments were repeated and yielded similar results.

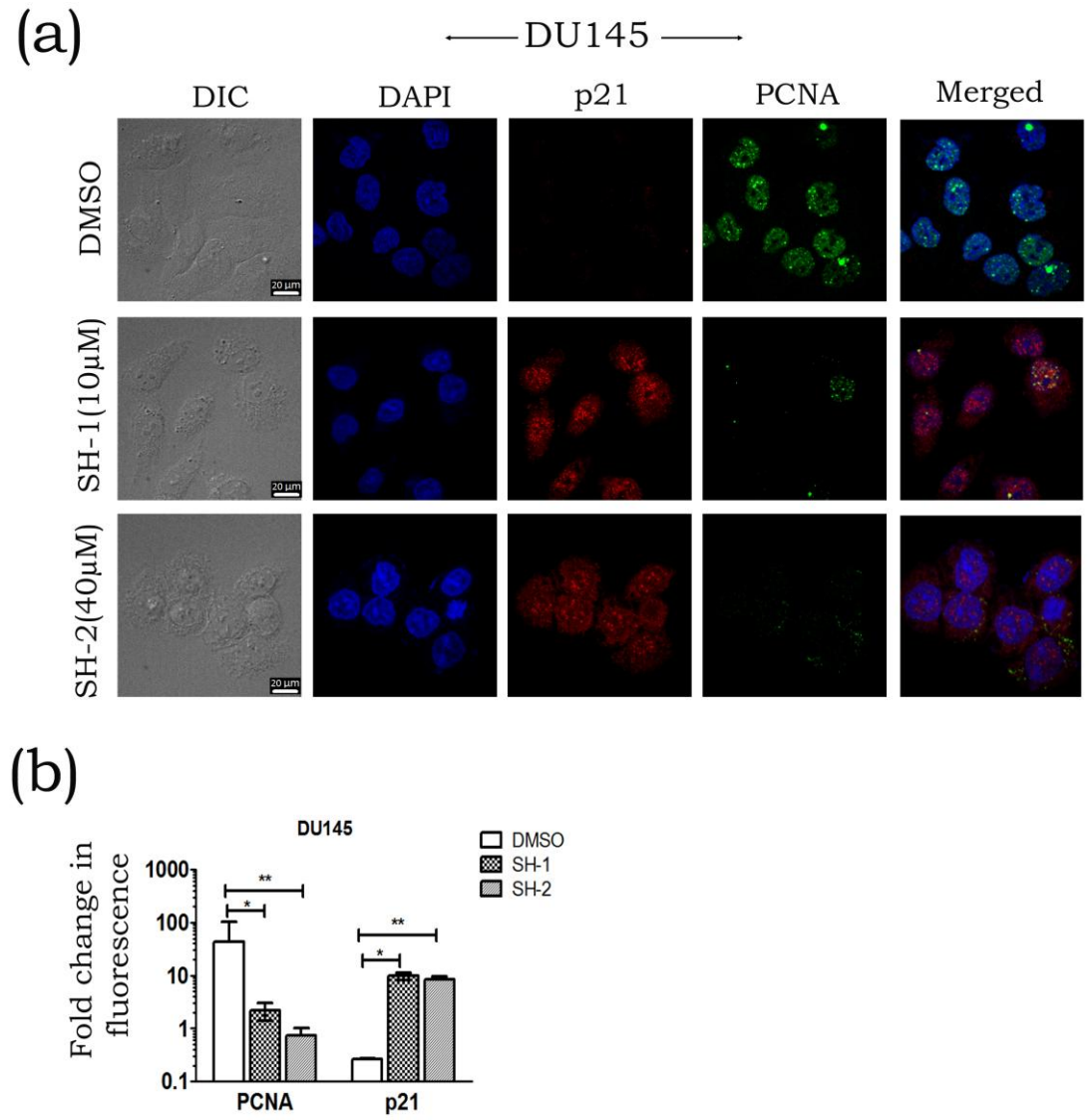

Figure. 3.18. Compound SH-1 and SH-2 inhibits nuclear expression of PCNA in DU145 cell.

DU145 cells were plated on coverslips in 6-well plates and treated with10µM and 40µM of compounds SH-1 and SH-2 respectively for 48 hours. Cells were fixed in 4% PFA followed by permeabilization with 0.01% Triton-x-100. After incubating with PCNA and p21 primary (1:50 dilution) and secondary (1:10,000) FITC labeled antibody, cells were mounted on slides in antifade mounting media. DAPI was used to counterstain nucleus. Slides were observed at 60X under ANDOR SPINNING DISK confocal microscope using ANDOR iQ 2.7 software (scale bar: 20µm). (a) The merged image is showing localization of PCNA and p21. (b) Quantitation from microscopic images was done using n number (n>50) of cells for each set. All experiments were repeated and yielded similar results. *$p<0.05$, **$p<0.01$ represented as compared to control.

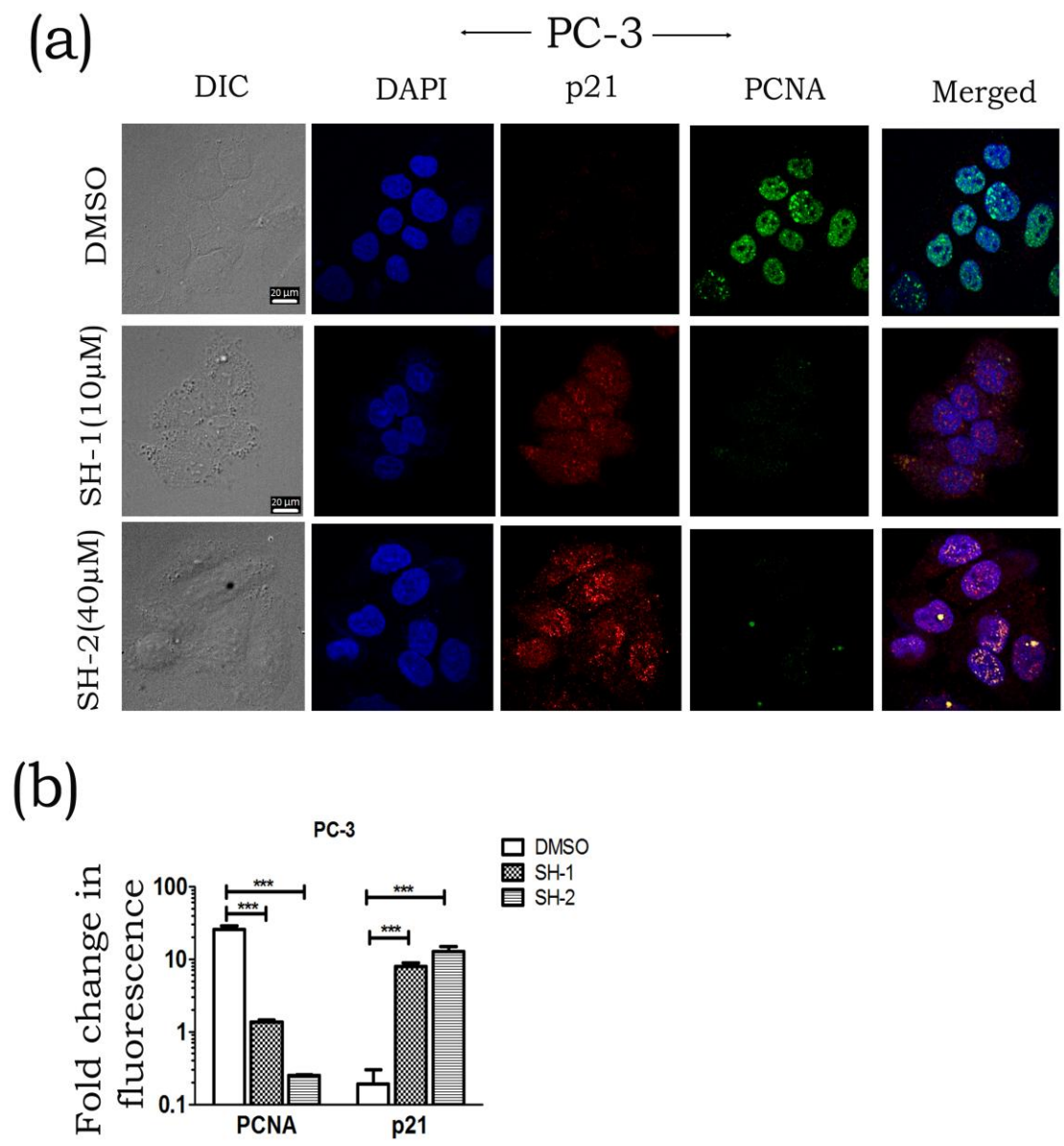

Figure. 3.19. Compound SH-1 and SH-2 inhibits nuclear expression of PCNA in the PC-3 cell.

PC-3 cells were plated on coverslips in 6-well plates and treated with10μM and 40μM of compounds SH-1 and SH-2 respectively for 48 hours. Cells were fixed in 4% PFA followed by permeabilization with 0.01% Triton-x-100. After incubating with PCNA and p21 primary (1:50 dilution) and secondary (1:10,000) FITC labeled antibody, cells were mounted on slides in antifade mounting media. DAPI was used to counterstain nucleus. Slides were observed at 60X under ANDOR SPINNING DISK confocal microscope using ANDOR iQ 2.7 software (scale bar: 20 m). (a)The merged image is showing localization of PCNA and p21. (b) Quantitation from microscopic images was done using n number (n>50) of cells for each set. All experiments were repeated and yielded similar results. ***p<0.001 represented as compared to control.

As shown in figure 3.12 and 3.16, both compounds induced the expression of p21 and inhibited PCNA, we next checked whether the inhibition in PCNA was associated with p21-upregulation. Immunoprecipitation was carried out using whole cell lysate with anti-p21 antibody and blotted with p21 and PCNA. Immunoprecipitation-western data of untreated cells (control) showed the PCNA expression, whereas SH-1 **(Fig. 3.17b and d)** and SH-2 **(Fig. 3.17c and e)** treated cells showed drastic decrease in PCNA expression by 72 hours. Also IP-blot of p21 showed upregulation in both cancer cells and that might have inhibited its association with PCNA. Next, we checked the cellular localization of PCNA. Immunofluorescence data showed the nuclear expression of PCNA in untreated cells. Treatment with either SH-1 or SH-2 inhibited nuclear PCNA in DU145 **(Fig. 3.18a)** and PC-3 **(Fig. 3.19a)**. The quantification of PCNA and p21 was done and showed an inhibition of PCNA by 58% and 70% and upregulation of p21 by 90% and 80% in SH-1 and SH-2 treated DU145 cells respectively **(Fig. 3.18b)**. In PC-3 cells, SH-1 and SH-2 induced p21 upregulation by 80% and 85%, and inhibited PCNA level by 60% and 90% respectively **(Fig. 3.19b)**.

These data suggested p21 upregulation, induced by SH-1 or SH-2, might have rendered the inhibition of PCNA in both cancer cell lines and that would have resulted in cell cycle arrest.

3.3.9 SH-1 and SH-2 induced proteasomal degradation of replication protein PCNA in DU145 and PC-3

Previous studies have shown that PCNA degradation takes place via ubiquitination (Matunis, 2002). To study whether either compound-induced inhibition of PCNA follows the notion, we used MG132, a proteasome inhibitor. SH-1 or SH-2 treatments were given with or without MG132 and protein expression was examined by the western blot.

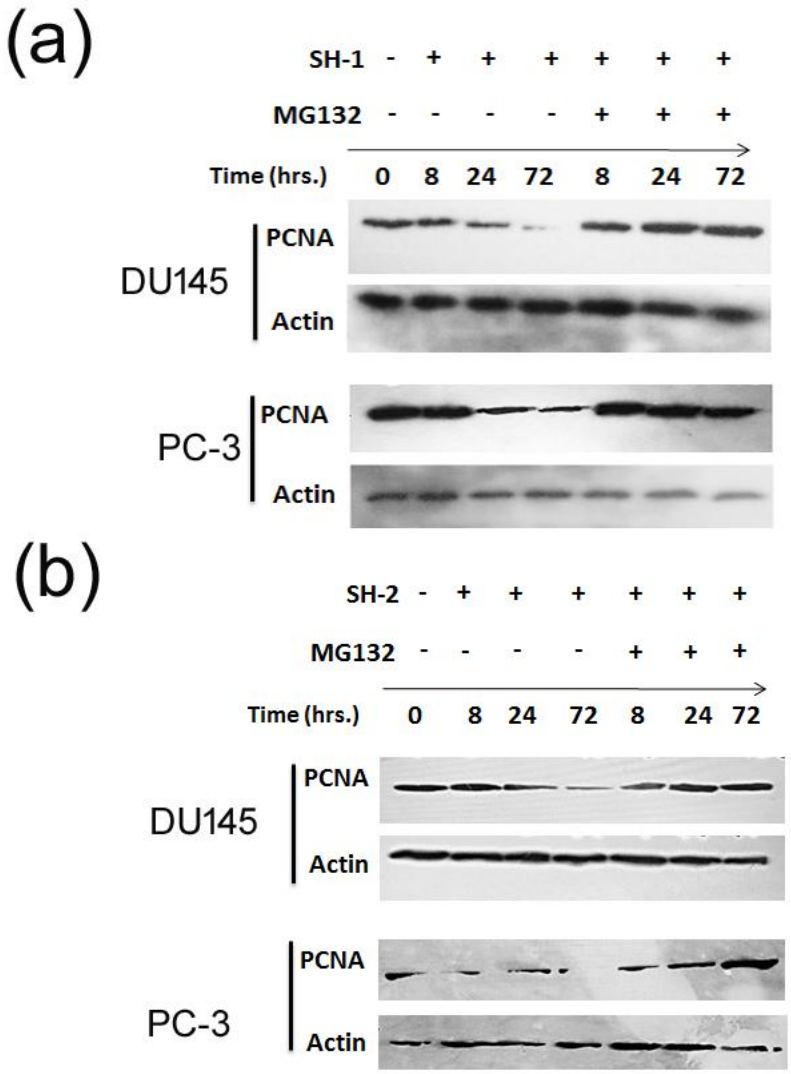

Figure. 3.20. SH-1 and SH-2 cause proteasome-mediated degradation of PCNA in DU145 and PC-3.

Cells were seeded in 6-well plates and after overnight incubation and treated with either (a) SH-1 or (b) SH-2 in the absence or presence of proteasome inhibitor MG132 (final concentration 10μM). Cells were incubated for the indicated time points. Western blots showed that MG132 rescued the inhibition of PCNA by either compound in both cancer cells.

The data showed reduction in PCNA in absence of the proteasomal inhibitor, MG132, but this is blocked when MG132 is used, suggesting clearly that the compounds induced PCNA proteasomal degradation in both cancer cell lines in a time dependent manner **(Fig. 3.20)**.

These results suggested that PCNA, an important player in DNA synthesis, was rendered to proteasomal degradation by SH-1 and SH-2 in DU145 and PC-3 cell lines.

3.4. Discussion

Most of the present available cancer therapies involve not only higher dosage but also long term administration. In most of the cases, cancer treatment results in systemic toxicity and drug resistance. An ideal drug should be more efficient at lowest possible doses in order to avoid undesired damages to the healthy tissues. In conversant with this notion, cell cycle evaluation was done with the subcytotoxic concentrations of SH-1 and SH-2, the minimum concentrations which induced significant toxicity in MTT experiments, shown in chapter-2. The *in-vitro* cell cycle data demonstrated that treatment of prostate cancer cells with these compounds resulted in cell cycle arrest. SH-1 arrested cells in S-phase and compound SH-2 did that in G_1 phase of the cell cycle. Most of the available anti-cancer drugs are used for prolonged time causing severe discomfort to the patients. Withdrawn of the drugs results in relapse of the disease. This might be due to the revival of proliferation of the cancerous cells after removal of the drug. We checked what happens when the compounds were removed 72 hours post-treatment. Our *in-vitro* withdrawal cell cycle data showed that cell cycle was adversely affected even three days post withdrawal, though the cell death was more when treated continuously for 6 days. The data showing the increase in cell death even after the withdrawal, inferred to the inability of cells recovery once they were exposed to either compound. The sub-G_1 population, which represents the dead cells, increased with the increase in exposure time. After 6-days of treatments, owing to the increase in cell death, various distinct cellular populations could not be observed. As discussed above, the adverse effects of cancer drugs on noncancer healthy tissues present a serious pathological drawback. The compounds were also evaluated on the noncancer cells, NIH-3T3. The cell cycle data in the NIH-3T3 suggested that both compounds at their respective IC_{50} concentrations exerted a considerable amount of polyploidy and death. However, at the subcytotoxic concentrations of SH-1 and SH-2, which are much lower than their IC_{50} values, fibroblast cells were not affected, indicating the

dose-dependent response of compounds. These data strengthened the notion that at a lower concentration, compounds kill cancer cells selectively. So these compounds were further characterized only at subcytotoxic concentrations.

Both compounds induced morphological changes selectively in the cancerous cells that lead to inhibition of cell proliferation and ultimately cell death. The wound healing data showed significant inhibition of cell migration in cancerous cell which further supported SH-1 and SH-2 as a potent inhibitor of cancer cell proliferation. On the other hand the cell morphology and cell proliferation of noncancer fibroblast cell lines were unaffected.

A cell cycle is executed by time bound expression and regulation of cyclins/CDKs complexes and their inhibition can result in cell cycle blockage (Vermeulen,K.,Van Bockstaele,D.R.,Berneman et al., 2003). Western data showed that compound SH-1 inhibited cyclin A and cyclin A-associated CDK2 activity**.** SH-2 inhibited cyclin D1 and cyclin E and cyclin E-associated CDK2 activity**.** These data reinstated that SH-1 arrested cells at S-phase were brought about by the inhibition of S-phase-specific cyclin A-CDK2 interaction and SH-2 resulted G_1-phase arrest was by the inhibition of G_1 specific cyclin E-CDK2 interaction. Further, both the compounds resulted in an elevated level of mRNA and protein expression level of p21, a CDK inhibitory protein known to inhibit the cyclin E-CDK2 and cyclin A-CDK2 interaction and thus the kinase activity (Jin et al., 2003). Both the compounds induced p21 nuclear localization and CDK2 cytoplasmic localization in both cells. The increased level of p21 might have cross-talked to cyclin-CDK complex thus brining about their dissociation and disruption of the cell cycle. Tumor suppressor protein p53 is a well-known transcriptional regulator of p21 and is implicated in cell proliferation and apoptotic function (El-Deiry et al., 1993). p21 can also perform its inhibitory function independent of p53 (Galanos et al., 2016; Karimian et al., 2016; Macleod et al., 1995). It is known that tumor suppressor protein, BRCA1 can transcriptionally regulate p21 (Abbas and Dutta, 2009; Somasundaram, 2003). PC-3 cells are $p53^{-/-}$ cell line therefore we checked BRCA1, one of the upstream regulators of p21. Our western data suggested the upregulation of BRCA1 by both compounds individually and that was coherent with the p21 upregulation. Immunofluorescence data suggested that both BRCA1 and p21 localize to the nucleus upon treatments. p21 is unique among the known CKIs in a way that it has two binding sites. N-terminus

interacts and inhibits the cyclin-CDK complexes, and control cell cycle progression. C-terminus interacts and inhibits the DNA polymerase processivity factor, PCNA, and halts DNA replication (Cayrol et al., 1998). Our western blotting data indicated a considerable amount of inhibition of PCNA by SH-1 and SH-2. Both compounds induced p21 that might have inhibited the PCNA. PCNA inhibition resulted in the halt of DNA synthesis and inturn replication block. To show the effect of compounds on p21-PCNA interaction, IP was done. There was inhibition of p21-PCNA interaction in the treated cancer cells. Our microscopic data revealed that treatment with either compounds reduced the expression of nuclear PCNA. Further to check whether the decrease in PCNA level is due to proteasomal degradation, cells were treated with MG132, "a proteasome inhibitor". In the absence of the proteasomal inhibitor, reduction in PCNA level was observed, but this reduction was blocked in the MG132 treated cells, suggesting clearly that the compounds induced proteasomal degradation of PCNA in both cancer cell lines. This in turn resulted in the replication block.

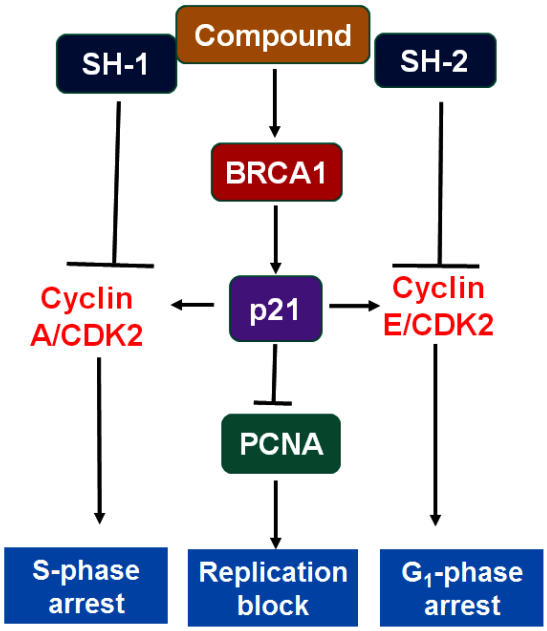

Figure. 3.21. Proposed model for mechanism of action of SH-1 and SH-2.

Compound SH-1 and SH-2 induce BRCA1 which in turn upregulates p21. P21 inhibits PCNA and that blocks replication. The induced p21 also inhibits cyclinA-CDK2 and cyclinE-CDK2 interaction by SH-1 and SH-2 respectively that brings about S-phase or G_1-phase arrest of cell cycle respectively.

A model for the possible mechanism of action was proposed based on the data obtained **(Figure. 3.21)**. Both compounds SH-1 and SH-2 induced BRCA1 which in turn upregulated the expression of p21. p21 inturn inhibited PCNA and resulted in replication block . The induced p21 also inhibited cyclinA-CDK2 and cyclinE-CDK2 interaction that brought about cell cycle arrest at S -phase or G_1-phase respectively. The present study suggested that these compounds might prove to be promising antiproliferative agents in metastatic prostate cancer cell lines, DU145 and PC-3.

3.5. References

Abbas, T. and Dutta, A. (2009). 'P21 in Cancer: Intricate Networks and Multiple Activities'. *Nature Reviews Cancer*, 9(6): 400–414.

Boss, D.S., Schwartz, G.K., Middleton, M.R., Amakye, D.D., Swaisland, H., Midgley, R.S., Ranson, M., et al. (2009). 'Safety, tolerability, pharmacokinetics and pharmacodynamics of the oral cyclin-dependent kinase inhibitor AZD5438 when administered at intermittent and continuous dosing schedules in patients with advanced solid tumours'. *Annals of Oncology*, 21(4): 884–894.

Cayrol, C., Knibiehler, M. and Ducommun, B. (1998). 'p21 binding to PCNA causes G1 and G2 cell cycle arrest in p53-deficient cells'. *Oncogene*, 16(3): 311–320.

Cazzalini, O., Perucca, P., Savio, M., Necchi, D., Bianchi, L., Stivala, L.A., Ducommun, B., et al. (2008). 'Interaction of p21CDKN1A with PCNA regulates the histone acetyltransferase activity of p300 in nucleotide excision repair'. *Nucleic Acids Research*, 36(5): 1713–1722.

Chen, R., Wierda, W.G., Chubb, S., Hawtin, R.E., Fox, J.A., Keating, M.J., Gandhi, V., et al. (2009). 'Mechanism of action of SNS-032, a novel cyclin-dependent kinase inhibitor, in chronic lymphocytic leukemia'. *Blood*, 113(19): 4637–4645.

Drobnjak, M., Osman, I., Scher, H.I., Fazzari, M. and Cordon-Cardo, C. (2000). 'Overexpression of cyclin D1 is associated with metastatic prostate cancer to bone'. *Clin Cancer Res*, 6(5): 1891–1895.

El-Deiry, W.S., Tokino, T., Velculescu, V.E., Levy, D.B., Parsons, R., Trent, J.M., Lin, D., et al. (1993). 'WAF1, a potential mediator of p53 tumor suppression'. *Cell*, 75(4): 817–825.

Funk, J.O., Waga, S., Harry, J.B., Espling, E., Stillman, B. and Galloway, D.A. (1997). 'Inhibition of CDK activity and PCNA-dependent DNA replication by p21 is blocked by interaction with the HPV-16 E7 oncoprotein.' *Genes & development*, 11(16): 2090–100.

Galanos, P., Vougas, K., Walter, D., Polyzos, A., Maya-Mendoza, A., Haagensen, E.J., Kokkalis, A., et al. (2016). 'Chronic p53-independent p21 expression causes genomic instability by deregulating replication licensing.' *Nature cell biology*, 18(7): 777–89.

Jin, Y.H., Choi, J.S., Shin, S., Lee, K.Y., Park, J.H. and Lee, S.K. (2003).

'Panaxadiol selectively inhibits cyclin A-associated Cdk2 activity by elevating p21WAF1/CIP1 protein levels in mammalian cells'. *Carcinogenesis*, 24(11): 1767–1772.

Johnson, D.G. and Walker, C.L. (1999). 'Cyclins and cell cycle checkpoints.' *Annual review of pharmacology and toxicology*, 39: 295–312.

Karimian, A., Ahmadi, Y. and Yousefi, B. (2016). 'Multiple functions of p21 in cell cycle, apoptosis and transcriptional regulation after DNA damage'. *DNA Repair*, 42: 63–71.

Macleod, K.F., Sherry, N., Hannon, G., Beach, D., Tokino, T., Kinzler, K., Vogelstein, B., et al. (1995). 'p53-Dependent and independent expression of p21 during cell growth, differentiation, and DNA damage'. *Genes and Development*, 9(8): 935–944.

Malumbres, M. and Barbacid, M. (2001). 'To cycle or not to cycle: a critical decision in cancer.' *Nature reviews. Cancer*, 1(3): 222–31.

Marshall, J.L., Bangalore, N., El-Ashry, D., Fuxman, Y., Johnson, M., Norris, B., Oberst, M., et al. (2002). 'Phase I study of prolonged infusion bryostatin-1 in patients with advanced malignancies'. *Cancer Biology and Therapy*, 1(4): 409–416.

Matunis, M.J. (2002). 'On the road to repair: PCNA encounters SUMO and ubiquitin modifications'. *Mol Cell*, 10(3): 441–442.

McClue, S.J., Blake, D., Clarke, R., Cowan, A., Cummings, L., Fischer, P.M., MacKenzie, M., et al. (2002). 'In vitro and in vivo antitumor properties of the cyclin dependent kinase inhibitor CYC202 (R-roscovitine).' *International journal of cancer. Journal international du cancer*, 102(5): 463–468.

Parry, D., Guzi, T., Shanahan, F., Davis, N., Prabhavalkar, D., Wiswell, D., Seghezzi, W., et al. (2010). 'Dinaciclib (SCH 727965), a novel and potent cyclin-dependent kinase inhibitor.' *Molecular cancer therapeutics*, 9(8): 2344–2353.

Pérez-tenorio, G., Berglund, F., Merca, A.E., Nordenskjöld, B.O., Rutqvist, L.E., Skoog, L. and Stål, O. (2006). 'Cytoplasmic p21 WAF1 / CIP1 correlates with Akt activation and poor response to tamoxifen in breast cancer'. *International Journal of Oncology*: 1031–1042.

Phelps, M.A., Lin, T.S., Johnson, A.J., Hurh, E., Rozewski, D.M., Farley, K.L., Wu,

D., et al. (2009). 'Clinical response and pharmacokinetics from a phase 1 study of an active dosing schedule of flavopiridol in relapsed chronic lymphocytic leukemia'. *Blood*, 113(12): 2637–2645.

Puyol, M., Mart??n, A., Dubus, P., Mulero, F., Pizcueta, P., Khan, G., Guerra, C., et al. (2010). 'A Synthetic Lethal Interaction between K-Ras Oncogenes and Cdk4 Unveils a Therapeutic Strategy for Non-small Cell Lung Carcinoma'. *Cancer Cell*, 18(1): 63–73.

Rowinsky, E.K., Rizzo, J., Ochoa, L., Takimoto, C.H., Forouzesh, B., Schwartz, G., Hammond, L.A., et al. (2003). 'A phase I and pharmacokinetic study of pegylated camptothecin as a 1-hour infusion every 3 weeks in patients with advanced solid malignancies.' *Journal of clinical oncology : official journal of the American Society of Clinical Oncology*, 21(1): 148–157.

Somasundaram, K. (2003). 'Breast cancer gene 1 (BRCA1): role in cell cycle regulation and DNA repair--perhaps through transcription.' *Journal of cellular biochemistry*, 88(6): 1084–91.

Toogood, P.L., Harvey, P.J., Repine, J.T., Sheehan, D.J., VanderWel, S.N., Zhou, H., Keller, P.R., et al. (2005). 'Discovery of a potent and selective inhibitor of cyclin-dependent kinase 4/6'. *Journal of Medicinal Chemistry*, 48(7): 2388–2406.

Vermeulen,K.,Van Bockstaele,D.R.,Berneman, Z.N., Vermeulen, K., Van Bockstaele, D.R. and Berneman, Z.N. (2003). 'The cell cycle:a review of regulation,deregulation and therapeutic targets in cancer'. *Cell Proliferation*, 36(3): 131–149.

Warfel, N.A. and El-Deiry, W.S. (2013). 'p21WAF1 and tumourigenesis'. *Current Opinion in Oncology*, 25(1): 52–58.

CHAPTER-4

INHIBITION OF p38MAPK PATHWAY

4.1. Introduction

Cell signaling is indispensable for the proper functioning and cellular integrity. Several intracellular signaling pathways are involved in cell communication in response to stimuli. The p38MAPK, a stress-activated kinase, is triggered by the external conditions like "oxidative stress, exposure to UV radiations, heat and chemical signals, and pro-inflammatory cytokines like tumor necrosis factor and interleukin1 (Del Reino et al., 2014)." These environmental cues trigger a MAPK-associated cascade to render the downstream outcome of the signal. MAP kinases are proline-directed kinases and are activated when threonine and tyrosine residues present in their activation loop are phosphorylated. Four isoforms of p38 are present in the cells namely "p38α, p38β, p38γ and p38□" (Wang et al., 2008). p38α is extensively studied and involved in eliciting various stress associated cellular responses. Cytokines confer resistance during the treatment of cancer and play a major role in triggering the differentiation role of p38MAPK (Winzen et al., 1999; Zarubin and Han, 2005). The cell survival function of p38 comprises the phosphorylation of "Activating Transcription Factor-2 or ATF-2". Studies have reported that ATF-2 can crosstalk with many cell cycle associated proteins and thereby promote the cell proliferation (Persengiev and Green, 2003). The cell survival functions of ATF-2 are also attributed to its ability to inhibit the pro-apoptotic proteins and bring about the p38-associated evasion of apoptosis in many cancer (Walluscheck et al., 2013). It can also bind to the cyclins and modulate the cell cycle checkpoints. Some studies have also shown that ATF-2 induces the transcription of NF-κb and promote the expression of proto-oncogenes like cyclin D1 and c-Myc (Joyce et al., 1999). In addition to that, the "survival role of p38" has been shown to be associated with phosphorylation of MK2. The phosphorylated MK2 further phosphorylates Hsp27, "the small heat shock protein" which has been reported in promoting processes, such as "actin organization, chaperoning, ROS-inhibition, inhibition of apoptosis etc." (Arrigo et al., 2005). The various functions of

phosphorylated and unphosphorylated forms of Hsp27 have been reported and are summarized **(Fig. 4.1)**.

In this chapter, the molecular docking of SH-1 and SH-2 was done to determine the possible interaction sites on the p38MAPK protein. Structurally MAP kinase p38 has two important binding sites which are "ATP and DFG (Asp-Phe-Gly) binding site." These binding sites regulate the activation of p38. Molecular docking is based on "lock-and-key" mechanism which provides the best possible and stable ligand/target-protein complex. The stable is this complex the higher is the binding affinity of ligand and the target protein. Computational docking is used to screen large libraries of compounds and refine these compounds to a manageable subset. Docking is based upon algorithms that are encoded with the chemical interactions and associated forces that play a role in the interaction between two molecules. Majorly, two specifications are assigned to the "docking program," to successfully define a possible interaction between target and ligand. One is "search algorithm" and other is "scoring function". "Glide molecular docking software (Friesner et al., 2006)" provides a virtual screening of compounds at the two high accuracy level. First, it scans the compounds at high-throughput and filters out non-specific interactions. Secondly, all possible interacting compounds are passed through extremely accurate-binding criteria. The receptor protein, to which all potential ligands are directed, usually takes the structure of a grid in the "GLIDE-based docking".

Docking program with these two compounds were done for all the 4 isoforms of p38. Out of these, p38α showed the best results. In chapter-3, both SH-1 and SH-2 inhibited cell proliferation in both cancer cells; these compounds were further accessed for their effects on the phosphorylation of p38MAPK pathway, a stress-induced mitogen-activated protein kinase, Hsp27, a small heat shock protein and transcription factor ATF-2.

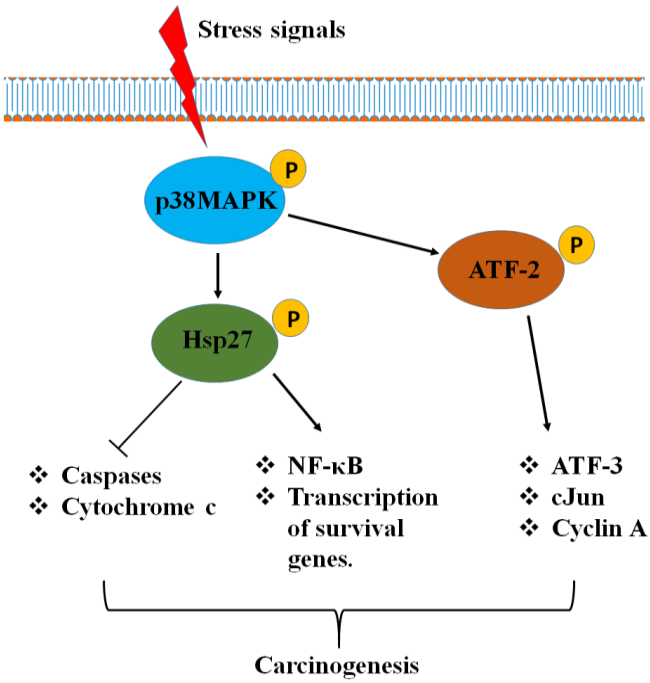

Figure. 4.1. Diagrammatic representation of the role of p38MAPK pathway in the promotion of carcinogenesis.

The environmental stress in cancer cells phosphorylates p38MAPK. The P-p38 phosphorylates its direct substrate ATF-2 which in turn activates the pro-survival genes viz. ATF-3, cJun and cyclin A. p38 also activates Hsp27 via MK2 pathway and triggers NF-κB pathway in the nucleus. P-Hsp27 promotes proliferation by inhibiting apoptotic machinery.

4.2. Methodology

4.2.1. Molecular docking of compounds

4.2.1.1. Protein preparation

The structure of the p38α protein "(PDB, id 1A9U" and "PDB, id 1KV2" co-crystallized with SB203580 and Birb 796 inhibitors were obtained from the "PDB database (www.rcsb.org)". Similarly, crystal structures of "human mitogen-activated protein kinase 11 or p38 beta" in complex with nilotinib (PDB id 3GDP), p38-gamma (PDB id 1CM8), and p38 delta kinase (PDB id 3COI), Human b-RAF bound to a DFG-Out inhibitor TAK-632 (PDB id 4KSP), Human c-ABL kinase domain bound with a DFG-Out inhibitor AP24534 (PDB id 3OXZ) were downloaded from PDB database (www.rcsb.org). The co-crystallized heteroatoms including inhibitors and water molecules with the protein structures were removed. Since all the protein structure were not complete, missing residues in all of them were constructed using

Prime module of GLIDE. The protein preparation wizard of GLIDE was exploited in preparing all the protein structure. Protein preparation wizard assigns bond orders and adds hydrogen atoms explicitly. Finally using the default "OPLS_2005" molecular mechanics force field, protein structures were minimized using "impref minimization wizard".

4.2.1.2. Inhibitor preparation

Chemical structure of Ligand SH-1 and SH-1 were drawn and converted to 3D format by clean in the 3D utility of Marvin sketch. Using Ligprep preparation wizard of GLIDE docking tool we prepared both SH-1 and SH-2 inhibitors, and a maximum of 32 tautomers for both the inhibitors in the pH range of 7.0±2.0 was generated.

4.2.1.3. Receptor Grid preparation and protein-ligand docking

We used two different grids for the docking of SH-1 and SH-2 inhibitors, one for the ATP and other for the DFG binding site. For DFG- out confirmation we used "Val-50, Lys-53, Ser-61, Arg-67, Glu-71, Leu-74, Val-83, Thr-106, Met-109, Ile-141, Ile-146, Arg-149, Ile-166, Asp-168, Phe-169, and Gly-170" (Gill et al., 2014). Since the all four isoforms of p38 map kinase share same DFG-binding site, thus we kept these residues constant for all the four isoforms. Since DFG-site is present in many other proteins and to study the binding efficiency SH-1 and SH-2 inhibitors, we also performed *in silico* docking for c-ABL and b-RAF proteins. The active sites for both the proteins were defined with residues "Glu (500), Thr (507), Trp (530), Cys (531), Gly (533), Asp (593), Phe (594) for b-RAF and residues Tyr (253), Glu (286), Thr (315), Phe (317), Met (318), Ile (360), His (361), Asp (381), Phe (382) for c-ABL protein". To prepare GRID of these active site residues, GLIDE grid preparation wizard was used. The size of the grid was restricted to 25Å and *in silico* docking was performed by keeping active site grid as rigid, and all tautomeric confirmations of the SH-1 and SH-2 inhibitors were treated as flexible. For ATP binding site we used different grid comprising of residues "Val -30, Ser-32, Gly- 33, Arg-34, Tyr-35, Val-38, Arg-51, Val-52, Lys-53, Glu-71, Leu- 74, Leu-75, Ile-84, Leu-86, Leu-104, Val-105, Thr-106, His-107, Leu-108, Met-109, Asp-112, Leu-167, Asp-168, Phe-169, Leu-171" (Gill et al., 2013).

4.2.1.4. Post-docking analysis

The post-docking analysis was performed using Xscore program, liginteraction suit available in Schrödinger program and chimera visualization tool was utilized for the preparation of figures.

4.2.2. Biological evaluation

4.2.2.1. Cell lines and reagents

Human prostate carcinoma cell lines, "DU145 and PC-3", and human fibroblast cell line, "NIH-3T3", were obtained from American Type Culture Collection and maintained as described in chapter-2. Antibodies used from santacruz were: ATF-2 total (sc-187), Hsp27 total (sc-59562) and actin (sc-1615). Antibodies; phospho-p38 (#9216), p38 total (#9212), phospho-ATF-2 (#9221) and phospho-Hsp27 (#2401) were obtained from cell signaling. ATF-2 fusion protein (#9224L) was obtained from cell signaling. Other chemicals, Histone H1 type3 (H5505), rhodamine123 (546054) and 2',7'-dichlorofluorescein diacetate (DCFH-DA) (D6883) were obtained from Sigma-Aldrich. QIAzol from QIAGEN (cat-79306), SYBER Green Mix from "Applied Biosystem" (4367659) and Verso cDNA synthesis kit from Thermo Scientific (AB-1453/B) were used. Other reagents were obtained in their high molecular grade.

4.2.2.2. Western blot

Western blot technique was used to check and analyze the expression level of the proteins in response to the synthetic compounds. The cells (7x 10^4/ml) were plated in 100mm dishes. **(The detail is provided in "Materials and methods" section of chapter-1)**.

4.2.2.3. Quantitative Real Time-PCR (qRT-PCR)

Real-time PCR of p38MAPK and Hsp27 was performed using the "Power SYBR-Green master mix" (Applied Biosystems) **(The detail is provided in "Materials and methods" section of chapter-3)**. Primer pairs and run method, used in the experiments, are listed in the appendix section.

4.2.2.4. *In-vitro* p38MAPK kinase assay

About 200µg of whole cell lysate was incubated with ~1µg of the anti-poshpho-p38MAPK primary antibody for 6 hours at 4°C on the end-to-end rotor in a 500-µl reaction volume. Subsequently, 40µl of equilibrated "protein A/G PLUS-Agarose beads" (santacruz) were incubated with the antibody–protein complex for overnight at 4°C. The beads were washed with ice-cold 1XPBS twice and suspended in 1X kinase assay buffer. The catalytic activity of p38MAPK was assayed in the reaction buffer containing kinase assay buffer, "100 µM [γ-^{32}P] ATP (6000 Ci/mmol)" and 2.5µg of ATF-2 fusion protein. Reaction mixtures were incubated at 30°C for 40 min and were stopped by boiling it with "Laemmli buffer" for 5 min at 100°C. The supernatant was run on the SDS–PAGE followed by staining and destaining. The phosphorylation level in "histone-H1" was analyzed by autoradiography of SDS–PAGE gel.

4.2.2.5. Immunofluorescence assay

The cellular localization of p38MAPK and Hsp27 was studied by immunofluorescence. Briefly, cancer cells ($7x10^3$ cells/ml) were seeded in 6-well plates over the coverslip and exposed to desired concentration of DMSO or either of the compound for the 48 hours **(The detail is provided in "Materials and methods" section of chapter-3)**.

4.2.2.6. Statistical analysis

All experiments were carried out minimally for three times. Statistical analyses were performed using "Graph Pad Prism software". Experimental data were expressed as means ±S.D. and the significance of differences was analyzed by "ANOVA test". Values of $P < 0.05$ were considered statistically significant. Blots were densitometrically quantitated.

4.3. Results

4.3.1. Molecular docking of SH-1 and SH-2 with p38α

We first performed molecular docking of SH-1 and SH-2 inhibitors with ATP and DFG binding sites of p38α. Our docking scores were much better for DFG site as compared to ATP binding site with Glide docking scores of -9.580 and -9.855 kcal/mol for DFG site in comparison to docking scores of -2.720 and -4.352 kcal/mol for ATP binding site. We later performed molecular docking for of SH-1 and SH-2 inhibitors to DFG sites of different isoforms of p38MAPK and also with other kinases (Human b-RAF and Human c-ABL kinase). Docking scores of -4.803, -4.565, -5.563, -2.892 and -2.595 kcal/mol were computed for SH-1 inhibitor against p38β, p38γ and p38□ kinases and Human b-RAF and Human c-ABL kinase. Similarly, computation of docking scores for SH-2 inhibitor for the p38 beta, gamma and delta kinases and human b-RAF and human c-ABL kinase was -4.809, -3.761, -5.421, -3.338 and -3.467 kcal/mol respectively **(Table. 4.1).** Post-docking analysis of SH-1 with DFG binding site demonstrates the formation of 3 hydrogen bonds, 16 hydrophobic interactions and 2 polar interactions between SH-1 and DFG site of p38 alpha **(Fig. 4.2 and Table. 4.1).** Also, post-docking analysis of SH-2 with DFG binding site demonstrates the formation of 2 hydrogen bonds, 16 hydrophobic interactions and 2 polar interactions between SH-2 and DFG site of p38 alpha **(Fig. 4.3 and Table. 4.2).**

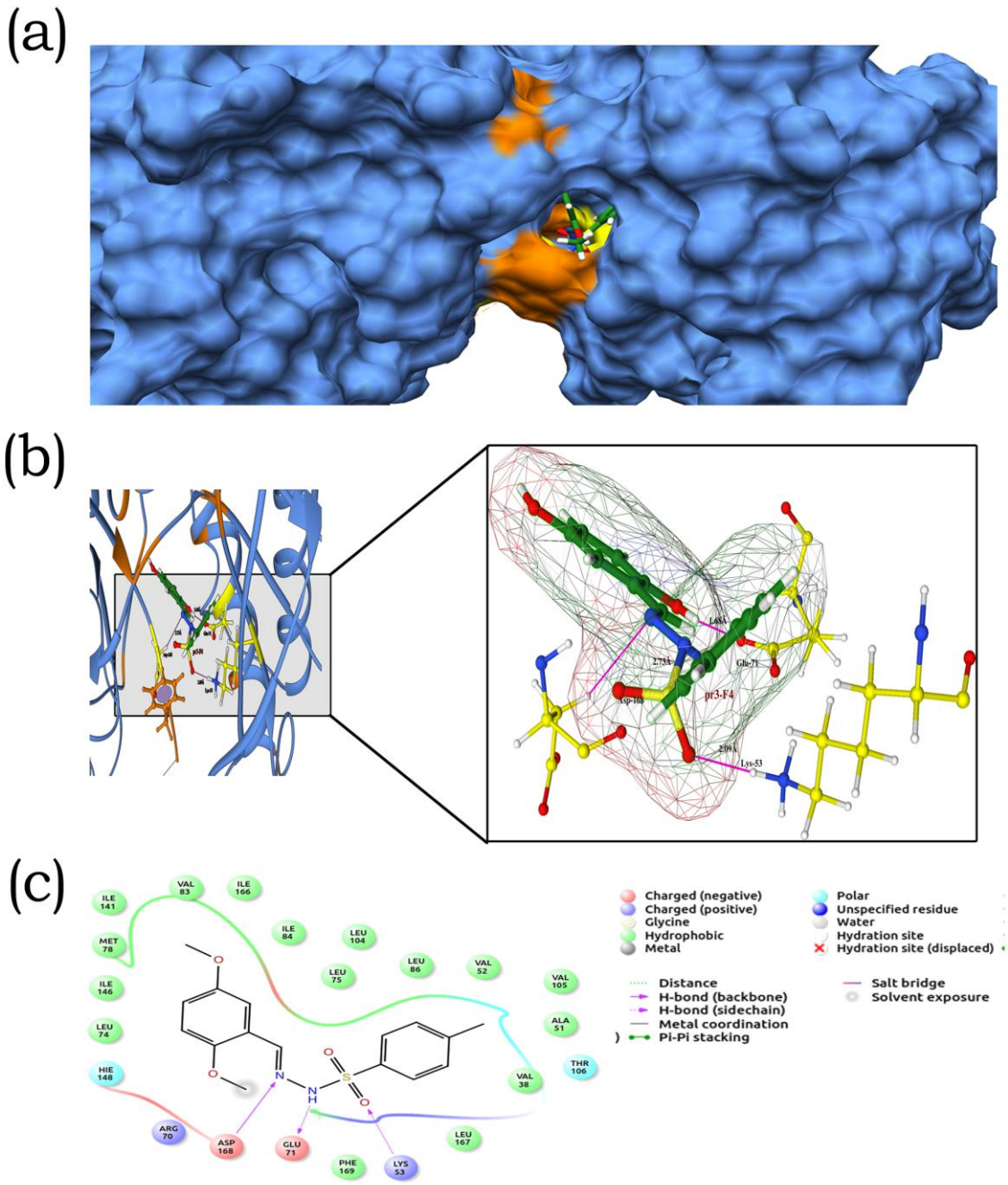

Figure. 4.2. Molecular docking of SH-1 with DFG binding sites of p38 alpha.

(a) Surface structure of SH-1 and p38α (DFG site), protein coloured blue, active site contrasting purple and SH-1 brown. (b) Secondary structure of p38α (DFG site) with hydrogen bonds in magenta. (c) 2D structure of p38α (DFG site) and SH-1 interactions showing hydrogen bonds (bold and dashed magenta lines) and residues forming hydrophobic interactions (Green) and polar interactions (cyan).

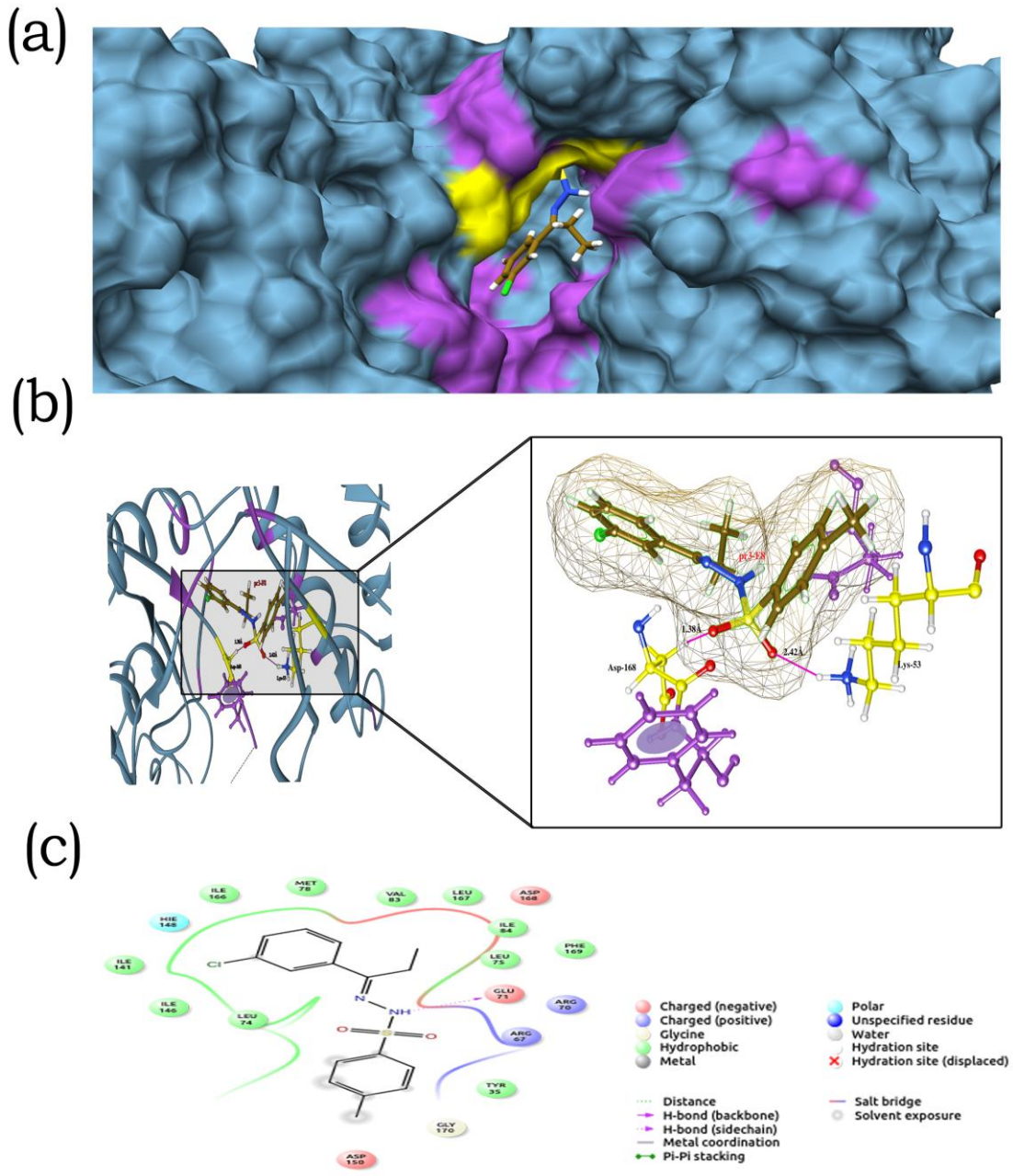

Figure. 4.3. Molecular docking of SH-2 with DFG binding sites of p38 alpha.
(a) Surface structure of SH-2 and p38α (DFG site), protein coloured blue, active site contrasting purple and SH-2 brown. (b) Secondary structure of p38α (DFG site) with hydrogen bonds in magenta. (c) 2D structure of p38α (DFG site) and SH-2 interactions showing hydrogen bonds (bold and dashed magenta lines) and residues forming hydrophobic interactions (Green) and polar interactions (cyan).

		SH-1 Inhibitor		SH-2 Inhibitor		
Active site/protein	Glide Score (Kcal/mol)	Glide Emodel (Kcal/mol)	Xscore (Kcal/mol)	Glide Score (Kcal/mol)	Glide Emodel (Kcal/mol)	Xscore (Kcal/mol)
DFG site/p38 alpha	-9.580	-65.550	-8.80	-9.855	-64.784	-9.60
ATP site/p38 alpha	-2.72	-45.885	-4.61	-4.352	-47.868	-5.02
DFG site/p38 Beta	-4.803	-45.986	-5.89	-4.809	-47.231	-5.85
DFG site/p38 Gamma	-4.565	-50.853	-6.01	-3.761	-45.145	-4.56
DFG site/p38 Delta	-5.563	-49.063	-4.29	-5.421	-33.658	-5.43
DFG site/c-ABL kinase	-2.892	-33.281	-3.28	-3.338	-45.402	-4.47
DFG site/b-RAF kinase	-2.595	-47.610	-2.85	-3.467	-49.560	-4.25

Table. 4.1. Glide docking scores, Emodel values, and relative Xscores for SH-1 and SH-2 inhibitors against different active site of corresponding target proteins.

Inhibitor	Hydrogen bonds	Hydrophobic interactions	Polar interactions
SH-1	Lys-53, Glu-71, Asp-168	Val-38, Ala-51, Ala-52, Leu-74, Leu-75, Me-78, Val-83, Ile-84, Leu-86, Leu-104, Val-105, Ile-141, Ile-146, Ile-166, Leu-167, Phe-169	Thr-106, His-148
SH-2	Lys-53 and Asp-168	Val-38, Ala-51, Ala-52, Leu-74, Leu-75, Me-78, Val-83, Ile-84, Leu-86, Leu-104, Val-105, Ile-141, Ile-146, Ile-166, Leu-167, Phe-169	Thr-106, His-148

Table. 4.2. List of Hydrogen bonds, hydrophobic interactions and Polar interactions formed by SH-1 and SH-2 inhibitors against DFG site of p38 alpha.

4.3.2. SH-1 and SH-2 inhibit phosphorylation of p38MAPK and its downstream target Hsp27 in DU145 and PC-3 cells

The p38MAPK pathway is activated by various cellular stresses and promote cell proliferation and survival in many types of cancer (Thornton and Rincon, 2009). Phosphorylation of Hsp27 is attributed to the generation of castrate-resistant prostate cancer (Zoubeidi et al., 2010). The modulating effect of SH-1 and SH-2 on the phosphorylation of p38 and Hsp27 were checked. The western blot data indicated that both SH-1**(Fig. 4.4)** and SH-2 **(Fig. 4.5)** inhibited the phosphorylation of p38 (Thr180/Tyr182) and its downstream target Hsp27 (Ser82). After 12 hours of treatment, the downregulation of P-p38 was more visible in a time-course manner.

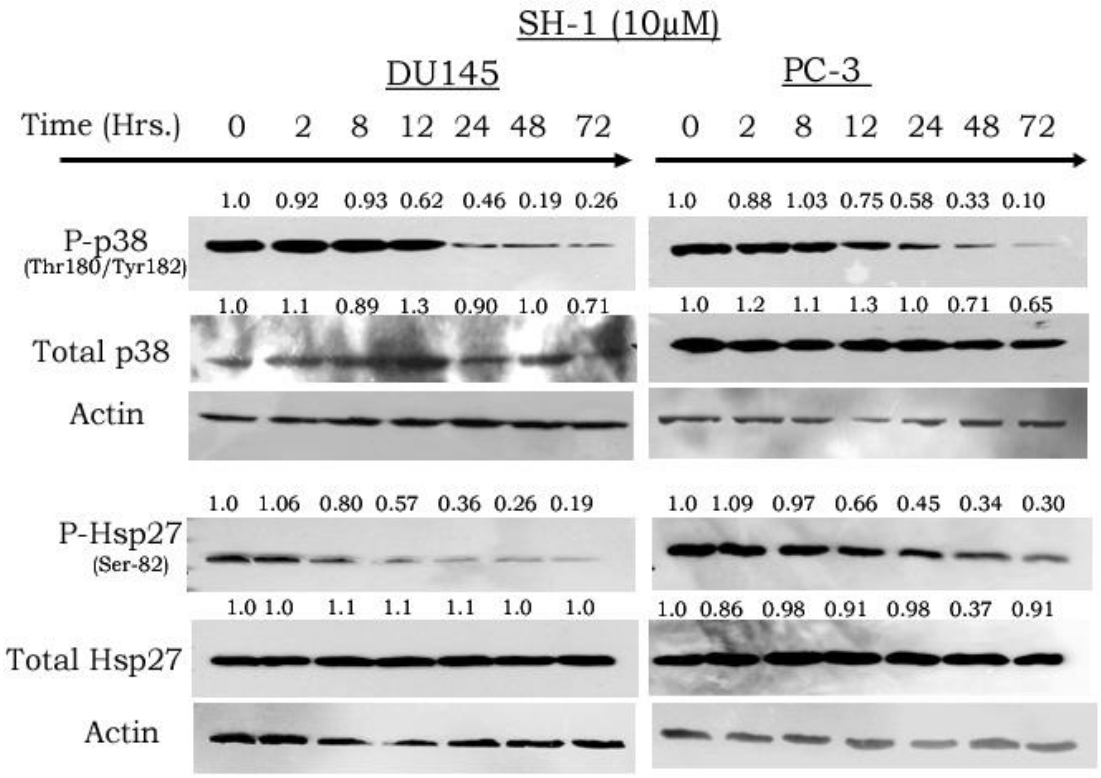

Figure. 4.4. Inhibition of phosphorylation of p38 and Hsp27 by SH-1 in DU145 and PC-3 cell lines.

DU145 and PC-3 cells were incubated with 10μM of SH-1 for the different indicated times and whole cell lysate was used for western blotting. SH-1 inhibited the phosphorylation of p38 and Hsp27 in a time dependent way in both cell lines. The expression level of both phospho-p38 and phospho-Hsp27 were densitometrically normalized with their respective total protein expression. The total level of p38 and Hsp27 were normalized with their respective actin. All experiments were repeated and yielded similar results.

Phosphorylated proteins were densitometrically normalized to the total expression of corresponding proteins. As shown by the densitometry, SH-1 downregulated P-p38 up to 70% in DU145 and 90% in PC-3 after 72 hours incubation **(Fig. 4.4).** The P-Hsp27 level was inhibited by 80% in DU145 and 70% in PC-3 by SH-1 post 72 hours incubation **(Fig. 4.4)**. Compounds SH-2 inhibited P-p38 by 60% and 75% and P-Hsp27 by 40% and 55% in DU145 and PC-3 respectively post 72 hours treatment **(Fig. 4.5)**. When normalized with respective actin, the total or unphosphorylated form of both p38 and Hsp27 demonstrated moderate inhibition, but not to the extent the phosphorylated form was inhibited.

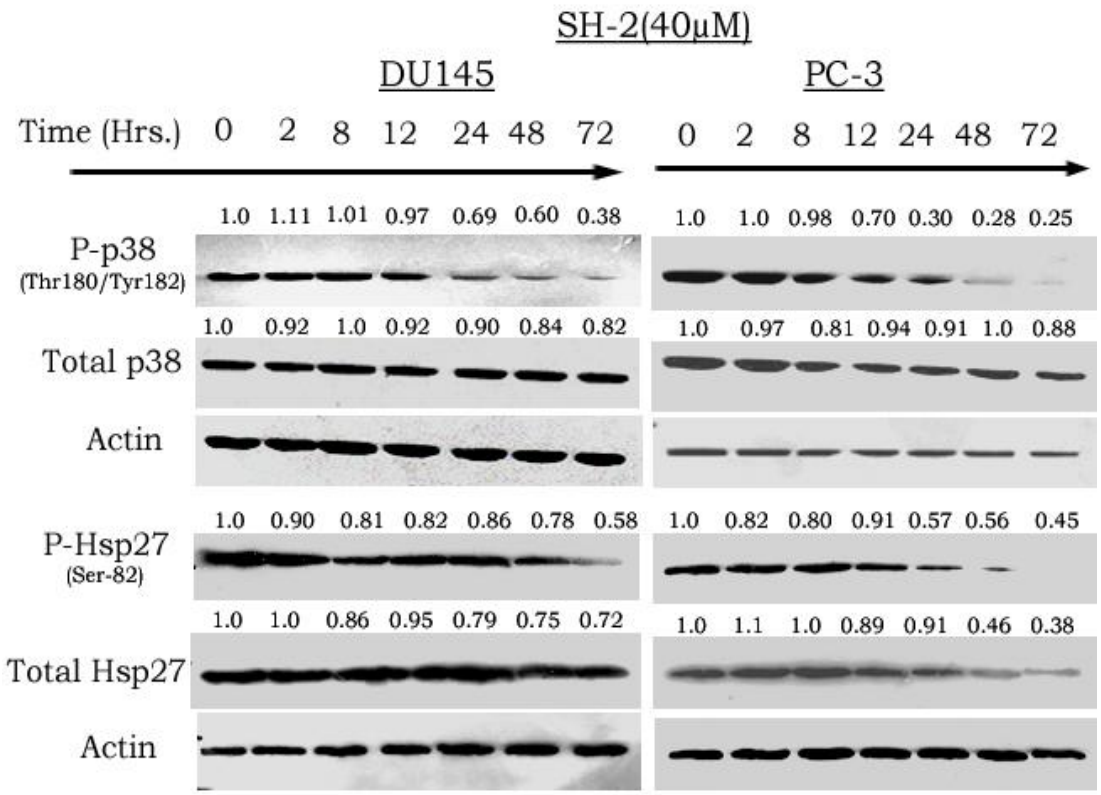

Figure. 4.5. Inhibition of phosphorylation of p38 and Hsp27 by SH-2 in DU145 and PC-3 cell lines.

DU145 and PC-3 cells were incubated with 40μM of SH-2 for the different indicated times and whole cell lysate was used for western blotting. SH-2 inhibited the phosphorylation of p38 and Hsp27 in a time dependent way in both cell lines. The expression level of both phospho-p38 and phospho-Hsp27 were densitometrically normalized with their respective total protein expression. The total level of p38 and Hsp27 were normalized with their respective actin. All experiments were repeated and yielded similar results

As stated above, the densitometry data showed a significant inhibition of p38MAPK cell survival pathway proteins in both cancer cell lines. The inhibitory effect was prominent post 12-hour compound treatment. We also checked the expression of P-p38 and P-Hsp27 in noncancer fibroblast cells, NIH-3T3. When compared between the cancerous and non-cancerous cells, data clearly showed that at 72 hours, approximately 50-60% phosphorylation of the p38 and Hsp27 was inhibited in the cancerous cells whereas the non-cancerous cells remained unaffected **(Fig. 4.6)**.

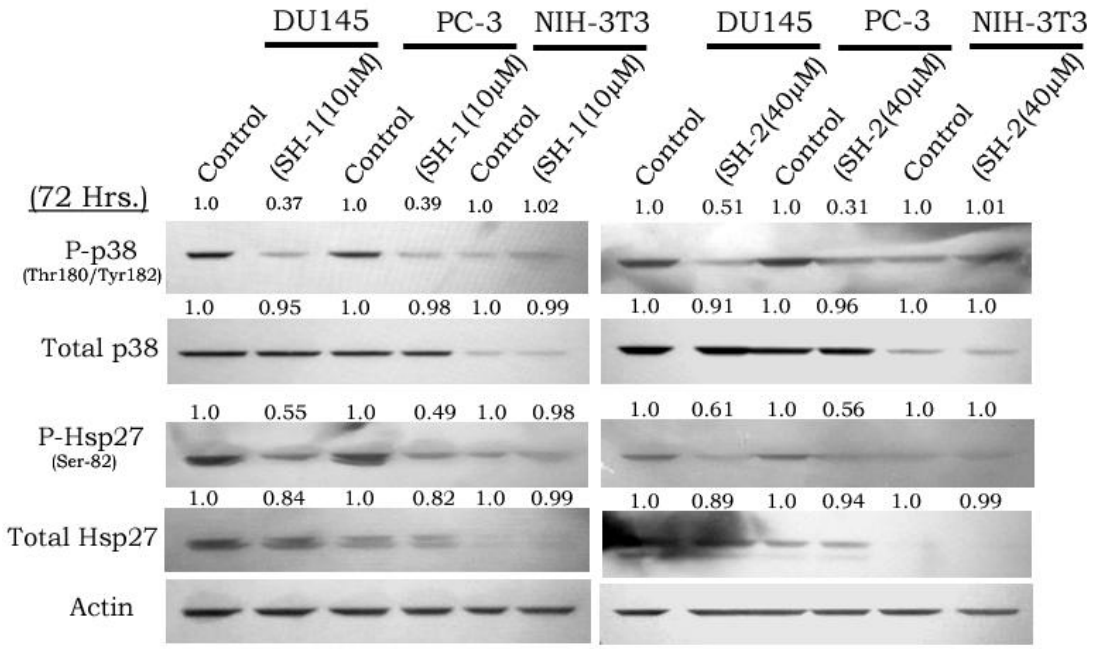

Figure. 4.6. Comparative Inhibition analysis of phosphorylated forms of p38 and Hsp27 by SH-1 and SH-2 in cancerous and noncancerous cells.

DU145, PC-3 and noncancerous fibroblast NIH-3T3 cells were incubated with 10μM of SH-1 and 40μM of SH-2 for 72 hours. Whole cell lysate was used for western blotting. Compound SH-1 and SH-2 could not inhibit the phosphorylation of p38 and Hsp27 in fibroblast cell line. The total level of p38 and Hsp27 were normalized with the respective actin. The densitometry data of both phospho-p38 and phosphor-Hsp27 showed no difference in NIH-3T3. Actin served as loading control. All experiments were repeated and yielded similar results.

Our data suggested the inhibition of p38MAPK and Hsp27 phosphorylation by SH-1 and SH-2 selectively in prostate cancer cells.

4.3.3. SH-1 and SH-2 inhibit mRNA level of p38 and Hsp27 in DU145 and PC-3 cell lines

Our data showed that the levels of unphosphorylated p38 and Hsp27 were also downregulated, so we further investigated the expression of mRNA to check whether p38 and Hsp27 were down-regulated at the transcriptional level.

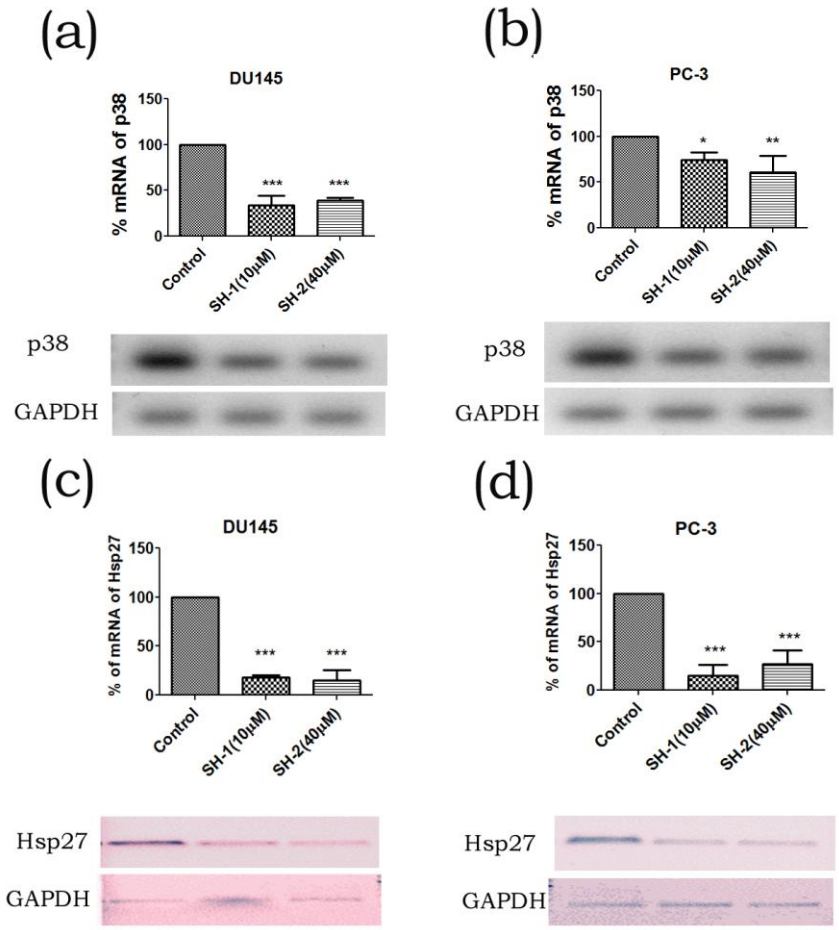

Figure. 4.7. Inhibition of mRNA of p38 by SH-1 and SH-2 in DU145 and PC-3 cell lines.

Cells were incubated with 10μM of SH-1 and 40μM of SH-2 for 72 hours. Total RNA was isolated using QIAzol method and cDNA was prepared. Quantitative PCR was done using SYBR-green master mix. Corresponding ct values of p38 were normalized with GAPDH and plotted values for (a) DU145 and (b) PC-4. The corresponding reaction samples were analysed on 1.0% agarose gel and EtBr fluorescence were captured. All experiments were repeated and yielded similar results. *$p<0.05$, **$p<0.01$, and ***$p<0.001$, represented as compared to control.

Total RNA was isolated and used to synthesize cDNA. "SYBR-Green-Based Real-Time Quantitative PCR" was carried out to study the expression of the p38 and Hsp27. The results indicated that SH-1 and SH-2 treatments resulted in about 70% and 60% p38-mRNA inhibition respectively in DU145 **(Fig. 4.7a)**, whereas PC-3 cells showed about 30% and 40% p38-mRNA suppression by SH-1 and SH-2 respectively **(Fig. 4.7b)**. The mRNA expression profile of Hsp27, post 72-hours treatment, showed the inhibition of about 80% by SH-1 and 85% by SH-2 in DU145

(Fig. 4.7c), while in PC-3 cells that were 86% and 74% by SH-1 and SH-2 respectively **(Fig. 4.7d)**. In both cases, the level of inhibition was significant and showed $p<0.01$, though the inhibition of Hsp27 mRNA was more prominent as compared to p38 mRNA in both cancer cell lines. The RT-PCR reaction mixtures were analyzed on 1.5% agarose gel which showed the corresponding band intensities.

Our data suggested that p38MAPK and downstream Hsp27 might be inhibited at the transcriptional level by both compounds in these cancer cell lines.

4.3.4. SH-1 and SH-2 inhibit nuclear localization of P-p38 and P-Hsp27 in DU145 and PC-3 cell lines

In androgen-independent prostate cancer, high Hsp27 activity lead to the inhibition of apoptosis and promote cell survival (Rocchi et al., 2005). Un-phosphorylated Hsp27 has predominantly localized to the cytoplasm while its phosphorylation by p38MAPK, the upstream regulator, induces its translocation to perinuclear and nuclear regions. To further explore the effect of SH-1 and SH-2, the expression and subcellular localization of P-p38 and P-Hsp27 were investigated in DU145 and PC-3 cells. As shown in the results, the untreated cells indicated nuclear P-p38 localization while P-Hsp27 was found both in the nucleus and cytoplasm, though it is predominantly present in the cytoplasm, in both DU145 **(Fig 4.8a)** and PC-3 **(Fig. 4.9a)** cells. The treatment with either SH-1 or SH-2 inhibited nuclear P-p38 and both nuclear and cytoplasmic P-Hsp27 in both DU145 **(Fig 4.8a)** and PC-3 **(Fig 4.9a)** cells. The expression levels of P-p38 and P-Hsp27 were quantitated and plotted. The histogram indicated around 50% and 70% inhibition of P-p38 by SH-1 and SH-2 respectively,

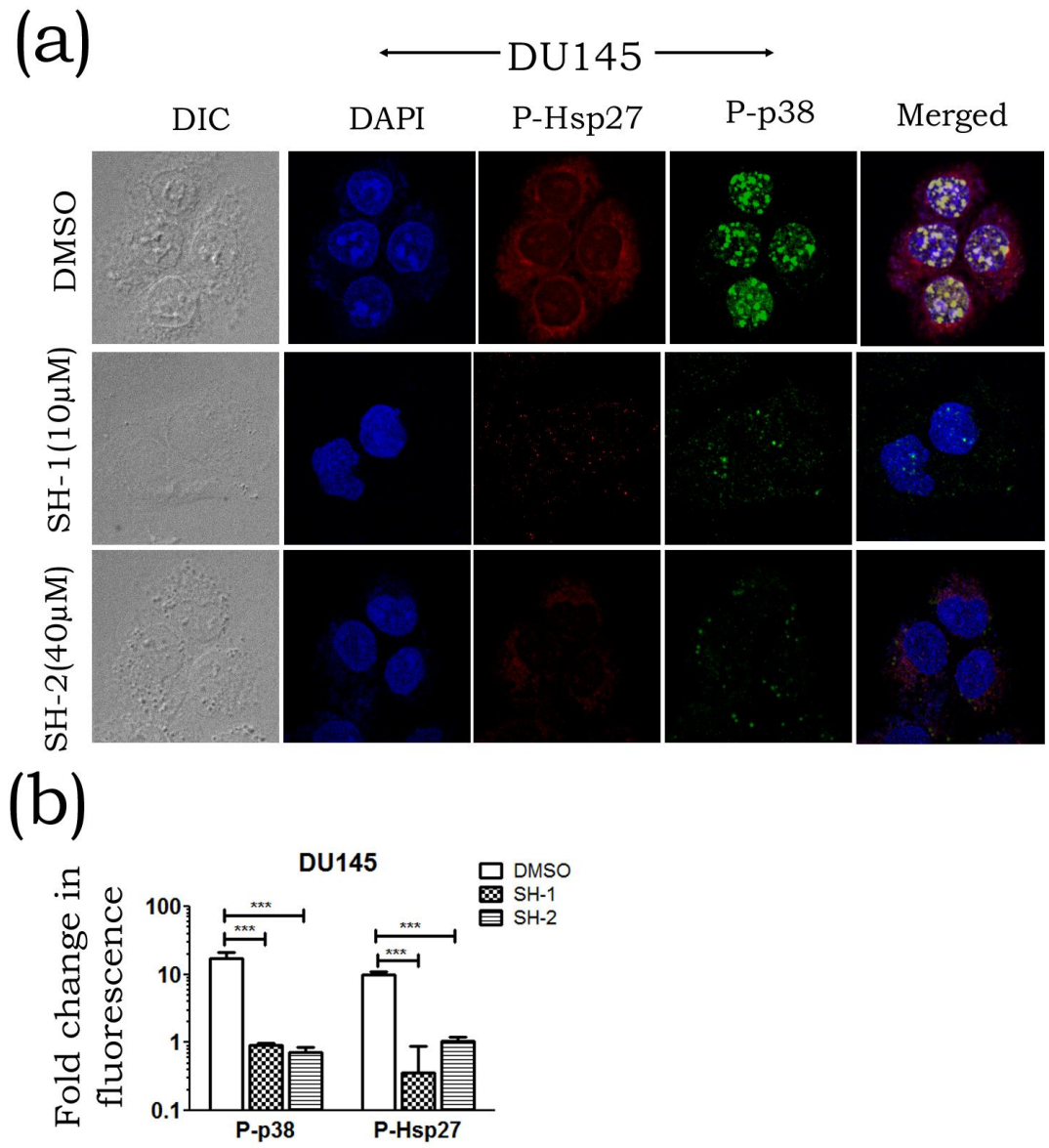

Figure. 4.8. SH-1 and SH-2 inhibit nuclear localization of P-p38 and P-Hsp27 in DU145.

DU145 cells were plated over coverslips in 6-well plates and treated with either 10µM of SH-1 or 40µM of SH-2 for 48 hours. Cells were fixed in 4% PFA followed by permeablization with 0.01% Triton-x-100. After incubating with anti-phospho-p38 and anti-phospho-Hsp27 (1:50 dilution) followed with secondary (1:10,000) FITC labelled antibody, cells were mounted over slides in antifade mounting media. DAPI was used to counterstain nucleus. Slides were observed at 60X under ANDOR SPINNING DISK confocal microscope using ANDOR iQ 2.7 software (scale bar: 20µm). (a) Merged image is showing co-localization of P-p38 and P-Hsp27. (b) Quantitation from microscopic images were done using n number (n>50) of cells for each set. All experiments were repeated and yielded similar results. ***p<0.001, represented as compared to control.

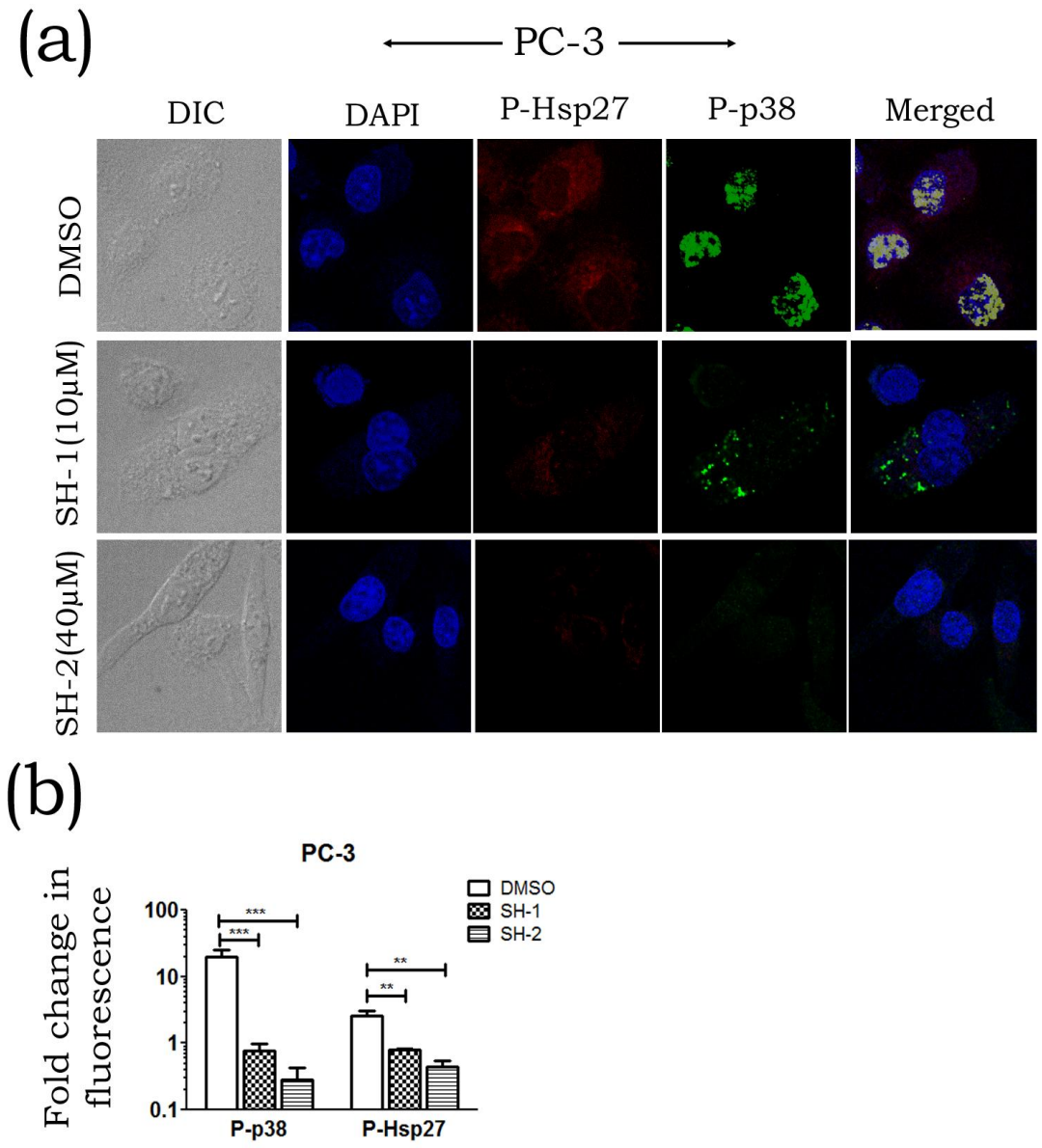

Figure. 4.9. SH-1 and SH-2 inhibit nuclear localization of P-p38 and P-Hsp27 in PC-3.

PC-3 cells were plated over coverslips in 6-well plates and treated with either 10μM of SH-1 or 40μM of SH-2 for 48 hours. Cells were fixed in 4% PFA followed by permeablization with 0.01% Triton-x-100. After incubating with anti-phospho-p38 and anti-phospho-Hsp27 (1:50 dilution) followed with secondary (1:10,000) FITC labelled antibody, cells were mounted over slides in antifade mounting media. DAPI was used to counterstain nucleus. Slides were observed at 60X under ANDOR SPINNING DISK confocal microscope using ANDOR iQ 2.7 software (scale bar: 20μm). (a) Merged image is showing co-localization of P-p38 and P-Hsp27. (b) Quantitation from microscopic images were done using n number ($n>50$) of cells for each set. All experiments were repeated and yielded similar results. ***$p<0.001$, represented as compared to control

while both compounds inhibited P-Hsp27 by 50% in DU145 **(Fig. 4.8b)**. In PC-3 cells, SH-1 inhibited both P-p38 and P-Hsp27 by 50%, and SH-2 inhibited by 75%-80% P-p38 and P-Hsp27 **(Fig 4.9b)**.

Our localization study showed that both compounds inhibited nuclear level of P-p38 and both nuclear and cytoplasmic P-Hsp27, and that might block the survival and anti-apoptotic functions of Hsp27 in prostate cancer cell lines.

4.3.5. Inhibition of p38 mediated phosphorylation of ATF-2 by SH-1 and SH-2

The p38MAPK activates its direct downstream target ATF-2 which is an inhibitor of apoptosis (Raingeaud et al., 1995).

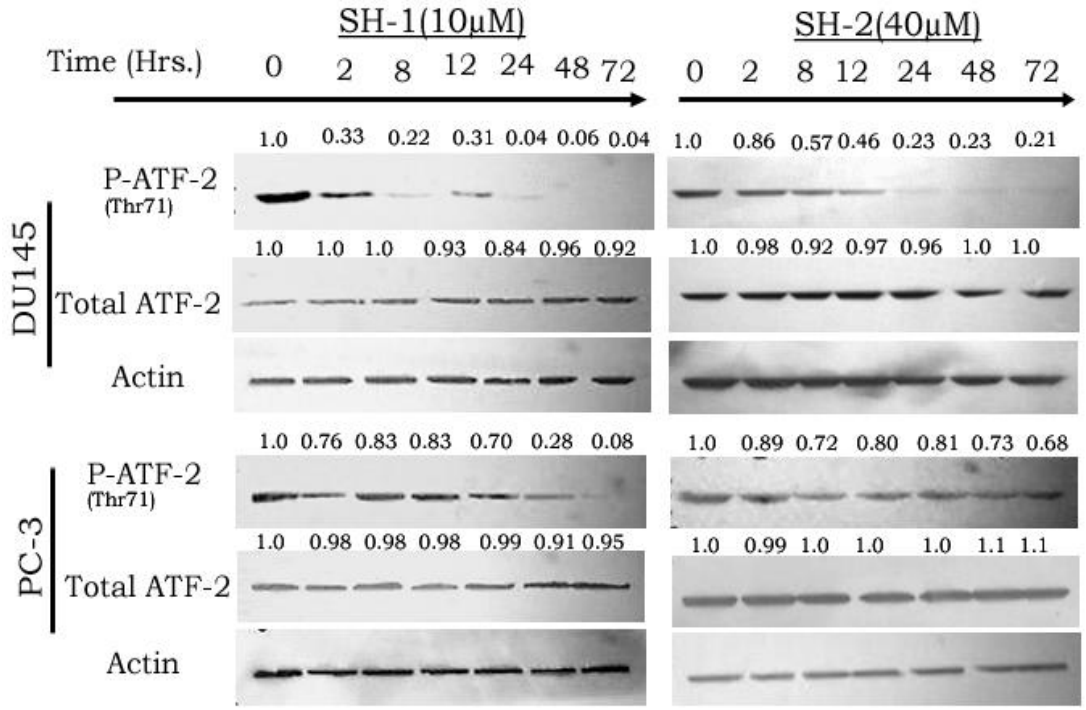

Figure. 4.10. SH-1 and SH-2 inhibited the p38-dependent phosphorylation of ATF-2 in DU145 and PC-3 cell lines.

DU145 and PC-3 cells were incubated with 10μM of SH-1 and 40μM of SH-2 for various indicated time periods. Whole cell lysate was used for western blotting. Anti-phospho-ATF-2(Thr71) was used to detect phosphorylation level of ATF-2. The expression level of phospho-ATF-2 and total ATF-2 were densitometrically normalized with respective actin. Both SH-1 and SH-2 inhibited the P-ATF-2 in both cell lines. Experiments were repeated and yielded similar results.

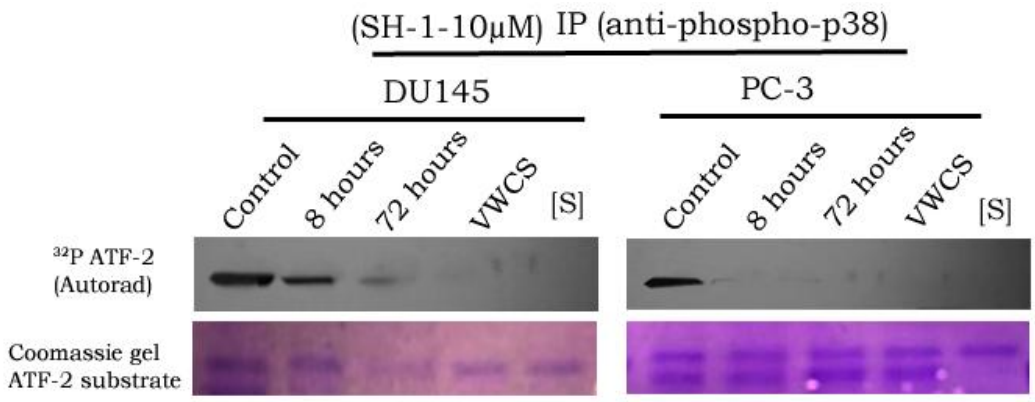

Figure. 4.11. *In-vitro* p38 kinase assay using ATF-2 as substrate in DU145 and PC-3 exposed with SH-1.

DU145 and PC-3 cells were incubated with 10μM of SH-1 and 100μM of VWCS peptide for various indicated time periods. 300μg protein was used for immunoprecipitation with anti-phospho-p38. IP beads were processed and used in in-vitro radio isotope based kinase assay. Purified ATF-2 was used as substrate. Coomassie stained ATF-2 served as loading control. All experiments were repeated and yielded similar results.

ATF-2-transcribed genes can mediate cell proliferation and survival (Persengiev and Green, 2003). We, therefore, checked the phosphorylation status of ATF-2 (P-ATF-2) in DU145 and PC-3 cell lines. Western blot with anti-P-ATF-2 (Thr71) and anti-total ATF-2 showed an inhibitory effect on P-ATF-2 in a time-dependent manner without affecting the total ATF-2 expression level. The densitometry-quantification indicated that SH-1 and SH-2 inhibited phosphorylation of ATF-2 totally by 72 hours post-treatment in DU145 cells **(Fig. 4.10)**. PC-3 cells also showed 100% inhibition of P-ATF-2 by SH-1. However, 31% inhibition was observed post 72 hours Sh-2-treatment **(Fig. 4.10)**. The *in-vivo* inhibition in p38-mediated phosphorylation of ATF-2 was further validated by performing *in-vitro* p38 kinase-activity assay using purified ATF-2 as substrate. Whole cells lysate was used for the immunoprecipitation with anti-phospho-p38 antibody and IP-beads were employed in the radioisotope-based kinase assay. VWCS (Gill et al., 2013), a known peptide inhibitor of p38 was used as a positive control in the reaction. Our kinase data showed that the inhibition of the phosphorylation of ATF-2 started 8 hours post-treatment and 100% by 72 hours treatment **(Fig. 4.11)**. The phospho-ATF-2 inhibition was thereby corroborated with inhibition of p38MAPK phosphorylating activity.

These results suggested that phosphorylation of ATF-2 was inhibited due to the inhibition of phosphorylation of p38MAPK in both cancer cell lines exposed to either compound.

4.4. Discussion

The p38MAPK, a stress-activated kinase, is activated by the genetic insults or environmental stresses. Studies have looked beyond this traditional role of p38MAPK and shown its role in cell survival (Thornton and Rincon, 2009). Molecular docking studies of SH-1 and SH-2 against ATP and DFG binding sites of p38 alpha map kinases as the target, was performed. Based on these studies we observed that the docking scores and Emodel values for both the inhibitors were more for DFG binding site as compared to ATP binding site. This data suggested that both the inhibitors exhibited relatively more binding affinity for the DFG binding site than the ATP binding site. Post-docking analysis for SH-1 demonstrated the formation of three hydrogen bonds, sixteen hydrophobic interactions, and two polar interactions, while SH-2 formed two hydrogen bonds, sixteen hydrophobic interactions and two polar interactions against DFG site of p38 alpha, indicating a high binding affinity for DFG site. “p38 map kinase” is a family of four isoforms and is reported to have homologous structures. To determine the specificity, we further performed molecular docking of SH-1 and SH-2 against DFG site of the other isoforms of p38 map kinase, viz. “p38β, p38γ, and p38□”. The Docking scores and “Emodel values” for these three isoforms were much less in comparison to the DFG site of p38α MAPK **(Table. 4.1)**, suggesting that both of these inhibitors might have specificity for the binding to DFG site of P38 alpha only and not with the other isoforms. It is known that kinases have homology in their active sites irrespective of their family. Human b-RAF and Human c-ABL kinases are reported to share active site similarity with p38MAPK family proteins. Thus, we also performed molecular docking studies for SH-1 and SH-2 against the DFG sites of human b-RAF and Human c-ABL kinases. Our docking results suggest that both the inhibitors SH-1 and SH-2 have very less affinity for human b-RAF and Human c-ABL kinases, which is even less than the affinity for the other p38 isoforms except p38α. We

observed that the docking scores for both the inhibitors, SH-1 and SH-2 are quite similar in almost all the docking studies. These similarities in docking scores for SH-1 and SH-2 inhibitors is due to similarities in their structures, as they both differ in just one functional group **(Fig. 2.2b, chapter-2)**.

Many pharmacological inhibitors of p38 MAPK are being developed for invasive cancer therapy (Gill et al., 2013). Our *in-vitro* data suggested a clear inhibition of the phosphorylated p38MAPK in metastatic prostate cancer cell lines, suggesting a potential role of SH-1 and SH-2 in cancer therapeutics. The survival role of p38MAPK may be largely associated with its MK2 (MAPK Activated Protein Kinase2) dependent phosphorylation of Hsp27, a molecular chaperone (Shiryaev et al., 2011). To check whether P-p38MAPK inhibition affected P-Hsp27, we checked the expression of P-Hsp27 and found a decrease in protein phosphorylation level in both cancer cell lines. The unphosphorylated forms of both p38 and Hsp27 were moderately affected. To get an insight picture, we checked their mRNA level to know whether they were affected at the transcriptional level. Our qRT-PCR data indicated that both compounds, individually, inhibited transcription level of p38 and Hsp27 as evident from the mRNA expression level in both cancer cells. Hsp27 expresses both in the nucleus and the cytoplasm and is implicated in localization based functions. Cytoplasmic localization of P-Hsp27 regulates, majorly, chaperoning functions which contribute to "membrane stability, actin polymerization, cell migration, cell survival" (Rousseau et al., 1997). Studies have reported that p38MAPK phosphorylates Hsp27 at serine residues 15, 78, and 82, that makes Hsp27 capable of translocating to the nucleus (Geum et al., 2002). In the nucleus, P-Hsp27 protects the DNA from damage by responding to genetic stresses and perform its survival functions (Korber et al., 1999). Our results showed, apart from nuclear, the cytoplasmic localization of P-Hsp27 which might be due to other types of post-translational modification of this protein (Kostenko and Moens, 2009). Our microscopy data indicated that both SH-1 and SH-2 individually inhibited the nuclear expression of phosphorylated forms of both p38 and Hsp27 in both cancer cell lines. We checked the expression level of these proteins in noncancerous fibroblast cell line, NIH-3T3. Our *in-vitro* data indicated that in the non-cancerous cells, the expression of the P-p38 and P-Hsp27 remained unaffected. The data clearly

shows the inhibition of stress-induced protein and their phosphorylation selectively in the cancer cells.

Apart from Hsp27, p38MAPK regulates gene expression by phosphorylation of the transcription factor, the activating transcription factor-2 (ATF-2). The P-p38MAPK directly interatcs and activates ATF-2 and NF-κB in the nucleus, and that association mediates proliferation signals in tumor cells through transcriptional activation of key cell cycle regulators (Koul et al., 2013; Recio and Merlino, 2003). Our immunoblot results showed that phosphorylation of ATF-2 was inhibited by both SH-1 and SH-2 in a time-dependent manner in both DU145 and PC-3. These data reinstated that both compounds not only inhibited the p38 associated phosphorylation of Hsp27 but also inhibited phosphorylation of ATF-2 which might have resulted in the transcriptional downregulation of the cell cycle regulatory proteins. These data supported the broad spectrum signaling inhibitory effect of these compounds.

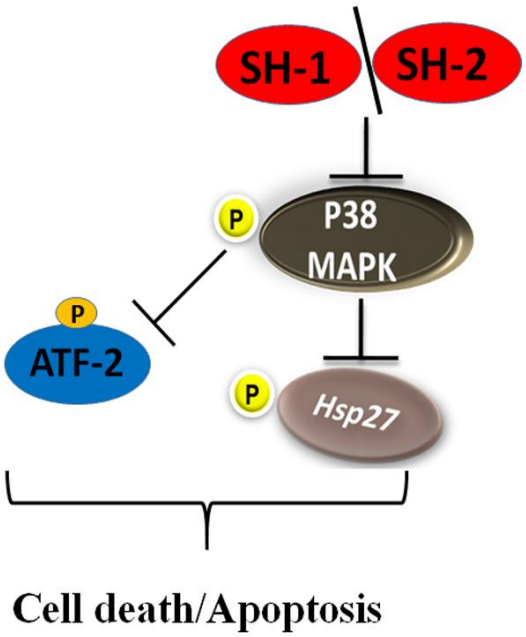

Figure. 4.12. Proposed hypothetical model for p38MAPK inhibition by SH-1 and SH-2.

Both SH-1 and SH-2 inhibit the phosphorylation of p38, which further blocks the phosphorylation of ATF-2. The inhibition of p38 also leads to inactivation of Hsp27. Unphosphorylated ATF-2 and Hsp27 are not able to upregulate the cancer survival genes which in turn result in cellular death.

Based on the findings, a hypothetical model was proposed **(Fig. 4.12)**. Both SH-1 and SH-2 inhibit the phosphorylation of p38, which further blocks the phosphorylation of ATF-2, a transcription factor. The inhibition of p38 also leads to inactivation of P-Hsp27. As a result, the unphosphorylated ATF-2 and Hsp27 are refrained from activating the cancer survival genes.

4.5. References

Arrigo, A., Virot, S., Chaufour, S., Firdaus, W., Kretz-Remy, C. and Diaz-Latoud, C. (2005). 'Hsp27 consolidates intracellular redox homeostasis by upholding glutathione in its reduced form and by decreasing iron intracellular levels.' *Antioxidants & redox signaling*, 7(3–4): 414–22.

Friesner, R.A., Murphy, R.B., Repasky, M.P., Frye, L.L., Greenwood, J.R., Halgren, T.A., Sanschagrin, P.C., et al. (2006). 'Extra precision glide: Docking and scoring incorporating a model of hydrophobic enclosure for protein-ligand complexes'. *Journal of Medicinal Chemistry*, 49(21): 6177–6196.

Geum, D., Son, G.H. and Kim, K. (2002). 'Phosphorylation-dependent cellular localization and thermoprotective role of heat shock protein 25 in hippocampal progenitor cells'. *Journal of Biological Chemistry*, 277(22): 19913–19921.

Gill, K., Nigam, L., Singh, R., Kumar, S., Subbarao, N., Chauhan, S.S. and Dey, S. (2014). 'The rational design of specific peptide inhibitor against p38α MAPK at allosteric-site: A therapeutic modality for HNSCC'. *PLoS ONE*, 9(7): 1–10.

Gill, K., Singh, A.K., Kapoor, V., Nigam, L., Kumar, R., Holla, P., Das, S.N., et al. (2013). 'Development of peptide inhibitor as a therapeutic agent against head and neck squamous cell carcinoma (HNSCC) targeting p38alpha MAP kinase.' *Biochimica et biophysica acta*, 1830(3): 2763–9.

Joyce, D., Bouzahzah, B., Fu, M., Albanese, C., D'Amico, M., Steer, J., Klein, J.U., et al. (1999). 'Integration of Rac-dependent regulation of cyclin D1 transcription through a nuclear factor-??B-dependent pathway'. *Journal of Biological Chemistry*, 274(36): 25245–25249.

Korber, P., Zander, T., Herschlag, D. and Bardwell, J.C. (1999). 'A new heat shock protein that binds nucleic acids.' *The Journal of biological chemistry*, 274(1): 249–56.

Kostenko, S. and Moens, U. (2009). 'Heat shock protein 27 phosphorylation: kinases, phosphatases, functions and pathology.' *Cellular and molecular life sciences : CMLS*, 66(20): 3289–3307.

Koul, H.K., Pal, M. and Koul, S. (2013). 'Role of p38 MAP Kinase Signal Transduction in Solid Tumors.' *Genes & cancer*, 4(9–10): 342–59.

Persengiev, S.P. and Green, M.R. (2003). 'The role of ATF/CREB family members in cell growth, survival and apoptosis'. *Apoptosis*, 8(3): 225–228.

Raingeaud, J., Gupta, S., Rogers, J.S., Dickens, M., Han, J., Ulevitch, R.J. and Davis, R.J. (1995). 'Pro-inflammatory cytokines and environmental stress cause p38 mitogen-activated protein kinase activation by dual phosphorylation on tyrosine and threonine'. *Journal of Biological Chemistry*, 270(13): 7420–7426.

Recio, J.A. and Merlino, G. (2003). 'Hepatocyte growth factor/scatter factor induces feedback up-regulation of CD44v6 in melanoma cells through Egr-1.' *Cancer research*, 63(7): 1576–1582.

Del Reino, P., Alsina-Beauchamp, D., Escos, a, Cerezo-Guisado, M.I., Risco, a, Aparicio, N., Zur, R., et al. (2014). 'Pro-Oncogenic Role of Alternative p38 Mitogen-Activated Protein Kinases p38gamma and p38delta, Linking Inflammation and Cancer in Colitis-Associated Colon Cancer'. *Cancer Res*, 74(21): 6150–6160.

Rocchi, P., Beraldi, E., Ettinger, S., Fazli, L., Vessella, R.L., Nelson, C. and Gleave, M. (2005). 'Increased Hsp27 after androgen ablation facilitates androgen-independent progression in prostate cancer via signal transducers and activators of transcription 3-mediated suppression of apoptosis'. *Cancer Research*, 65(23): 11083–11093.

Rousseau, S., Houle, F., Landry, J. and Huot, J. (1997). 'p38 MAP kinase activation by vascular endothelial growth factor mediates actin reorganization and cell migration in human endothelial cells'. *Oncogene*, 15(18): 2169–2177.

Shiryaev, A., Dumitriu, G. and Moens, U. (2011). 'Distinct roles of MK2 and MK5 in cAMP/PKA- and stress/p38MAPK-induced heat shock protein 27 phosphorylation.' *Journal of molecular signaling*, 6(1): 4.

Thornton, T.M. and Rincon, M. (2009). 'Non-classical p38 map kinase functions: Cell cycle checkpoints and survival'. *International Journal of Biological Sciences*, 5(1): 44–52.

Walluscheck, D., Poehlmann, A., Hartig, R., Lendeckel, U., Schönfeld, P., Hotz-Wagenblatt, A., Reissig, K., et al. (2013). 'ATF2 knockdown reinforces oxidative stress-induced apoptosis in TE7 cancer cells'. *Journal of Cellular and Molecular Medicine*, 17(8): 976–988.

Wang, H., Xu, Q., Xiao, F., Jiang, Y. and Wu, Z. (2008). 'Involvement of the p38

Mitogen-activated Protein Kinase {alpha}, {beta}, and {gamma} Isoforms in Myogenic Differentiation'. *Mol. Biol. Cell*, 19(4 %U http://www.molbiolcell.org/cgi/content/abstract/19/4/1519 %8 April 1, 2008): 1519–1528.

Winzen, R., Kracht, M., Ritter, B., Wilhelm, A., Chen, C.Y.A., Shyu, A. Bin, Müller, M., et al. (1999). 'The p38 MAP kinase pathway signals for cytokine-induced mRNA stabilization via MAP kinase-activated protein kinase 2 and an AU-rich region-targeted mechanism'. *EMBO Journal*, 18(18): 4969–4980.

Zarubin, T. and Han, J. (2005). 'Activation and signaling of the p38 MAP kinase pathway'. *Cell Res*, 15(1): 11–18.

Zoubeidi, A., Zardan, A., Wiedmann, R.M., Locke, J., Beraldi, E., Fazli, L. and Gleave, M.E. (2010). 'Hsp27 promotes insulin-like growth factor-I survival signaling in prostate cancer via p90Rsk-dependent phosphorylation and inactivation of BAD'. *Cancer Research*, 70(6): 2307–2317.

CHAPTER-5

INHIBITION OF PYRUVATE KINASE M2 (PKM2) PATHWAY AND INDUCTION OF APOPTOSIS: MEDIATED BY ROS

5.1. Introduction

The reactive oxygen species (ROS) are the unintended but inevitable metabolic outcomes of oxidizing agents. Cellular systems have antioxidant defence mechanism which maintains cellular ROS homeostasis. In cancer cells, due to oxidative stress, a comparatively higher amount of ROS is found. The optimum level of ROS is widely maintained by the reduced glutathione (GSH). The metabolic machinery of cancer cells differs from the normal cells. The metabolism of glucose provides NADPH which constantly supplies GSH, and that rescues cancer cells from ROS-induced damage. In cancer cells, pyruvate is converted to lactic acid in the cytosol. The preferential pyruvate fermentation in cancer cells is called "Warburg effect or aerobic glycolysis" (Warburg, 1956). The modulation of glucose metabolism triggers the upregulation of genes involved in the high glucose uptake and survival under hypoxic condition (Mathupala et al., 2001). Pyruvate kinase (PK) is a crucial enzyme that catalyse the conversion of phosphoenolpyruvate to pyruvate in the glycolysis (Altenberg and Greulich, 2004). Mammalian cells express four different isoforms of PK namely "L, R, M1 and M2", which are specified on the basis of their persistence in different tissue types. The alternative splicing of pre-mRNA of PK generates M1 and M2 isoforms from exon 9 and 10 respectively (Matlin et al., 2005). These M1 and M2 isoforms are known as PKM1 and PKM2 respectively. PKM2 is abundantly found in cancer cells. PKM2 has been shown to interact with hypoxia inducible factor 1 α (HIF-1α) in the hypoxic condition and stimulates glucose metabolism (Luo and Semenza, 2011). In almost all human cancer types the epidermal growth factor receptors (EGFR) persist in an active form and has been shown in driving the PKM2 to the nucleus (Yang et al., 2011). Generally, PKM2 occurs in two forms, one is highly active tetrameric form and other is less active dimeric form. The dimeric form carries out kinase function which is indispensable in performing its transcriptional

activity in the nucleus, where it enhances the promoter activity and expression of c-Myc and cyclin D1 gene (Lu, 2012). Further, c-Myc induces the transcriptional activation of PKM2 by binding to exon 9, which triggers preferential splicing of exon 10 and the formation of PKM2 (David et al., 2010). Both HIF-1α and c-Myc have been reported to induce PKM2 via mammalian target of rapamycin (mTOR) pathway (Sun et al., 2011). The metabolic and transcriptional role of PKM2 have been shown in the following figure **(Fig. 5.1)**.

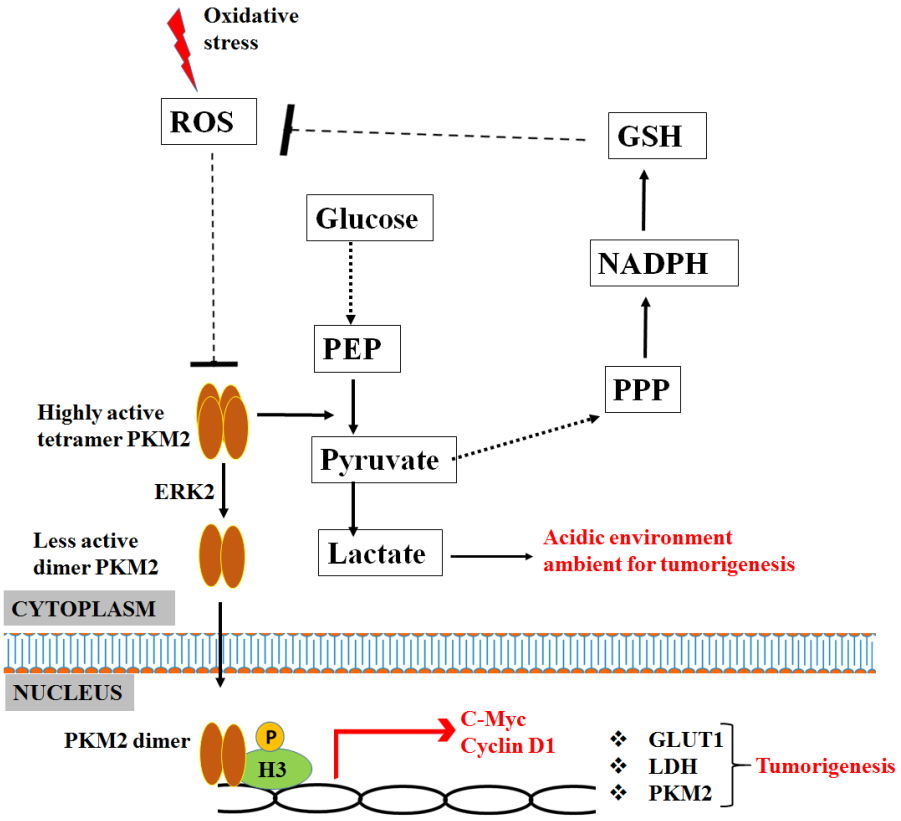

Figure. 5.1. Diagrammatic representation of PKM2 metabolism in cancer cells.

The highly active tetrameric form of PKM2 catalyzes the conversion of phosphoenolpyruvate (PEP) into pyruvate that is, instead of going to pentose phosphate pathway (PPP), diverted to the formation of lactate. The resultant low level of NADPH is insufficient to control the high oxidative stress in cancer cells. The less active dimeric form of PKM2 goes to the nucleus and phosphorylates histone-H3 (P-H3), and that stimulates the transcriptional activation of proto-oncogenes c-myc and cyclin D1.

ROS has paradoxical functions wchic can be exploited in cancer therapy. By activating the cell cycle growth factors via receptor tyrosine kinase, ROS facilitate cancer cell viability at a low level, but higher levels of ROS induces cell death (Ralph et al., 2010). ROS can induce mitochondrial permeabilization and cell death followed by the release of cytochrome c. These toxic cytochrome c activates anti-apoptotic protein Bax/Bak. Members of the Bcl-2 family of proteins have a pivotal role in regulating the apoptotic pathway. Bcl-2 protein, a member of this family, associated with the mitochondrial membrane, suppresses apoptosis. Another molecule, survivin, negatively regulates apoptosis by inhibiting caspase-3 activation. Survivin is overexpressed in many cancers, including prostate cancer which might promote the conditions for metastasis and tumorigenesis.

In this chapter, the effects of SH-1 and SH-2 were examined on the expression of PKM2 and its downstream molecule histone-H3 and c-Myc. Effects on ROS generation, mitochondrial membrane potential and apoptosis were also checked.

5.2. Methodology

5.2.1. Cell lines and reagents

Human prostate carcinoma cell lines, DU145 and PC-3, and human fibroblast cell line, NIH-3T3, were obtained from American Type Culture Collection and maintained as described in chapter-2. Antibodies used from santacruz were: PARP1 (sc-7150), caspase-3 (sc-1226), Phospho-histone H3 (sc-8656), survivin (sc-17779), bcl-2 (7382), and actin (sc-1615). PKM2 (#3192) from cell signaling and c-Myc (9E10) from Abcam, were obtained. Histone H1 type3 (H5505), Rhodamine123 (546054) and 2',7'-dichlorofluorescein diacetate (DCFH-DA) (D6883) were obtained from Sigma-Aldrich. QIAzol from QIAGEN (cat-79306), "SYBR-Green Mix from Applied Biosystem" (4367659) and "Verso cDNA synthesis kit" from Thermo Scientific (AB-1453/B) were used.

5.2.2. Western blot

Western blot technique was used to check and analyze the expression level of the proteins in response to the synthetic compounds. The cells (7x 10^4/ml) were plated

in 100mm^2 dishes. **(The detail is provided in "Materials and methods" section of chapter-1)**.

5.2.3. Reactive oxygen species (ROS) generation assay

ROS generation in control and compound-treated cells was measured by flow cytometry following staining with DCFH-DA. Briefly, desired cells were seeded (6x 10^4/ml) in six-well plates, allowed to attach overnight and exposed to DMSO (control) or desired concentrations of compound for 72 hours. The cells were stained with 5µM "DCFH-DA" for 45 min at 37^0C, and the fluorescence was measured by flow cytometry (BD Bioscience).

5.2.4. Measurement of mitochondrial membrane potential (MMP)

MMP assay in control and compound-treated cells was carried out by flow cytometry following staining with Rhodamine 123. Briefly, desired cell line was seeded (6x 10^4/ml) in 6-well plates and exposed to DMSO (control) or specific concentrations of either SH-1 or SH-2 for specified time. The cells were stained with 5µM "Rhodamine 123" for 45 min at 37^0C, and the fluorescence was measured by flow cytometry (BD Bioscience).

5.2.5. Quantitative Real Time-PCR (qRT-PCR)

Real-time PCR of PKM2 and c-Myc was performed using the "Power SYBR-Green master mix" (Applied Biosystems). **(The detail is provided in "Materials and methods" section of chapter-3)**. Primer pairs used in the experiments are listed in the appendix section.

5.2.6. Immunofluorescence study

The cellular localization of phospho-histone H3 and c-Myc was investigated by immunofluorescence. Briefly, cancer cells ($7x10^3$ cells/ml) were seeded in 6-well plates over the coverslip and exposed to desired concentration of compounds for the 48 hours. **(The detail is provided in "Materials and methods" section of chapter-3).**

5.2.7. Statistical analysis

Each experiment was repeated more than three times and significance was measured by one way or two way ANNOVA. The data shown are the mean from three parallel experiments. $\alpha = p<0.05$, $\beta = p<0.01$, $\gamma = p<0.001$ compared to control.

5.3. Results

5.3.1. SH-1 and SH-2 inhibit expression of PKM2 in prostate cancer cell lines, DU145 and PC-3

Pyruvate Kinase M2 (PKM2) is one of the four isoforms of PK that have been reported abundantly expressed in most of the cancer (Mazurek, 2011). The SH-1 or SH-2 treated DU145 and PC-3 cells were examined for the expression of PKM2, both at the protein as well as at the mRNA level. Immunoblot data showed a time-dependent inhibition of the PKM2 protein in both the cancer cell lines. The densitometry analysis of western blot data indicated that, at 72 hours post-treatment, SH-1 inhibited PKM2-protein expression by 70% in DU145 and 88% in PC-3 cells **(Fig. 5.2a)**. Compound SH-2 downregulated the PKM2 protein by 68% in DU145 and 84% in PC-3 cells **(Fig. 5.2b)**. The mRNA level was checked to know the effect of either compound at the transcriptional level. PKM2 mRNA expression was inhibited by 70% and 80% in DU145 cells **(Fig. 5.3a)** and by 75% and 45% in PC-3 cells **(Fig. 5.3b)** post 72 hours exposure to SH-1 and SH-2 respectively.

Our data showed that both, SH-1 and SH-2, inhibited PKM2 at transcriptional as well as at translational level in DU145 and PC-3 cells.

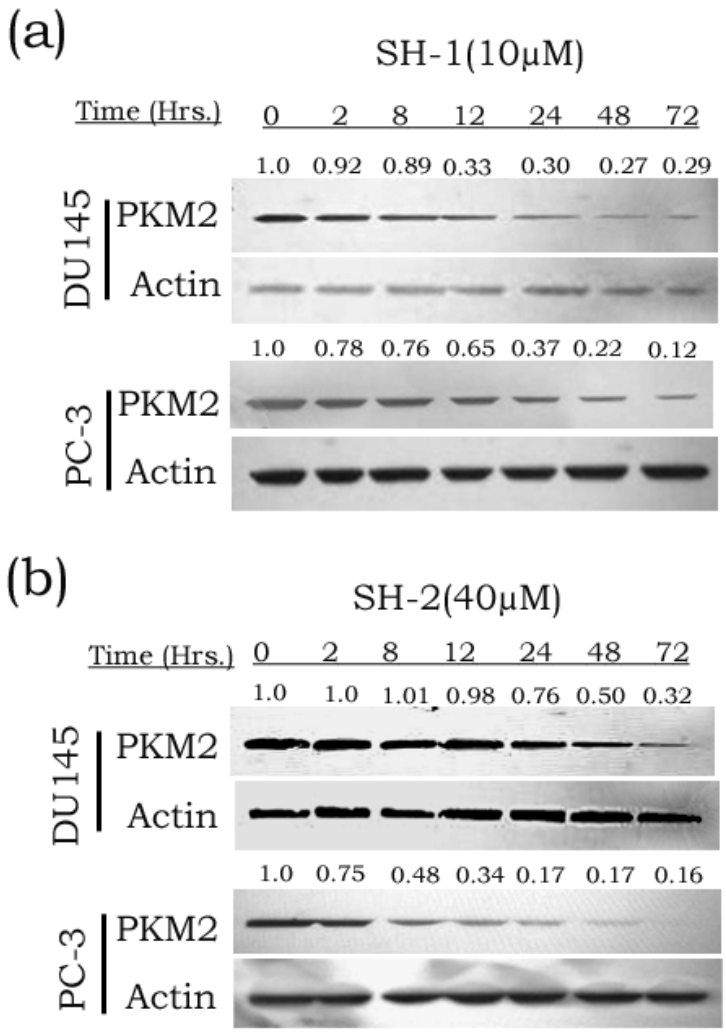

Figure. 5.2. SH-1 and SH-2 inhibits the protein expression of PKM2 in DU145 and PC-3 cell lines.

Cells were plated and incubated with 10μM of SH-1 (a) and 40μM of SH-2 (b) for the different indicated times. Cells were harvested at stipulated times, lysed and whole cell lysate was used for immunoblotting. Data showed significant inhibition of PKM2 by either SH-1 (a) or SH-2 (b) in a time dependent manner. The expression of PKM2 was densitometrically normalized with the respective actin bot. Each blot was repeated and yielded similar results.

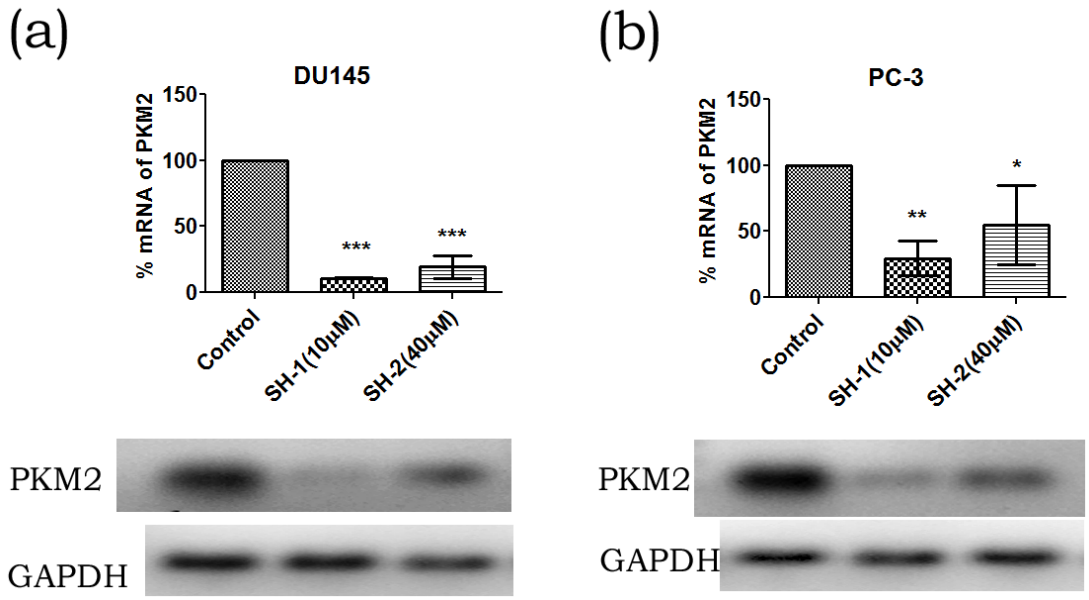

Figure. 5.3. Inhibition of mRNA of PKM2 by SH-1 and SH-2 in DU145 and PC-3 cell lines.

Cells were incubated with 10μM of SH-1 and 40μM of SH-2 for 72 hours. Total RNA was isolated using QIAzol method and cDNA was prepared. Quantitative PCR was done using SYBR-green master mix. Corresponding ct values of PKM2 expression were normalized with GAPDH and plotted values for (a) DU145 and (b) PC-3. The corresponding reaction samples were analysed on 1.0% agarose gel and EtBr fluorescence were captured. Experiments were repeated and yielded similar results. *p<0.05, **p<0.01, and ***p<0.001 were presented as compared to control.

5.3.2. SH-1 and SH-2 inhibit phosphorylation of histone H3 and expression of c-Myc in DU145 and PC-3 cell lines

The transcriptional regulation in eukaryotes is majorly regulated by post-transcriptional modification of the histone octamers, constituting the core nucleosome protein, by either acetylation, phosphorylation, methylation, or ubiquitination (Lee et al., 2010). The phosphorylation of histone H3 at Ser10, Ser28, and Thr11 can lead to acetylation of adjacent Lys residue and chromatin decondensation (Peterson and Laniel, 2004; Baek, 2011).

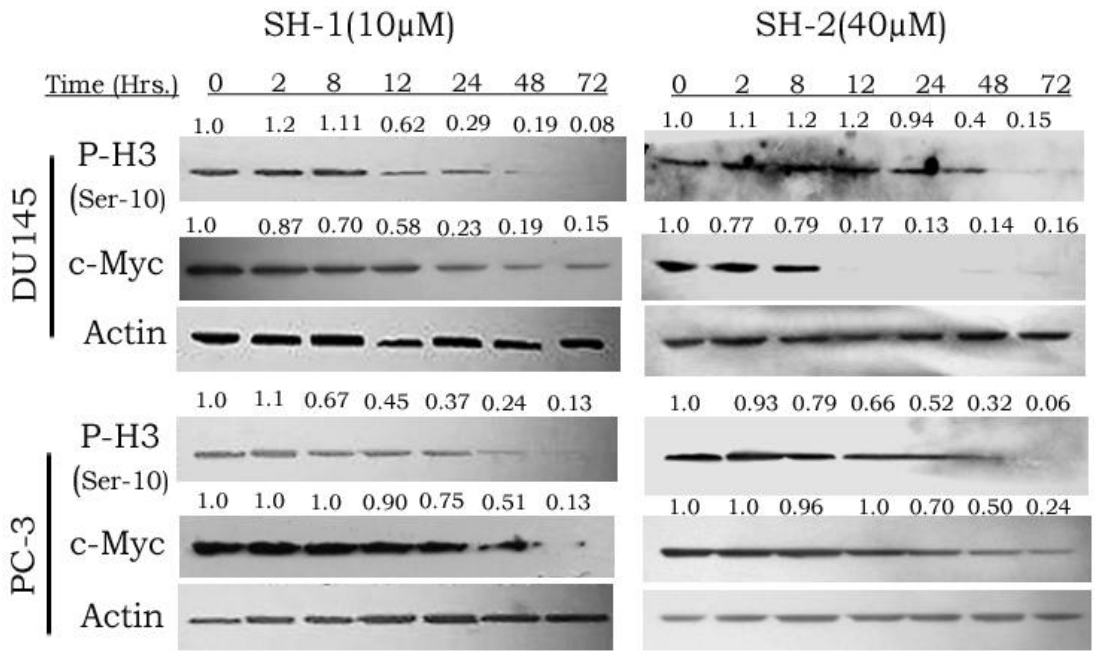

Figure. 5.4. SH-1 and SH-2 inhibit the phopho-histone-3 and c-Myc in DU145 and PC-3 cell lines.

Cells were plated and incubated with 10μM of SH-1 and 40μM of SH-2 for the different indicated times. Cells were harvested at stipulated times, lysed and whole cell lysate was used for immunoblotting. Data showed significant inhibition of P-H3 and c-Myc by both SH-1 and SH-2 in a time dependent manner. The expression of P-H-3 and c-Myc were densitometrically normalized with the respective actin bot. Each blot was repeated and yielded similar results.

Recent studies have shown that PKM2 phosphorylates histone H3 at T11 and promote transcription of pro-oncogenes c-Myc and cyclin D1 (Yang et al., 2012). To understand the functional regulation of PKM2, under these conditions, we checked the phosphorylation of histone H3 and c-Myc in prostate cancer cells after the treatment. Both the compounds individually inhibited the phosphorylation of histone-H3 protein (P-H3). The densitometry data showed that by 72 hours, P-H3 expression was totally inhibited in both DU145 and PC-3 cells treated with either SH-1 or SH-2 **(Fig. 5.4)**. Phosphorylation of histone H3 activates the transcription of c-Myc gene (Yang et al., 2012). We next examined the level of c-Myc, both at the mRNA and at the protein level.

The mRNA expression of c-Myc was downregulated approximately by 75% in SH-1 and SH-2-treated DU145 cells **(Fig. 5.5a)**, while PC-3 cells showed about 85-90% inhibition by the compounds **(Fig. 5.5b)**. The protein expression of c-Myc was inhibited by 85% and 75% in DU145 cells and by 87% and 76% in PC-3 cells by SH-1 and SH-2 respectively **(Fig. 5.4)**. Already we have shown in the chapter-3 that in the presence of SH-1, cyclin D1 was decreased in PC-3 **(Fig. 3.8)** but remained unaffected in DU145, while cyclin D1 was downregulated by SH-2 **(Fig. 3.10)** in both the cell lines.

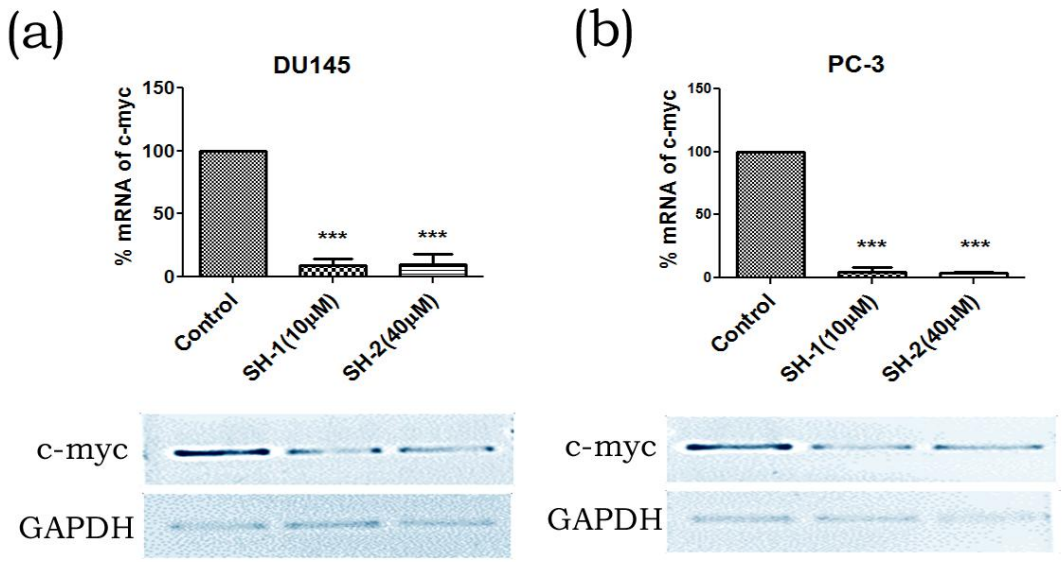

Figure. 5.5. Inhibition of mRNA of c-Myc by SH-1 and SH-2 in DU145 and PC-3 cell lines.

Cells were incubated with 10μM of SH-1 and 40μM of SH-2 for 72 hours. Total RNA was isolated using QIAzol method and cDNA was prepared. Quantitative PCR was done using SYBR-green master mix. Corresponding ct values of c-myc expression were normalized with GAPDH and plotted values for (a) DU145 and (b) PC-3. The corresponding reaction samples were analysed on 1.0% agarose gel and EtBr fluorescence were captured. Experiments were repeated and yielded similar results. ***$p<0.001$ was presented as compared to control.

Our data indicated that both compounds downregulated the expression of PKM2 and inhibited the subsequent transcription of proto-oncogene c-Myc and cyclin D1 in prostate cancer cell lines.

5.3.3. SH-1 and SH-2 inhibit the nuclear interaction of P-H3 and c-Myc in DU145 and PC-3 cell lines

As shown in results **(Fig. 5.4)**, both compounds significantly inhibited c-Myc in cancer cells, we next checked the cellular localization of P-H3 and c-Myc upon treatment with either of the compound by immunofluorescence. The control panel showed that c-Myc is localized both in the nucleus and cytoplasm, though the expression was more prominent in the nucleus in case of DU145 cells **(Fig. 5.6a)**.

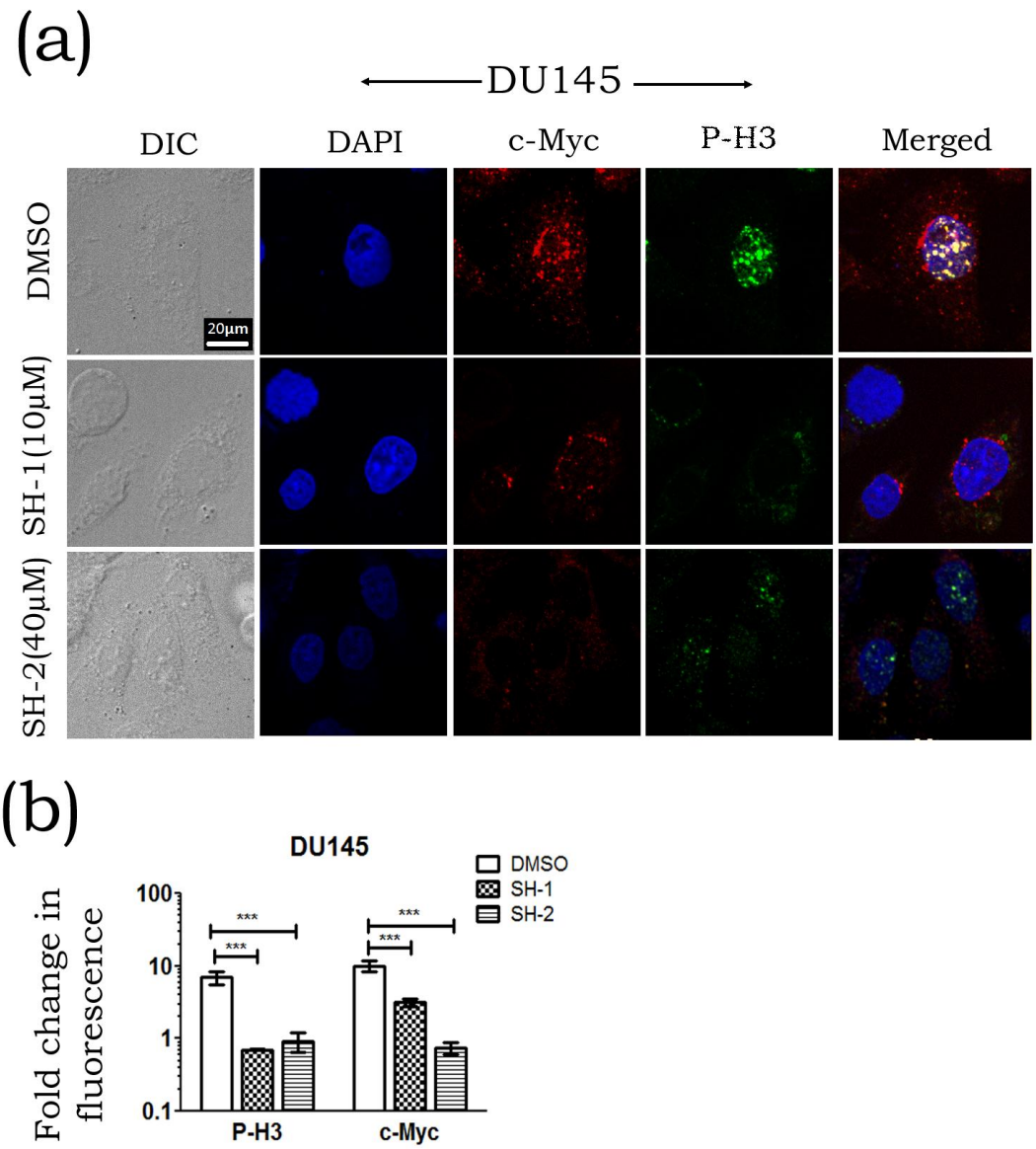

Figure. 5.6. SH-1 and SH-2 inhibit nuclear localization of phospho-histone H-3 and c-Myc in DU145.

Cells were plated over coverslips in 6-well plates and treated with either 10µM of SH-1 or 40µM of SH-2 for 48 hours. Cells were fixed in 4% PFA followed by permeablization with 0.01% Triton-x-100. After incubating with primary (1:50 dilution) and secondary (1:10,000) FITC labelled antibody, cells were mounted over slides in antifade mounting media. DAPI was used to counterstain nucleus. Slides were observed at 60X under ANDOR SPINNING DISK confocal microscope using ANDOR iQ 2.7 software (scale bar: 20µm). (a) Merged image is showing co-localization of phospho-histone-H-3 and c-Myc. (b) Quantitation from microscopic images were done using n number (n>50) of cells for each set. All experiments were repeated and yielded similar results. ***p<0.001 was presented as compared to control.

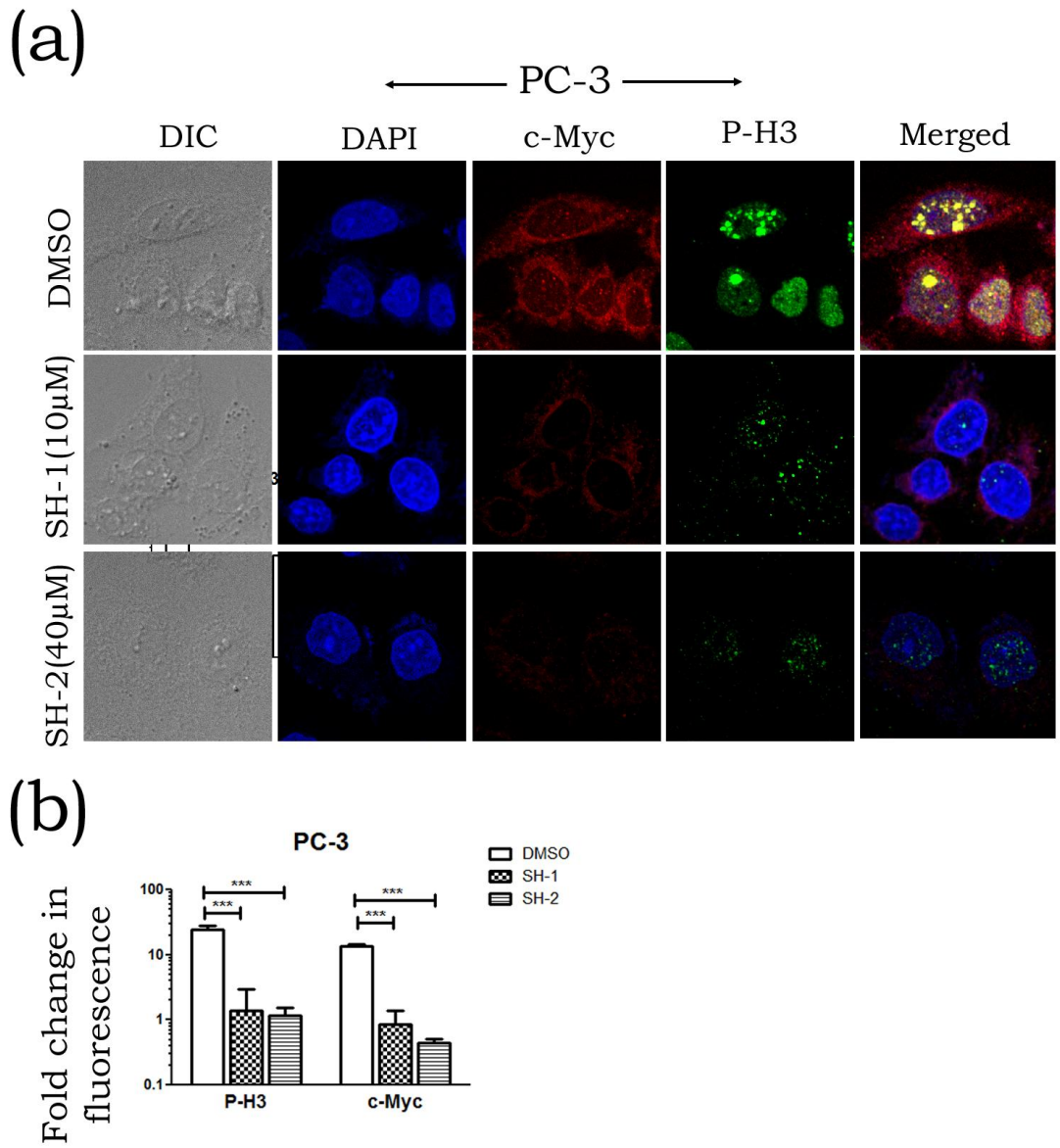

Figure. 5.7. SH-1 and SH-2 inhibit nuclear localization of phospho-histone H-3 and c-Myc in PC-3.

Cells were plated over coverslips in 6-well plates and treated with either 10µM of SH-1 or 40µM of SH-2 for 48 hours. Cells were fixed in 4% PFA followed by permeablization with 0.01% Triton-x-100. After incubating with primary (1:50 dilution) and secondary (1:10,000) FITC labelled antibody, cells were mounted over slides in antifade mounting media. DAPI was used to counterstain nucleus. Slides were observed at 60X under ANDOR SPINNING DISK confocal microscope using ANDOR iQ 2.7 software (scale bar: 20µm). (a) Merged image is showing co-localization of phospho-histone H-3 and c-Myc. (b) Quantitation from microscopic images were done using n number (n>50) of cells for each set. All experiments were repeated and yielded similar results. ***p<0.001 was presented as compared to control.

The P-H3 was expressed exclusively in the nucleus in the untreated samples. Merge panel showed the overlapping or colocalization of the proteins in both DU145 **(Fig. 5.6a)** and PC-3 cells **(Fig. 5.7a)**. After treatment with either SH-1 or SH-2 for 48 hours, both P-H3 and c-Myc were inhibited. Treatment with either either of the compound not only abolished the interaction of P-H3 and c-Myc but also resulted in significant depletion in their expression in both DU145 **(Fig. 5.6a)** and PC-3 **(Fig. 5.7a)** cell lines. The relative expression of c-Myc and P-H3 in treated and untreated cells was quantified, which showed that P-H3 was inhibited by about 50% and 42% and c-Myc was inhibited by 28% and 49% by SH-1 and SH-2 respectively in DU145 cells **(Fig. 5.6b)**. The PC-3 cells showed 55% and 60% inhibition in P-H3 and 62% and 69% inhibition in c-Myc by SH-1 and SH-2 respectively **(Fig. 5.7b)**.

Our data showed that both SH-1 and SH-2 inhibited the expression and colocalization of nuclear P-H3 and c-Myc in both prostate cancer cell lines.

5.3.4. SH-1 and SH-2 induce reactive oxygen species (ROS) level in DU145 and PC-3

One of the hallmarks of cancer cells is increased the level of ROS as compared to the normal cells and this makes the cancer cells more susceptible to a further increase in the ROS level. We checked the ROS-production using DCFH-DH dye in DU145, PC-3 and NIH-3T3 cells followed by flow cytometry. Our data indicated a significant time-dependent increase in ROS generation in SH-1-treated **(Fig. 5.8a and b)** or SH-2-treated **(Fig. 5.8c and d)** both cancer cells. Chapter-2 indicated that the fibroblast cell, NIH-3T3, were least sensitive to compound induced toxicity, the ROS level in fibroblast cells was examined here. At 72 hours, fibroblast cells did not show any increase in ROS as compared to 30-40% increase in ROS level in the cancer cells **(Fig. 5.9).** H_2O_2 (10µM) was used as positive control for ROS generation assay.

These data suggested a selective increase in ROS generation in cancerous cells by both the compounds.

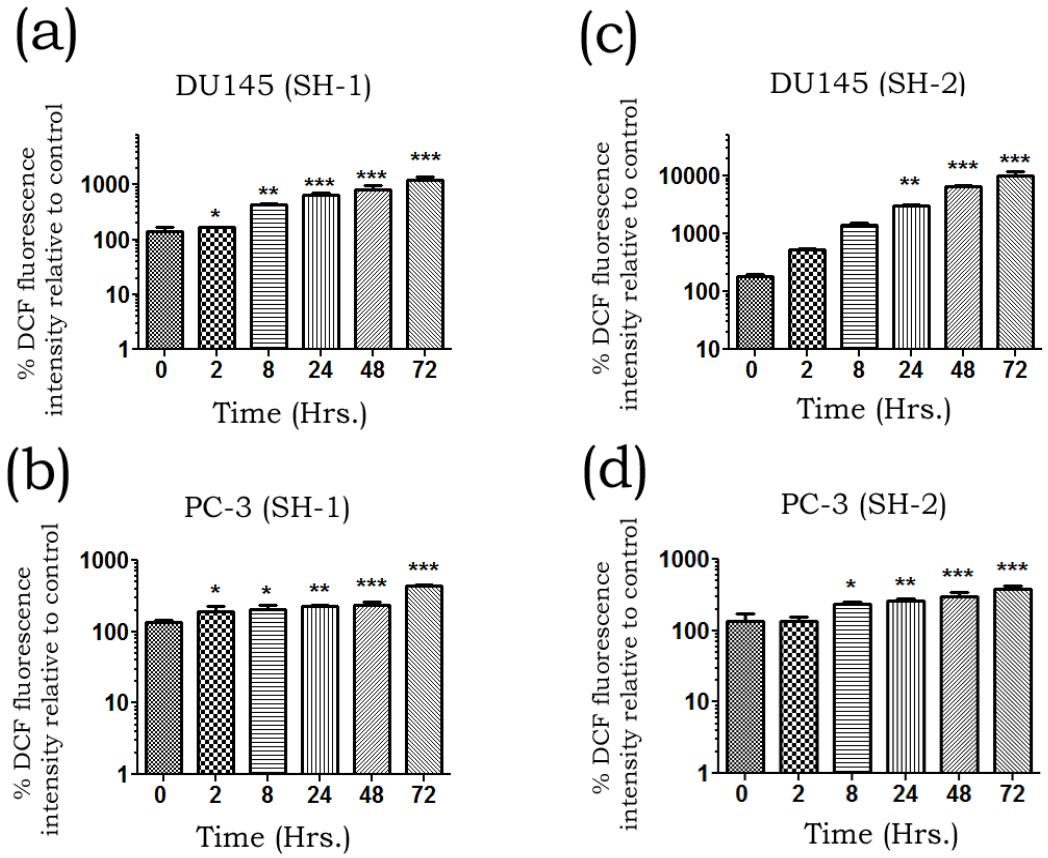

Figure. 5.8. Time dependent evaluation of ROS generation by SH-1 and SH-2.

Cells were plated and treated with 10µM of SH-1 and 40µM of SH-2 for various indicated time intervals. Cells were harvested and incubated with DCFH-DA (10µM) and fluorescence was measured by flow cytometry. Treatment resulted in induction of ROS in DU145 cells, treated with either SH-1 (a) or SH-2 (c) and PC-3 cells, treated with either SH-1 (b) or SH-2 (d) in a time dependent manner. Experiments were repeated and yielded similar results. The data shown are the mean ±S.D. from three independent experiments. *p<0.05, **p<0.01, ***p<0.001 were presented as compared to control.

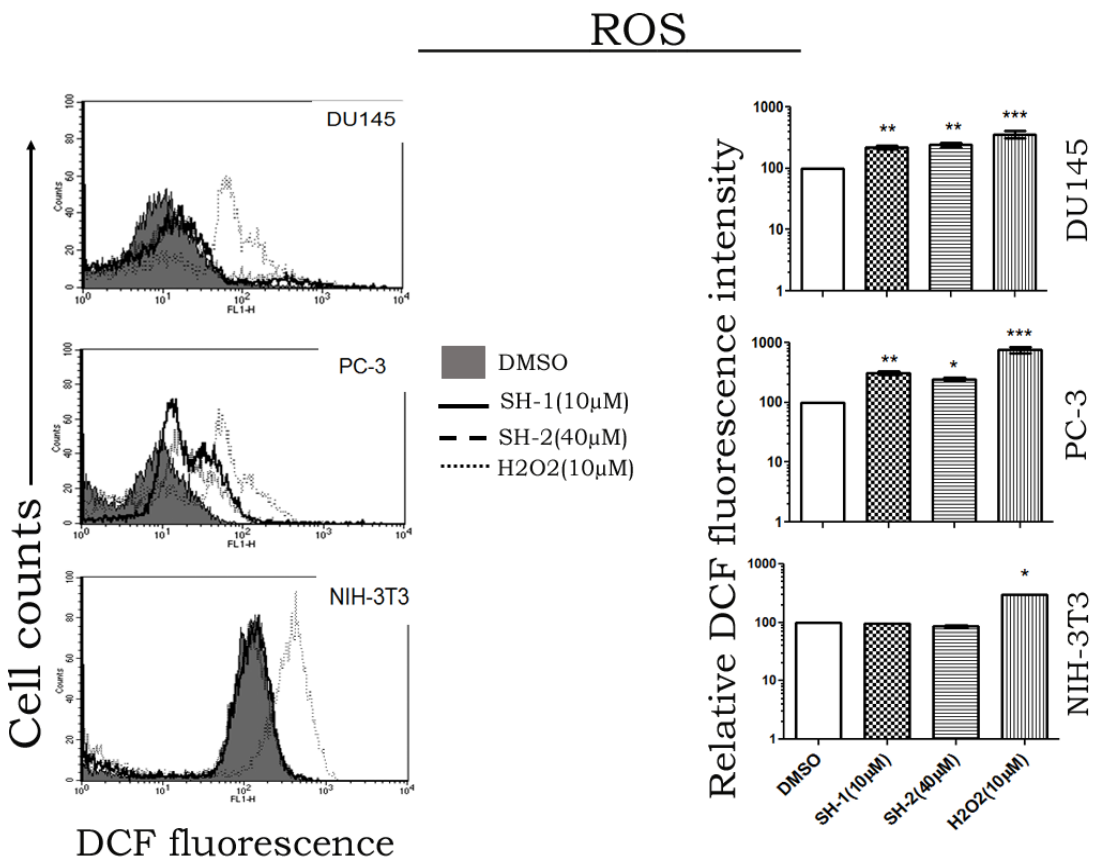

Figure. 5.9. Demonstration of ROS generation by SH-1 and SH-2 in cancerous and noncancerous cells.

DU145, PC-3 and NIH-3T3 cells were plated and treated with either 10µM or 40µM of SH-1 or SH-2 respectively for 72 hours. Cells were harvested and incubated with DCFH-DA (10µM) and fluorescence was measured by flow cytometry. H_2O_2 (10µM) was used as positive control. Treatment resulted in induction of ROS in DU145 and PC-3 but not in NIH-3T3 cell line. Experiments were repeated and yielded similar results. The data shown are the mean ±S.D. from three independent experiments. *p<0.05, **p<0.01, ***p<0.001 were presented as compared to control.

5.3.5. SH-1 and SH-2 inhibit mitochondrial membrane potential (MMP) in DU145 and PC-3

The increase in cell death, ROS, and inhibition of PKM2 prompted us to look for the effect of these compounds on mitochondrial membrane integrity. We checked the mitochondrial membrane potential.

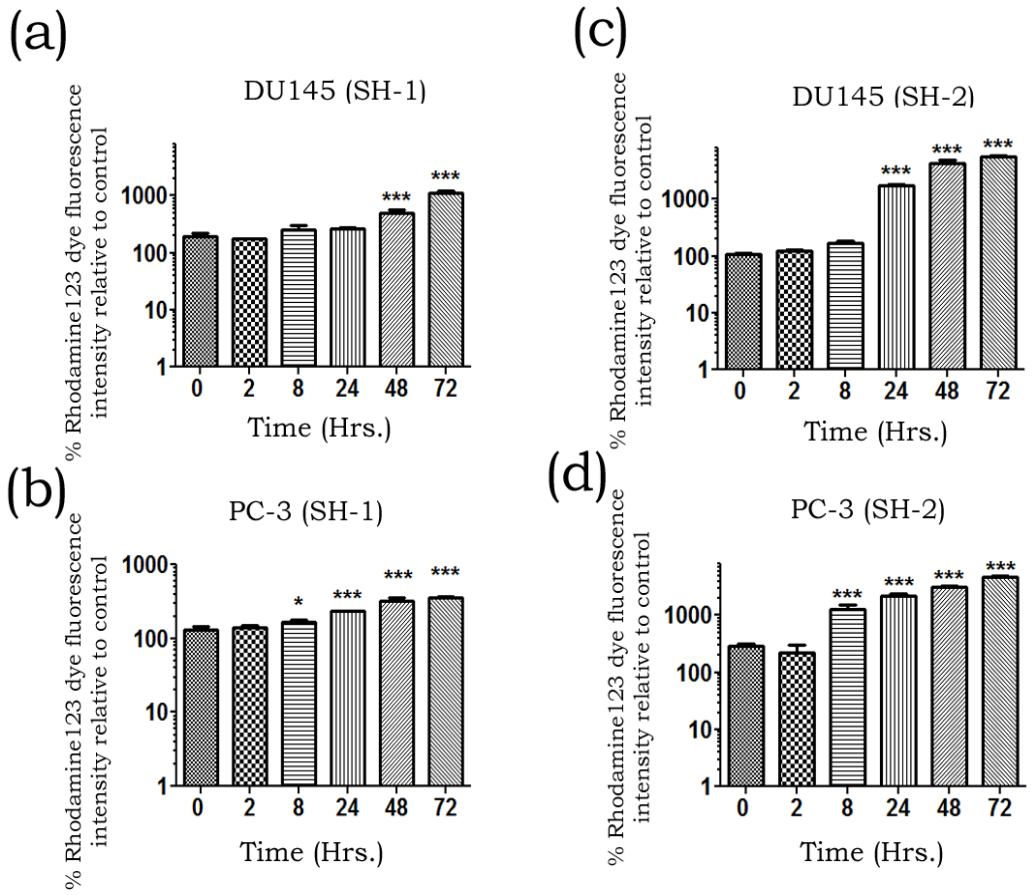

Figure. 5.10. SH-1 and SH-2 disrupts mitochondrial membrane potential (MMP) in a time dependent manner.

Cells were plated and treated with 10µM of SH-1 and 40µM of SH-2 for various indicated time intervals. Cells were harvested and incubated with Rhodamine 123 (10µM) and fluorescence was measured by flow cytometry. Both SH-1 and SH-2 disrupted MMP significantly in DU145 cells, treated with either SH-1 (a) or SH-2 (c) and PC-3 cells, treated with either SH-1 (b) or SH-2 (d) in a time dependent manner. Experiments were repeated and yielded similar results. The data shown are the mean ±S.D. from three independent experiments. *$p<0.05$, ***$p<0.001$ were presented as compared to control.

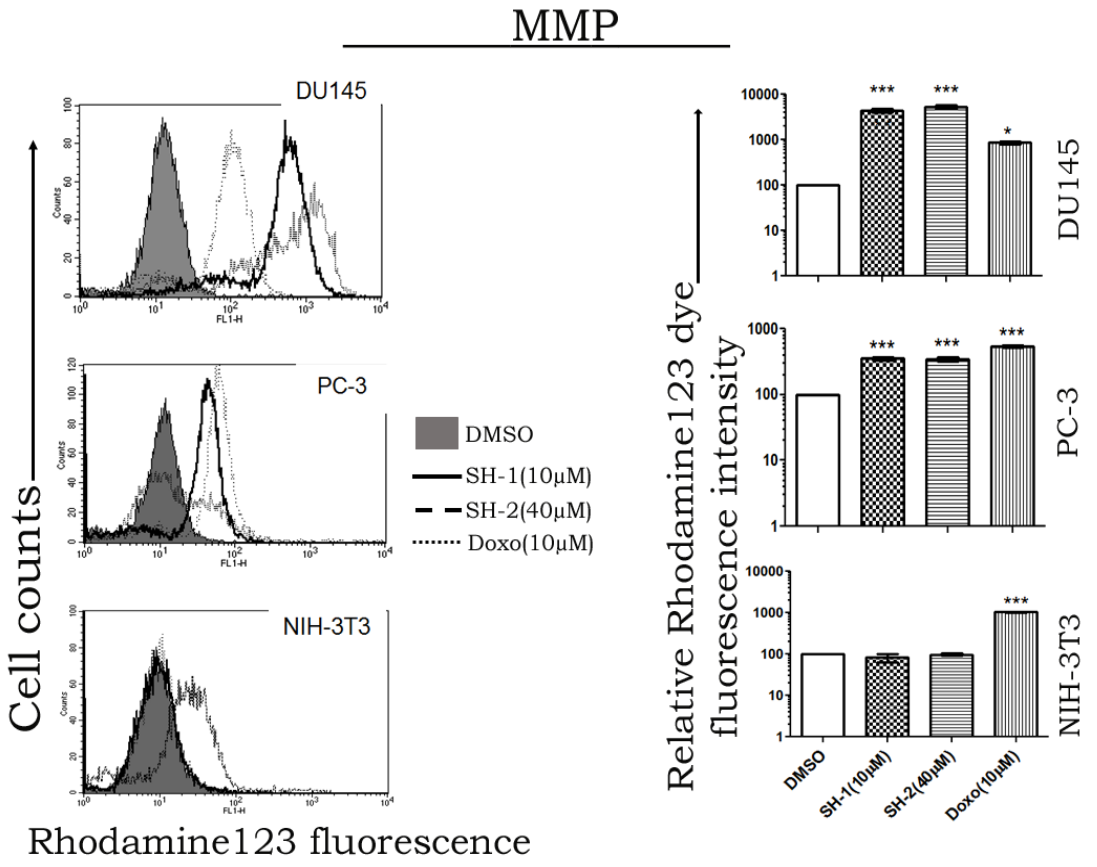

Figure. 5.11. Demonstration of MMP by SH-1 and SH-2 in cancerous and noncancerous cells.

DU145, PC-3 and NIH-3T3 cells were plated and treated with either 10μM or 40μM of SH-1 or SH-2 respectively for 72 hours. Cells were harvested and incubated with Rhodamine 123 (10μM) and fluorescence was measured by flow cytometry. Doxorubicin (10μM) was used as positive control. Both SH-1 and SH-2 disrupted MMP significantly in cancer cell lines DU145 and PC-3 but not in NIH-3T3 cell line. Experiments were repeated and yielded similar results. The data shown are the mean ±S.D. from three independent experiments. *p<0.05, ***p<0.001 were presented as compared to control.

We used cationic fluorescent dye Rhodamine 123, which can diffuse into the mitochondrial matrix and reflect the change of MMP. Higher concentration of Rhodamine dye (10μM) was used so that disruption in membrane potential would result in more influx of dye in mitochondria and higher rhodamine fluorescence. Fluorescence emission was measured by flow cytometry. Our data indicated a significant time-dependent increase in MMP disruption in SH-1 **(Fig. 5.10a, b)** and SH-2-treated **(Fig. 5.10c and d)** cancer cells. The data, post 72 hours treatment,

indicated about 40% inhibition in MMP in both cancer cells, while the fibroblast cells remained unaffected **(Fig. 5.11).** Doxorubicin (10µM) was used as positive control for MMP assay.

The results show that both compound drastically disrupted the mitochondrial membrane potential selectively in cancer cells that might have triggered by an increase in ROS.

5.3.6. SH-1 and SH-2 induced mitochondrial apoptosis in both prostate cancer cell lines, DU145 and PC-3

The sub-G_1 populations of cell cycle data obtained from SH-1 and SH-2 treatment **(chapter-3, Fig. 3.1 and 3.2)** were plotted **(Fig. 5.12a, c, 5.13a, c)**. The increase in sub-G_1 cell population, induction of ROS and disruption of mitochondrial membrane potential intrigued us to study whether the compound-induced cell death was due to apoptosis. PARP [Poly (ADP-ribose) Polymerase], which is a well-known DNA repair protein, respond to the initial DNA damage and is cleaved in apoptosis (Boulares et al., 1999). We checked the expression of PARP in cancer cells treated for indicated time interval. The data indicated that both SH-1 **(Fig. 5.12b and d)** and SH-2 **(Fig. 5.13b and d)** induced the cleavage of PARP in a time-dependent manner in both the cancerous cell lines. These data indicated that the cell death, brought about by either SH-1 or SH-2, involved the cellular apoptosis.

Mitochondrial pathway of apoptosis involves many signals which can modulate mitochondrial membrane potential and mitochondrial permeability. Therefore, we studied the role of both compounds on the expression of major proteins involved in this pathway. Cytochrome *c* release is known indicator of caspase-3 cleavage during mitochondria-dependent apoptosis. Pro-caspase-3 is processed into two subunits of 20 and 11 kDa. The 20 kDa subunit is auto-processed into an active subunit of 17 kDa. The western blot study showed that drug treatment induced cleavage of pro-caspase-3 in a time-dependent manner post 24 hours in SH-1 **(Fig. 5.12b and d)** and SH-2 **(Fig. 5.13b and d)** treated cell lines. Anti-apoptotic proteins Bcl-2 and survivin are overexpressed in many cancer and inhibit Bax/Bak which promote the

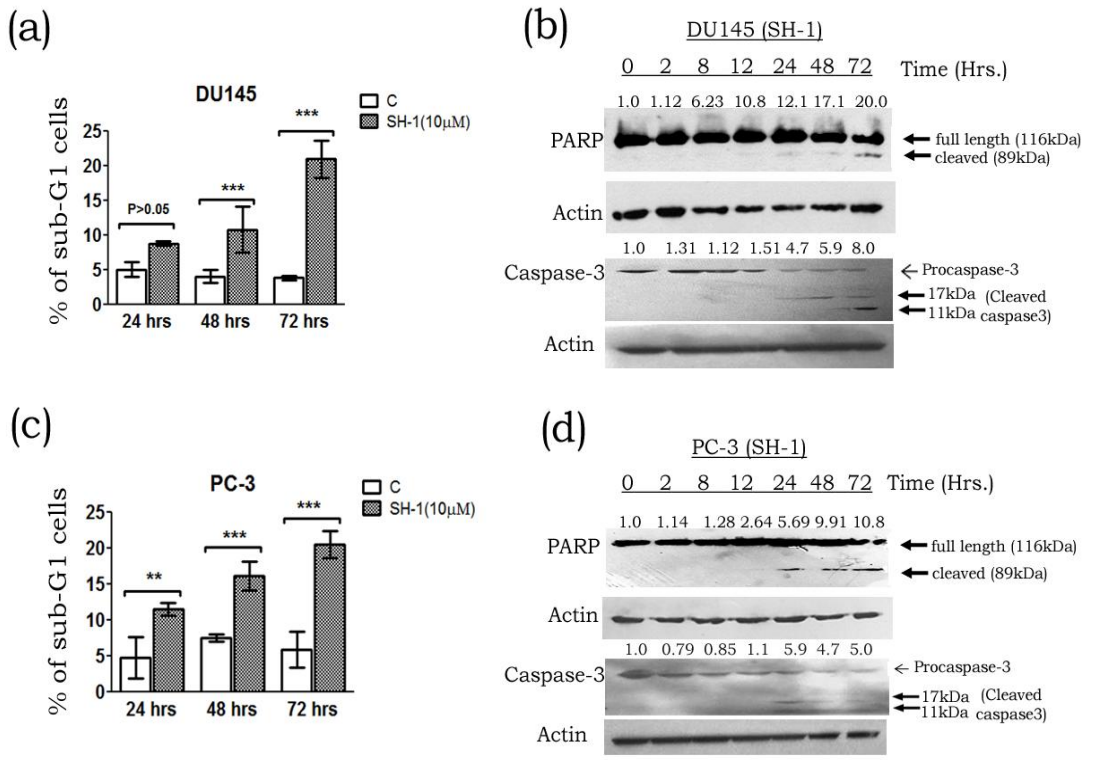

Figure. 5.12. SH-1 induces the apoptotic cell death in DU145 and PC-3 cell lines.

DU145 and PC-3 cells were incubated with 10μM of SH-1 for the various indicated time periods. Cells were harvested at their stipulated time point, lysed and whole cell lysate was used for immunoblotting. SH-1 induced the sub-G_1 cells in both DU145 and PC-3 **(Figure. 3.3, chapter 3)**. The sub-G1 cells, which indicate dead cells, were plotted against their respective control in both DU145 (a) and PC-3 (c) cell lines. Western blotting data showed that SH-1 cleaved the full length PARP and caspase-3 in both DU145 (b) and PC-3 (d) cells. The cleaved products of PARP and caspase-3 were densitometrically normalized with their respective actin blots. Each blot was repeated and yielded similar results. The data shown are the mean ±S.D. from three independent experiments. **p<0.01, ***p<0.001were presented as compared to control.

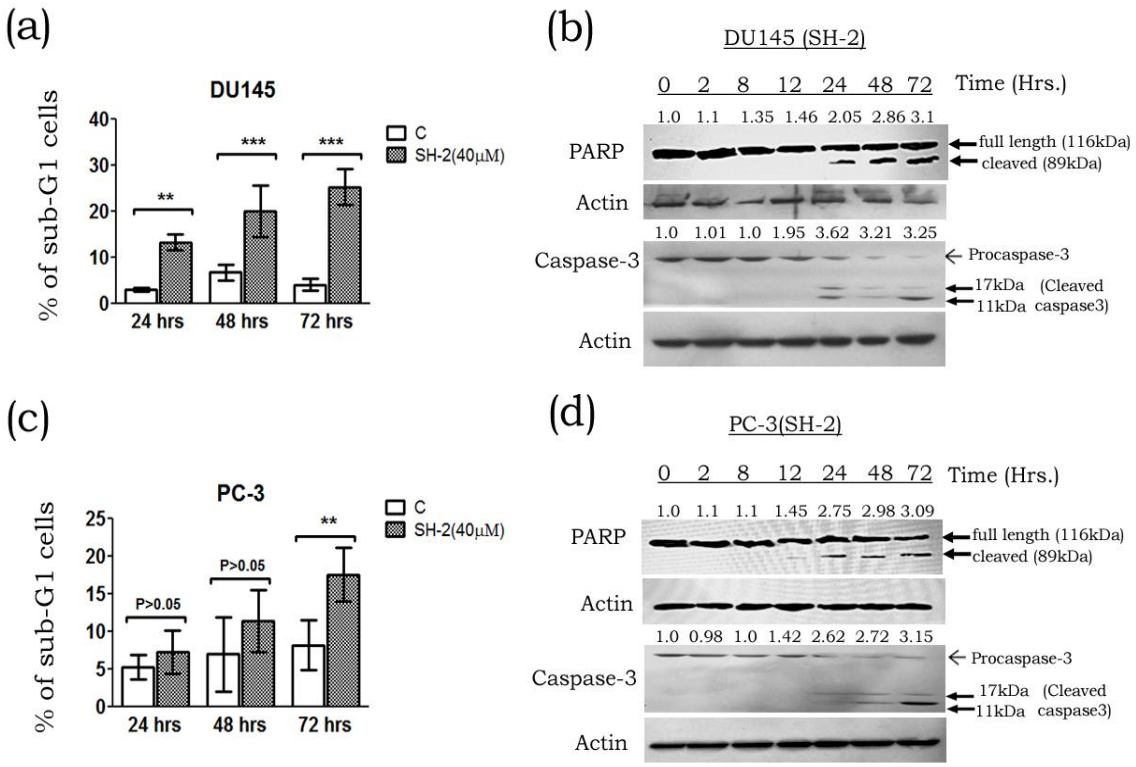

Figure. 5.13. SH-2 induces the apoptotic cell death in DU145 and PC-3 cell lines.

DU145 and PC-3 cells were incubated with 40μM of SH-2 for the various indicated time intervals. Cells were harvested at their stipulated time point, lysed and whole cell lysate was used for immunoblotting. SH-2 induced the sub-G_1 cells in both DU145 and PC-3 **(Figure. 3.3, chapter 3)**. The sub-G1 cells, which indicate dead cells, were plotted against their respective control in both DU145 (a) and PC-3 (c) cell lines. Western blotting data showed that SH-2 cleaved the full length PARP and caspase-3 in both DU145 (b) and PC-3 (d) cells. The cleaved products of PARP and caspase-3 were densitometrically normalized with their respective actin blots. Each blot was repeated and yielded similar results. The data shown are the mean ±S.D. from three independent experiments. **p<0.01, ***p<0.001 were presented as compared to control.

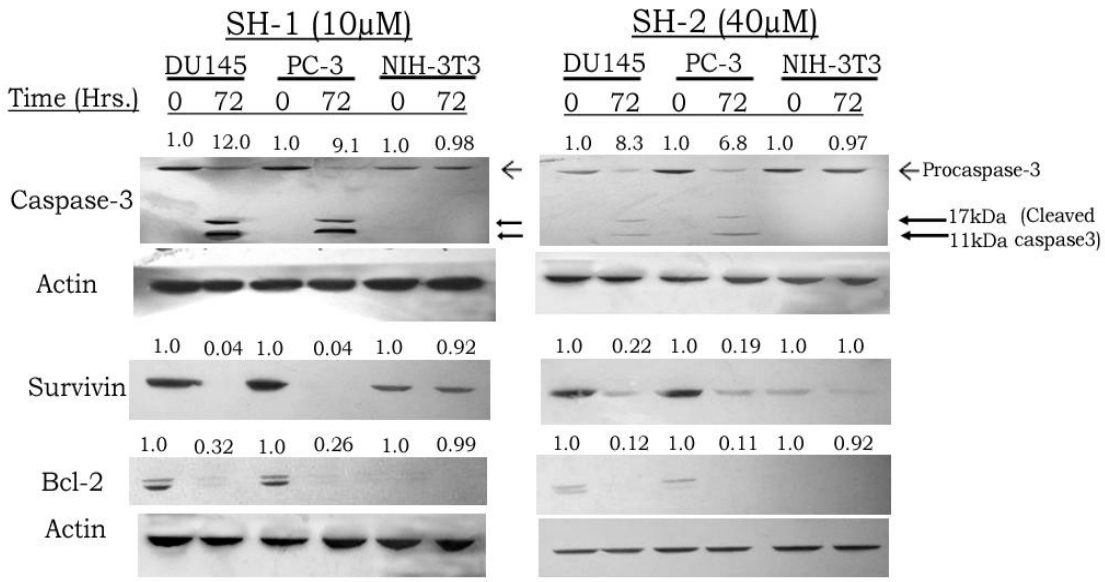

Figure. 5.14. SH-1 and SH-2 induced apoptotic cascade in cancerous cells not in fibroblast cell line NIH-3T3.

DU145, PC-3 and NIH-3T3 cells were incubated with 10µM of SH-1 and 40µM of SH-2 for 72 hours. Cells were harvested, lysed and whole cell lysate was used for immunoblotting. Western blotting data showed that neither SH-1 nor SH-2 could cleave caspase-3 in its active subunits in fibroblast cells. Further the expression level of survivin and bcl-2 remained constant in treated and untreated fibroblast cells. Cleaved caspase-3, survivin and bcl-2 expressions were densitometrically normalized with their respective actin blot. Each blot was repeated and yielded similar results.

release of cytochrome-c. The western blots of Bcl-2, survivin, and caspase-3, were densitometrically quantified which showed that 72 hours post-SH-1 exposure resulted in an increase in cleavage of caspase-3 by 12-fold and 9-fold in DU145 and PC-3 respectively, and by 7-8 fold in SH-2 treatment cancer cells **(Fig. 5.14)**. The expression of survivin and Bcl-2 were inhibited up to 90% in cancer cells **(Fig. 5.14)**. Interestingly in the non-cancerous cell line, NIH-3T3, the expression of all these proteins remained unaltered in the presence of either of the compound **(Fig. 5.14)**.

These data suggested the selective induction of apoptosis in both cancer cells teated with either SH-1 or SH-2.

5.4. Discussion

The cancer cells are under high metabolic pressure as compared to their normal counterparts. The PKM2 has been found to be induced in many types of cancer, wherein it pushes the glucose metabolism in the aerobic pathway. The dimeric form of PKM2 plays a key role in the Warburg effect (Christofk et al., 2008), while the highly active tetrameric form is implicated in the perpetuation of gene transcription required for cell proliferations (Dong et al., 2016). In glycolytic signaling, enzyme pyruvate kinase regulates a rate limiting step involving the formation of ATP and pyruvate from phosphoenolpyruvate (PEP) (Koppenol et al., 2011). PKM2 regulates transcription by modulating the histones, especially H3. Post-transcriptional modification of histones plays a fundamental role in the condensation or decondensation of chromatin thus regulating the transcription. Histone H3 is phosphorylated at various serine, threonine, and tyrosine residues and that lead to the acetylation of lysine residue required in mitosis (Baek, 2011; Peterson and Laniel, 2004). Ser10 phosphorylation of histone H3 has been reported to induce cancer (Li et al., 2013). Histone H3 phosphorylation by PKM2 promotes transcription of proto-oncogenes c-myc and cyclin D1 (Yang et al., 2012). Our data showed that both the compounds individually inhibited PKM2 expression, both at the transcription as well as at the translational level. Further, both the compounds blocked the Ser10 phosphorylation of histone H3, and the level of the c-Myc and cyclin D1 was also downregulated. The interaction of nuclear P-H3 and c-Myc was also blocked in DU145 and PC-3 cells. c-Myc, a proto-oncogene, is regulated by several molecular mechanisms and induced in many types of cancer (Dang, 2012). It upregulates cyclins and downregulates cyclin inhibitor p21 and thus promotes cell proliferation. In the presence of either of the compounds, mRNA level of c-myc was downregulated, showing their effects on the transcription level and asserting their anti-proliferating effect. In chapter-3, we have shown an increase in the expression level of the CDK-inhibitor, p21 in the presence of either of the compound. The decreased level of c-Myc level might not be able to downregulate the expression of p21, and thus p21 was able to block cell proliferation.

The ROS production is the metabolic outcome of increased metabolic processes, mitochondrial dysfunction, and peroxisome activity (Murphy, 2013). High ROS

levels are known to damage proteins and DNA and can be exploited to kill cancer cells (Wang and Yi, 2008; Khan et al., 2012; Raj et al., 2011). The loss of MMP may be corroborated with the production of high ROS (Liou and Storz, 2010). In majority of cancer cells, mitochondria function aberrantly and produce energy rather directly by glycolysis (Jose et al., 2011). Therefore, we further evaluated the level of ROS in both prostate cancer cells and found that both compounds increased ROS level significantly. The increase in ROS may, in turn, disrupt the mitochondrial membrane integrity. Therefore, we next checked the integrity of mitochondrial membrane in both cancer cells. Our data indicated that both compounds disrupted the MMP in both cancer cell lines in a dose-dependent manner. In chapter-3, our cell cycle data indicated that treatment of both cancer cell lines with either compound resulted in an increase in sub-G_1 cell population in a time-dependent manner. To investigate whether the cell death was due to cellular apoptosis, we performed the western blot of PARP, a well-characterized DNA repair protein and a marker of apoptosis. The cleavage of PARP indicated that arrested cells were apoptosized with increase in exposure time. Intrinsic apoptosis implicates several undesirable modulations in mitochondria and its cellular signaling (Cai and Jones, 1999; Yee et al., 2014). The MMP and ROS data further intrigued us to know how expression level of mitochondria-dependent apoptotic proteins was affected. Members of the Bcl-2 family of proteins have a pivotal role in regulating the apoptotic pathway. Bcl-2, a member of this family, suppress apoptosis and is associated with the mitochondrial membrane. Another molecule survivin inhibits caspase-3 activation, hence carries out negative regulation of apoptosis. Survivin is overexpressed in many cancers, including prostate cancer which might promote the conditions for metastasis and tumorigenesis (Zhu et al., 2005; Jha et al., 2012). Furthermore, the elevated levels of survivin in the primary tumor is frequently linked with a poor prognosis for patients (Jha et al., 2012). Our results clearly showed the down-regulation of survivin and Bcl-2 expression, and increase in caspase-3 cleavage selectively in the cancerous cells suggesting their vital role in the induction of apoptosis in both metastatic prostate cancer cells. The expression of these apoptotic proteins were unaltered in compound treated non-cancerous fibroblast cell line.

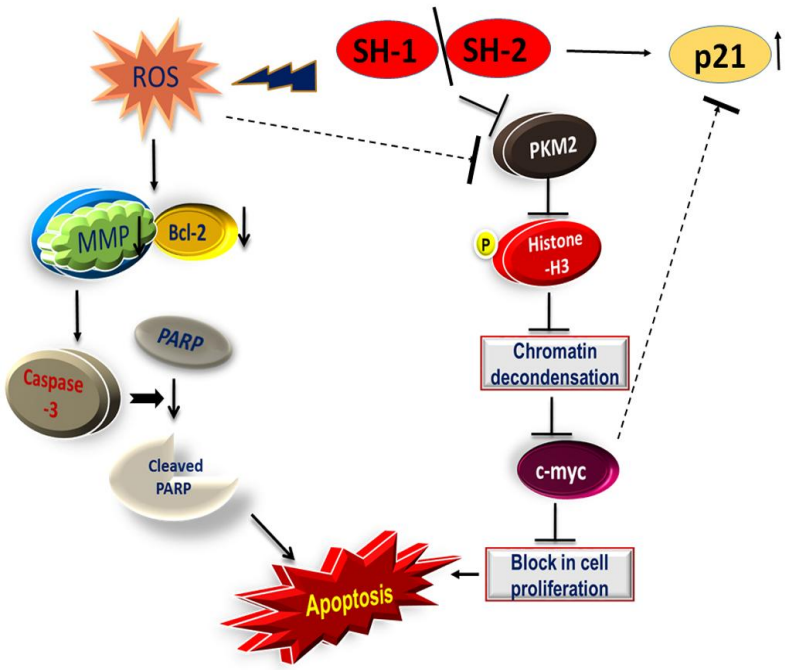

Figure. 5.15. Proposed hypothetical mechanism of inhibitory-action of SH-1 and SH-2 on PKM2 pathway and apoptosis.

Both compounds escalate ROS level which inhibits the membrane potential of mitochondria and release of cytochrome c. The inhibition of anti-apoptotic protein Bcl-2 results in the activation of effector caspase-3. Caspase-3 cleaves PARP and finally cell is apoptosized. The glycolytic enzyme PKM2 is inhibited by either compound and by high ROS level as well. The inhibition of PKM2 leads to the dephophorylation of histone-H3 and further inhibition of the transcription of pro-oncogene c-Myc. Inhibition of c-Myc may not be able to inhibit the upregulation of p21 and that results in inhibition in cell proliferation and apoptosis.

A hypothetical model is suggested based on the above data. As summarized in figure **(Fig. 5.15)**, both SH-1 and SH-2 induce oxidative stress by elevating the ROS level which inhibits the membrane potential of mitochondria and stimulates the release of cytochrome c. Cytochrome c inhibits the anti-apoptotic protein Bcl-2, and that results in the activation of effector caspase-3. Caspase-3 cleaves PARP and finally renders the cells to apoptosis. Both the compounds may inhibit the glycolytic enzyme PKM2 directly or by the ROS. The inhibition of PKM2 leads to the inhibition of the phosphorylation of histone-H3 and further inhibition of the transcription of pro-oncogene c-Myc. Inhibition of c-Myc may not be able to inhibit p21 and that results in inhibition in cell proliferation and apoptosis.

5.5. References

Altenberg, B. and Greulich, K.O. (2004). 'Genes of glycolysis are ubiquitously overexpressed in 24 cancer classes'. *Genomics*, 84(6): 1014–1020.

Baek, S.H. (2011). 'When Signaling Kinases Meet Histones and Histone Modifiers in the Nucleus'. *Molecular Cell*, 42(3): 274–284.

Boulares, a H., Yakovlev, A.G., Ivanova, V., Stoica, B. a, Wang, G., Iyer, S., Smulson, M., et al. (1999). 'Role of Poly (ADP-ribose) Polymerase (PARP) Cleavage in Apoptosis'. *The Journal of biological chemistry*, 274(33): 22932–22940.

Cai, J. and Jones, D.P. (1999). 'Mitochondrial redox signaling during apoptosis'. *Journal of Bioenergetics and Biomembranes*, 31(4): 327–334.

Christofk, H.R., Vander Heiden, M.G., Harris, M.H., Ramanathan, A., Gerszten, R.E., Wei, R., Fleming, M.D., et al. (2008). 'The M2 splice isoform of pyruvate kinase is important for cancer metabolism and tumour growth'. *Nature*, 452(7184): 230–233.

Dang, C. V. (2012). 'MYC on the path to cancer'. *Cell*, 149(1): 22–35.

David, C.J., Chen, M., Assanah, M., Canoll, P. and Manley, J.L. (2010). 'HnRNP proteins controlled by c-Myc deregulate pyruvate kinase mRNA splicing in cancer.' *Nature*, 463(7279): 364–8.

Dong, G., Mao, Q., Xia, W., Xu, Y., Wang, J., Xu, L. and Jiang, F. (2016). 'PKM2 and cancer: The function of PKM2 beyond glycolysis (Review)'. *Oncology Letters*, 11(3): 1980–1986.

Jha, K., Shukla, M. and Pandey, M. (2012). 'Survivin expression and targeting in breast cancer.' *Surgical oncology*, 21(2): 125–131.

Jose, C., Bellance, N. and Rossignol, R. (2011). 'Choosing between glycolysis and oxidative phosphorylation: A tumor's dilemma?' *Biochimica et Biophysica Acta - Bioenergetics*, 1807(6): 552–561.

Khan, M.I., Mohammad, A., Patil, G., Naqvi, S.A.H., Chauhan, L.K.S. and Ahmad, I. (2012). 'Induction of ROS, mitochondrial damage and autophagy in lung epithelial cancer cells by iron oxide nanoparticles'. *Biomaterials*, 33(5): 1477–1488.

Koppenol, W.H., Bounds, P.L. and Dang, C. V. (2011). 'Otto Warburg's contributions to current concepts of cancer metabolism.' *Nature reviews. Cancer*, 11(5): 325–37.

Lee, J.S., Smith, E. and Shilatifard, A. (2010). 'The Language of Histone Crosstalk'. *Cell*, 142(5): 682–685.

Li, B., Huang, G., Zhang, X., Li, R., Wang, J., Dong, Z. and He, Z. (2013). 'Increased phosphorylation of histone H3 at serine 10 is involved in Epstein-Barr virus latent membrane protein-1-induced carcinogenesis of nasopharyngeal carcinoma.' *BMC cancer*, 13(1): 124.

Liou, M.-Y. and Storz, P. (2010). *Reactive oxygen species in cancer*

Lu, Z. (2012). 'Nonmetabolic functions of pyruvate kinase isoform M2 in controlling cell cycle progression and tumorigenesis'. *Chinese Journal of Cancer*, 31(1): 5–7.

Luo, W. and Semenza, G.L. (2011). 'Pyruvate kinase M2 regulates glucose metabolism by functioning as a coactivator for hypoxia-inducible factor 1 in cancer cells.' *Oncotarget*, 2(7): 551–556.

Mathupala, S.P., Rempel, A. and Pedersen, P.L. (2001). 'Glucose catabolism in cancer cells: Identification and characterization of a marked activation response of the type II hexokinase gene to hypoxic conditions'. *Journal of Biological Chemistry*, 276(46): 43407–43412.

Matlin, A.J., Clark, F. and Smith, C.W.J. (2005). 'Understanding alternative splicing: towards a cellular code.' *Nature reviews. Molecular cell biology*, 6(5): 386–98.

Mazurek, S. (2011). 'Pyruvate kinase type M2: A key regulator of the metabolic budget system in tumor cells'. *International Journal of Biochemistry and Cell Biology*, 43(7): 969–980.

Murphy, M.P. (2013). 'Mitochondrial dysfunction indirectly elevates ROS production by the endoplasmic reticulum'. *Cell Metabolism*, 18(2): 145–146.

Peterson, C.L. and Laniel, M.-A. (2004). 'Histones and histone modifications.' *Current biology : CB*, 14: R546–R551.

Raj, L., Ide, T., Gurkar, A.U., Foley, M., Schenone, M., Li, X., Tolliday, N.J., et al. (2011). 'Selective killing of cancer cells by a small molecule targeting the stress

response to ROS.' *Nature*, 475(7355): 231–4.

Ralph, S.J., Rodríguez-enríquez, S., Neuzil, J. and Moreno-sánchez, R. (2010). 'Molecular Aspects of Medicine Bioenergetic pathways in tumor mitochondria as targets for cancer therapy and the importance of the ROS-induced apoptotic trigger'. *Molecular Aspects of Medicine*, 31(1): 29–59.

Sun, Q., Chen, X., Ma, J., Peng, H., Wang, F., Zha, X., Wang, Y., et al. (2011). 'Mammalian target of rapamycin up-regulation of pyruvate kinase isoenzyme type M2 is critical for aerobic glycolysis and tumor growth.' *Proceedings of the National Academy of Sciences of the United States of America*, 108(10): 4129–4134.

Wang, J. and Yi, J. (2008). 'Cancer cell killing via ROS: To increase or decrease, that is a question'. *Cancer Biology and Therapy*, 7(12): 1875–1884.

Warburg, O. (1956). 'Injuring of Respiration the Origin of Cancer Cells'. *Science*, 123(3191): 309–14.

Yang, W., Xia, Y., Hawke, D., Li, X., Liang, J., Xing, D., Aldape, K., et al. (2012). 'PKM2 Phosphorylates Histone H3 and Promotes Gene Transcription and Tumorigenesis'. *Cell*, 150(4): 685–696.

Yang, W., Xia, Y., Ji, H., Zheng, Y., Liang, J., Huang, W., Gao, X., et al. (2011). 'Nuclear PKM2 regulates β-catenin transactivation upon EGFR activation'. *Nature*, 478(7375): 118–122.

Yee, C., Yang, W. and Hekimi, S. (2014). 'The intrinsic apoptosis pathway mediates the pro-longevity response to mitochondrial ROS in C elegans'. *Cell*, 157(4): 897–909.

Zhu, H., Chen, X.-P., Zhang, W.-G., Luo, S.-F. and Zhang, B.-X. (2005). 'Expression and significance of new inhibitor of apoptosis protein survivin in hepatocellular carcinoma.' *World Journal of Gastroenterology*, 11(25): 3855–3859.

CHAPTER-6

IN-VIVO TOXICITY STUDY OF COMPOUNDS

6.1. Introduction

The deleterious side effects from both chemotherapy and radiation have been of grave concerns in cancer therapy. The most common side effects are "dizziness, audio-visual impairment, nausea, diarrhea, loss of hair, sensory loss, loss of appetite, leading to malnutrition, loss of white blood cells, permanent organ damage or failure, internal bleeding, paralysis" (Lung cancer guide book, 2013; Redd et al., 2001). Doxorubicin, "an anthracycline glycoside antibiotic", is used against different types of cancer (Terry Priestman, 2012; BLUM and CARTER, 1974). However, its use in chemotherapy is confined due to the severe toxic effects on healthy tissue (Shinoda et al., 1999). Docetaxel and Paclitaxel belong to taxane family, has been approved by FDA to be used against a broad range of malignancies including prostate cancer (S. and Y., 2012; Qi et al., 2013). These drugs are being administered in combination with other drugs to enhance the therapeutic potentials. However, the side effects elicited by these drugs have always been a dark truth(Shelley et al., 2006; Partridge et al., 2001; Love et al., 1989). When doxorubicin is used along with docetaxel or paclitaxel, the metabolic conversion of former increases cardiac toxicity (Minotti et al., 2001).

In previous chapters, the selective deleterious effects of SH-1 and SH-2 on prostate cancer cell lines DU145 and PC-3 were observed, which included inhibition of cell proliferation, cell cycle arrest, induction of pro-apoptotic proteins, inhibition of MMP, induction of ROS and the apoptosis. The evaluation of these compounds on noncancer cell line NIH-3T3 suggested that cancer cell lines were more sensitive to the compounds than the noncancer counterpart. This chapter includes *in-vivo* toxic evaluation of SH-1 and SH-2 in BALB/c mice. Animals were given the treatment on an alternate day and an acute study of 20 days was conducted. After compound treatment, levels of ROS and glutathione (GSH), superoxide dismutase (SOD), lipid

peroxides (TBARS), and catalase (CAT) were checked in blood and in tissues viz. liver, kidney and prostate gland.

6.2. Methodology

6.2.1. Chemicals

OPT or "1,10-Phenanthroline monohydrate" (cat-GRM1138), TBA or "2-Thiobarbituric acid (cat-RM1594)", DTNB or "5,5'-Dithiobis(2-nitrobenzoic acid)" (cat- GRM1677), GSH or "Glutathione reductase" (cat- 210068901), NEM or "N–Ethylmaleimide (cat-RM1498)", NADPH (cat-RM393), NBT or "Nitroblue tetrazolium chloride" (cat-RM578), PMS or "Phenazine methosulphate" (cat-MB206), "tetra-Sodium pyrophosphate anhydrous" (cat-GRM7515), and trichloroacetic acid (cat- 0219605780) were obtained from HI Media. Triple distilled water prepared by "Millipore" was used in making the reagents. The additional commercially available routine chemicals were obtained in their highest purity grade.

6.2.2. Animals

Randomly bred BALB/c male mice of 4-6 weeks old and 22±2.0 g of weight, were used for the experiments. All animals were maintained in a well air-conditioned rooms of "animal facility at Jawaharlal Nehru University" (JNU), New Delhi. They were properly maintained on a standard "ad libitum pellet-diet" and tap water with regular alternate cycles of 12 hours of light and darkness. All animals were provided with human care in compliance with the "Committee for the Purpose of Control and Supervision of Experiments on Animals (CPCSEA)." The Animal Ethics Committee of JNU approved (IAEC code-22/2015 dated November 19, 2015) the protocols for the experiments.

Animals were randomly grouped into three separate set of three mice each. Set-I (Control) animals were given DMSO, as a vehicle of test compounds, intraperitoneally using small 1 ml syringe. Set-II and set-III animals was treated with either SH-1 or SH-2 respectively with a dose of 25mg/kg of animal body weight.

The treatments were given on an alternate day for 20 days. All aseptic care were taken into account during treatments.

6.2.3. Preparation of blood hemolysate and tissue homogenate

One day before sacrifice, 300µl of blood was collected intraorbitally using capillary and stored immediately in heparin. Animals were then sacrificed by cervical dislocation, and the stomach was cut open longitudinally. Immediately, the liver was perfused with a high amount of ice-cold normal saline and removed. Kidney, and prostate glands were carefully removed, having no extraneous tissue, and rinsed in cold 1XPBS. The separated organs were blotted dry, weighed quickly and homogenized. Tissue homogenization was done with "0.1M phosphate buffer (pH-7.4) @ 1g/ ml buffer (100%)" and was further diluted in the same buffer to make it 20%.

6.2.4. Reactive oxygen species (ROS) measurement

ROS measurement was done with a slight modification of the standard protocol described by Socci et al. (Socci et al., 1999). The amount of ROS in blood and tissues was measured by using "2',7'-dichlorofluorescein diacetate (DCFDA)" dye, which is converted to fluorescent DCF by cellular oxidative species. Briefly, 5% RBC hemolysate and 1% tissue homogenate were prepared in ice-cold 40 mM Tris–HCl buffer (pH 7.4), and was further diluted to 0.25% with the above buffer. The samples were divided into two equal parts (2 mL each). In one part, 40 µl of 1.25 mM DCFDA in methanol was added for ROS estimation. Another fraction in which 40 µl of methanol was added served as a control for tissue/hemolysate autofluorescence. Samples were incubated in a water bath for 15 min at 37ºC. Fluorescence was recorded at 488 nm excitation and 525 nm emission wavelength using a fluorescence plate reader and expressed in "DCF formed/min" per ml of RBC or mg tissue.

6.2.5. Reduced glutathione (GSH) measurement

For blood glutathione (GSH) measurement, the standard method prescribed by Ellman (Ellman, 1959). was used with few modifications. In brief, 0.2 mL of whole

blood was added to 1.8 mL of distilled water and incubated for 10 minutes at 37°C for complete hemolysis. After that, 3 mL of 4% sulfosalicylic acid was added, and the mixture was centrifuged at 2500 *g* for 15 minutes. The dusty supernatant (0.2 mL) was mixed with 0.4 mL DTNB and 1 mL phosphate buffer. Absorbance recorded at 412 nm was used for the calculation of GSH concentration and expressed as mg/ml of RBCs.

Tissue GSH content was measured with a slight modification of the protocol as described by Hissin and Hilf(Hissin and Hilf, 1976). Briefly, 0.375 ml of 20% homogenate was dissolved in 1.125 mL of phosphate–EDTA buffer and 0.5 mL of 25% HPO3, which resulted in protein precipitation. The mixture was centrifuged at 4°C, 10,000 *g* for 5 minutes and the supernatant was collected. 0.2ml of above supernatant was added in 1.8ml of phosphate–EDTA buffer and 0.1ml of OPT. The whole reaction was vortexed and kept at RT for 15 minutes in the dark. After mixing well, absorbance was recorded at 420 nm and GSH was calculated as mg/g of tissue.

6.2.6. Thiobarbituric acid (TBA) reactive substances

Measurement of lipid peroxidation in blood and tissue was done by the published method described by Pachauri et al(Pachauri and Flora, 2015). Briefly, 100µl of hemolysate was mixed with 0.2 ml of 8% SDS followed by addition of 1.5 ml of 20% acetic acid and 1.5 ml of 0.8% freshly prepared TBA. To this solution, 0.7 ml distilled water was added, and the mixture was boiled at 95°C for 60 minutes till a pink color appeared. After cooling to room temperature, 1ml cold distilled water was added and centrifuged @ 6000rpm, 4°C for 15 minutes.

For tissue, 0.5ml of 20% homogenate was dissolved in 0.5ml of 0.15 M KCl (5% w/v) and was incubated for 30 minutes at 37°C followed by the addition of I ml 10% TCA The reaction mixture centrifuged at 4000 rpm for 15 min. To 0.5ml of supernatant, added 0.5 ml of TBA and the mixture was boiled at 95°C for 10 minutes till a pink color appeared. After cooling the tubes at room temperature, 1ml distilled water was added.

For both blood and tissue, Malondialdehyde (MDA) formation, a key component in lipid peroxidation, was determined by reading the absorbance at 535 nm. The

absorbance of the supernatant was read at 535 nm, and the values were expressed as nanomoles of MDA/mL blood or µg/g tissue weight in tissue samples.

6.2.7. Superoxide dismutase (SOD) assay

The activity of antioxidant SOD from tissue was determined by the method as described by Kakkar (Kakkar et al., 1984) and that from blood was done with modification of prescribed method by Weinterbour (Winterbourn et al., 1975). For blood SOD assay, A reaction containing 0.3 ml hemolysate 0.3 ml PMS, 0.3 ml NBT, 0.8 ml distilled water and 0.2 ml NADH was prepared. For tissue SOD activity, 0.35 ml 20% homogenate was mixed with 0.75 ml of phosphate buffer and the reaction mixture was centrifuged at 2500 rpm, 4^{o}C for 10 minutes. Next, 0.2 ml of supernatant was taken and mixed with 1.2 ml of sodium pyrophosphate, 0.3 ml of PMS, 0.3 ml of NBT, 0.2 ml of hemolysate and homogenate, 0.8 ml of distilled water and 0.2 ml of NADH. In addition to this mixture, a blank reaction was prepared which did not contain tissue protein or blood protein. All reaction mixtures were incubated at 37^{o}C for 90 seconds followed by addition of 1 ml of acetic acid. The reaction mixtures were kept at room temperature for 10 minutes, and the absorbance was recorded at 560nm.

6.2.8. Catalase (CAT) assay

Catalase activity in purified erythrocytes and tissues was assayed following the procedure of Sinha et al., (1972). Reaction mixture using 1 ml of phosphate buffer, 0.1ml of hemolysate and homogenate, 0.4 ml of distilled water and 0.2 ml of H_2O_2 was prepared. The control mixture was prepared; containing 1 ml of phosphate buffer, 0.5ml of distilled water and 0.2 ml of H_2O_2. Both the mixtures were incubated at 37^{o}C for 15 min and reaction was stopped by the addition of 2 ml of acetic acid with dichromate (1:3 ratio of 5% potassium dichromate in distilled water and glacial acetic acid respectively). Above mixture was boiled for 15 min and the mixture was cooled and absorbance was recorded at 570 nm.

6.2.9. Protein determination of blood and tissue.

Total protein in blood and tissue samples was measured by the standard method of Bradford (Bradford, 1976) Before protein estimation both blood and tissue homogenates were processed. Heparinized blood was centrifuged at 500 rpm, $4^{o}C$ for 10 minutes and obtained supernatant was further centrifuged at 12000 rpm, $4^{o}C$ for 15 minutes. The supernatant was collected and used for protein estimation. For tissue, 0.2ml of tissue homogenate was mixed in 0.2ml of TCA and kept overnight for precipitation. The mixture was centrifuged at 2000 rpm for 10 minutes. The supernatant was discarded, and protein pellet was dissolved in 0.2ml of 0.1N NaOH, which was used for protein estimation. The estimation was done in triplicates with different volumes of lysates. Bovine serum albumin (BSA) was used as a standard, and OD was taken at 650 nm.

6.2.10. Statistical analysis

Experimental data were accessed by the method of one-way analysis of variance (ANOVA) using Graph pad prism and then followed by post-Dunnett's multiple comparison tests. The data shown are the mean from three parallel experiments. * = $p<0.05$, ** = $p<0.01$, *** = $p<0.001$ compared to control. $P>0.05$ was considered nonsignificant.

6.3. Results

6.3.1. Effect of SH-1 and SH-2 on Lipid peroxidation and ROS in the blood, liver, Kidney, and Prostate gland of mice

In-vivo toxic evaluation of SH-1 and SH-2 using blood and various tissues samples of mice exposed to SH-1 or SH-2 were done using the standard protocols. A higher level of ROS causes oxidative damage to the biomolecules, including lipids. The ROS level was measured in mice exposed to either DMSO, SH-1 or SH-2. The ROS-blood data indicated the values of 0.0051±0.12 in DMSO-treated, 0.0051±0.09 in SH-1-treated and 0.0052±0.15 in SH-2-treated mice **(Fig. 6.1a)**.

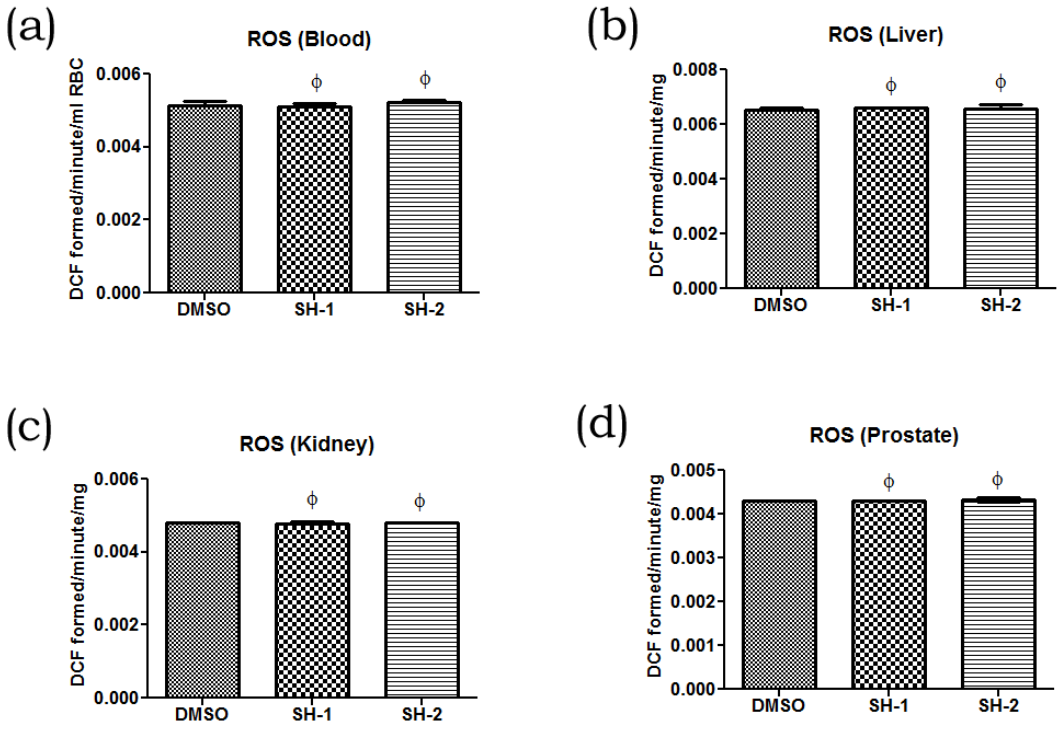

Figure. 6.1. Effect on ROS level in different tissues of mice exposed to either SH-1 or SH-2.

DMSO-exposed mice worked as control vehicle in all assays. The level ROS were measured in terms of the amount of active DCF formed/minute/ml of RBCs or per mg tissue. The fluorescent intensity of DCF was measured in (a) blood, (b) liver, (c) kidney, (d) prostate gland. The calculated values were represented as histograms. Values for each experiment are mean ±SD; n=3. ϕ represents $p>0.05$ with respect to control group.

ROS-liver data showed the values of 0.0065±0.13 in DMSO-treated, 0.0066±0.05 in SH-1-treated and 0.0065±0.14 in SH-2 treated mice **(Fig. 6.1b)**. ROS-kidney data showed the values of 0.0048±0.10 in DMSO treated, 0.0047±0.15 in SH-1-treated and 0.0048±0.09 in SH-2 treated mice **(Fig. 6.1c).** ROS-prostate data showed the values of 0.0043±0.15 in DMSO-treated, 0.0043±0.08 in SH-1-treated and 0.0043±0.07 in SH-2 treated mice **(Fig. 6.1d).** These results clearly indicated that in DMSO, SH-1 or SH-2 treated tissues, ROS level remained unchanged.

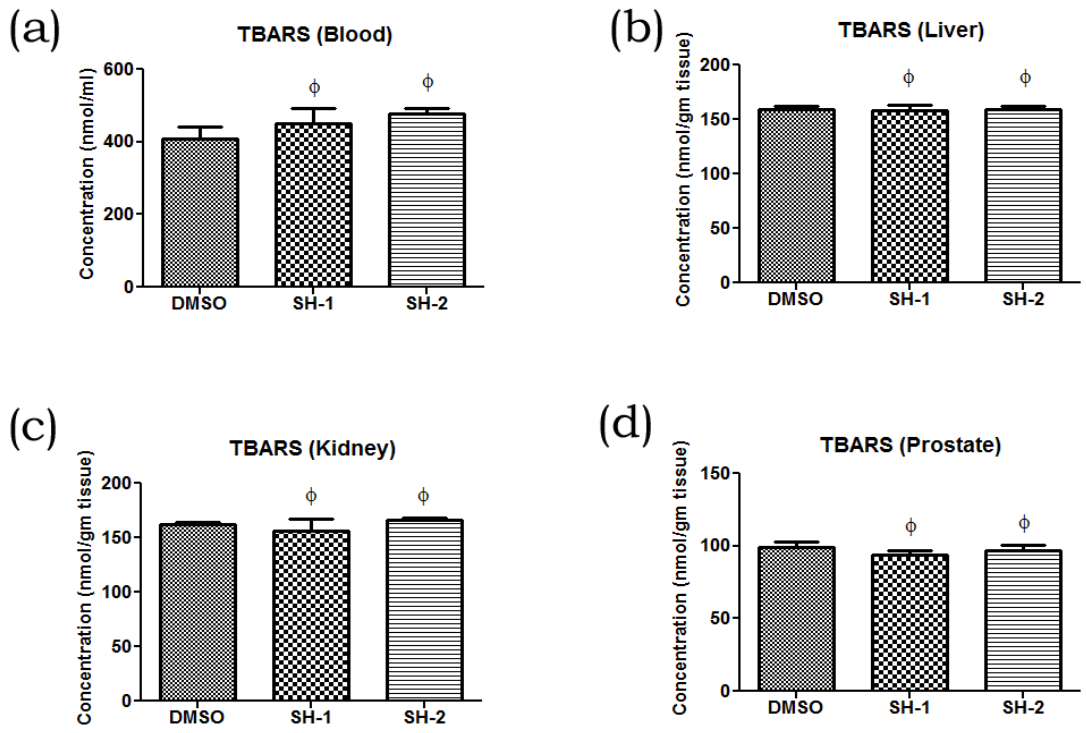

Figure. 6.2. Effect on TBARS in different tissues of mice exposed to either SH-1 or SH-2.

DMSO-exposed mice worked as control vehicle in all assays. The level of thiobarbituric reactive substances (TBARS) in mice, exposed to either compound, are expressed in nanomoles of TBARS per gm of tissue. The fluorescent intensities were measured in (a) blood, (b) liver, (c) kidney, (d) prostate gland. The calculated values were represented as histograms. Values for each experiment are mean ±SD; n=3. ϕ represents $p>0.05$ with respect to control group.

The relative levels of the antioxidants are measured to know whether a compound is toxic or not. The lipid peroxidation by oxidative species involves the conversion of

unsaturated fatty acids to lipid aldehydes. Malondialdehyde (MDA) is one of these lipid peroxidation byproducts (Girotti, 1998) that can react with thiobarbituric acid (TBA) and forms the fluorescent product. These TBA reacting agents are called TBA-reactive substances or TBARS. The TBARS assay was done with different tissues in mice exposed to DMSO or either of the compound. The TBARS-blood data indicated the values of 407.5±14.5 in DMSO treated, 450.0±18.1 in SH-1-treated and 477.5±12.5 in SH-2-treated mice **(Fig. 6.2a)**. TBARS-liver data showed the values of 159.5±8.3 in DMSO treated, 158.2±12.7 in SH-1-treated and 159.2±11.2 in SH-2 treated mice **(Fig. 6.2b)**. TBARS-kidney data showed the values of 162.0±2.2 in DMSO treated, 156.5±10.2 in SH-1-treated and 165.75±3.4 in SH-2 treated mice **(Fig. 6.2c).** TBARS-prostate data showed the values of 98.75±3.9 in DMSO treated, 93.5±3.7 in SH-1-treated and 97.0±4.3 in SH-2 treated mice **(Fig. 6.2d)**. These data demonstrated that the production of MDA in the treated samples remained unaffected with respect to the control samples.

6.3.2. Effect of SH-1 and SH-2 on antioxidant enzymes (GSH, SOD, and CATALASE) in the blood, liver, Kidney, and Prostate gland of mice

As stated above, the cells are equipped with the defense machinery to cope up with the higher level of antioxidants. “reduced glutathione (GSH), superoxide dismutase (SOD) and catalase (CAT)” are the significant players of antioxidant machinery. They convert superoxides into nontoxic molecules. The levels of these antioxidants were measured in mice exposed to DMSO or either of the compound. The GSH-blood data indicated the values of 0.566±1.50 in DMSO-treated, 0.491±1.51 in SH-1-treated and 0.603±2.1 in SH-2-treated mice **(Fig. 6.3a)**. GSH-liver data showed the values of 0.90±0.02 in DMSO treated, 0.86±0.01 in SH-1-treated and 0.85±0.01 in SH-2 treated mice **(Fig. 6.3b)**. GSH-kidney data showed the values of 0.83±0.02 in DMSO treated, 0.77±0.06 in SH-1-treated and 0.76±0.05 in SH-2 treated mice **(Fig. 6.3c).** GSH-prostate data showed the values of 1.99±0.09 in DMSO treated, 0.186±0.13 in SH-1-treated and 0.183±0.02 in SH-2 treated mice **(Fig. 6.3d)**. The histogram of respective values indicated that, with respect to control, the GSH level did not get altered by either compound.

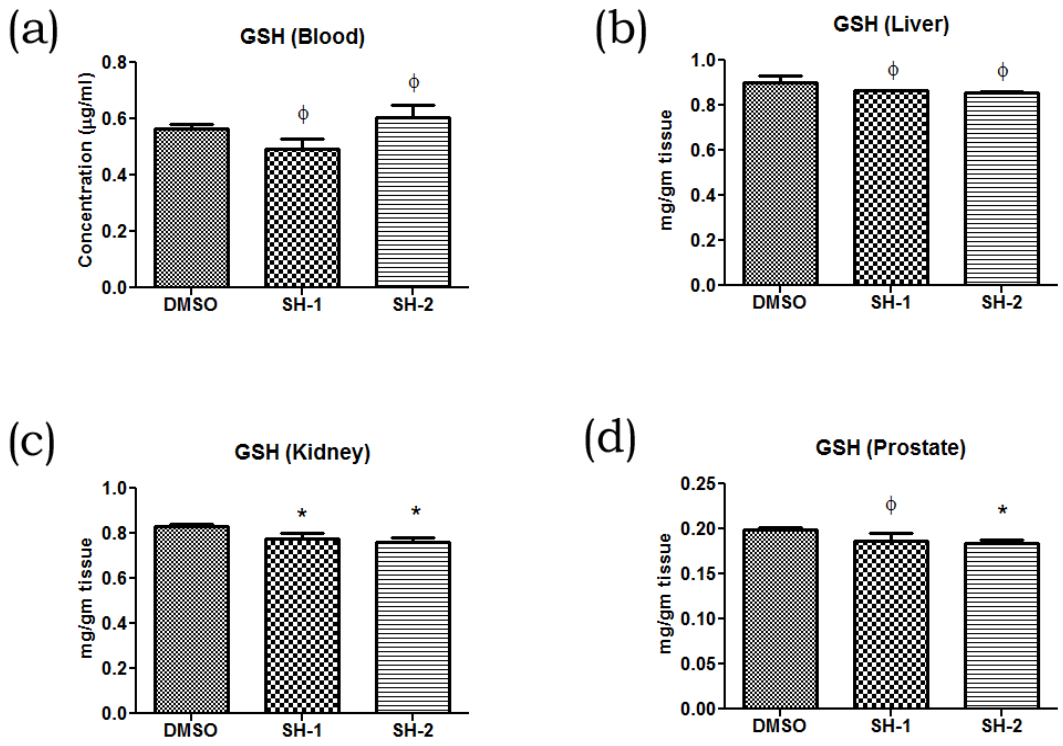

Figure. 6.3. Effect on GSH in different tissues of mice exposed to either SH-1 or SH-2.

DMSO-exposed mice worked as control vehicle in all assays. The level of reduced glutathione (GSH) was given in terms of mg/gm of tissue. The fluorescent intensities were measured in (a) blood, (b) liver, (c) kidney, (d) prostate gland. The calculated values were represented as histograms. Values for each experiment are mean ±SD; n=3. ϕ represents $p>0.05$ with respect to control group.

Next, the activity of antioxidant enzyme SOD was measured. The SOD-blood data indicated the values of 1.36±1.1 in DMSO-treated, 1.31±1.06 in SH-1-treated and 0.94±0.91 in SH-2-treated mice **(Fig. 6.4a)**. SOD-liver data showed the values of 2.00±0.50 in DMSO treated, 1.80±0.12 in SH-1-treated and 1.81±0.19 in SH-2 treated mice **(Fig. 6.4b)**. SOD-kidney data showed the values of 2.05±0.09 in DMSO treated, 1.81±0.10 in SH-1-treated and 1.75±0.12 in SH-2 treated mice **(Fig. 6.4c).** SOD-prostate data showed the values of 1.80±0.05 in DMSO treated, 1.60±0.8 in SH-1-treated and 1.86±1.0 in SH-2 treated mice **(Fig. 6.4d)**.

The histogram of respective values indicated that SOD activity in the treated samples remained unaffected with respect to the control samples.

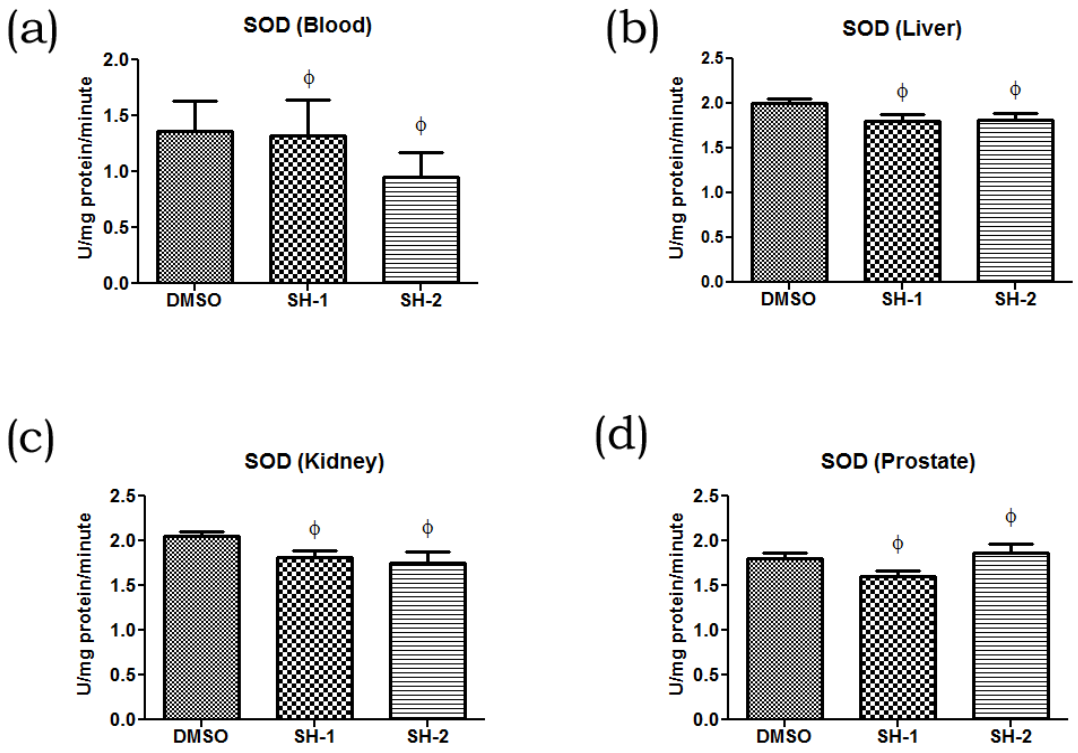

Figure. 6.4. Effect on SOD activity in different tissues of mice exposed to either SH-1 or SH-2.

DMSO-exposed mice worked as control vehicle in all assays. Superoxide dismutase (SOD) activity was measured and expressed in unit/mg tissue protein/minute. The fluorescent intensities were measured in (a) blood, (b) liver, (c) kidney, (d) prostate gland. The calculated values were represented as histograms. Values for each experiment are mean ±SD; n=3. ϕ represents $p>0.05$ with respect to control group.

The activity of catalase was measured in these tissues as per the method described in materials and method. The CAT-blood data indicated the values of 535.01±24.8 in DMSO-treated, 574.1±45.2 in SH-1-treated and 684.8±21.2 in SH-2-treated mice **(Fig. 6.5a)**. CAT-liver data showed the values of 4254.7±41.02 in DMSO treated, 4389.1±52.0 in SH-1-treated and 4368.6±49.0 in SH-2 treated mice **(Fig. 6.5b)**. CAT-kidney data showed the values of 4302.0±83.0 in DMSO treated, 3813.9±77.0 in SH-1-treated and 4546.1±38.5 in SH-2 treated mice **(Fig. 6.5c).**

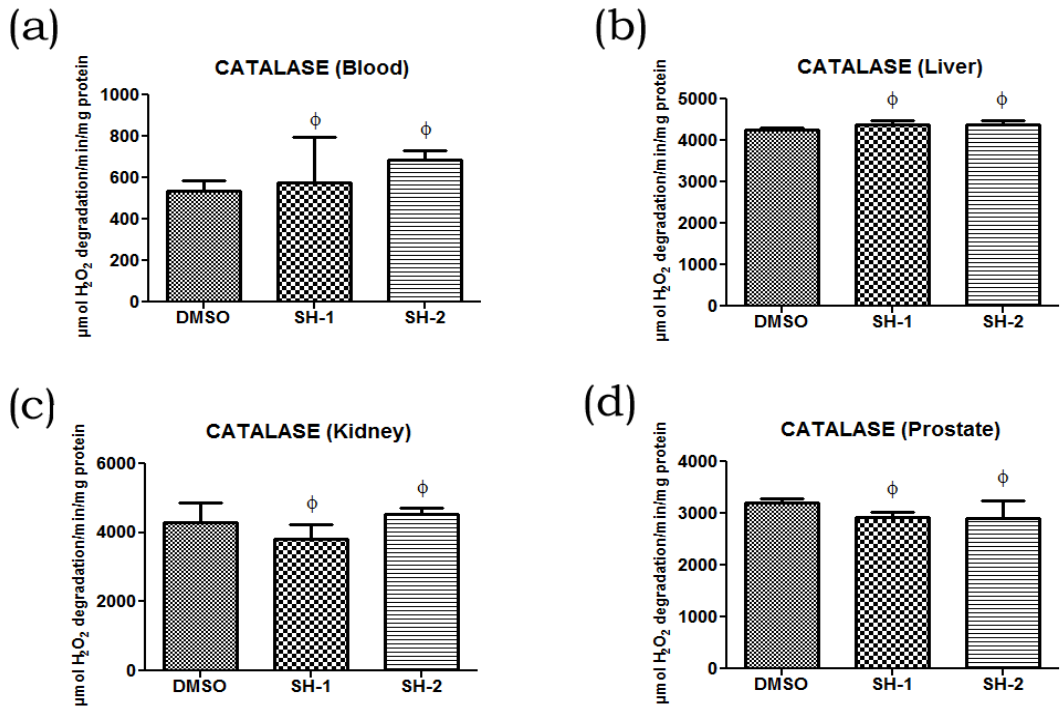

Figure. 6.5. Effect on Catalase activity in different tissues of mice exposed to either SH-1 or SH-2.

DMSO-exposed mice worked as control vehicle in all assays. The Catalase enzyme activity was assessed and expressed in µmole H_2O_2 degradation/min/mg prostate protein. The fluorescent intensities were measured in (a) blood, (b) liver, (c) kidney, (d) prostate gland. The calculated values were represented as histograms. Values for each experiment are mean ±SD; n=3. ϕ represents $p>0.05$ with respect to control group.

CAT-prostate data showed the values of 3197.7±20.1 in DMSO treated, 2916.5±24.2 in SH-1-treated and 2903.5±47.9 in SH-2 treated mice **(Fig. 6.5d)**. The histogram of respective values indicated that the catalase activity in the tissue, treated with either compound, remained unaltered with respect to the control samples.

6.4. Discussion

Apart from the external toxicity, a cell itself forms many toxic agents as a part of the metabolic activities. For example, the oxidative species are constantly formed, and the homeostasis is restored and maintained by the antioxidant defense machinery. In the cell, the levels and activities of these antioxidants are often modulated upon receiving external toxic agents. With the introduction of toxins, the membrane lipids

are metabolized to active lipid species, which in turn can damage the cell membrane (Barja, 2004). In the present study, the ROS profile from treated and untreated mice clearly indicated that these compounds at specified concentration could not trigger the level of ROS in blood and tissues. Sometimes, the low level of ROS is hard to measure and bypass the detection system, to overcome this problem TBARS assay was performed. TBARS are the index of lipid peroxidation by the oxidative species, and that can provide better insight about the toxicity of a compound. The TBARS, data in blood and tissues indicated that neither of the compound alters the amount of MDA, an important product of lipid peroxidation. Moreover, TBARS data was in coherence with the ROS data. The reduced glutathione (GSH) quenches the higher level of ROS and protect cells from the oxidative damages (Chang et al., 1991). Though insignificant, there was a slight decrease in GSH values in the SH-1 and SH-2 treated kidney and SH-2 treated prostate samples. The toxicological studies on the total GSH level revealed that neither SH-1 nor SH-2 could modulate the GSH level significantly. The cellular antioxidant system functions with the enzymatic activity of proteins which can scavenge the harmful oxidants into neutral bio-molecules. SOD and catalase are the examples of such scavengers (Weydert and Cullen, 2010). SOD can react with an active O_2^- and convert it into the water while catalase can convert hydrogen peroxide into oxygen and water. The activities of these enzymes were checked on compound exposured samples, and the data showed that it remained significantly unaltered in the treated samples with respect to the control samples. Liver is the biggest source of metabolic activities and more susceptible to the toxic substances. The various antioxidant based assay could not detect any significant change by compound treatments in the liver.

The fibroblast data from previous chapters indicated that the cells were unaffected by both SH-1 and SH-2 compounds. The present *in-vivo* toxicity data further supported the fibroblast data. The preferential killing of cancer cells by SH-1 and SH-2 advocate their potential anticancer property and could be used in prostate cancer therapy.

6.5. References

Barja, G. (2004). 'Free radicals and aging'. *Trends in Neurosciences*, 27(10): 595–600.

BLUM, R.H. and CARTER, S.K. (1974). 'AdriamycinA New Anticancer Drug with Significant Clinical Activity'. *Annals of Internal Medicine*, 80(2): 249–259.

Bradford, M.M. (1976). 'A rapid and sensitive method for the quantitation of microgram quantities of protein utilizing the principle of protein-dye binding'. *Analytical Biochemistry*, 72(1–2): 248–254.

Chang, W.C., Chen, S.H., Wu, H.L., Shi, G.Y., Murota, S. and Morita, I. (1991). 'Cytoprotective effect of reduced glutathione in arsenical-induced endothelial cell injury.' *Toxicology*, 69(1): 101–10.

Ellman, G.L. (1959). 'Tissue sulfhydryl groups'. In *Archives of Biochemistry and Biophysics*. pp. 70–77.

Girotti, A.W. (1998). 'Lipid hydroperoxide generation, turnover, and effector action in biological systems.' *Journal Of Lipid Research*, 39(8): 1529–1542.

Hissin, P.J. and Hilf, R. (1976). 'A fluorometric method for determination of oxidized and reduced glutathione in tissues'. *Analytical Biochemistry*, 74(1): 214–226.

Kakkar, P., Das, B. and Viswanathan, P.N. (1984). 'A modified spectrophotometric assay of superoxide dismutase'. *Indian Journal of Biochemistry and Biophysics*, 21(2): 130–132.

Love, R.R., Leventhal, H., Easterling, D. V and Nerenz, D.R. (1989). 'Side effects and emotional distress during cancer chemotherapy.' *Cancer*, 63(3): 604–612.

Lung cancer guide book. (2013). 'Chemotherapy side effects profile'. *Lung cancer guide book*: 384–395.

Minotti, G., Saponiero, A., Licata, S., Menna, P., Calafiore, A.M., Teodori, G. and Gianni, L. (2001). 'Paclitaxel and docetaxel enhance the metabolism of doxorubicin to toxic species in human myocardium'. *Clinical Cancer Research*, 7(6): 1511–1515.

Pachauri, V. and Flora, S.J.S. (2015). 'Combined Efficacy of Gallic Acid and MiADMSA with Limited Beneficial Effects Over MiADMSA Against Arsenic-induced Oxidative Stress in Mouse'. : 1–10.

Partridge, a H., Burstein, H.J. and Winer, E.P. (2001). 'Side effects of chemotherapy and combined chemohormonal therapy in women with early-stage breast cancer.' *Journal of the National Cancer Institute. Monographs*, 2115(30): 135–142.

Qi, W.-X., Shen, Z., Lin, F., Sun, Y., Min, D., Tang, L.-N., He, A.-N., et al. (2013). '【メタアナリシス】 転移性乳癌に対するPTX vs DTX系レジメンのメタアナリシス'. *Current medical research and opinion*, 29(2): 117–25.

Redd, W.H., Montgomery, G.H. and DuHamel, K.N. (2001). 'Behavioral intervention for cancer treatment side effects.' *Journal of the National Cancer Institute*, 93(11): 810–23.

S., Y. and Y., D. (2012). 'Docetaxel plus prednisone versus mitoxantrone plus prednisone as firstline chemotherapy for metastatic castration-refractory prostate cancer: Long-term effects and safety in chinese'. *International Journal of Urology*, 19: 155.

Shelley, M., Harrison, C., Coles, B., Staffurth, J., Wilt, T.J. and Mason, M.D. (2006). 'Chemotherapy for hormone-refractory prostate cancer.' *The Cochrane database of systematic reviews*, (4): CD005247.

Shinoda, K., Mitsumori, K., Yasuhara, K., Uneyama, C., Onodera, H., Hirose, M. and Uehara, M. (1999). 'Doxorubicin induces male germ cell apoptosis in rats'. *Archives of Toxicology*, 73(4–5): 274–281.

Socci, D.J., Bjugstad, K.B., Jones, H.C., Pattisapu, J.V. and Arendash, G.W. (1999). 'Evidence That Oxidative Stress Is Associated with the Pathophysiology of Inherited Hydrocephalus in the H-Tx Rat Model'. *Experimental Neurology*, 155(1): 109–117.

Terry Priestman. (2012). *Cancer Chemotherapy in Clinical Practice*

Weydert, C.J. and Cullen, J.J. (2010). 'Measurement of superoxide dismutase, catalase and glutathione peroxidase in cultured cells and tissue'. *Nature protocols*, 5(1): 51–66.

Winterbourn, C.C., Hawkins, R.E., Brian, M. and Carrell, R.W. (1975). 'The estimation of red cell superoxide dismutase activity'. *The Journal of laboratory and clinical medicine*, 85: 337–41.

CHAPTER-7

SUMMARY

Prostate cancer is one of the leading cause of deaths. Change in the life standards and food hobbits are several reasons for the increase of prostate cancer especially in the industrial countries. The major problem lies in the late appearance of diagnostic symptoms in men. In the process of treatment, the disease often stops responding to the drugs and this emanate from the problem of drug resistance. The present drugs, used for cancer therapies, have many side-effects. Arylsulfonylhydrazones of 2-formylpyridine N-oxide and 2- formylpyridine 1-oxide have been shown to possess potent activity against several transplanted murine tumor (May and Sartorelli, 1978; Loh et al., 1980). To enhance the cancer tissue specificity and minimize systemic toxicity, a series of 10 sulphonylhydrazone derivatives were prepared by substituting at various positions of the phenyl rings of toluene sulphonylhydrazones and named as "PR-3 series". These compounds were provided by Professor Amir Azam, Jamia Milia University, New Delhi. Compounds were screened for their toxic effects on metastatic prostate cancer cells DU145 and PC-3. Two of these compounds viz. SH-1 or *N*'-[(1*E*)-(2,5-dimethoxyphenyl)methylene]-4-methylbenzenesulfonohydrazide and SH-2 or (E)-*N*-(1-(3-chlorophenyl)propylidene)-4-methylbenzene sulfonohydrazide were taken for the further detailed study. Both compounds SH-1 and SH-2 exerted considerable amount of cell death at their IC_{50} concentrations, 60µM and 70µM in DU145 and PC-3 respectively. High doses of the drugs induce systemic toxicity and resistance, therefore subcytotoxic concentrations, 10µM for SH-1 and 40µM for SH-2, were used for their characterization on cancer cells. These lower concentrations are the minimum ones which adversely affected the cancer cells and resulted in 25-30 % killing. SH-1 induced S-phase arrest and downregulation of cyclin A, while SH-2 induced G_1-phase arrest and inhibition of cyclin D1 and cyclin E Our *in-vitro* withdrawal cell cycle data showed the increase in cell death even after the compounds were withdrawn, inferring the irreversible killing effect of these compounds. However, noncancerous-fibroblast, NIH-3T3 cells were unaffected by the subcytotoxic concentrations of either of the compound. The CDK-inhibitor p21 was induced, both at transcriptional and translational level, by

both compounds in the cancer cells. p53, tumor suppressor protein, regulates the p21 expression.

DU145 cells have mutated p53, and PC-3 cells are $p53^{-/-}$ cell lines. BRCA1 (Breast Cancer1), a tumor suppressor protein, transcriptionally activates p21 and is known to express in both DU145 and PC-3. Both SH-1 and SH-2 upregulated the expression and nuclear localization of BRCA1and p21. The induced p21 inhibited cyclin A/CDK2 and cyclin E/CDK2 interactions, resulting in S-phase and G1-phase arrest of cell cycle in both cancer cells. C-terminus of p21 interacts and inhibits PCNA, and halts DNA replication (Cayrol et al., 1998). The downregulation of PCNA induced by either of compound indicated that p21 might have inhibited PCNA, thus replication block in both cancer cells. PCNA was degraded proteasomely, as shwon by the proteasomal inhibitor-MG132 data.

The interactions these 2 compounds with p38MAPK were first checked by docking program. For this all the 4 isoforms, "α, β, γ, and □ " of p38 were used Results showed best interaction with the DFG binding site of p38. Many pharmacological inhibitors of p38 MAPK have been developed for invasive cancer therapy (Gill et al., 2013). The survival role of p38MAPK is associated with the downstream phosphorylation of Hsp27 and transcription factor ATF-2 (Shiryaev et al., 2011). Our data indicated inhibition of phosphorylated p38 and Hsp27. The total expression level of p38 and Hsp27 were highly inhibited at transcriptional while those were moderately inhibited at translational level by either of the compound. Our *in-vitro* data indicated that in the non-cancerous cells, the expression of the P-p38 and P-Hsp27 remained unaffected. The P-p38 dependent phosphorylation of ATF-2 was also inhibited in both cancer cells.

The cancer cells are under high metabolic pressure as compared to their normal counterparts. The PKM2, one of the isoforms of pyruvate kinase (PK), has been found to be induced in many types of cancer, wherein it pushes the glucose metabolism in the aerobic pathway (Dong et al., 2016). In cancer cells, PKM2 regulates transcription by modulating the histones, especially H3 and activates the transcription of proto-oncogenes c-Myc and cyclin D1 (Weiwei Yang et al., 2012). Both SH-1 and SH-2 inhibited PKM2 and its associated phosphorylation of H3 and transcription of c-Myc and cyclin D1. PKM2 is translocated to the nucleus by ERK1/2, where it performs it transcriptional role (W Yang et al., 2012). The

inhibition of p38MAPK might have blocked the nuclear translocation of PKM2 and that lead to the inhibition in P-H3 and subsequent activation of proto-oncogenes c-Myc and cyclin D1. The decreased level of c-Myc level might not have been able to downregulate the expression of p21, and thus p21 was able to block cell proliferation. High ROS levels are known to damage DNA, MMP, and can be exploited to kill cancer cells (Wang and Yi, 2008; Khan et al., 2012; Raj et al., 2011; Liou and Storz, 2010). Our data indicated that both compounds disrupted the MMP and induced ROS in both cancer cell lines in a dose-dependent manner. Higher level of ROS can inhibit PKM2 and trigger antioxidant signals (Anastasiou, 2011). Our data inferred that compound induced ROS might be responsible for inhibition of PKM2 in both DU145 and PC-3. To investigate whether the cell death, induced by either compound, was due to cellular apoptosis, the expression of PARP was checked and found its time dependent cleavage in both cancer cells. Higher ROS level induced-cytochrome c inhibits the anti-apoptotic protein Bcl-2, and that results in the activation of effector caspase-3. The inhibition of mitochondrial apoptotic players, Bcl-2 and survivin and induction of caspase-3 cleavage, further supported the apoptotic nature of cell death induced by SH-1 and SH-2. These apoptotic remained unaffected at the subcytotoxic concentrations in noncancerous fibroblast cells.

The toxic implications of both compounds were also evaluated in *in-vivo* mouse model system. The investigation of superoxide dismutase (SOD) and glutathione (GSH), the lipid peroxides (TBARS), catalase (CAT) and ROS level in were carried out in blood and tissue samples (liver, kidney and prostate gland) of BALB/c mice exposed to either SH-1 or SH-2. The biochemical data clearly indicated insignificant effects on these enzymes in the mice.

These study supported the broad spectrum signaling inhibitory effect of these compounds in metastatic prostate cancer cell DU145 and PC-3. The preferential killing of cancer cells by SH-1 and SH-2 advocate their potential anticancer property and could be used in prostate cancer therapy.

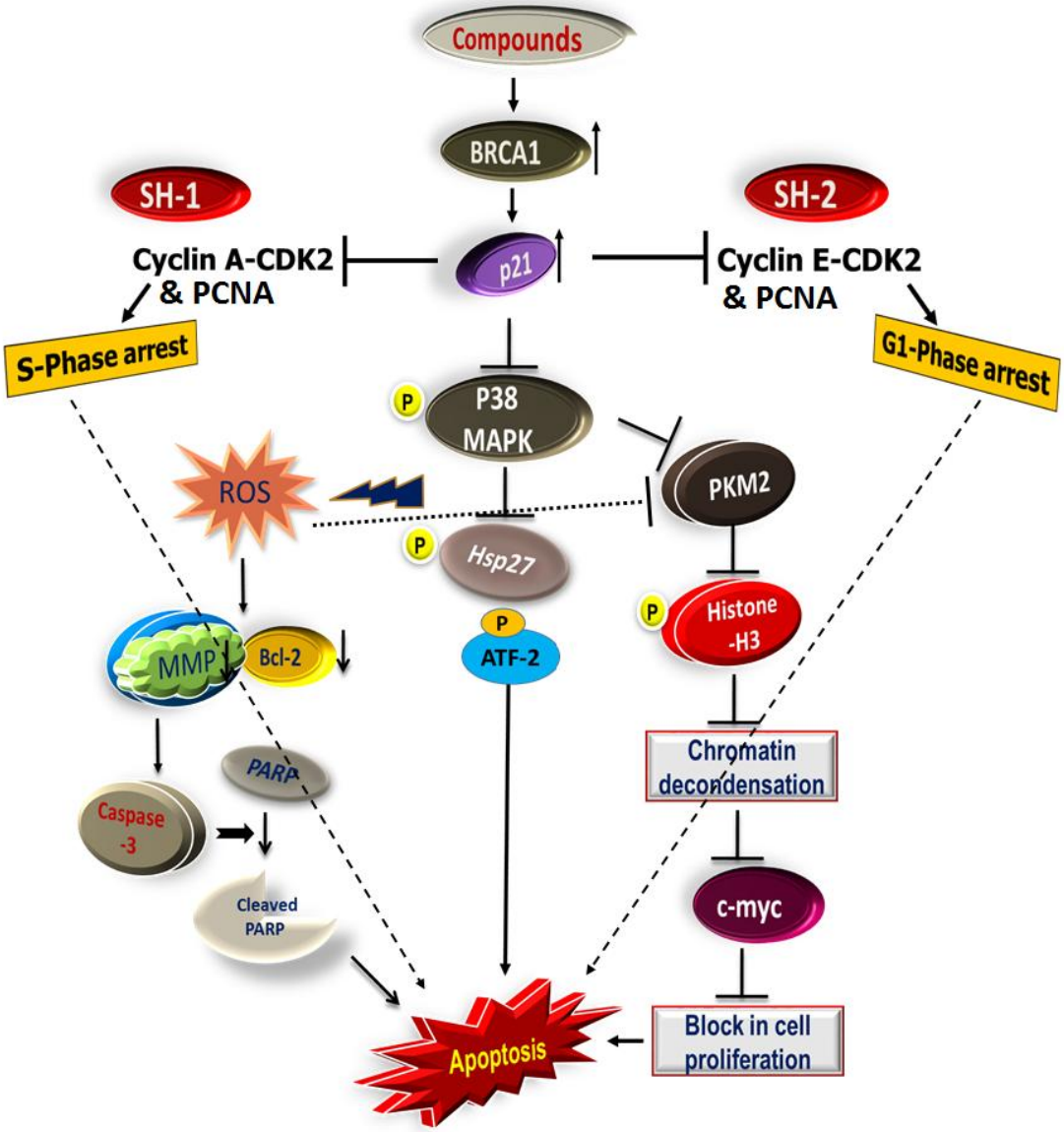

Proposed model for mechanism of action of SH-1 and SH-2 in prostate cancer cell lines DU145 and PC-3

References

Anastasiou, D. (2011). 'Inhibition of pyvate kinase M2 by reactive Oxygen Species contributes to cellular Antioxydant responses'. *Science*, 334(December): 1278–1283.

Cayrol, C., Knibiehler, M. and Ducommun, B. (1998). 'p21 binding to PCNA causes G1 and G2 cell cycle arrest in p53-deficient cells'. *Oncogene*, 16(3): 311–320.

Dong, G., Mao, Q., Xia, W., Xu, Y., Wang, J., Xu, L. and Jiang, F. (2016). 'PKM2 and cancer: The function of PKM2 beyond glycolysis (Review)'. *Oncology Letters*, 11(3): 1980–1986.

Gill, K., Singh, A.K., Kapoor, V., Nigam, L., Kumar, R., Holla, P., Das, S.N., et al. (2013). 'Development of peptide inhibitor as a therapeutic agent against head and neck squamous cell carcinoma (HNSCC) targeting p38alpha MAP kinase.' *Biochimica et biophysica acta*, 1830(3): 2763–9.

Khan, M.I., Mohammad, A., Patil, G., Naqvi, S.A.H., Chauhan, L.K.S. and Ahmad, I. (2012). 'Induction of ROS, mitochondrial damage and autophagy in lung epithelial cancer cells by iron oxide nanoparticles'. *Biomaterials*, 33(5): 1477–1488.

Liou, M.-Y. and Storz, P. (2010). *Reactive oxygen species in cancer*

Loh, W., Cosby, L.A. and Sartorelli, A.C. (1980). 'Synthesis and antineoplastic activity of phenyl-substituted phenylsulfonylhydrazones of 1-pyridinecarboxaldehyde 1-oxide'. *Journal of Medicinal Chemistry*, 23(6): 631–634.

May, J.A. and Sartorelli, A.C. (1978). 'Antineoplastic properties of arylsulfonylhdrazones of 3-formylpyridazine 2-oxide and 4-formylpyrimidine 3-oxide'. *Journal of medicinal chemistry*, 21(12): 1333—1335.

Raj, L., Ide, T., Gurkar, A.U., Foley, M., Schenone, M., Li, X., Tolliday, N.J., et al. (2011). 'Selective killing of cancer cells by a small molecule targeting the stress response to ROS.' *Nature*, 475(7355): 231–4.

Shiryaev, A., Dumitriu, G. and Moens, U. (2011). 'Distinct roles of MK2 and MK5 in cAMP/PKA- and stress/p38MAPK-induced heat shock protein 27 phosphorylation.' *Journal of molecular signaling*, 6(1): 4.

Wang, J. and Yi, J. (2008). 'Cancer cell killing via ROS: To increase or decrease, that is a question'. *Cancer Biology and Therapy*, 7(12): 1875–1884.

Yang, W., Xia, Y., Hawke, D., Li, X., Liang, J., Xing, D., Aldape, K., et al. (2012). 'PKM2 Phosphorylates Histone H3 and Promotes Gene Transcription and Tumorigenesis'. *Cell*, 150(4): 685–696.

Yang, W., Zheng, Y., Xia, Y., Ji, H., Chen, X., Guo, F., Lyssiotis, C.A., et al. (2012). 'ERK1/2-dependent phosphorylation and nuclear translocation of PKM2 promotes the Warburg effect'. *Nat Cell Biol*, 14(12): 1295–1304.

List I: Stock solutions and reagents

All solutions were prepared in deionized, ultra-filtered water from a water purification system (Millipore, USA). All solutions were sterilized by autoclaving at 15 lbs /square inch for 20 min, unless stated otherwise.

Ampicillin stock solution (100 mg/ml)

1 gm of ampicillin was dissolved in 10 ml of autoclaved water. The solution was filter sterilized using 0.2 µm filter. Aliquots were stored at -20^{o}C.

RNaseA stock solution (1 mg/ml)

10 mg of RNase A was dissolved in 10 ml of autoclaved 10 mM Tris-Cl (pH 8.0). The solution was filter sterilized using 0.2 µm filter. Aliquots were stored at -20^{o}C until needed.

DNaseI stock solution (1 mg/ml)

10 mg of DNaseI was dissolved in 10 ml of autoclaved 10 mM Tris-Cl (pH 8.0). The solution was filter sterilized using 0.2 µm filter. Aliquots were stored at -20^{o}C until needed.

TE (storage buffer)

Dissolve 10 mM Tris-HCl, pH 8.0 and 1 mM EDTA in 1 Liter of water and sterilize by autoclaving..

1 M Tris.HCl (pH 8.0)

Dissolved 121.14 g of Trizma™ base (Tris base) in water and pH was adjusted to 8.0 using 6 N HCl and volume was made up to 1000ml with water.

DMEM Incomplete medium

DMEM was dissolved in 900 ml of autoclaved water, $NaHCO_3$ was added to final concentration of, pH was adjusted to 7.2. Volume was made up to 1 liter and media was filtered with 0.22 µm filter before use.

Freezing mixture for cell lines

Freezing mixture for cell lines made of 5% DMSO, 20% FBS in DMEM. Filter-sterilize; store frozen.

0.5 M EDTA (pH 8.0)

18.61 gm of EDTA was dissolved in 80 ml water. The pH was adjusted to 8.0 with NaOH pellets. The volume was made up to 100 ml.

TAE Buffer (pH 8.5)

50 X stock solutions was prepared by dissolving

242 g Tris base,

57.1 ml glacial acetic acid,

37.2 g $Na_2EDTA\text{-}2H_2O$ (2 mM)

6X DNA Gel Loading Dye

Bromophenol blue	0.25%
Xylene cyanole FF	0.25%
Glycerol	30%

Gel Loading Dye was prepared in water, and stored in aliquots at 4^oC.

Ethidium bromide (10 mg/ml)

0.1 gm of ethidium bromide was dissolved in 8 ml of autoclaved water. The volume was made up to 10 ml. Aliquots were stored in dark at room temperature.

30% Acrylamide solution

29 gm of acrylamide and 1 gm of N, N'- methylene bisacrylamide were dissolved in 90 ml of autoclaved water (29:1). The final volume was made up to 100 ml and the solution was stored in a dark bottle at 4^oC.

10% SDS solution

5 gm of SDS was dissolved in 40 ml of autoclaved water. The final volume was made up to 50 ml and stored at room temperature.

10% APS

1 gm of ammonium persulphate was dissolved in 8 ml of autoclaved water. The final volume was made up to 10 ml. Aliquots were stored at -20^{o}C.

1.5 M Tris base (pH 8.8)

18.1 gm of Tris base was dissolved in 80 ml of water and the pH was adjusted to 8.8 with concentrated HCl and the final volume was made up to 100 ml.

1 M Tris base (pH 6.8)

12.1 gm of Tris base was dissolved in 80 ml of water and the pH was adjusted to 6.8 with concentrated HCl and the final volume was made up to 100 ml.

5X SDS PAGE sample loading dye

β-Mercaptoethanol	15%
SDS	15%
Bromophenol blue	0.6%
Glycerol	50%

Electrode buffer

Glycine	192 mM
Tris base	25 mM
SDS	0.1%

The buffer was prepared in autoclaved water.

12% Resolving gel

30% Acrylamide solution	4.0 ml

1.5 M Tris HCl (pH 8.8)	2.5 ml
Autoclaved water	3.35 ml
10% SDS solution	100 µl
10% APS solution	50 µl
TEMED	8 µl

Stacking gel

30% Acrylamide solution	0.65 ml
1 M Tris HCl (pH 6.8)	0.65 ml
Autoclaved water	3.65 ml
10% SDS solution	50 µl
10% APS solution	25 µl
TEMED	6 µl

Staining solution

Coomassie brilliant blue	0.25%
Methanol	40%
Glacial acetic acid	10%

Destaining solution

Methanol	40%
Glacial acetic acid	10%

Transfer buffer (pH 8.3)

Glycine	192 mM
Tris base	25 mM
Methanol	20%

Kinase assay buffer (pH-7.4)

$MgCl_2$	10 mM
Tris-Cl (pH-7.4)	50 mM
DTT	1mM

Cell lysis buffer

Tris-Cl (pH-8.0)	50 mM
NaCl	150 mM
EDTA	2mM
Glycerol	10%
NP-40	1%

PBS-Tween

0.5 ml of Tween 20 was added to 1000 ml of autoclaved 1X PBS.

1.25 mM DCFDA

3 mg of DCFDA powder was dissolved in 5 ml of DMSO or methanol. This should be used freshly in the reaction.

10 mM DTNB or Ellman's reagent

40 mg of DTNB powder was dissolved in 10 ml of methanol. This should be used freshly in the reaction**.**

0.2M H_2O_2

741 µl of 30% hydrogen peroxide was dissolved in 9.259 ml of distilled water. This should be used freshly in the reaction

180 µM PMS

3.06 mg of PMS powder was dissolved in 10 ml of double distilled water.

780 µM NADPH

8.0 mg of PMS powder was dissolved in 15 ml of double distilled water.

300 µM NBT

5.0 mg of PMS powder was dissolved in 20 ml of methanol.

5.55 mM OPT

1.0 mg of OPT powder was dissolved in 10 ml of methanol.

List II: Sequences of primers and run-method used in qRT-PCR

The primer sequences, either referred from other published journals or synthesized using PubMed primer design tool, were obtained from Sigma in high purity grade.

1. **p21 (Nucleic Acids Res. 2006; 34(2): 543–554)**

   Forward primer- 5′-GCAGACCAGCATGACAGATTT-3′

   Reverse primer- 5′-GGATTAGGGCTTCCTCTTGGA-3′

2. **p38 (NCBI Reference Sequence: NM_001315.2)**

   Forward primer- 5'-ATGCCGAAGATGAACTTTGC -3'

   Reverse primer- 5'-TCTTATCTGAGTCCAATACAAGCATC-3'

3. **Hsp27 (Black et al. 2011 June 1; 253(2): 112–120)**

   Forward primer- 5'-AAGCTAGCCACGCAGTCCAA-3'

   Reverse primer- 5'-CGACTCGAAGGTGACTGGGA-3'

4. **PKM2 (NCBI Reference Sequence: NM_002654.5)**

   Forward primer- 5'-ATCGTCCTCACCAAGTCTGG -3'

   Reverse primer- 5'-GAAGATGCCACGGTACAGGT -3'

5. **c-myc (Cell. 2005 Sep 23;122(6):947-56)**

   Forward primer- 5′-TACCCTCTCAACGACAGCAG-3′

   Reverse primer- 5′-GGGCTGTGAGGAGGTTTG-3′

6. **GAPDH (NCBI Reference Sequence: NM_002046.5)**

   Forward primer- 5'-AGCCTCAAGATCATCAGCAATG -3'

   Reverse primer- 5'-ATGGACTGTGGTCATGAGTCCTT-3'

PCR-reaction run method

Real-time quantitative PCR was performed in a 7500 Real-Time PCR System (Applied Biosystems) using the Power SYBR-Green master mix (Applied Biosystems). The PCR cycling conditions were: 40 cycles of 15 second at 95°C, 30 second at 56°C and 30 second at 72°C. Fold inductions were calculated using the formula 2 (DD Ct), where ΔΔ Ct is the ΔCt (treatment) –ΔCt (DMSO), ΔCt is Ct(gene of interest)-Ct(endogenous control) and Ct refers to the cycle at which the threshold is crossed.

List III: Publications, patents, and presentations

Publications:

1. Saba tariq[a], Fernando Avecilla[b], **Guru Prasad Sharma**[c], Neelima Mondal[c] ,Amir Azama*. Design, synthesis and biological evaluation of Quinazolin-4(3*H*)-one Schiff base conjugates as potential antiamoebic agents. **Journal of Saudi Chemical Society. 2016 July 14;** ISSN 1319-6103, http://dx.doi.org/10.1016/j.jscs.2016.05.006.

2. Narayanaswamy N, Das S, Samanta PK, Banu K, **Sharma GP**, Mondal N, Dhar SK, Pati SK, Govindaraju T. Sequence-specific recognition of DNA minor groove by anNIR-fluorescence switch-on probe and its potential applications. **Nucleic Acids Res. 2015 Oct 15**; 43(18):8651-63.

Patents:

S.No.	Title	Inventors	Complete filing date	Application Number
1.	*N*'-[(1*E*)-(2,5-dimethoxyphenyl)methylene]-4-methylbenzene (SH-1): Potential anti-cancer drug for prostate cancer	Amir Azam, Neelima Mondal, **Guru Prasad Sharma**, Afreen Inam	25.01.2016	201611002689
2.	(E)-*N*-(1-(3-chlorophenyl)propylidene)-4-methylbenzene sulfonohydrazide (SH2): Potential molecule against prostate cancer	Amir Azam, Neelima Mondal, **Guru Prasad Sharma**, Afreen Inam	03.02.2016	201611003778

Conferences:

1. Given oral presentation under **"Emerging Spark"** category on "**p38 MAPK signaling mediates mitochondrial apoptosis induced by novel synthetic hydrazone derivative SH-2 in metastatic prostate cancer cell lines"** at **Biosparks-2016**, School of Life Science, Jawaharlal Nehru University, New Delhi (**18-19 March 2016**).
2. Presented poster on "**Induction of apoptosis by novel synthetic hydrazine derivatives in metastatic prostate cancer cell lines"** at International symposium on Role of Herbals in Cancer Chemoprevention and Treatment, Jawaharlal Nehru University, New Delhi (**09-10 February 2016**).
3. Presented poster on "**Inhibition of PCNA, p38MAPK and Pyruvate Kinase M2 by novel synthetic compound F4 in metastatic prostate cancer cell lines"** at International symposium on Current Advances in Radiobiology, Stem cells and Cancer research, Jawaharlal Nehru University, New Delhi (**19-21 February 2015**).
4. Presented poster on "**Inhibition of replication, MAPK (Mitogen Activated Protein Kinase) pathway and S-phase arrest by novel synthetic compound F4in prostate cancer cell lines"** at XXXVIII All India Cell Biology Conference and International symposium on 'Cellular Response to Drugs,' CSIR-Central Drug research Institute, Lucknow (**10-12 December 2014**).
5. Given oral presentation on "**Replication block and S-phase arrest of cell cycle by novel synthetic compound F4 on prostate cancer cell lines DU-145 and PC3."** at 5th International Conference on Stem Cells and Cancer (ICSCC-2014): Proliferation, Differentiation and Apoptosis, Jawaharlal Nehru University, New Delhi (**08-10 November 2014**) **Awarded for best oral presentation.**
6. Given oral presentation on "**Study of anticancer properties of novel synthetic compound(s) on Prostate Cancer cell lines"** at **Biosparks-2014**, School of Life Science, Jawaharlal Nehru University, New Delhi (**21-22 March 2014**).
7. Presented poster on "**Study of anticancer properties of novel synthetic compound(s) on Prostate Cancer cell lines"** at 20th ISCB International Conference (ISCBC-2014) Chemistry and Medicinal Plants in Translational Medicine for Healthcare, department of Chemistry, Delhi University, New Delhi (**01-04 March 2014**).

LIST-IV. List of figures

LIST-V. List of tables